



**AUSTRALIA**

**University of Southern Queensland  
Faculty of Health, Engineering and Sciences**

**TRIBOLOGICAL BEHAVIOUR OF GRAPHITE/DATE PALM  
FIBRES REINFORCED EPOXY COMPOSITES**

A dissertation submitted by

**Abdullah Al-Ajmi 006**

**10 231 64**

For the award of

***Doctor of Philosophy***

**August 2013**

Principal Supervisor: Dr. B.F. Yousif

## Abstract

Natural fibres are becoming alternative candidates to synthetic fibres because of their environmental and economic advantages. In this study, the mechanical and the tribological performance of epoxy composites (ECs) based on date palm fibres (DPFs) was evaluated and compared with neat epoxy (NE). The work is divided into three stages: fibre optimisation, graphite optimisation and final composite selection.

Different fibre diameters (0.3–0.7 mm) and concentration of sodium hydroxide (NaOH) (zero to nine per cent) were used in preparing the fibre. For optimisation purposes, the interfacial adhesion between the DPFs and the epoxy matrix was studied using a new fragmentation technique that considers the influence of the NaOH treatment and the fibre diameter. At this stage, the results revealed that NaOH treatment significantly influences both the fibre strength and the fibre interfacial adhesion. Six per cent NaOH exhibited the optimum concentration to gain good mechanical properties for the EC, since it can maintain good interfacial adhesion, while maintaining good fibre strength.

In the second stage, the influence of the graphite weight presentation on ECs was evaluated from a mechanical and tribological perspective. Different weight percentages were used in the sample preparation (zero to seven per cent) for tensile, hardness and adhesive wear experiments. In the first part of this study, ultimate tensile strength and modulus of elasticity values and fracture morphology are determined. In the second part, specific wear rate, friction coefficient, interface temperature and surface morphology of the composites are determined. The results are discussed to gain the optimum mixing ratio of graphite with epoxy. The results revealed that there is a significant influence of the weight fraction of the graphite on both mechanical and tribological performance of the composites. Intermediate weight percentage of three weight per cent graphite in the EC was considered the optimum from both mechanical and tribological performance, since there is a slight reduction in the tensile properties and significant improvement to the hardness, wear and frictional characteristics. The modification on the wear track roughness significantly controlled the wear and

frictional behaviour of the composites. Micrographs of the worn surface showed different wear mechanisms, depending on the content of the graphite in the composites. Softening and fragmentation appeared with low content of graphite presence in the composite, since there was no sign of aggregation or detachments of fillers.

From the second stage on the graphite percentage in the composite, it was concluded that three weight per cent of graphite in the ECs represents the optimum content from mechanical and tribological perspectives. In the third stage, the mechanical and tribological performance of the ECs based on three weight per cent graphite, DPF and three weight per cent graphite plus DPF are discussed and compared with NE. Further, the tribological performance of the composites is discussed, considering two different adhesive wear techniques: block on ring (BOR) and block on disk (BOD). This stage revealed that DPF is able to improve the mechanical properties of the ECs with no signs of pull out or debonding of the fibres. The main fracture mechanism was breakage in the fibre, fracture in the resinous regions and micro-cracks with graphite presence in the composites. Further, the addition of the three weight per cent of the graphite into the date fibre/ECs contributed to the improvement of the ECs; the fibres assisted in strengthening the surface, while the graphite generated the lubricant film transfer. Tribological experimental configuration significantly controlled the wear behaviour of the composite; the wear performance worsened under BOD compared to BOR because of the high thermo-mechanical loading in the case of BOD compared to BOR.

## List of publications

Shalwan, A\*\* & Yousif, BF 2013, 'In state of art: mechanical and tribological behaviour of polymeric composites based on natural fibres', *Materials & Design*, vol. 48, June, pp 14–24.

Shalwan, A\*\* & Yousif, BF 2014, 'Investigation on interfacial adhesion of date palm/epoxy using fragmentation technique', *Materials & Design. Volume 53*, Pages 928–937.

Shalwan, A\*\* & Yousif, BF 2013 in press, 'Correlation between mechanical and tribological performance of polymer composite materials', *International Journal of Precision Technology*, August.

Shalwan, A\*\* & Yousif, BF 2013, 'Influence of graphite content on mechanical and wear characteristics of epoxy composites', under review August 2013, *Wear*.

Shalwan, A\*\* & Yousif, BF 2013, 'Mechanical, wear and frictional performance of epoxy composites based on date palm fibres and graphite filler', under consideration since July 2013 *Tribology Letter*.

Arhaim, YH, Shalwan, A\*\* & Yousif, BF 2013, 'Correlation between frictional force, interface temperature and specific wear rate of fibre polymer composites', *Advanced Materials Research*, vol. 685, pp. 45–49.

\*\*Note: the candidate used his Arabic surname (Shalwan, A) instead of the English (Al-Ajmi, A.)

## Certification of thesis

I certify that the ideas, designs and experimental work, results, analyses and conclusions set out in this thesis are entirely my own effort, except where otherwise indicated and acknowledged.

I further certify that the work is original and has not been previously submitted for assessment in any other course or institution, except where specifically stated.

Abdullah Al-Ajmi

006 10 231 64

\_\_\_\_\_  
Signature of Candidate

\_\_\_\_\_  
Date

Endorsement

\_\_\_\_\_  
Signature of Principle Supervisor

\_\_\_\_\_  
Signature of Associate  
Supervisor

\_\_\_\_\_  
Date

\_\_\_\_\_  
Date

## **Acknowledgements**

I would like to express my most sincere appreciation to my PhD project supervisors Dr B. F. Yousif and Prof. Dr. Kin Tak Lau for their support, encouragement, valuable input and guidance provided at every stage of this thesis. I would also like to extend my gratitude towards the entire departmental and technical staff for their assistance and support in using the facilities and materials for conducting the experimental work.

In addition, I wish to express my deepest appreciation to my family members for their constant support throughout this study, especially my mother and my son Mohammed. I would like to extend my appreciation to my friends for their encouragement.

My particular appreciation is also extended to the University of Southern Queensland for financial support during this study.

# Contents

<b>List of tables</b> .....	<b>x</b>
<b>List of figures</b> .....	<b>xi</b>
<b>Chapter 1: Introduction</b> .....	<b>1</b>
1.1 Introduction .....	1
1.2 Objectives .....	4
1.3 Project significance .....	5
1.4 Organisation of the thesis .....	5
<b>Chapter 2: Literature review</b> .....	<b>8</b>
2.1 Mechanical properties of natural fibres/polymer composites .....	8
2.1.1 Influence of natural fibres on mechanical behaviour of polymeric composites .....	8
2.1.2 Interfacial adhesion of natural fibres .....	11
2.1.3 Effect of fibre orientation on mechanical properties .....	16
2.1.4 Effect of volume fraction .....	16
2.1.5 Effect of fibre physical properties .....	18
2.2 Tribological performance of polymeric composites based on natural fibres ...	19
2.2.1 Influence of natural fibres on tribological behaviour of polymeric composites .....	19
2.2.2 Effect of treatments .....	26
2.2.3 Operating parameters .....	28
2.2.4 Frictional behaviour .....	29
2.3 Possible reduction of friction coefficient .....	31
2.3.1 Liquid lubricants .....	31
2.3.2 Solid lubricants .....	35
2.4 Chapter summary .....	37
<b>Chapter 3: Methodology</b> .....	<b>39</b>
3.1 Introduction .....	39
3.2 Materials selection and preparation .....	41
3.2.1 Date palm fibre preparation and treatment .....	41
3.3 Preparation of samples .....	43
3.3.1 Single fibre tensile test .....	43
3.3.2 Fragmentation test specimens .....	43
3.3.3 Composite specimens preparation .....	44
3.4 Experimental procedure .....	47
3.4.1 Mechanical properties .....	49
3.4.1.1 <i>Single fibre tensile test</i> .....	49
3.4.1.2 <i>Single fibre fragment test</i> .....	49
3.4.1.3 <i>Tensile experiments of the composites</i> .....	50
3.4.2 Tribological experiments .....	51

3.4.3 Calibration and measurement technique of friction coefficient .....	55
<b>Chapter 4: Interfacial adhesion of date palm/epoxy using fragmentation technique .....</b>	<b>56</b>
4.1 Introduction .....	56
4.2 Influence of fibre treatment on surface morphology .....	58
4.2.1 Optical microscope micrographs morphology .....	58
4.2.2 Scanning electron microscope morphology .....	60
4.3 Single fibre tensile test .....	63
4.4 Single fibre fragmentation tensile test .....	68
4.5 Comparison to other published works .....	79
4.6 Chapter summary .....	82
<b>Chapter 5: Influence of graphite content on mechanical and wear characteristics of epoxy composites .....</b>	<b>83</b>
5.1 Introduction .....	83
5.2 Tensile properties of graphite/epoxy composites .....	83
5.2.1 Stress strain diagram, ultimate TS and modulus of elasticity .....	83
5.2.2 Fracture behaviour of the epoxy composites .....	86
5.3 Tribological performance of the epoxy composites based on different graphite contents .....	93
5.3.1 Running in and steady state of the adhesive wear .....	93
5.3.2 Running in and steady state of the coefficient of friction .....	95
5.3.3 Frictional heat in the interface of graphite/epoxy composites .....	98
5.4 Surface observations .....	101
5.4.1 Roughness modifications of the wear track .....	101
5.4.2 Roughness of the composite surface .....	103
5.4.3 Scanning electron microscopy observation .....	106
5.4.3.1 <i>Micrographs of NE worn surface</i> .....	106
5.4.3.2 <i>Micrographs of one weight per cent graphite/epoxy worn surface</i> .....	108
5.4.3.3 <i>Micrographs of three weight per cent graphite/epoxy worn surface</i> .....	109
5.4.3.4 <i>Micrographs of five weight per cent graphite/epoxy worn surface</i> .....	110
5.4.3.5 <i>Micrographs of seven weight per cent graphite/epoxy worn surface</i> .....	112
5.5 Comparison with previous works .....	113
5.6 Chapter summary .....	116
<b>Chapter 6: Mechanical and wear characteristics of DPF and graphite filler/ECS .....</b>	<b>117</b>
6.1 Introduction .....	117
6.2 Tensile properties of date palm/graphite/epoxy composites .....	117
6.2.1 Stress strain diagram, ultimate tensile stress and modulus of elasticity of date palm/graphite/epoxy composites .....	117
6.2.2 Fracture behaviour date palm/graphite/epoxy composites .....	124
6.2.3 Shore D hardness of the selected composites .....	126



6.3 Tribological performance of date palm/graphite/epoxy composites under BOR technique .....	127
6.3.1 Wear behaviour of date palm/graphite/epoxy composites .....	127
6.3.2 Frictional behaviour of date palm/graphite/epoxy composites .....	129
6.3.3 Observation on the worn surfaces after BOR tests .....	133
6.3.3.1 <i>Roughness modifications of the wear track</i> .....	133
6.3.3.2 <i>Roughness of the composite surface</i> .....	134
6.3.3.3 <i>SEM observation</i> .....	135
6.4 Tribological performance of date palm/graphite/epoxy composites under BOD technique .....	138
6.4.1 Wear and frictional behaviour of date palm/graphite/epoxy composites	139
6.4.2 Observation on the worn surfaces of date palm/graphite/ECs after BOR testing .....	143
6.5 Discussion and arguments with previous works .....	147
6.6 Correlation between mechanical and tribological properties .....	150
6.7 Chapter summary .....	154
<b>Chapter 7: Conclusions and recommendations .....</b>	<b>160</b>
7.1 Conclusion.....	160
7.2 Recommendations .....	162
<b>References .....</b>	<b>1635</b>
<b>Appendix A: Samples of the collected thermal image for graphite/ECs at different operating parameters and graphite contents .....</b>	<b>17582</b>
<b>Appendix B: Samples of the collected thermal image and roughness profile for graphite/date palm fibre/ECs at different operating parameters and test configurations .....</b>	<b>1793</b>
<b>Appendix C : Figures of the collection between mechanical and tribological properties .....</b>	<b>201</b>
<b>C.1 Completed figures of the correlation between mechanical properties and specific wear rate .....</b>	<b>201</b>
<b>C.2 Completed figures of the correlation between mechanical properties and friction coefficient .....</b>	<b>208</b>
<b>Glossary of Terms .....</b>	<b>213</b>

## List of tables

Table 2.1: Comparisons between various existing fibre-reinforced composites .....	17
Table 2.2: Adhesive wear and coefficient friction result of neat polymers and natural fibre composites under dry contact .....	22 Table
3.1: Specimen sets of the SFTT .....	43
Table 3.2: Technical specifications of the newly developed machine (Yousif 2012) .....	53
Table 4.1: Summary of the previous works on optimum diameter and chemical treatment concentration on mechanical behaviour of fibre/polymer composites .....	81
Table 5.1: Summary of the previous works on effect of adding filler tribological behaviour of polymer composite .....	115
Table 6.1: Published works on tensile properties of natural fibre reinforce epoxy or polyester composites .....	121
Table 6.3: Summary of previous works on effect of natural fibres and fillers on tribological behaviour of polymer composite .....	148
Table 6.4 correlation coefficient of individual mechanical properties with coefficient of friction and specific wear rate.	156
Table 6.5 Correlation coefficient of two mechanical properties combined with coefficient of friction and specific wear rate. .	157
Table 6.6 Correlation coefficient of two or more than two mechanical properties combined with coefficient of friction and specific wear rate.	158

## List of figures

Figure 1.1: Number of synthetic and natural fibre-reinforced polymeric composite articles. Source: www.ScienceDirect.com. Keywords used: natural fibres, reinforcement, polymers and synthetic fibres .....	2
Figure 1.2: Layout of the thesis .....	7
Figure 2.1: Some mechanical properties of natural fibre/polymer composites .....	10
Figure 2.2: Scheme of reaction of fibre surface with NaOH treatment .....	12
Figure 2.3: Tensile strength of polymeric composites based on natural fibres with/without treatment .....	15
Figure 2. 4: Specific wear rate and friction coefficient of some polymeric composites under dry contact conditions .....	25
Figure 2.5: Schematic drawing showing the effect of treating the natural fibres on the wear behaviour of polymeric composites.....	28
Figure 2.6: Specific wear rate and friction coefficient of some polymeric composites under wet contact conditions .....	34
Figure 2.7: Influence of solid lubricants on the frictional behaviour of polymeric composites .....	36
Figure 3.1: Schematic drawing showing the procedure of experimental study .....	40
Figure 3.2: (a) date palm tree, (b) extracted fibres, (c) fibres classification .....	42
Figure 3.3: (a) SFFT specimen geometry, (b) SFFT mould and fibre position .....	44
Figure 3.4: (a) tensile specimen dimensions, (b) used tensile test mould .....	45
Figure 3.5: (a) tribological specimen geometry, (b) tribological mould and fibre position .....	46
Figure 3.6: a) tensile specimens, b) BOD-tribological specimen, c) BOR-tribological test .....	48
Figure 3.7: (a) single fibre specimen, (b) fixing single fibre specimen in tensile test machine .....	49
Figure 3.8: (a) some of SFFT specimens, (b) fixing specimen in tensile machine ....	50
Figure 3.9: The tribo-test machine. ....	52
Figure 3.10: Fibre orientations with respect to the sliding direction .....	54

Figure 3.11: Calibration chart for measuring friction force .....	55
Figure 4.1: Optical images of fibre surface (D = 0.3 mm)—(a) untreated, (b) at 3% NaOH, (c) at 6% NaOH (d) at 9% NaOH.....	59
Figure 4.2: (a) optical microscope micrographs for three different diameters of fibre with defects, (b) scheme of cross-section of fibre with lumen and defects .....	60
Figure 4.3: Micrographs of the untreated DPF .....	61
Figure 4.4: Treated DPF with different NaOH concentrations .....	62
Figure 4.5: Tensile behaviour of the single DPF (0.3 mm diameter) treated with different NaOH concentrations .....	63
Figure 4.6: Tensile behaviour of the single DPF (0.5 mm diameter) treated with different NaOH concentration .....	64
Figure 4.7: Tensile behaviour of the single DPF (0.7 mm diameter) treated with different NaOH concentrations .....	64
Figure 4.8: Effect of diameter of fibre and NaOH treatment on TS on single fibre ..	66
Figure 4.9: Effect of diameter of fibre and NaOH treatment on strain at fracture on single fibre .....	66
Figure 4.10: Effect of diameter of fibre and NaOH treatment on modulus of elasticity on single fibre .....	67
Figure 4.11: Tensile behaviour of the single DPF fragmentation test (0.3 mm diameter) treated with different NaOH concentrations .....	69
Figure 4.12: Tensile behaviour of the single DPF fragmentation test (0.5 mm diameter) treated with different NaOH concentrations .....	70
Figure 4.13: Tensile behaviour of the single DPF fragmentation test (0.7 mm diameter) treated with different NaOH concentrations and NE .....	71
Figure 4.14: Effect of diameter of fibre and NaOH treatment on tensile stress of date palm/EC .....	72
Figure 4.15: Effect of fibre diameter and NaOH treatment on shear stress on fibre of date palm/EC.....	73
Figure 4.17: Microscopy of fragmentation samples after testing the treated DPF (3% NaOH)/epoxy .....	75
Figure 4.18: Microscopy of fragmentation sample after testing the treated DPF	

(6% NaOH)/epoxy .....	76
Figure 4.19: Microscopy of fragmentation sample after testing the treated DPF	
(9% NaOH)/epoxy .....	77
Figure 4.20: Schematic drawing showing the treatment effect of different concentration (0%, 3%, 6% and 9%) on surface and structure fibre .....	79
Figure 5.1: Stress strain diagrams of graphite/ECs .....	84
Figure 5.2: Ultimate TS and modulus of elasticity of graphite/ECs .....	86
Figure 5.3: Micrographs of the NE after tensile testing—st = stretching, de = detachment, fr = fracture .....	87
Figure 5.4: Micrographs of the 1% graphite/ECs after tensile testing—cr = cracks, sl = shear lips, rl = river-like pattern .....	88
Figure 5.5: Micrographs of 3% graphite/ECs after tensile testing—rl = river-like pattern, gp = graphite particle .....	89
Figure 5.6: Micrographs of 5% graphite/ECs after tensile testing—rl = river-like pattern, gp = graphite particle, de = debonding, ag = aggregation .....	90
Figure 5.7: Micrographs of 7% graphite/ECs after tensile testing—de = debonding, ag = aggregation, cr = cracks, fr = fracture .....	91
Figure 5.8: Shore D hardness of graphite/ECs .....	92
Figure 5.9: Specific wear rate v. sliding distance of graphite/ECs .....	94
Figure 5.10: Schematic drawing representing the running in and steady state .....	94
Figure 5.11: Specific wear rate at the steady state of the graphite/ECs after 7.5 km sliding distance .....	95
Figure 5.12: Coefficient of friction v. sliding distance of the composites .....	96
Figure 5.13: Coefficient of friction at the steady state of the composites after 7 km sliding distance .....	98
Figure 5.14: Heat distribution in the interface and both rubbed surfaces of the NE after 2.52, 5.04 and 7.56 km sliding distances at sliding velocity of 2.8 m/s and applied load of 50 N .....	99
Figure 5.15: Interface temperature of graphite/ECs surface at the end of the adhesive loadings .....	100
Figure 5.16: Samples of the roughness profile of the counterface .....	102

Figure 5.17: Ra roughness values of the counterface surface after adhesive loadings for 7.56 km sliding distance .....	103
Figure 5.18: Samples of the roughness profile of the composite surfaces after 7.56 km sliding distance at sliding velocity of 2.8 m/s and applied load of 50 N .....	105
Figure 5.19: Ra roughness values of graphite/ECs surface after adhesive loadings for 7.56 km sliding distance .....	106
Figure 5.20: Micrographs of NE after adhesive testing—fg = fragmentation, so = softening, fr = fracture .....	107
Figure 5.21: Micrographs of 1% graphite/ECs after adhesive testing—fg = fragmentation, so = softening, fr = fracture, gr = graphite, dt = detachment, cr = crack .....	109
Figure 5.22: Micrographs of 3% graphite/ECs after adhesive testing—so = softening, fr = fracture, pg = patch of graphite, df = deformation .....	110
Figure 5.23: Micrographs of 5% graphite/ECs after adhesive testing—so = softening, fr = fracture, fl = film transfer, df = deformation .....	111
Figure 6.1: Stress strain diagram of different ECs based on graphite and/or DPFs.	118
Figure 6.2: Ultimate TS and modulus of elasticity of different ECs based on graphite and/or DPF. NE = neat epoxy, GE = 3% graphite/epoxy, FE = DPFE, GFE = 3 wt% graphite/date palm fibre/epoxy .....	119
Figure 6.3: Micrographs of DPFE composite after tensile test. ....	125
Bo = bonded, Ep = Epoxy, Br = breakage, Rl = river-like, Tr = Trichome .....	126
Figure 6.5: Shore D hardness of different ECs based on graphite and/or DPF. NE = neat epoxy, GE = 3% graphite/epoxy, FE = DPFE, GFE = 3 wt% graphite/date palm fibre/ epoxy .....	127
Figure 6.6: Specific wear rate v. applied load of different ECs based on graphite and/or DPF after 5.04 km sliding distance using BOR technique .....	128
Figure 6.7: Reduction in specific wear rate at the steady state of different ECs based on graphite and/or DPF at 70 N applied load using BOR technique .....	129

Figure 6.8: Coefficient of friction v. sliding load of different ECs based on graphite and/or DPF using BOR technique .....	130
Figure 6.9: Reduction in COF at the steady state of different ECs based on graphite and/or DPF at 70 N sliding load using BOR technique .....	131
Figure 6.10: Interface temperature of different ECs based on graphite and/or DPF at different applied loads after 5.04 km sliding distance using BOR technique .....	132
Figure 6.11: Roughness values of the counterface surface after adhesive loadings of different ECs based on graphite and/or DPF at 50 N applied load using BOR technique .....	134
Figure 6.12: Roughness values of the specimen surface of different ECs based on graphite and/or DPF after adhesive loadings at 50 N using BOR technique for 5 km sliding distance .....	135
Figure 6.13: Micrographs of DPF/ECs after testing under 50 N applied load using BOR technique .....	136
Bo = bonded, So =Softening, Db =debonding .....	136
Figure 6.14: Micrographs of date palm/3 wt% graphite/ECs after testing at 50 N using BOR technique .....	138
Cr= cracks, Db =debonding .....	138
Figure 6.15: Specific wear rate v. sliding distance of different ECs based on graphite and/or DPF using BOD technique .....	140
Figure 6.16: Reduction in specific wear rate at the steady state of different ECs based on graphite and/or DPF at 70 N km sliding load using BOD technique .....	140
Figure 6.17: Specific wear rate of the selected composites using BOR and BOD techniques after applied load 50 N. ....	141
Figure 6.18: Coefficient of friction v. sliding load of different ECs based on graphite and/or DPF using BOD technique .....	142
Figure 6.19: Interface temperature of different ECs based on graphite and/or DPF at different applied loads using BOD technique .....	142

Figure 6.20: Roughness values of the counterface surface after adhesive of different ECs based on graphite and/or DPF loadings at 50 N using BOD technique .....	143
Figure 6.21: Micrographs of the date palm/3 wt% graphite/ECs after the experiments using BOD under low applied loads. Fr = fragmentation, Ab = abrasive, Pg = ploughing, Cr = crack, Bo = bonded, Po = pull out, Fl = film transfer .....	144
Figure 6.22: Micrographs of the date palm/3 wt% graphite/ECs after the experiments using BOD under high applied loads. Pl = pull out fibre, Pg = ploughing, Fl = film transfer, Db = debonding.....	146
Figure 6.23: Correlation between the individual mechanical properties and specific wear rate of the studied materials .....	152
Figure 6.24: Correlation between selective combined mechanical properties and specific wear rate of the studied materials .....	153
Figure A.3: Heat distribution in the interface and both rubbed surfaces of the 5%Gr-EC after 2.52, 5.04 and 7.56 km sliding distances at sliding velocity of 2.8 m/s and applied load of 50 N .....	177
Figure A.4: Heat distribution in the interface and both rubbed surfaces of the 7%Gr-EC after 2.52, 5.04 and 7.56 km sliding distances at sliding velocity of 2.8 m/s and applied load of 50 N .....	178
Figure B.1: Heat distribution in the interface and both rubbed surfaces of the NE at 20, 30, 40, 50 N sliding loads at sliding velocity of 2.8 m/s and sliding distance 5.04 km (BOR) .....	180
Figure B.2: Heat distribution in the interface and both rubbed surfaces of the GE at 20, 30, 40, 50 N sliding loads at sliding velocity of 2.8 m/s and sliding distance 5.04 km (BOR) .....	182
Figure B.3: Heat distribution in the interface and both rubbed surfaces of the FE at 20, 30, 40, 50 N sliding loads at sliding velocity of 2.8 m/s and sliding distance 5.04 km (BOR) .....	184
Figure B.4: Heat distribution in the interface and both rubbed surfaces of the GFE at 20, 30, 40, 50 N sliding loads at sliding velocity of 2.8 m/s and sliding distance 5.04 km (BOR) .....	186



Figure B.5: Heat distribution in the interface and both rubbed surfaces of the NE at 20, 30, 40, 50 N sliding loads at sliding velocity of 2.8 m/s and sliding distance 2.52 km (BOD) .....	188
Figure B.6: Heat distribution in the interface and both rubbed surfaces of the GE at 20, 30, 40, 50 N sliding loads at sliding velocity of 2.8 m/s and sliding distance 2.52 km (BOD) .....	190
Figure B.7: Heat distribution in the interface and both rubbed surfaces of the FE at 20, 30, 40, 50 N sliding loads at sliding velocity of 2.8 m/s and sliding distance 2.52 km (BOD) .....	192
Figure B.8: Heat distribution in the interface and both rubbed surface of the GFE at 20, 30, 40, 50 N sliding loads at sliding velocity of 2.8 m/s and sliding distance 2.52 km (BOD) .....	194
Figure B.9: Roughness values of the counterface surface after adhesive loadings of different ECs based on graphite and/or DPF at 50 N applied load using BOR technique .....	195
Figure B.10: Roughness values of the specimen surface of different ECs based on graphite and/or DPF before adhesive loadings at 50 N using BOR technique .....	196
Figure B.11: Roughness values of the specimen surface of different ECs based on graphite and/or DPF after adhesive loadings at 50 N using BOR technique .....	197
Figure B.12: Roughness values of the counterface surface after adhesive of different ECs based on graphite and/or DPF loadings at 50 N using BOD technique .....	198
Figure C. 1 correlation between specific wear rate and modulus of elasticity .....	199
Figure C. 2 correlation between specific wear rate and elongation at break .....	199
Figure C. 3 correlation between specific wear rate and hardness .....	200
Figure C. 4 correlation between specific wear rate and tensile strength .....	200
Figure C. 5 correlation between specific wear rate and the combination of modulus of elasticity and tensile strength .....	201

Figure C. 6 correlation between specific wear rate and the combination of modulus of elasticity, tensile strength and elongation at break .....	201
Figure C. 7 correlation between specific wear rate and the combination of modulus of elasticity, tensile strength, hardness and elongation at break .....	202
Figure C. 8 correlation between specific wear rate and the combination of tensile strength and elongation at break .....	202
Figure C. 9 correlation between specific wear rate and the combination tensile strength and hardness .....	203
Figure C. 10 correlation between specific wear rate and the combination of modulus of elasticity and elongation at break .....	203
Figure C. 11 correlation between specific wear rate and the combination of modulus of elasticity and hardness .....	204
Figure C. 12 correlation between specific wear rate and the combination of hardness and elongation at break .....	204
Figure C. 13 correlation between specific wear rate and the combination of modulus of elasticity, hardness and elongation at break .....	205
Figure C. 14 correlation between friction coefficient and tensile strength .....	206
Figure C. 15 correlation between friction coefficient and modulus of elasticity .....	206
3 Figure C. 16 correlation between friction coefficient and tensile elongation at break .....	207
Figure C. 17 correlation between friction coefficient and hardness .....	207
Figure C. 18 correlation between friction coefficient and the combination of modulus of elasticity and tensile strength .....	208
Figure C. 19 correlation between friction coefficient and the combination of modulus of elasticity, tensile strength and elongation at break .....	208
Figure C. 20 correlation between friction coefficient and the combination of modulus of elasticity, tensile strength, hardness and elongation at break .....	209
Figure C. 21 correlation between friction coefficient and the combination of tensile strength and elongation at break .....	209

Figure C. 22 correlation between friction coefficient and the combination of tensile strength and hardness .....	210
Figure C. 23 correlation between friction coefficient and the combination of modulus of elasticity and elongation at break .....	210
Figure C. 24 correlation between friction coefficient and the combination of modulus of elasticity and hardness .....	211
Figure C. 25 correlation between friction coefficient and the combination of hardness and elongation at break .....	211
Figure C. 26 correlation between friction coefficient and the combination of modulus of elasticity, hardness and elongation at break .....	212

## List of abbreviations

ABS	Acrylonitrile butadiene styrene
ASTM	American Society for Testing and Materials
BFRP	Betelnut fibres reinforced in polyester
BOD	Block on disk
BOR	Block on ring
CFRP	Coir fibre-reinforced polyester
CPC	Cotton-polyester composite
Df	Fibre diameter
DPF	Date palm fibre
DPFE	Date palm fibre-reinforced epoxy
EC	Epoxy composite
GJ	Gigajoule
GR	Graphite powder
HDPE	High-density polyethylene
ICMF	Incomplete maturation fibres
KFRE	Kenaf fibre-reinforced epoxy
MoS <sub>2</sub>	Molybdenum disulfide
NaOH	Sodium hydroxide
NE	Neat epoxy
PA	Polyamides
PEEK	Polyarylethe-retherketone
PLA	Polylactic acid
PMMA	polymethyl methacrylate
PP	Polypropylene
PPESK	Polyphatalazinone ether sulfone ketone

PPE	Polyphthalazinone ether
PPS	Polyphenylene sulfide
PTFE	Poly-tetrafluoroethylene

Ra	Roughness average
RNFPC	Reinforced natural fibre polymer composite
SCRP	Sugarcane fibre/polyester composite
SEM	Scanning electron microscopy
SiC	Silicon carbide
SFFT	Single fibre fragmentation test
SFTT	Single fibre tensile test
SP	Sisal fibres/polyester composites
T-OPRP	Treated oil palm fibre-reinforced polyester
TS	Tensile strength
T-SP	Treated sisal fibres/polyester composites
UHMWPE	Ultra-High Molecular Weight Polyethylene
US	United States
UT-OPRP	Untreated oil palm fibre-reinforced polyester
UT-SP	Untreated sisal fibres/polyester composites
Vf	Volume fraction
Ws	Specific wear rates
Wt	Weight



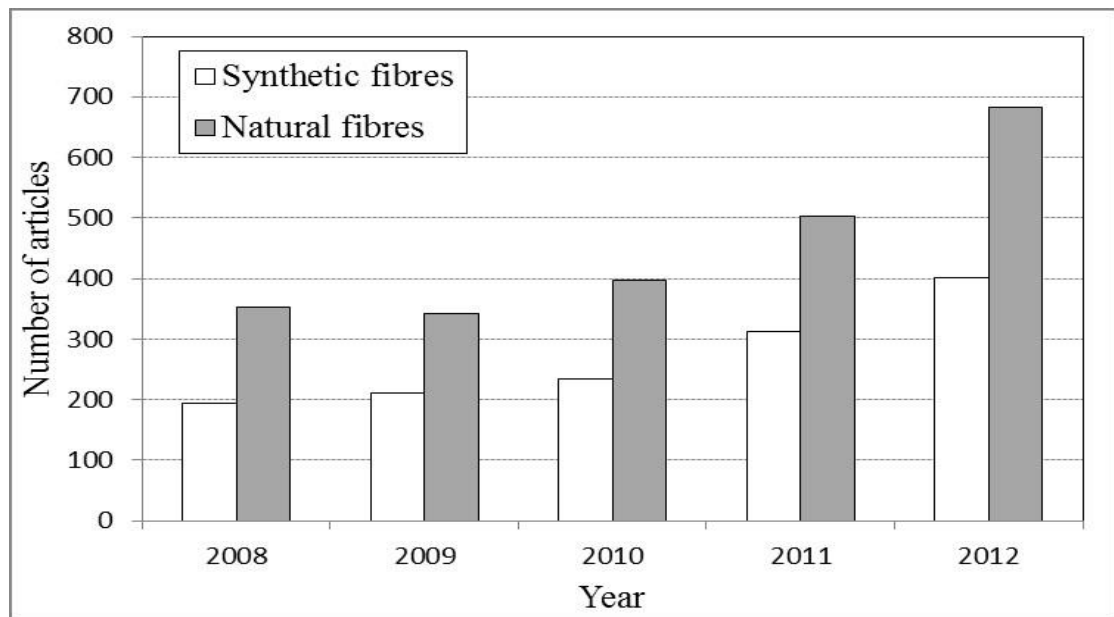
# Chapter 1: Introduction

## 1.1 Introduction

In the current era, environmental (pollution and emissions), renewable energy, recyclability and sustainability of materials awareness has increased. This has stimulated interest in the research and development of biodegradable and highperformance materials. Natural fibres are promising alternative reinforcement fibres to replace synthetic fibres for polymeric composites across different industrial applications. Natural fibres have several advantages over synthetic fibres: they are renewable, environmentally friendly, less expensive, flexible (regarding usage), lightweight, naturally recyclable and biodegradable. The most environmental key for natural fibres is their biodegradability which is the process of decomposing the materials rapidly by the action of microorganisms.

Natural fibres can be obtained from natural resources, such as plants, animals or minerals. With the rise of a global energy crisis and ecological risks, the unique advantages of plant fibres include abundance; non-toxicity; non-irritability to skin, eyes and respiratory system and non-corrosive properties. Plant-based, fibrereinforced polymer composites have attracted much interest because of their potential as alternative reinforcement to synthetic materials (Cheung et al., 2009, Wambua et al., 2003, Yousif, 2013b). Natural fibres have lower costs (US\$200– 1,000 per tonne) and use less energy to produce (four gigajoule [GJ] per tonne) than glass (US\$1,200–1,800 per tonne, 30 GJ energy to produce) and carbon (US\$12,500 per tonne, 130 GJ energy to produce) as reported by Thomas and Pothan (2009). The lower weight (20–30 wt%) and higher volume of natural fibres, compared to synthetic fibres, improves fuel efficiency and reduces emission in auto applications (Azwa et al., 2013, Yousif and Nirmal, 2011).

There is great focus on and interest in using bio-reinforcements. Numerous studies have strived to evaluate the influence of new reinforcements on composite performance under different loading conditions, including mechanical and tribological. Research on using different types of natural fibres for different polymers is ongoing; however, there is little understanding about such materials, their limitations and their solutions. In recent years, natural fibres, such as hemp, flax, jute, linen, kenaf, oil palm and bamboo, have drawn considerable attention in numerous applications, including automobiles, furniture, packing and construction as reported by many researchers such as (Joshi et al., 2004, Virk et al., 2010, Alawar et al., 2009b, Chand and Dwivedi, 2007, Saha et al., 2010, Rosa et al., 2009, Chin and Yousif, 2009, Yousif and Ku, 2012, Yousif et al., 2010a). Figure 1.1 shows the number of articles published on synthetic and natural fibres over the past five years, which indicates research interest in this topic. However, the participant authors found it necessary to address the common issues in using natural fibres and possible solutions to those issues. As such, the current review is motivated to address these issues and limitations from mechanical and tribological perspectives.



**Figure 1.1: Number of synthetic and natural fibre-reinforced polymeric composite articles.**  
**Source: www.ScienceDirect.com. Keywords used: natural fibres, reinforcement, polymers and synthetic fibres**



This thesis establishes a comprehensive collection of literature on natural fibres, their applications, limitations and possible solutions from mechanical and tribological perspectives. The literature was published in the *Materials and Design* journal and the main conclusions include:

- Surface characteristics, volume fraction ( $V_f$ ), physical properties and orientation of natural fibre have significant influences on the mechanical and tribological performance of composites. The nature of the fibres controls the mechanical and tribological behaviour of the composites. In other words, modification and critical selection of the fibres are necessary to gain high composite performance.
- There is no remarkable correlation reported between the mechanical and tribological performance of major polymeric composites. However, for natural fibre/polymer composites, treatment of the fibres has influenced both mechanical and tribological behaviours of the composites. Treating the natural fibres assists the stabilisation of the bonding area between the fibre and the matrix, which enhances the ability of the fibre to carry the load under mechanical and tribological loadings.
- Natural fibre polymeric composites suffer from high friction coefficient. Graphite is suggested as a solid lubricant for such composites, which may reduce the friction coefficient of the composite and maintain high wear characteristics. In contrast, using water as a lubricant for natural fibre/polymer composite may deteriorate the composite strength.

In light of the above, the current study is motivated to fully investigate the possibility of using new natural fibres (date palm) as reinforcement for mechanical and tribological applications. The interfacial adhesion properties of the fibres were studied using a new technique (fragmentation) that considered different fibre diameters and concentrations of sodium hydroxide (NaOH) treatment. Conversely, the addition of the graphite as a solid lubricant into the epoxy composites (ECs) was studied with different weight percentage of graphite in the composites to discover the optimum graphite content in the ECs. After identifying the optimum fibre diameter, NaOH

treatment concentration and graphite content percentage, the optimum mixture of the composites was achieved. The adhesive wear performance of the composites was studied using two different tribological techniques: block on ring (BOR) and block on disk (BOD).

## **1.2 Objectives**

The main objectives of this work are to:

1. establish a comprehensive literature on natural fibres, their applications and limitations
2. study the influence of the fibre diameter and NaOH concentration in the chemical treatment on the interfacial adhesion of the date palm fibre (DPF) with epoxy matrix, using the new technique, i.e., fragmentation; this will assist in selecting the optimum NaOH concentration and fibre diameter for the composite fabrications.
3. study the fundamental mechanical properties (tensile and hardness) of the date palm ECs, which will assist in correlating the tribological and mechanical performance of the composite
4. investigate the adhesive wear and frictional behaviour of the developed composite using BOR and BOD techniques, considering different applied loads and sliding distance
5. study the influence of the addition of different graphite fillers weight percentage (wt%) into the composite on the mechanical, the frictional and the adhesive wear performance of the composite at the applicable conditions
6. develop and understand the correlation between the mechanical and tribological performance of the selected composites.

### **1.3 Project significance**

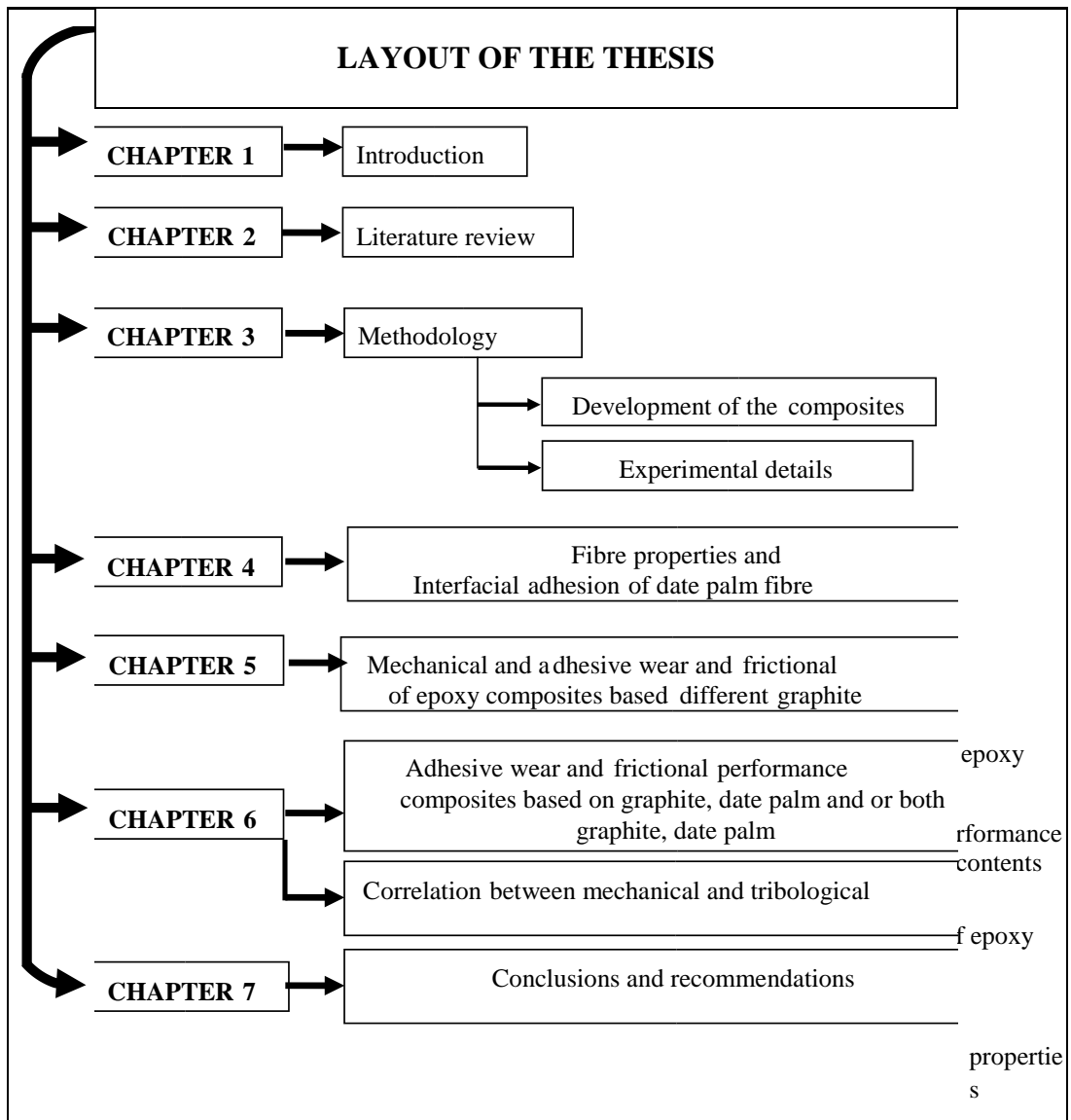
This project will affect different areas, including economic, environmental, industrial and scientific. The project's main significance includes:

- reduction of the friction coefficient of the natural fibre/polymer composites, which will set the platform for implementing the developed composites in the industries for parts exposed to tribological loading conditions, such as gears, bearings, bushes and slides.
- determination of the NaOH concentration in chemical treatment procedures, which will enhance the interfacial adhesion of natural fibres and overcome common problems and limitations in using natural fibres as reinforcement in polymeric composites
- development of a correlation model between the mechanical and tribological properties of the composites, as there is much debate in the literature about this
- publication of three international articles in high standard journals. In addition, after completion of the work, two articles will be written for publication in similar quality international journals.

### **1.4 Organisation of the thesis**

The thesis contains seven chapters, as shown in the layout of Figure 1.2. Chapter One presents a brief introduction of the importance of natural fibres as a reinforcing material for polymeric composites, as well as their benefits for the environment. Chapter Two introduces the literature review on natural fibre-reinforced polymer composites and their applications. It presents the relevant background information that has been recently reported for mechanical and tribological application. The merits, limitations and arguments on the effect of natural fibres on the mechanical and tribological performance of polymeric composites under various loading conditions are presented. Chapter Three describes the methodology covering the material selection and manufacturing processes, as well as the experimental procedure of the mechanical, fragmentation and tribological testing procedures. Chapter Four covers

influence of the fibre diameter and NaOH concentration on the mechanical properties of the fibre and the interfacial adhesion of the fibre with the matrix. In Chapter Five, the results and findings of the tests conducted on different ECs based on different weight percentage of graphite are discussed from mechanical and tribological perspectives to gain the optimum weight fraction of graphite. Chapter Six focuses on the mechanical and adhesive wear performance of the ECs, based on DPFs and/or three weight per cent graphite. Chapter Seven concludes with the findings of this thesis and provides recommendations for future work.



**Figure 1.2: Layout of the thesis**

## **Chapter 2: Literature review**

### **2.1 Mechanical properties of natural fibres/polymer composites**

#### **2.1.1 Influence of natural fibres on mechanical behaviour of polymeric composites**

From a mechanical perspective, natural fibres may enhance the mechanical properties of polymers, with some considerations and improvements to the surface characteristics of natural fibre. There are several factors related to natural fibres that influence the performance of the composites, including the interfacial adhesion, orientation, strength and physical properties. The mechanical efficiency of the fibre-reinforced polymer composites depends on the fibre-matrix interface and the ability to transfer stress from the matrix to fibre, as reported by many researchers (Fu and Lauke, 1996, Tungjitpornkull and Sombatsompop, 2009, Duval et al., 2011, Rouison et al., 2006, Beg and Pickering, 2008, Joseph et al., 1999, Alawar et al., 2009b, Hepworth et al., 2000, Rokbi et al., 2011, Rosa et al., 2009, Venkateshwaran et al., 2012, Yang and Luo, 2011).

Moisture absorption, impurities, orientation, Vf and physical properties of natural fibres play a constitutive role in determining the mechanical properties of fibre polymer composites. Figure 2.1 shows the effect of reinforcing polymers with different types of natural fibres on the mechanical properties of polymers. In most cases, natural fibre-reinforced polymer composites exhibit better mechanical properties than the pure matrix. In other words, using natural fibres as reinforcement for polymeric composites introduces positive effects on the mechanical behaviour of polymers.

Addition of jute fibres (Plackett et al., 2003) to polylactic acid (PLA) showed 75.8% enhancement to the tensile strength (TS) of PLA, while flax fibres exhibited a negative effect, with a decrease in the TS of composite by 16%. Conversely, kenaf

(Caulfield et al., 1999), hemp (Wambua et al., 2003) and cotton (Kim et al., 2008) improved the TS of polypropylene (PP) composites. TS of epoxy improved with the addition of jute fibres (H. Wells, 1980), but the jute fibres weakened the compressive strength. Meanwhile, jute enhanced all the mechanical properties of polyester composites (H. Wells, 1980). Jute/polyester composites have showed the maximum improvement in TS by 121%, compared to pure polyester.

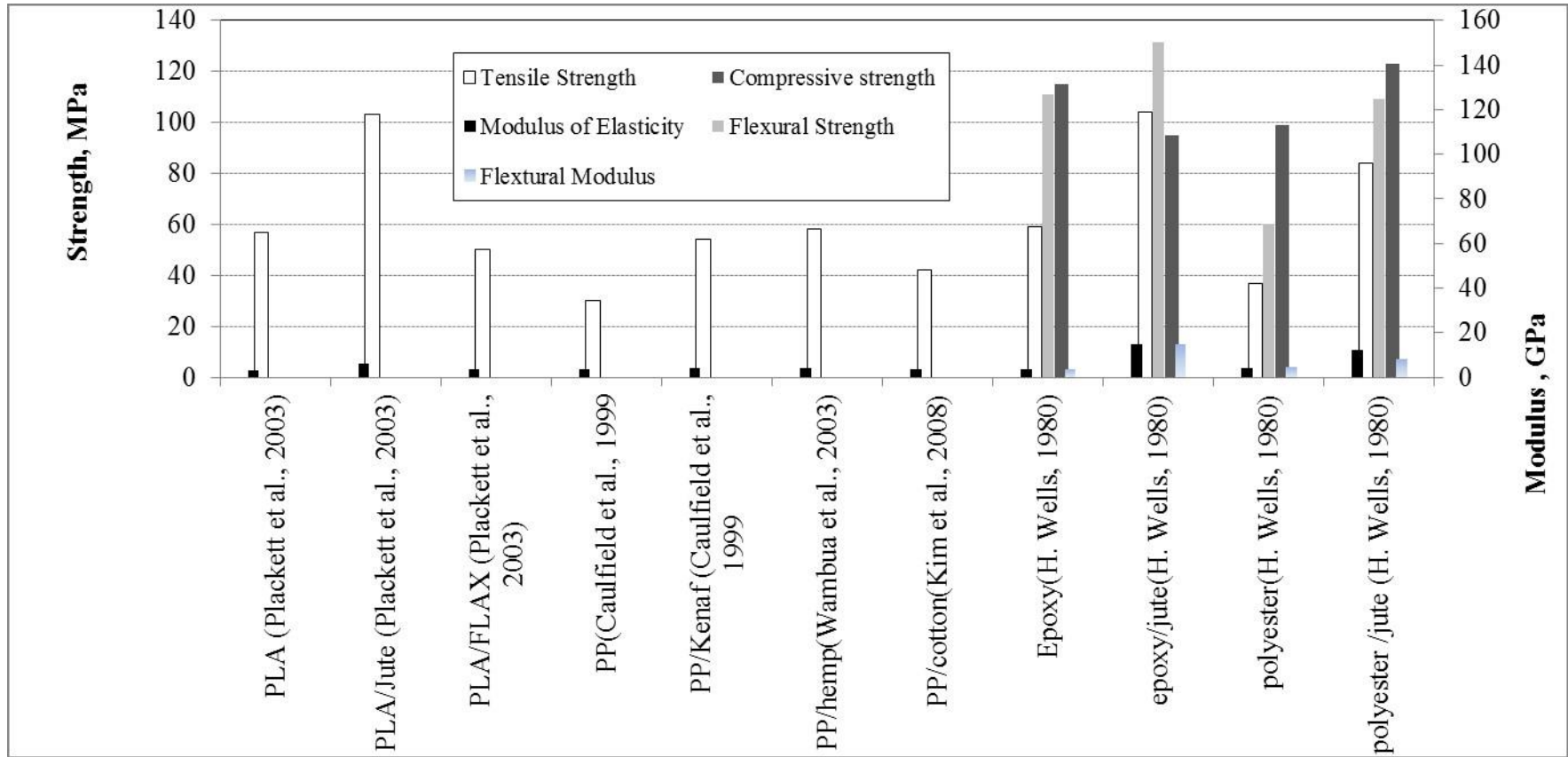


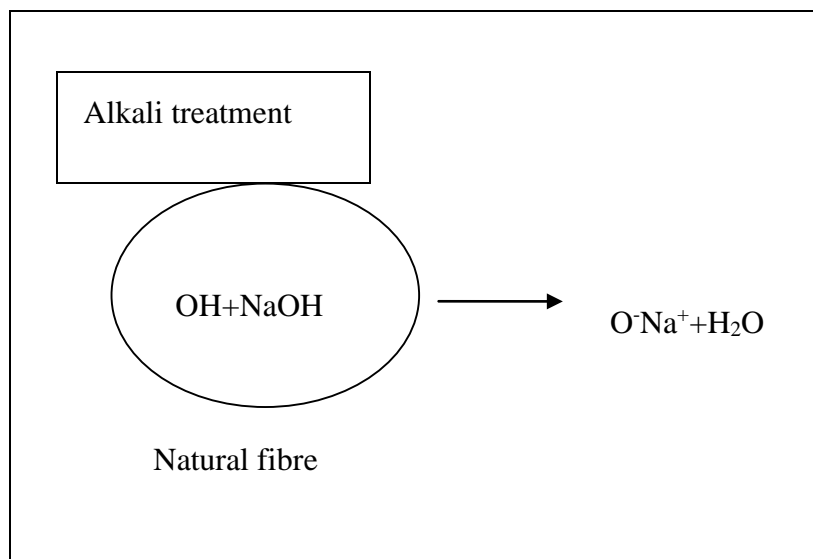
Figure 2.1: Some mechanical properties of natural fibre/polymer composites



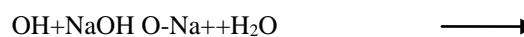


### 2.1.2 Interfacial adhesion of natural fibres

Mechanical properties of polymeric composites based on natural fibres strongly depend on the interface adhesion between the fibres and the polymer matrix (Haque et al., 2009, Rosa et al., 2009, Torres and Cubillas, 2005, Chin and Yousif, 2009, Yousif et al., 2010b). This is mainly because natural fibres are rich in cellulose, hemicelluloses, pectins and lignin, which are hydroxyl groups. Natural fibres tend to be strong polar and hydrophilic materials, while polymers exhibit significant hydrophobicity. In other words, there are significant compatibility problems between the fibre and the matrix, which weakens the interface area between natural fibres and matrices. However, many investigators reported that chemical treatments, such as bleaching, acetylation and alkali treatment may improve the matrix-fibre interfacial adhesion (Alawar et al., 2009b, Cantero et al., 2003, Haque et al., 2009, Saha et al., 2010, Hepworth et al., 2000, Yousif and El-Tayeb, 2009, Yousif and El-Tayeb, 2008a). These chemical treatments clean the surface of fibres from impurities, which in turn increases the roughness of the fibre surface and disrupts the moisture absorption process through removing the coat of hydroxide groups in fibre (see Figure 2.2).



Alkali treatment reaction:



### Figure 2.2: Scheme of reaction of fibre surface with NaOH treatment

Several works have attempted to study the influence of the type and concentration of chemical solution on fibre characteristics and their interfacial adhesion with various matrices. For example, Alawar et al. (2009a) investigated the effects of two kinds of chemical treatments in different concentrations (NaOH 0.5–5% and HCL 0.3–1.6 N) on surface morphology and the mechanical properties of DPF. The results revealed that NaOH enhances surface morphology of fibre and increases the number of pores on the fibre surface with an increase of the concentration. This could be due to increases in the harshness of reactions of NaOH on fibre when the soda concentration is increased. In addition, the TS and Young's modulus of the fibre have improved, compared with untreated fibre at low concentrations of alkali treatment. The optimum alkali concentration was at one per cent, where the TS enhanced by 300%, compared with untreated fibre. At high NaOH concentrations, the solution attacked the main construction components of the fibres, which weakened the fibre strength. Conversely, HCL treatment caused deterioration in the tensile and huge distortions on natural fibre surfaces; these were observed as a result of acid attack. Similar findings of HCL effects have been reported on bamboo fibres (Nguyen Tri Phuong et al., 2010).

With regard to the chemical treatment technique and conditions, Saha et al. (2010) studied the influence of alkali treatment (NaOH) on the TS of jute fibres under ambient temperatures and elevated temperatures at high pressure steaming conditions. The use of NaOH under all conditions had resulted in a rougher surface and better separation and removing of impurities, non-cellulosic materials, inorganic substance and wax. The range representing O–H stretching of hydrogen bond became less intense upon alkali treatment compared to untreated fibres. The TS and elongation at fibre breakage were improved by 65% and 38%, respectively, at elevated temperature and high-pressure steam conditions.

Many studies have used single fibre fragmentation tests (SFFT) to evaluate the interfacial shear ( $\sigma$ ) of natural fibre with matrix (Awal et al., 2011, Torres and

Cubillas, 2005, Valadez-Gonzalez et al., 1999b, Sawpan et al., 2011, Pihtili, 2009, Park et al., 2006, Yousif et al., 2006, Nirmal et al., 2010, Yousif et al., 2010b). As an example of this method, the interfacial shear of untreated and pre-treated sisal fibres (with stearic acid) with polyester matrix was studied by Torres and Cubillas (2005). The treatment of fibres had improved so that  $\sigma$  increased by about 23%, with respect to untreated fibre. This is due to size reduction and number of fibre clumps and agglomerates during standard processing operations, which enhances bonding between the fibre and the matrix. This has been observed on fractographs of the samples after testing, where untreated fibre showed large fibre pull out compared to treated fibre.

For the composites based on natural fibres, Figure 2.3 displays the influence of NaOH and saline treatment of natural fibres on the TS of bamboo/ PLA (Pickering et al., 2008), ramie/PLA (Yu et al., 2010), bamboo/PP (Pickering et al., 2008) and henequen/HDPE (Valadez-Gonzalez et al., 1999a) composites. It can be seen that the treated fibre/polymer composite showed better TS compared to the untreated fibre/polymer composite. Moreover, the TS of untreated bamboo/PLA composites is lower than the neat PLA by 30%, while the treated bamboo/PLA composite exhibited higher TS and modulus by about 10% and four per cent, respectively, compared to the neat PLA. The effects of NaOH or saline treatment on the TS of bamboo/PP and henequen/HDPE are similar to the bamboo/PLA composite results. Conversely, treated bamboo/PLA and ramie/PLA with NaOH is more efficient than saline treatment.

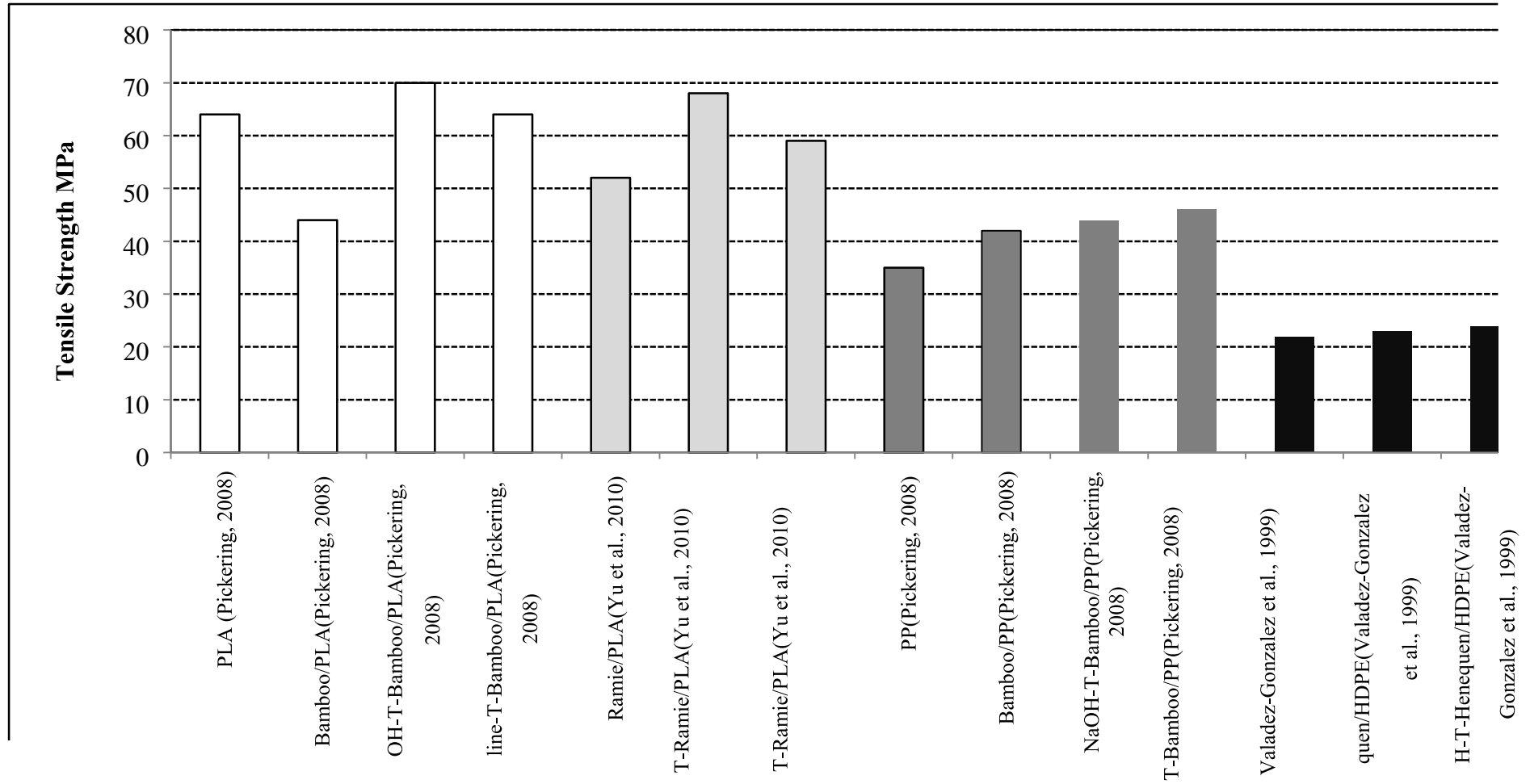


Figure 2.3: Tensile strength of polymeric composites based on natural fibres with/without treatment



### **2.1.3 Effect of fibre orientation on mechanical properties**

In fibre polymeric composites, the composite shape and surface appearance were defined by the matrix, while fibres acted as carriers of load and stress (stiffness and strength) under loading conditions. Therefore, the orientation of natural fibres will have significant effects, playing an important role in controlling the mechanical properties of the composites. It has been reported that Young modulus (E), Poisson ratio ( $\nu$ ) and TS of the alfa/polyester composites decreased with the increase of the fibre's orientation (0°, 10°, 30°, 45° and 90°), with respect to the direction of the applied load as reported by Zhang et al. (2008a). The reduction percentages of TS with respect to the change of fibre angles were 78% and 88%, when the fibres were oriented in 45° and 90° (transverse direction), respectively. At the transverse direction, the mechanical properties of fibre/polymer composites are controlled by the matrix rather than the fibres and vice versa. On the same level, all reported works on the natural fibre/polymer composites reached the same conclusion, for example, sisal/oil palm/natural rubber as described by Jacob et al. (2004) and others (Fu and Lauke, 1996, Herrera-Franco and Valadez-González, 2004, Jacob et al., 2004, Tungjitpornkull and Sombatsompop, 2009). However, this could not be correct in the case of other loadings. For instance, under tribological loading, orientation of the fibres exhibited different influences on the tribological performance of the composite. This will be clarified in the tribology section.

### **2.1.4 Effect of volume fraction**

Volume fraction (%) can be defined as fibre volume ratio to the total volume of the fibre composite times 100. In theoretical models, the increase of high strength fibre Vf leads to high tensile properties of fibre polymer composite, for instance, the proportional relation (Ku et al., 2011, Shibata et al., 2005, Venkateshwaran et al., 2012). However, from an experimental perspective, the increase of Vf over specific value always deteriorates the mechanical properties. Several studies have been conducted to find the optimum value of the natural fibre Vf in composites to gain

optimum mechanical properties. Some research on the optimum Vf of natural fibres in some polymeric composites are summarised in Table 2.1. It seems that there is no universal value of Vf of natural fibres in which optimum TS can be achieved. For example, each type of fibre has an optimum Vf, exhibiting good TS. This can be related to the nature of natural fibres and their characteristics in terms of strength, interfacial adhesion and physical property. Moreover, those reported works agreed that, at a high Vf  $\gg$  50%, the fibres tend to aggregate in the composite, which weakens the interfacial area and debonding between the fibres and matrix (Zhang et al., 2008a, Haque et al., 2009, Jacob et al., 2004, Ku et al., 2011, Lei et al., 2006, Shibata et al., 2005, Venkateshwaran et al.).

**Table 2.1: Comparisons between various existing fibre-reinforced composites**

Materials	Optimum TS at Vf (%)
Sisal-oil palm/natural rubber (Jacob et al., 2004)	$\approx$ 30
Coir/PP (Haque et al., 2009)	$\approx$ 15
Palm/PP(Haque et al., 2009)	$\approx$ 15
Hemp/PP (Hargitai et al., 2008)	$\approx$ 40–50
Flax/HDPE (Ku et al., 2011)	$\approx$ 20
Rice/HDPE (Venkateshwaran et al.)	$\approx$ 5–10
Kenaf/PP (Lee et al., 2009)	$\approx$ 40
Jute/PP (Lee et al., 2009)	$\approx$ 40
Hemp/PLA (Hu and Lim, 2007)	$\approx$ 35
Jute/PBS (Liu et al., 2009)	$\approx$ 20
Alfa/polyester (Zhang et al., 2008a)	$\approx$ 44
Sisal/rubber (Jacob et al., 2004)	$\approx$ 30
Oil palm/rubber (Jacob et al., 2004)	$\approx$ 30
Kenaf/ corn-starch (Shibata et al., 2005)	$\approx$ 50
Bagasse corn-starch (Shibata et al., 2005)	$\approx$ 50



Ramie cloth/polyester (Lei et al., 2006)	≈30
--	-----

### 2.1.5 Effect of fibre physical properties

The individual increases in length or decreases in diameter of natural fibres has positive effects on the mechanical properties of the polymer composite (Athijayamani et al., 2009, Aziz and Ansell, 2004, Beg and Pickering, 2008, Joseph et al., 1999, Liu et al., 2007, Mylsamy and Rajendran, 2011, Shibata et al., 2005, Andersons et al., 2005, Duval et al., 2011, Park et al., 2006, Rouison et al., 2006, Umer et al., 2011). A more than critical decrease of fibre length reduces the stress transfer efficiency between the matrix and the fibre. Moreover, maintaining the optimum Vf of fibres with short fibres increases the number of fibre ends that act as crack initiators, deteriorating the mechanical properties of composites.

Liu et al. (2007) found that the critical fibre length for kenaf/soy composite is six millimetres. Mylsamy and Rajendran (2011) found the optimum fibre length for agave/ECs is three millimetres. This difference in critical length is mainly due to the differences in the interfacial adhesion of the fibre with the matrix that, in turn, controls the shear between the fibre and the matrix. Conversely, small natural fibre diameters have a positive effect on the mechanical properties of fibre/polymeric composites. The explanation is that this behaviour ambushes the fibre structure, increasing the probability of defects in the fibre. Natural fibres are bundles of fine fibres called microfibrils; the strength keeping these microfibrils together is much lower than their TS. With the diameter of large fibres, the number of microfibrils increases in the fibre, which increases the probability of inter-cell failure and lower overall mechanical properties (Andersons et al., 2005, Duval et al., 2011, Park et al., 2006, Rouison et al., 2006, Umer et al., 2011).

## **2.2 Tribological performance of polymeric composites based on natural fibres**

### **2.2.1 Influence of natural fibres on tribological behaviour of polymeric composites**

Most industrial and manufacturing parts are exposed to tribological loadings, such as adhesive and abrasive, in their service. Therefore, tribological performance of materials is an essential consideration in the design of mechanical parts. In other words, understanding the tribological behaviour of natural fibre/polymer composites deserves equal consideration with the mechanical properties of those materials (Yousif et al., 2010a). Nevertheless, there is less literature on the effects of natural fibres on the tribo-performance of polymeric composites.

Some studies have emphasised that the tribology behaviour of composite polymers based on natural fibre is not intrinsic behaviour, arguing instead that it depends greatly on many processing parameters, including operating parameters, characteristics of polymer material, physical and interfacial adhesion properties of fibre, additives and contact condition. A few researchers have investigated the tribological behaviour of polymeric composites based on natural fibres, such as: kenaf (Chin and Yousif, 2009), oil palm (Yousif and El-Tayeb, 2008a), sisal (Chand and Dwivedi, 2008), cotton (Hashmi et al., 2007a), jute (Chand and Dwivedi, 2006), betelnut (Yousif et al., 2010a), bamboo (Nirmal et al., 2012b). From those reported works, there are a few issues that can be addressed, which are:

- Operating parameters influence the wear and frictional behaviour of the majority of polymer composites.
- Reinforcing the polymer with natural fibres may enhance the wear performance of the composite. However, it is not true for all composites. Therefore, further investigation is required.
- Chemical treatment of the natural fibres enhances the interaction between the fibres and the matrix at the interface. However, the type and the concentration of the chemical treatments will vary from type to type.

- Addition of solid lubricants controls the shear resistance in the interface zone. This could either enhance friction or wear behaviour or enhance the friction and worsen the wear. Optimisation is recommended.

Polymers have displayed different tribology behaviours with different types of natural fibres. Table 2.2 lists the most recent literature on the tribological performance of natural fibre/polymer composites associated with glass/polyester composites for comparison purposes. Further, the specific wear rate and fractional trends against sliding distance are given in the table. In general, one can say that a steady state can be achieved after a certain sliding distance. However, in the running period (first stage of the sliding), there is difference in the wear behaviour of the composites. In some cases, such as polyester (Yousif, 2009), chopped glass/polyester (Yousif and El-Tayeb, 2007b), cotton/polyester (Chand and Dwivedi, 2008) and kenaf/epoxy (Chin and Yousif, 2009), the composite showed low specific wear rate and an increase in the steady state stage, which is due to the adaption period of the two rubbed surfaces in the running in stage.

Moreover, in those works, it has been reported that the film generated on the counterface became smoother at the steady state than the running in stage. However, in coir/polyester (Yousif, 2009), sisal/polyester (Chand and Dwivedi, 2008), betelnut/polyester (Yousif et al., 2010a) and bamboo/ epoxy (Nirmal et al., 2012b), the opposite occurred, that is, high specific wear rate at the first stage and then reduced at the steady state because of the smoothening process occurring on both rubbed surfaces. This result argues that the characteristic of generated film on the counterface is the main factor in determining the wear behaviour of the composite.

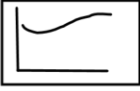


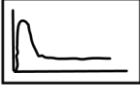
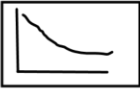

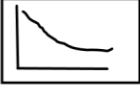

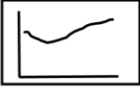

For the frictional behaviour of those composites, there are four categories of frictional trends. There is an increase in the friction coefficient at the running in stage, followed by the steady state (Umer et al., 2011, Chand and Dwivedi, 2008, Nirmal et al., 2012b). This indicates the stability of rubbed surface characteristics. In Yousif and El-Tayeb (Yousif and El-Tayeb, 2008c, Nirmal et al., 2012b, Yousif,


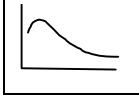
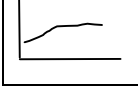
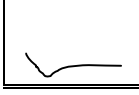
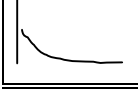
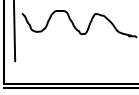
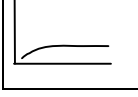
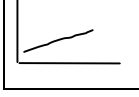
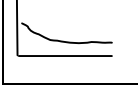
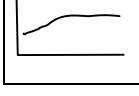
2009), there is a reduction in the friction coefficient in the steady stage compared to the running in stage. This is due to the smooth film transfer generated on the counterface and its high stability. Conversely, Chin and Yousif (Chin and Yousif, 2009, Yousif et al., 2010a, Yousif and El-Tayeb, 2008c, Chand and Dwivedi, 2006) showed fluctuation and increases in the friction coefficient value, which represent the instability of rubbed surface characteristics and modifications taking place during the sliding process.

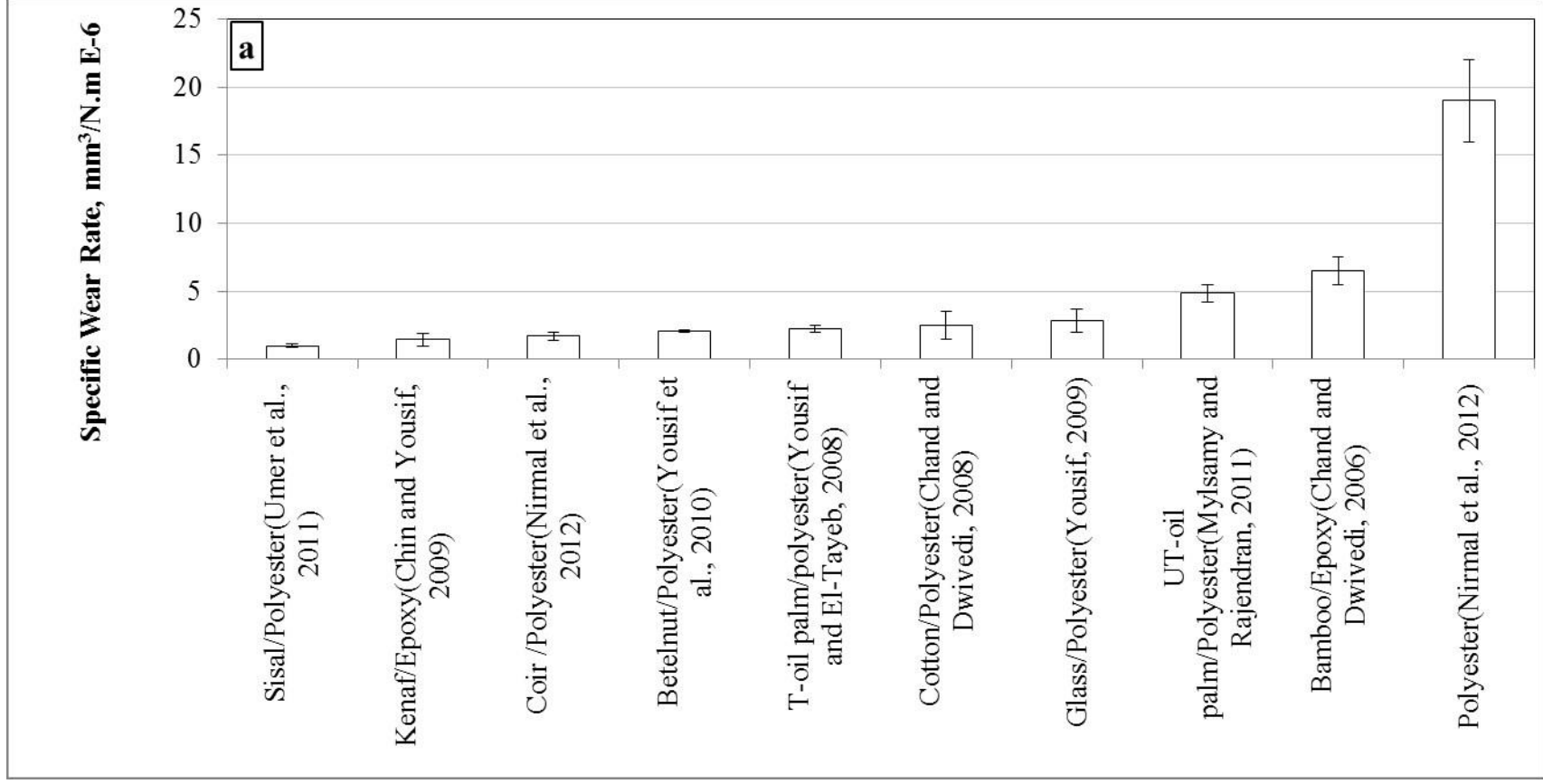
The data in Table 2.2 are extracted and represented in Figure 2.4 for comparison purposes. Figure 2.4 shows the specific wear rate (a) and friction coefficient (b) of the polymeric composite based on natural fibres. In designing components subjected to tribological loading, it is desirable to have low specific wear rates and either a high or low friction coefficient.

From Figure 2.4, it seems that there is no correlation between the wear and frictional behaviour of the composites. For example, sisal/polyester (Chand and Dwivedi, 2008) exhibited low specific wear rates and a relatively high friction coefficient. In another example (Chand and Dwivedi, 2008), cotton/polyester composites showed very high friction coefficients with a low specific wear rate. In bearing applications, a low friction coefficient with low specific wear rate is desirable. Therefore, the friction coefficient of natural fibre/polymer composite should be reduced with the addition of solid lubricants or use of the designed components in lubricant conditions. However, these actions may affect other characteristics, such as composite strength, physical properties and degradation ability. Further investigation is required.

**Table 2.2: Adhesive wear and coefficient friction result of neat polymers and natural fibre composites under dry contact**

<b>Materials/ operating parameters and conditions</b>	<b>Specific wear rate (Ws), mm<sup>3</sup>/N.m x10<sup>-5</sup></b>	<b>Friction coefficient</b>
Polyester (Yousif, 2009) Against stainless steel; 30-90 N applied load; Anti-Parallel orientation.	 $W_s = 16-22$ At 2.8m/s	 $\mu = 0.9-0.95$ At 2.8m/s
Chopped glass /Polyester (Yousif and El-Tayeb, 2007b) Against stainless steel; 50 N applied load; Anti-Parallel orientation.	 $W_s = 2-3.7$ At 3.9m/s	 $\mu = 0.23-0.7$ At 3.9m/s
Coir /Polyester (Yousif, 2009) Against stainless steel; 50 N applied load; Normal orientation.	 $W_s = 1.4-2.0$ At 2.8m/s	 $\mu = 0.57-0.8$ At 2.8m/s
Sisal/Polyester (Chand and Dwivedi, 2008) Against stainless steel; 100 N applied load; Randomly oriented fibres	 $W_s = 0.84-1.12$ At 1.75m/s	 $\mu = 0.6-0.65$ At 1.75m/s
Cotton/Polyester (Hashmi et al., 2007a) Against stainless steel; 20 N -80 N applied load; Randomly oriented fibres	 $W_s = 1.5-3.5$ At 2.22 m/s	 $\mu > 1$ At 2.22 m/s

<p>Untreated oil palm/Polyester (Yousif and El-Tayeb, 2008a)</p> <p>Against stainless steel; 50 N applied load; Randomly oriented fibres</p>	 <p>5.5</p> <p><math>W_s = 4.2-</math> <math>At 2.8m/s</math></p>	 <p>5.5</p> <p><math>\mu = 0.2-0.</math> <math>At 2.8 m/s</math></p>
<p>Treated oil palm/polyester (Yousif and El-Tayeb, 2008a)</p> <p>Against stainless steel; 20 N -80 N applied load; Randomly oriented fibres</p>	 <p>5</p> <p><math>W_s = 2-2.</math> <math>At 2.8m/s</math></p>	 <p><math>\mu = 0.45-0</math> <math>.57</math> <math>At 2.8 m/s</math></p>
<p>Betelnut/Polyester (Yousif et al., 2010a)</p> <p>Against stainless steel; 30 N -100 N applied load; Anti-Parallel Orientation.</p>	 <p><math>W_s = 2-2.2</math> <math>At 2.8 m/s</math></p>	 <p>5.5</p> <p><math>\mu = 0.22-0</math> <math>At 2.8m/s</math></p>
<p>Kenaf/Epoxy (Chin and Yousif, 2009)</p> <p>Against stainless steel; 30 N -90 N applied load; Normal Orientation.</p>	 <p><math>W_s = 1-1.9</math> <math>At 2.8 m/s</math></p>	 <p>4.2</p> <p><math>\mu = 0.36-0.</math> <math>At 2.8m/s</math></p>
<p>Bamboo/Epoxy (Nirmal et al., 2012b)</p> <p>Against stainless steel; 30 N -90 N applied load; Randomly oriented fibres</p>	 <p>7.5</p> <p><math>W_s = 5.5-</math> <math>At 2.8m/s</math></p>	 <p>6.4</p> <p><math>\mu = 0.57-</math> <math>At 2.8m/s</math></p>



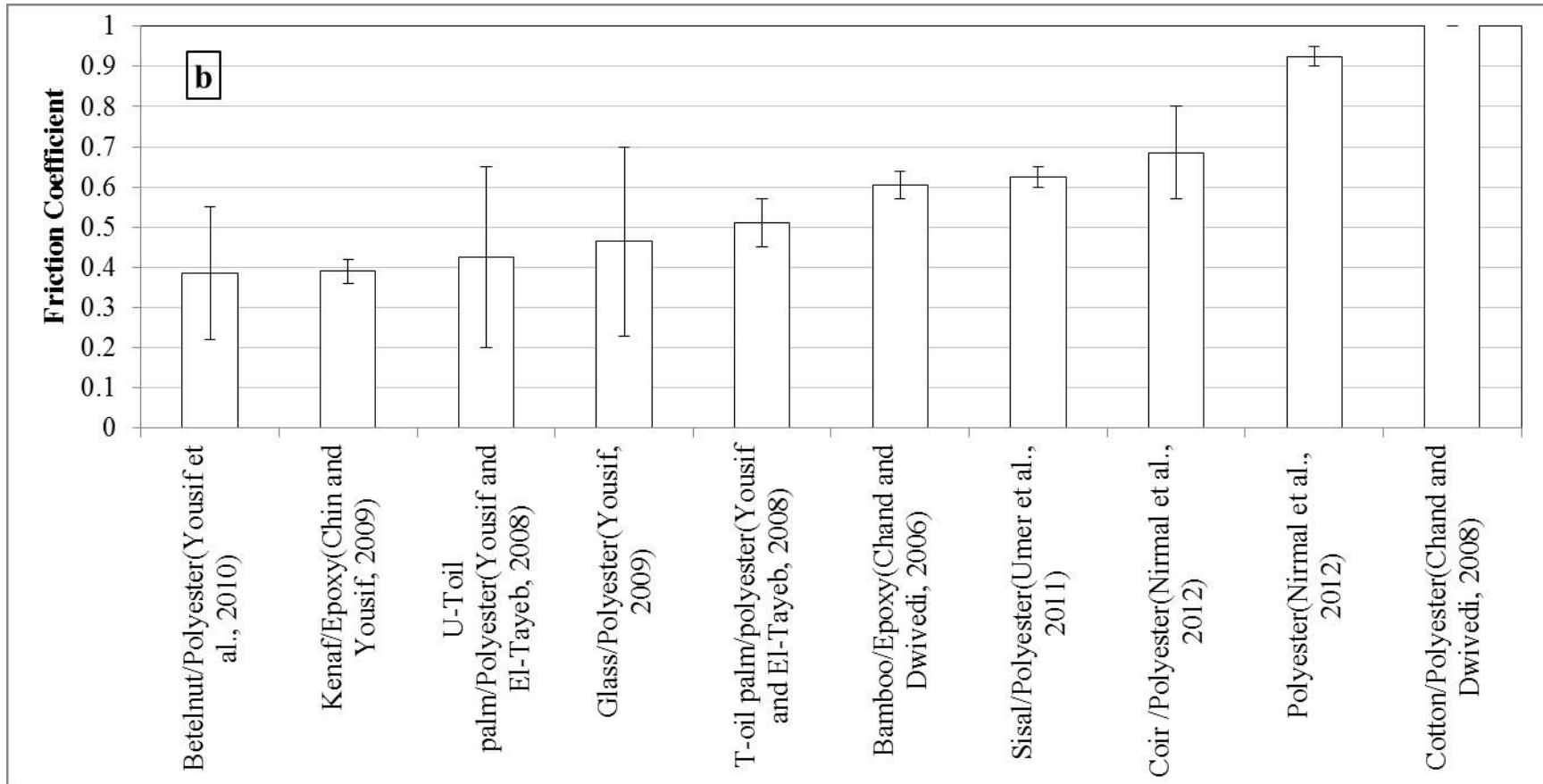


Figure 2. 4: Specific wear rate and friction coefficient of some polymeric composites under dry contact conditions





### 2.2.2 Effect of treatments

The interfacial adhesion of fibre with the matrix plays a substantial role in controlling the tribological properties of polymeric composites based on natural fibres (Chin and Yousif, 2009, Shinji, 2008, Yousif and El-Tayeb, 2008a). It is well known that natural fibres lack good interfacial adhesion with polymers. Chemical treatment of fibre is one common and useful technique used to enhance the interfacial adhesion between the natural fibres and the synthetic matrices. This treatment showed good results from a mechanical perspective, as mentioned previously.

With regard to the effect of chemical treatment on natural fibres as reinforcement and the tribological behaviour of polymeric composites, a few studies have looked at kenaf, oil palm, betelnut and sisal (Yousif and El-Tayeb, 2008a, Nirmal et al., 2010, Chand and Dwivedi, 2008, Chin and Yousif, 2009). These studies emphasise that a stronger interfacial adhesion between the fibres and matrix offers better tribological performance. Yousif and El-Tayeb (2008a) have investigated alkali treatment consequence (six per cent NaOH) on the tribological performance of treated and untreated oil palm fibre-reinforced polyester (T-OPRP and UT-OPRP) composites, using BOR technique (2008a). T-OPRP and UT-OPRP composites were experienced at different sliding distances (0.85 to 5 km), sliding velocities (1.7–3.9 m/s) and applied loads (30–100 N) under dry contact conditions. In general, the presence of either untreated or treated oil palm fibres in the polyester matrix promoted wear and friction performance by about 40–80% and 40–70%, respectively. Neat polyester showed poor results due to rapid polyester debris worn away from the interface, especially at the longer sliding distances, high-applied load and sliding velocity. TOPRP showed less specific wear rate by about 11% compared to UT-OPRP due to the enhancement of the adhesion characteristic between the oil palm fibres and the polyester matrix. Moreover, the scanning electron microscopy (SEM) observation on UT-OPRP worn surface showed debonding and bending of fibres and fragmentation and deformation on the resinous regions. Meanwhile, T-OPRP composite showed less damage compared to UT-OPRP, where no sign of fibres debonding was observed. The friction coefficient of T-OPRP composite seems to be steady, compared to UT-OPRP,

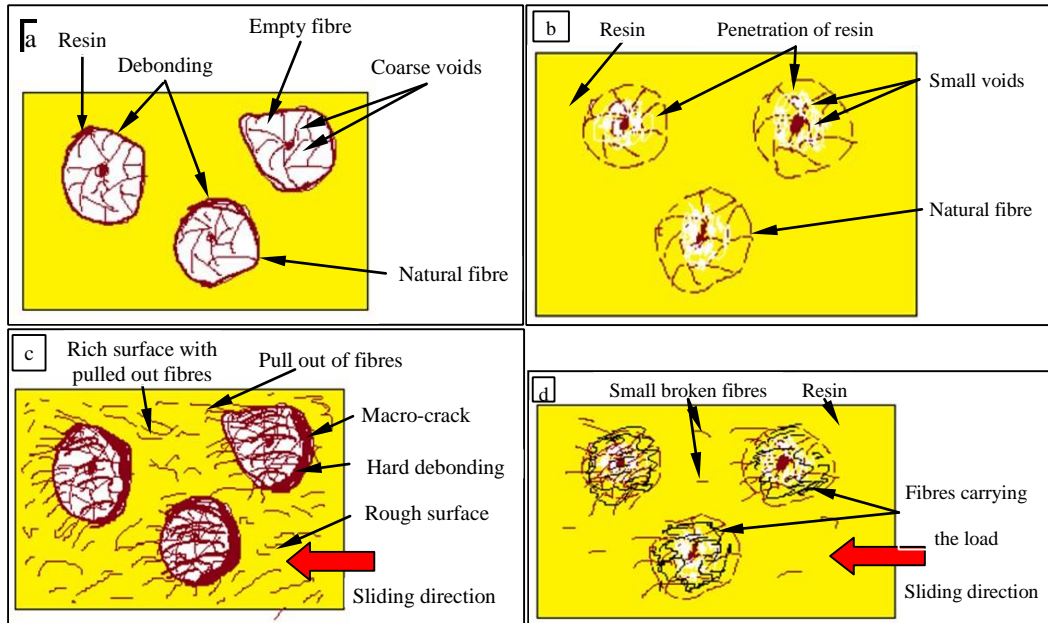
which showed fluctuating behaviour. This was due to modifications occurring on the counterface surface during the rubbing process (i.e., unstable behaviour).

The wear behaviour of untreated and treated betelnut fibres reinforced in polyester (BFRP) composites have been studied at the same conditions (applied load = 30 N, sliding velocity = 2.8m/s and under dry contact conditions) (2009). The comparison revealed that significant enhancement of wear performance occurred when the betelnut fibres were treated with six per cent NaOH. In general, the specific wear rate was in the order of 10 to eight for the treated betelnut fibres and 10 to five for the untreated betelnut fibres. This is due to the high interfacial adhesion of betelnut fibres with the polyester matrix preventing fibre pull out during the sliding (i.e., low removal of material).

Chand et al. (2008) studied the effect of chemical treatment (saline) of sisal fibres/polyester composite (SP) on the tribological behaviour of the composites. The specific wear rate of untreated-SP (UT-SP) was greater than treated-SP (T-SP). This was attributed to the poor bonding between UT-S fibre and polyester, leading to the easy detachment of the sisal fibres from the matrix during sliding. In contrast, the coefficient of material friction followed the order, pure polyester (.05) < SP (0.6–0.8) < T-SP (invalid value > 1), at an applied load of 20 N. The improvement of interfacial bonding reduces the pull out of fibre, which increases the resistance in the interface and leads to high friction coefficient.

Figure 2.5 suggests two different scenarios when the natural fibre/polymer composites slide against hard and smooth counterfaces, such as steel. In the case of untreated fibre, Figure 2.5a suggests an initial debonding of fibres that weakens the contact surface, leading to high damage on the composite surface, such as tear, breakage and fibre pull out, during sliding conditions (Figure 2.5c). This has been reported by studies on untreated natural fibre/polymer composites, such as oil palm/polyester (Yousif and El-Tayeb, 2008c) and coir/polyester (Nirmal et al., 2012b). However, in the case of treated natural fibre/polymer composite (Figure 2.5b), the possibility of fibre pull out is less because of the high interfacial adhesion property of the treated fibre compared

to the untreated fibre. In other words, the materials removal from the surface of treated fibre composite surface (Figure 2.5d) will be less than that of untreated ones (Figure 2.5c). This occurred when the kenaf/ECs was tested against a stainless steel counterface (Chin and Yousif, 2009).



**Figure 2.5: Schematic drawing showing the effect of treating the natural fibres on the wear behaviour of polymeric composites**

### 2.2.3 Operating parameters

El-Tayeb (El-Tayeb, 2008) reported that wear resistance of sugarcane fibre/polyester composites (SCRCP) increased significantly with increased loads (20–80 N). At higher loads, larger frictional heat generation resulted in a large amount of back transfer patches of polymer film, which were intermittently spread over the surface, shielding the composite surface from further damage. Chand and Dwivedi (2008) studied the effect of increasing load applied on the abrasive wear behaviour of sisal-polyester and found that the increasing applied load decreased the specific wear rate caused by the greater frictional heat, which softened the matrix on the composite surface. Chin and Yousif (2009) have found an insignificant effect of applied load (30–100 N) and

sliding velocity (1.1–3.9 m/s) on the specific wear rates of kenaf fibre-reinforced epoxy (KFRE) composite. Specific wear rates of KFRE composites exhibited a steady state after approximately 3 km sliding distance. Increases of applied load slightly increase the friction coefficient and the interface temperature. The worn surface revealed that the fibre ends are still well adhered in the matrix, with no sign of debonding or pull out at a lower applied load (50 N). While at higher applied load (70 N), the worn surface showed debonding of fibres and this was due to the high thermo-mechanical loading, which fastened the material removal from the resinous regions and weakened the interfacial area between the fibres and the matrix, but there was no sign of pull out of fibres. At higher applied loads of 100 N, micro-cracks became clear on the surface, which is due to the high side force, indicating the high wear resistance in the rubbing zone.

Yousif (2009) has investigated the effect of operation parameters, that is, applied load (10–30 N) and sliding distance (zero to 4.2 km) on the tribological behaviour of coir fibre-reinforced polyester (CFRP) composites. There is minimal difference in the friction coefficient and the interface temperature of CFRP composite at different applied load, that is, the average friction coefficient of CFRP composite at 10, 20 and 30 N was 0.61, 0.63 and 0.68, respectively. At a short range sliding distance (zero to seven kilometres), there is insignificant different in the friction of CFRP composites at all applied loads, while there is a reduction in friction coefficient of CFRP composites at longer sliding distance.

#### **2.2.4 Frictional behaviour**

In general, friction is the measure of energy that dissipates at the surface. Based on the three friction mechanisms (asperity deformation, adhesion and ploughing), quantitative treatment is proposed to determine the total friction coefficient. The behaviour of each one of these mechanisms depends on the contact surface topography, operation conditions and the type of material. Few works focused on investigating the friction behaviour of polymeric composites based on the natural fibres under dry sliding conditions (Yousif, 2009, Yousif and El-Tayeb, 2008a, Chin

and Yousif, 2009, Hashmi et al., 2007a, Chand and Dwivedi, 2008). Chin and Yousif (2009) have found that the presence of kenaf fibres in the composite reduced the frictional coefficient of epoxy from 0.75 to 0.56. It has been reported that a reduction of friction coefficient can be achieved when polyester is reinforced with coir, betelnut and oil palm fibres by about 30%, 46% and 60%, respectively (Yousif and El-Tayeb, 2008a, Yousif, 2009, Yousif et al., 2010a). This is attributed to the modification that took place on the counterface wear track and the topographical composite surfaces, that is, the role of this modification in the roughness of film transfer generation on counter face. In other words, the presence of natural fibres on the composite surface smoothed the film transfer on the counterface, which led to a decrease in the interlock between the asperities in contact, leading to low friction coefficient. However, the friction coefficient is still high for such materials to be used in tribological applications, such as bearing, sliding and bushes. Moreover, the low friction coefficient may sacrifice the wear performance of the material. The addition of cotton and sisal fibres to polyester composites significantly increased the friction coefficient by 46% and 50% compared to the neat polyester. This was due the low sensitivity of the cotton fibre to heat of friction as compared to polyester resin, which offered higher resistance to sliding movement.

It should be mentioned here that all the above works have been conducted on metal surface under adhesive wear loading condition. At those works, dry adhesive wear were performed under atmospheric temperature and humidity with applied load in range of 10 N - 100 N, sliding velocity of 1m/s - 4 m/s against a steel surface of less than 1  $\mu\text{m}$  Ra. Therefore, the current operating parameters are selected within the same range of the literature. Moreover, there are two possible solutions to overcome the high friction coefficient of the polymeric composites based on natural fibres, which are either introducing solid lubricants to the composites or operating the composites under wet contact conditions. This will be explained further in the coming sections.

## **2.3 Possible reduction of friction coefficient**

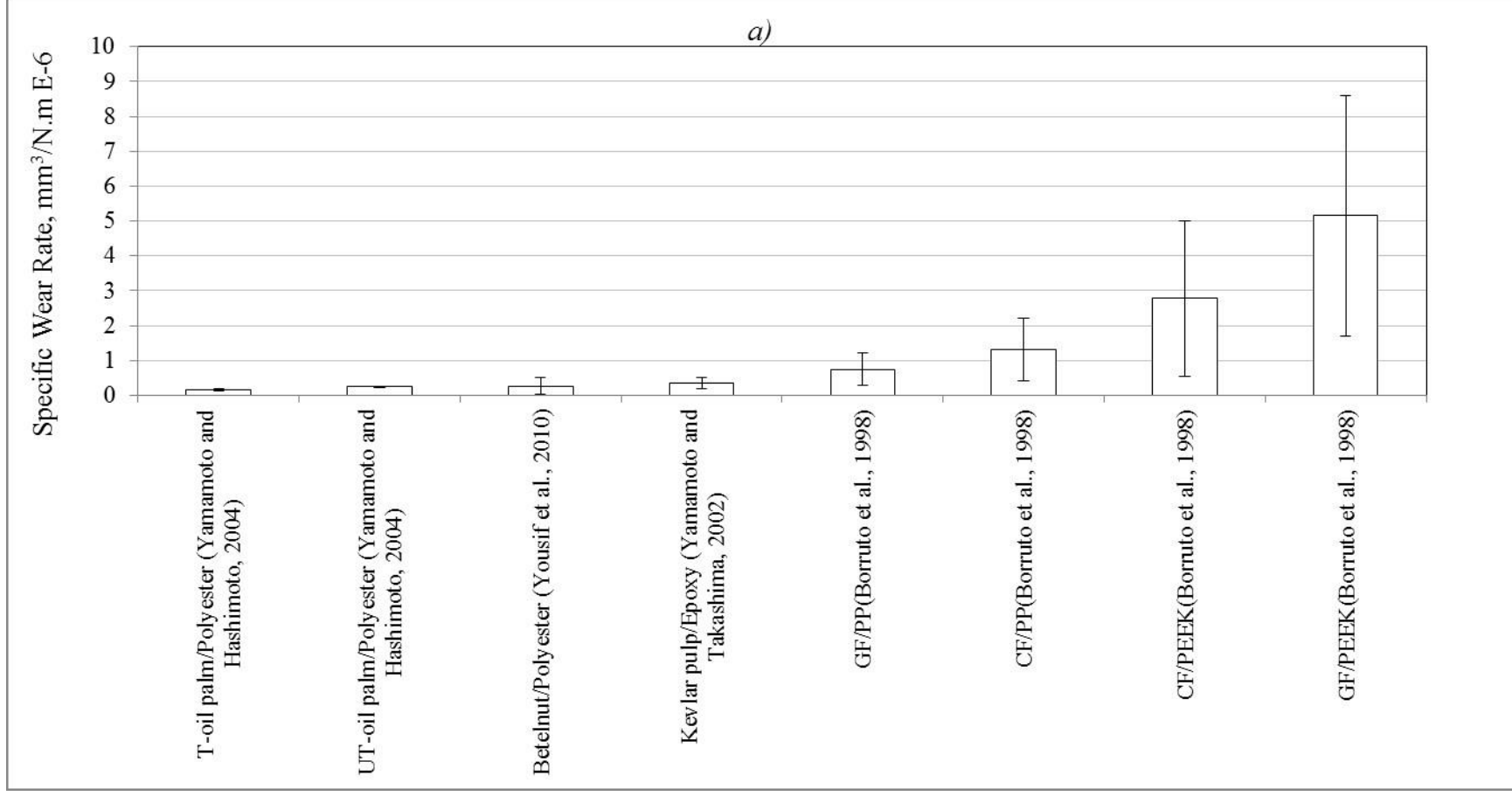
### **2.3.1 Liquid lubricants**

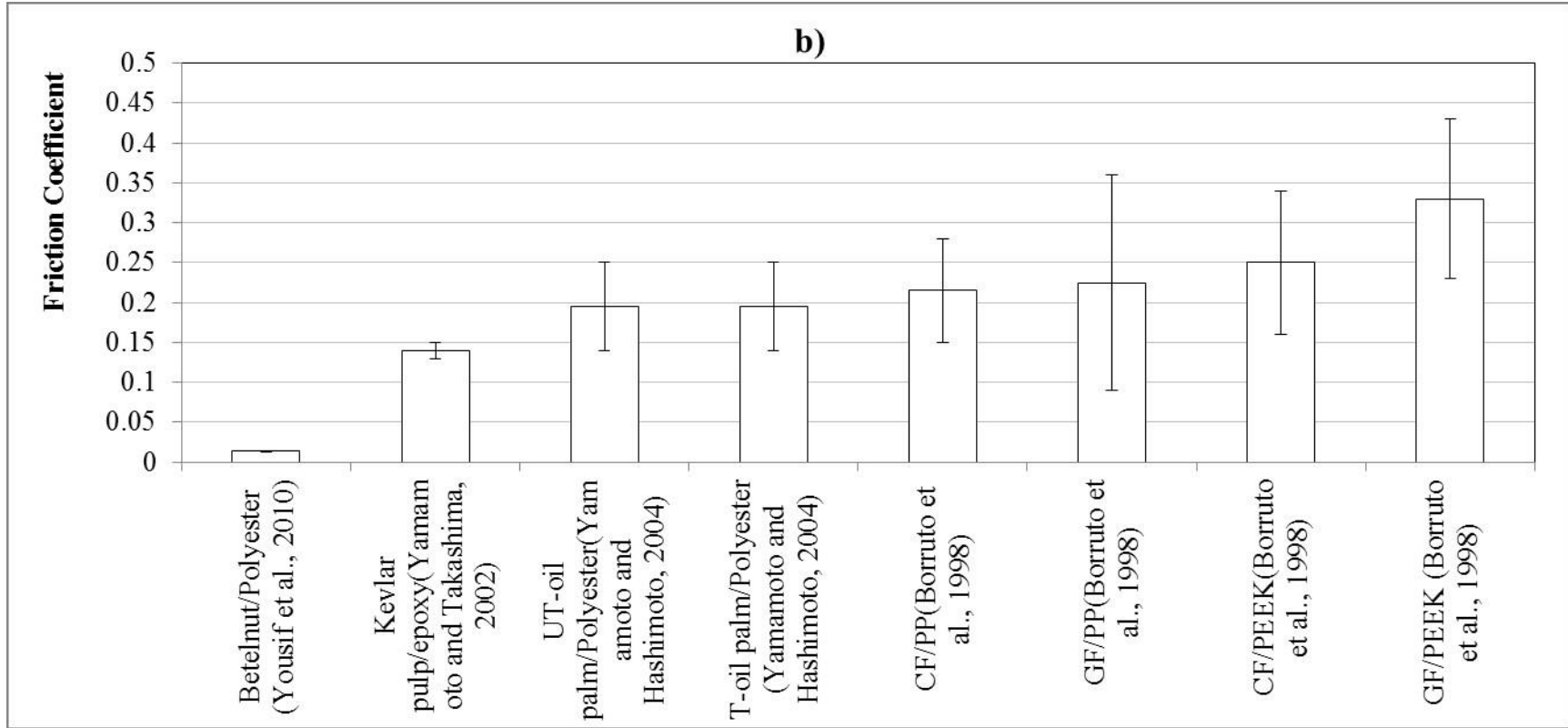
From the literature, the contact condition (wet/dry) has significant effects on the tribo-performance of polymeric composites based on synthetic fibres and/or additives. This effect could be positive or negative, as reported on different polymers. The tribological behaviour of some polymeric composites, such as PPS and PEEK were broken down under wet contact condition compared to dry because of lowering in the hardness of the surface layer of the composite (Yamamoto and Takashima, 2002). Moreover, the absence of the film transfer on the counterface led to transfer of the wear mechanism from adhesive to abrasive such that the worn debris and fibres in the interface attacked both surfaces (Wu and Cheng, 2006). However, the tribological behaviour of some polymeric composites, such as PA, UHMWPE (Borruto et al., 1998) and epoxy (Wu and Cheng, 2006) were enhanced under wet contact conditions compared to dry. This is mainly due to the water acting as a cooler and cleaner; that is, the water absorbs the heat generated by friction and removes the wear debris from the rubbing area. The friction and wear characteristics of carbon and glass/PEEK and PPS composites have been studied under wet contact conditions (Yamamoto and Hashimoto, 2004). The wear performance of the glass fibre/PEEK slightly improved the friction but exhibited poor resistance to wear. In contrast, carbon/PEEK showed good friction and wear characteristics under wet contact condition compared to dry ones. Consequently, there is an argument on the effect of the water as lubricant on the tribological behaviour of synthetic fibre/polymer composites.

With regard to the natural fibre/polymer composites, the tribological behaviour of palm fibre-reinforced polyester composites was studied under dry/wet adhesive mode (Yousif and El-Tayeb, 2008c). Under dry conditions, the untreated fibre/polyester exhibited poor wear characteristics, leading to debonding of the oil palm fibres during sliding, especially under severe conditions. The high interface temperature during dry adhesive condition led to softening of the polyester region and then pull out of fibre from the bulk to the surface. Water assisted absorption of the frictional heat, resulting in lower material removal and low friction coefficient compared to the dry contact conditions behaviour.

Recently, the adhesive wear and frictional performance of BFRP composites under dry and wet conditions at different operating parameters has been investigated (Yousif et al., 2010a). Under wet conditions, the coefficient frictional of BFRP composite was lower by about 94% than in dry conditions. This is due to reduction in the thermo-mechanical loading during the sliding (N.S.M, 2008, El-Sayed et al., 1995). Under dry contact conditions, the roughness of the generated film transfer on the counterface was significantly increased during the sliding, while, under wet contact conditions, there was no significant change in the wear track roughness. It should be considered here that the presence of water may lead to an increase in the moisture of natural fibres and considerable decrease in the mechanical properties of natural fibre (Bledzki and Gassan, 1999, Wambua et al., 2003, Dhakal et al., 2007, Chow et al., 2007). Figure 2.6 summarises the wear and friction of natural and synthetic fibre/polymer composite under wet contact conditions. Compared to the dry contact conditions, Figure 2.4 shows that presence of the water significantly reduces the specific wear rate and friction coefficient of the natural fibre/polymer composite, for example, oil palm/polyester (Yousif and El-Tayeb, 2008c, Yamamoto and Hashimoto, 2004) and betelnut/polyester (Yousif et al., 2010a). Moreover, one can notice that the natural fibre/polymer composite exhibited much better wear and frictional performance than the synthetic fibre/polymer composite. This is due to the abrasive nature of the synthetic fibres, which acts as a third body in the interface, causing severe damage on the composite surface, as reported by (Yousif and ElTayeb, 2008b).







**Figure 2.6: Specific wear rate and friction coefficient of some polymeric composites under wet contact conditions**



### 2.3.2 Solid lubricants

In polymer composites, selecting the right compositions assists in reaching special requirements for tribological applications. In other words, filling polymer composite with desired fillers and/or reinforcement is frequently employed for specific objectives. Many researchers studied the tribological behaviour of polymers containing solid lubricants, aiming to reduce the friction coefficient of the composites and maintain good wear performance. The frictional characteristics of polymers were enhanced dramatically by incorporating solid lubricants, such as graphite, molybdenum disulfide (MoS<sub>2</sub>) and poly-tetrafluoroethylene (PTFE), where fluid lubricants were undesirable and ineffective (Ben Difallah et al., 2012b, Bijwe and Indumathi, 2004, Samyn and De Baets, 2005, Zhang et al., 2008b, Cho et al., 2006, Theiler and Gradt, 2010, Xu et al., 2007, Zhang et al., 2009, Ye et al., 2009, Hashmi et al., 2007b). Figure 2.7 summarises the influence of solid lubricants on the frictional performance of polymeric composites. In general, it can be seen that the addition of the graphite to the cotton/polyester composite significantly reduced the friction coefficient of the composites (Chand and Dwivedi, 2008). PTFE showed a remarkable reduction in the friction coefficient value (<0.1) of the ECs compared to the reported friction coefficient value of neat epoxy (NE) (Chin and Yousif, 2009), kenaf/epoxy (Chin and Yousif, 2009) and MoS<sub>2</sub>/epoxy (Samyn and De Baets, 2005). PTFE could be promising fillers, which helps in enhancing the frictional performance of polymeric composites. Zhang et al. (2008b) studied the tribological properties of two solid lubricants: PTFE and graphite-filled polyphthalazinone ether sulfone ketone (PPESK) composites. The research revealed that the friction coefficient and wear rate of PPESK composites noticeably reduced by 65% compared with neat PPESK because of the lubricating transfer film formation steel counterface. However, it is known that PTFE has low support to the composite, in terms of wear performance of the composites (Yousif and El-Tayeb, 2008b, Ben Difallah et al., 2012a, Bijwe and Indumathi, 2004, Cho et al., 2006). Therefore, most of the reported works on the solid lubricant proposed the graphite as solid lubricant for polymeric composite, aiming for low friction coefficient and good wear performance.

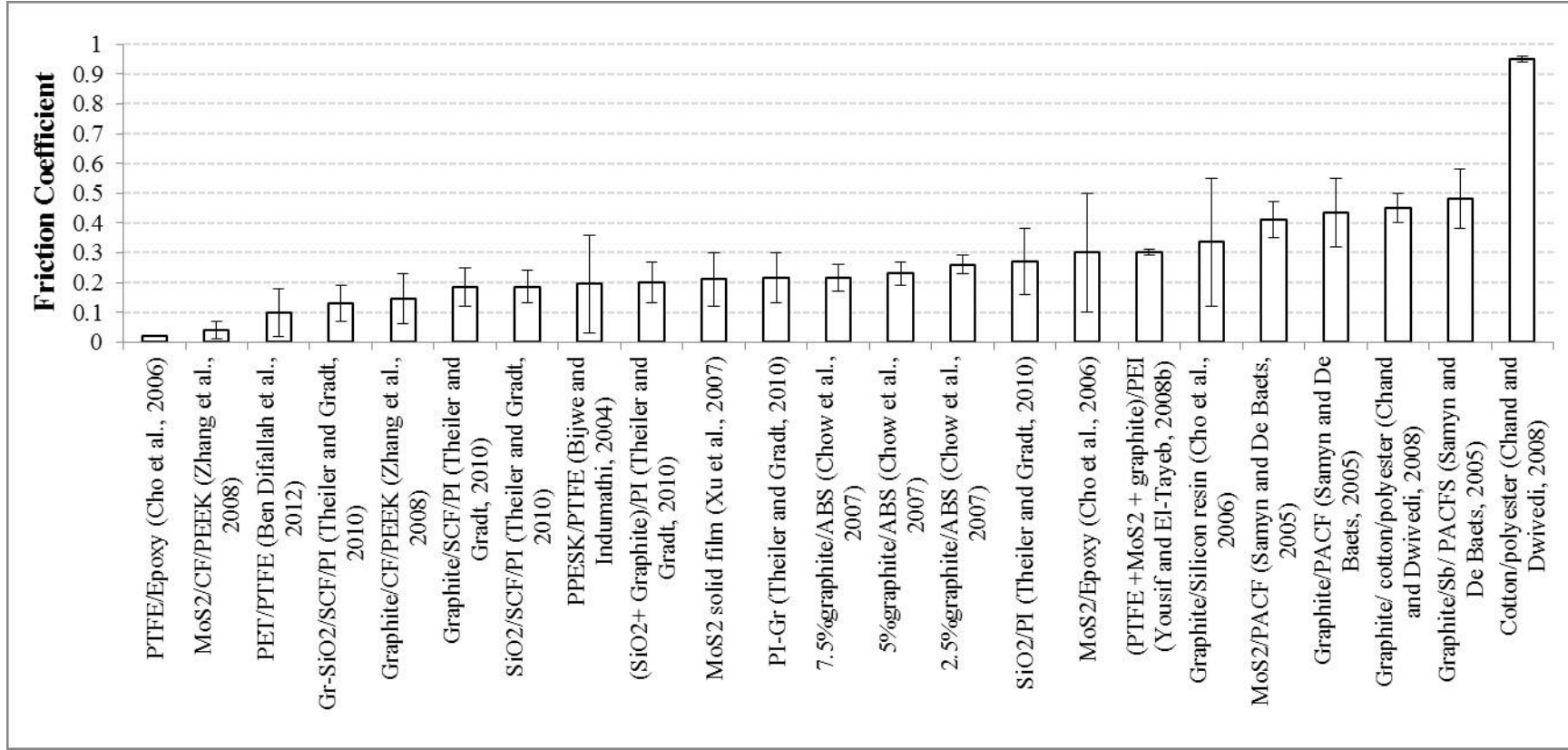


Figure 2.7: Influence of solid lubricants on the frictional behaviour of polymeric composites



Ben Difallah et al. (2012b) investigated the effects of graphite addition (zero to 7.5 wt%) on the wear resistance and friction coefficient of acrylonitrile butadiene styrene (ABS) matrix. In the study, ABS matrix exhibited lower friction coefficient and high wear resistance with the increase of the weight fraction of graphite in the polymer matrix. For example, a composite with 7.5 wt% graphite exhibited the lowest value of friction coefficient (0.18) compared to neat ABS (0.34). The reason for the low friction of polymers filling with graphite is that the transfer film contains graphite particles acting as a lubricant layer, which, in turn, reduces and hampers the direct contact between the polymer and the hard counterface.

Hashmi et al. (Hashmi et al., 2007b) investigated the friction behaviour of cottonpolyester composites (CPCs) and the effect of adding graphite as a filler to polyester composites. In the study, the friction coefficient decreased (0.95, 0.65, 0.6, 0.58 and 0.47) as the concentration of graphite increased (zero, 1.96, 3.84, 5.66 and 7.4 vol%). In the case of graphite filled CPCs, the contact temperature drastically reduced because of graphite's lamellar crystal structure. This is another reason for the low friction coefficient and good wear performance of the composites.

## **2.4 Chapter summary**

In this chapter, several reported works have been reviewed and several issues have been addressed with the usage of synthetic and/or natural fibres as reinforcements for the polymeric composites. The main points can be concluded as follows:

- Surface characteristics,  $V_f$ , physical properties and orientation of natural fibre have significant influence on the mechanical and the tribological performance of the composites. The nature of the fibres controls the mechanical and the tribological behaviour of the composites. In other words, modification and critical selection of the fibres are necessary to gain high composite performance.
- There is no remarkable correlation between the mechanical and tribological performance of major polymeric composites. However, for natural fibre/polymer composites, treatment of the fibres has influenced both mechanical and tribological behaviours of the composites. Treating the natural

fibres assisted in stabilising the bonding area between the fibre and the matrix, which enhanced the ability of the fibre to carry the load under mechanical and tribological loadings.

- Natural fibre polymeric composites suffer from high friction coefficient. It is suggested to use graphite as a solid lubricant for such composites, which may reduce the friction coefficient of the composite and maintain high wear characteristics. On the other hand, using water as lubricant for natural fibre/polymer composite may deteriorate the composite strength.
- The use of water as a lubricant deteriorates the wear performance of synthetic fibre/polymer composites by transferring the adhesive into three body abrasion wear mode. On the other hand, water assisted in cooling the rubbed surface, which, in turn, exhibited better wear and frictional performance, compared to the dry contact conditions.



## **Chapter 3: Methodology**

### **3.1 Introduction**

An overview of the experiments and the scope of the study is introduced in Figure 3.1. In Stage 1, the single fibre tensile test (SFTT) and the SFFT will be used to determine the optimum fibre diameter and NaOH concentration, seeking the high mechanical performance of the DPF reinforced ECs. These tests will be performed on different diameters of fibre (0.3, 0.5, 0.7 mm,  $\pm 0.05\text{mm}$ ) with different concentrations of NaOH treatment (3, 6, 9 wt%) and the mechanical properties results will be put under investigation and studied. In addition, the tensile and the tribological tests will be used to determine the optimum concentration of graphite additives (one, three, five and seven weight per cent), seeking the high mechanical and tribological performance of the graphite-ECs.

In Stage 2, the optimum fibre diameter, the optimum NaOH treatment concentration and the optimum graphite ratio will be used to fabricate three sorts of composites: graphite-ECs, fibre-reinforced ECs and fibre-reinforced-graphite composites. These composites will be examined by mechanical and tribological tests and compared with the NE composites to seek the high mechanical and tribological performance of the DPF reinforced ECs.

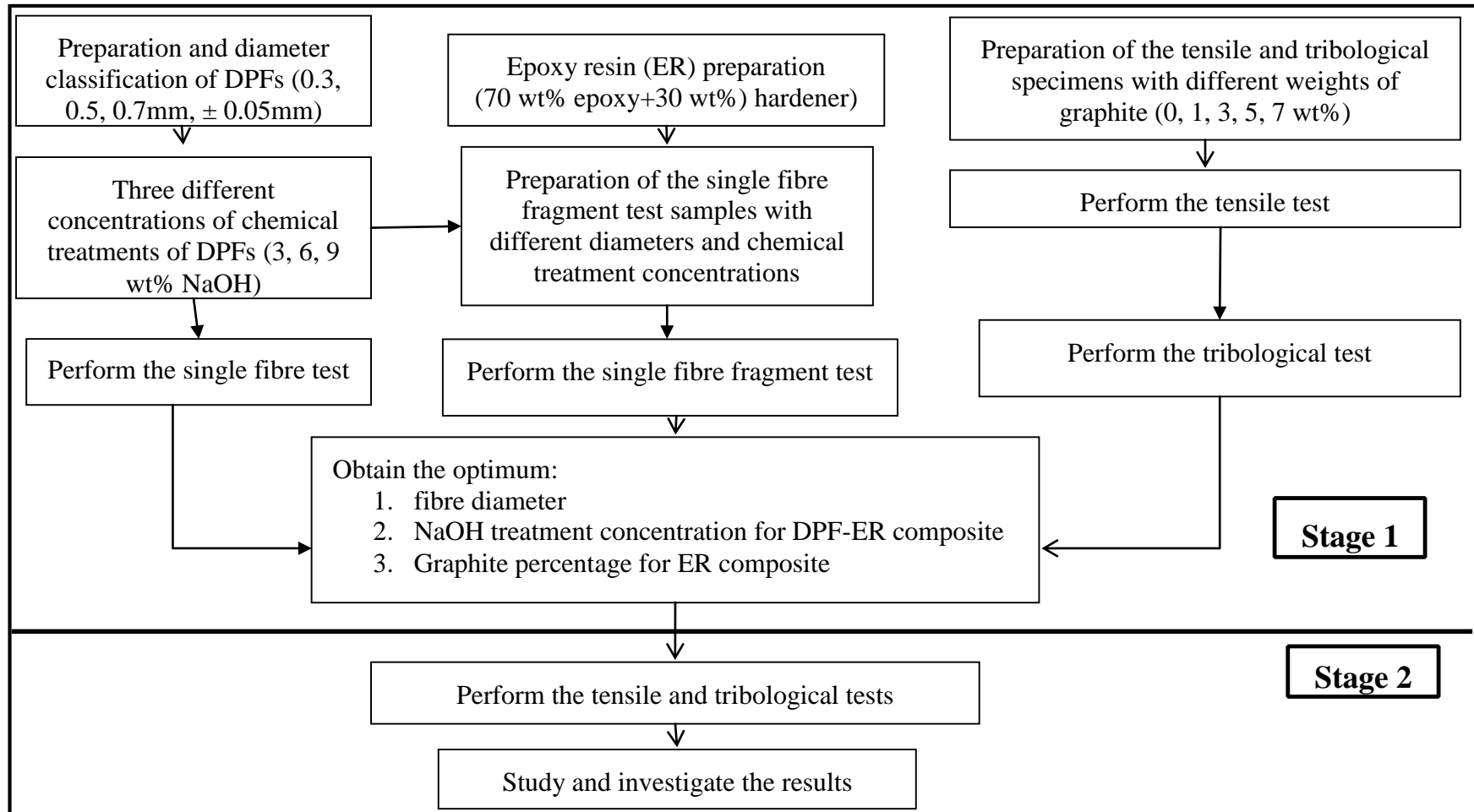


Figure 3.1: Schematic drawing showing the procedure of experimental study



## **3.2 Materials selection and preparation**

In addition to the advantages of natural fibres as an alternative option to the synthetic fibres, date palm trees are widely spread in large numbers in many countries and regions, such as the Middle East, Northern Africa, India and the United States (US). Moreover, date palms are considered perennial, making them a renewable resource of fibres. Using DPFs for reinforcing polymer composites is an attempt to create new manufacturing applications, in addition to their traditional and common applications, such as ropes and baskets, where there are no tangible industrial applications for the DPFs (Alawar et al., 2009b, Abu-Sharkh and Hamid, 2004, Kaddami et al., 2006). However, there is a shortage in investigated research in potentially using DPFs as a reinforcement for polymer composites for mechanical and tribological applications, compared with other natural fibres, such as flax, jute, hemp and coir (Baley, 2002, Bledzki and Gassan, 1999, Alawar et al., 2009b).

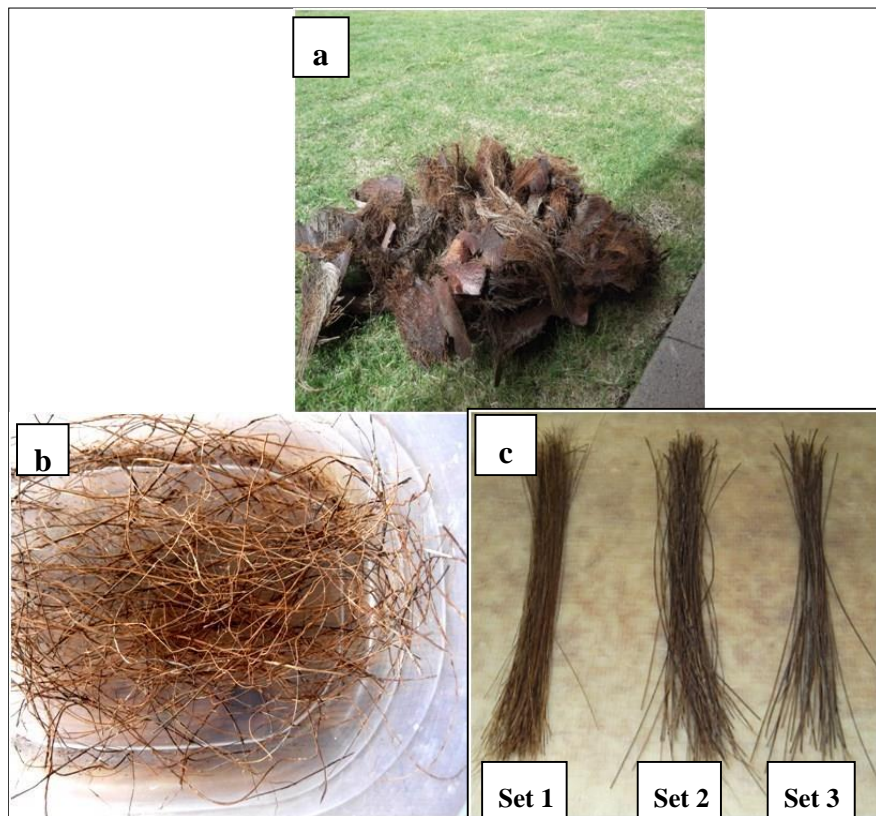
For the matrix selection, epoxy is considered to be one of the common, cheap and widely used resins for tribological applications (Wu and Cheng, 2006, Chin and Yousif, 2009, Nirmal et al., 2012b, Cheung et al., 2009). In the current study, epoxy resin (R246TX) was used as matrix material, which is supplied by Australian Calibrating Services Pty Ltd, Australia. The hardener used in the current work is Kinetix (H160 medium), which is supplied by LTL Composites Pty Ltd, Australia. The solid lubricant used in the current study is graphite powder (Gr). The 92% pure graphite filler size used in the current study is 45  $\mu\text{m}$  as supplied by Chem-Supply Pty Ltd, Australia.

### **3.2.1 Date palm fibre preparation and treatment**

Raw mesh (natural mat) surrounding the date palm tree stems was collected from a date palm farm in Kuwait. Samples of the collected mats are displayed in Figure 3.2a. The fibres were separated from the meshes manually and washed with a tap water and two per cent detergent solution to remove the contaminants, adhering dirt and dust. The extracted fibres were air dried for 48 hours at room temperature and samples of

the extracted fibres are shown in Figure 3.2b. At this stage, optical microscopy (Motic stereomicroscope, SMZ168 series) was used to check the fibre and select the desired ones. In addition, fibres were classified into three groups according to their diameters: Set 1 ( $0.3 \pm 0.05$  mm), Set 2 ( $0.5 \pm 0.05$  mm) and Set 3 ( $0.7 \pm 0.05$  mm), as shown in Figure 3.2c. In determining the fibre diameter, three measurements were taken at different cross sections in each fibre and average diameter was calculated. Then the fibres were cut to the desired length and preserved in polyethylene bags.

Fibres are treated with NaOH. First, the selected fibres are soaked in NaOH solution (three, six and nine weight per cent NaOH) for 24 hours at room temperature. Second, after treatment, the fibres are rinsed with fresh water and dried at room temperature for 24 hours. Finally, fibres were preserved in right polyethylene bags to reduce moisture absorption until they were used.



**Figure 3.2: (a) date palm tree, (b) extracted fibres, (c) fibres classification**

### 3.3 Preparation of samples

#### 3.3.1 Single fibre tensile test

The SFTT is aimed to determine the tensile properties for a single fibre. After preparation, classification and treatment fibres, the treated fibres were cut to desired length of 80 mm. Then, the treated fibres were classified into 12 sets, according to their diameters and NaOH treatment percentages, as shown in Table 3.1.

**Table 3.1: Specimen sets of the SFTT**

Sample	S1	S2	S3	S4	S5	S6	S7	S8	S9	S10	S11	S12
Df mm	0.3	0.3	0.3	0.3	0.5	0.5	0.5	0.5	0.7	0.7	0.7	0.7
NaOH (%)	0	3	6	9	0	3	6	9	0	3	6	9

#### 3.3.2 Fragmentation test specimens

The SFFT was developed by Kelly and Tyson (1965) and is used extensively to evaluate the interface properties (interfacial shear strength) of fibre-matrix composites (Kelly and Tyson, 1965, Awal et al., 2011, Torres and Cubillas, 2005). The current study is based on the Kelly and Tyson (1965) technique. Each test specimen for SFFT consists of a single fibre encapsulated in a chosen polymer and, normally, the specimen has a dogbone shape. The specimen is subjected to an increasing tensile load, which is transferred to the fibre through the fibre-matrix interface.

The specimens for the SFFT were prepared to study the interfacial adhesion of the DPFs with the epoxy matrix. The DPFs are classified into twelve sets, according to the fibre diameter (Df) and concentration of NaOH solution (zero to nine weight per cent), as listed in Table 3.1. Figure 3.3a and 3.3b show the specimen geometry and the used mould for SFFT. The mould was coated with a release agent (wax) before the fabrication. The prepared fibre was placed inside the mould. To ensure the correct alignment of the fibre, the two ends of each prepared fibre were fixed inside the mould before preparing the resin, as shown in Figure 3.3b. The resin mixture was prepared

by mixing the epoxy and the hardener with a ratio of 1:3, based on the industrial recommendation. The mixture was left for five to ten minutes to get rid of the bubbles. The mixture was poured carefully inside the cavity of the mould and a small steel tool was used to ensure the distribution of the matrix and the alignment of the fibres. The prepared sample was cured for 24 hours at atmospheric conditions. Next, the samples were removed from the mould and cured again in an oven with a temperature of 50°C for 24 hours. After curing, the specimens were ready for SFFT procedures. For each test, three specimens were tested and the average value of interfacial shear strength ( $\tau_c$ ) was taken.

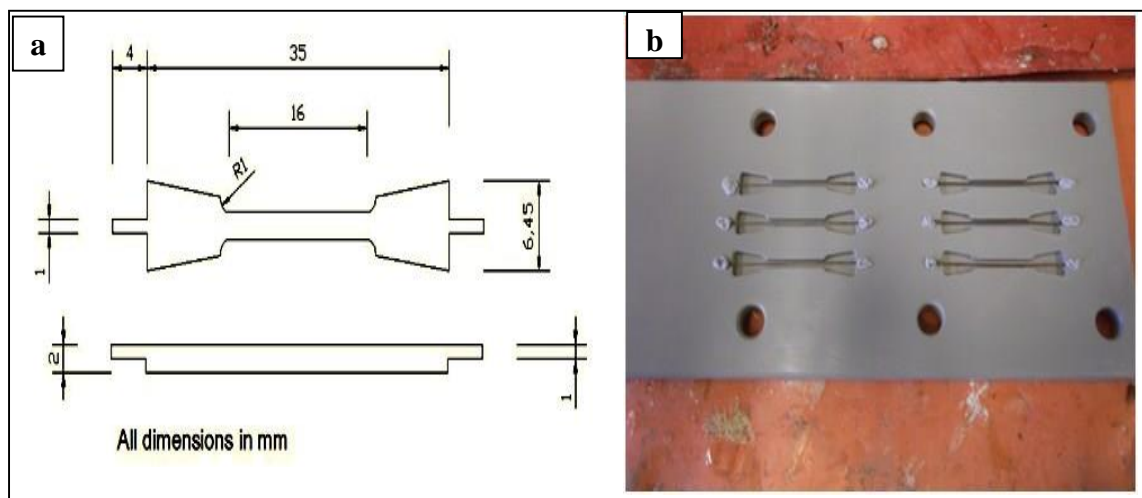
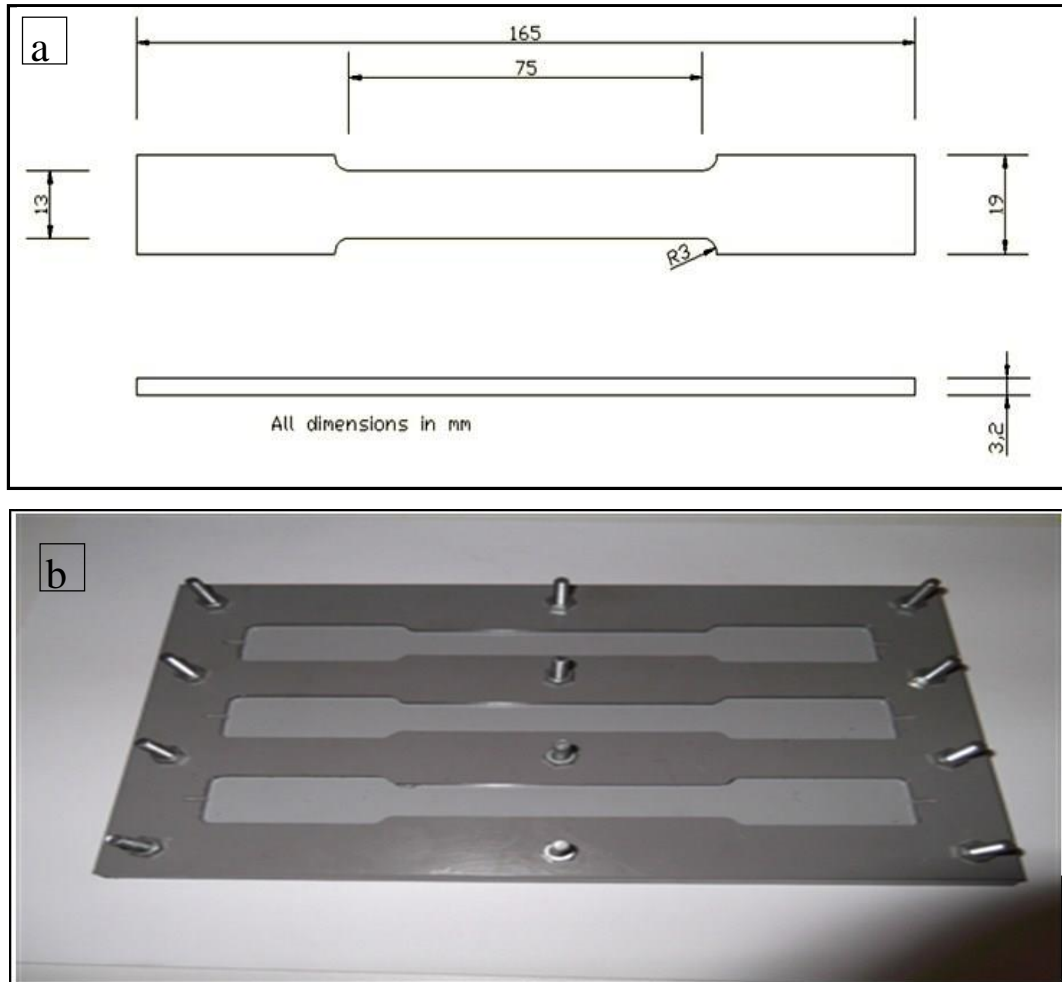


Figure 3.3: (a) SFFT specimen geometry, (b) SFFT mould and fibre position

### 3.3.3 Composite specimens preparation

The date palm fibre-reinforced epoxy (DPFE) specimens for the mechanical and tribological tests were prepared using the same procedure as for SFFT specimens with different mould dimensions and with/without graphite in epoxy resin. Further, the graphite addition was zero to seven weight per cent, with respect to the amount of epoxy used. In addition, the  $V_f$  in the matrix was fixed to approximately 35–40 volume per cent.

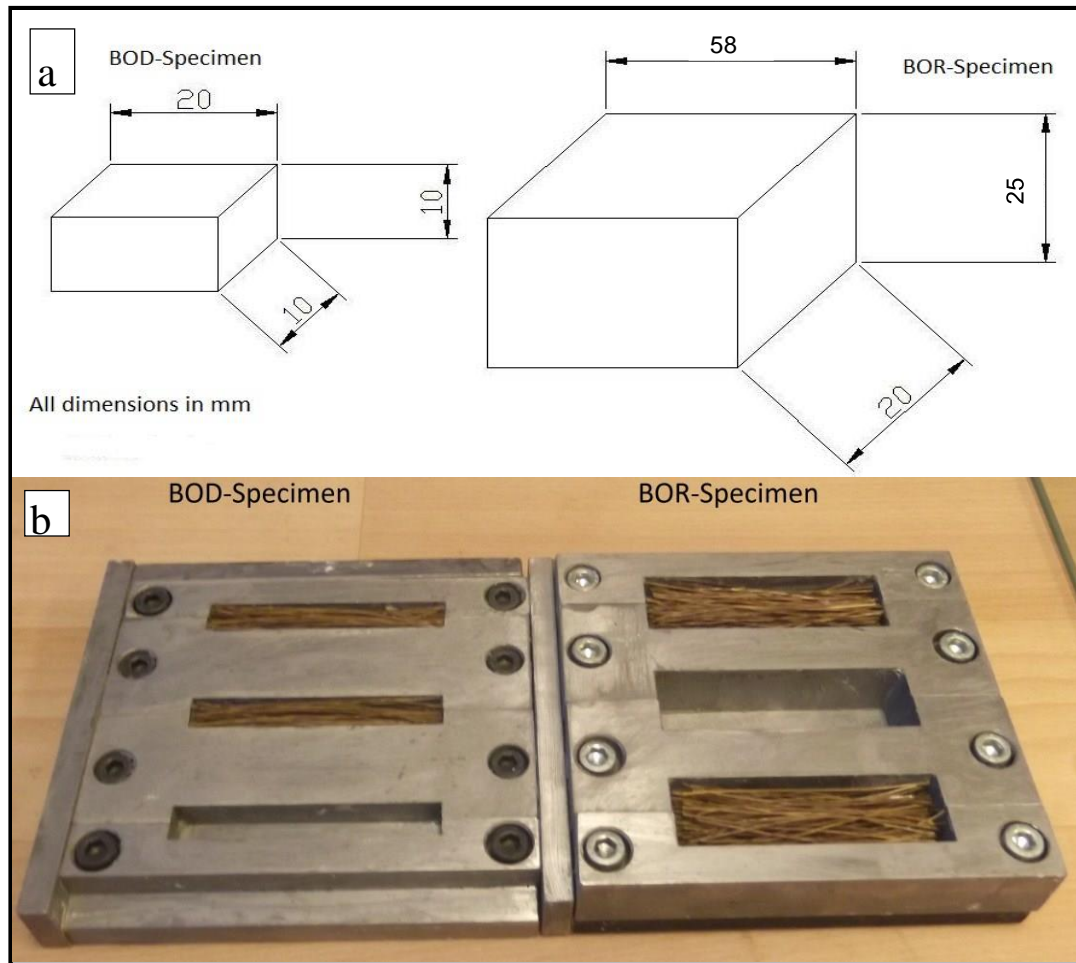
For the tensile testing samples, the samples were prepared based on ASTM (ASTM, 2000) standards, with the dimension (specimen geometry) and the used mould given in Figure 3.4 (ASTM, 2000).



**Figure 3.4: (a) tensile specimen dimensions, (b) used tensile test mould**

In the preparation of tribological composite specimens, two metal moulds were used to manufacture two types of tribological specimens for two tribological techniques (BOR and BOD). Figure 3.5a and 3.5b show the specimen dimensions and the used metal moulds for preparing the BOR and BOD specimens. The prepared specimens are cut into the desired dimension of 10 mm x 10 mm x 20 mm and 25 mm x 58 mm x 20 mm for tribological experiments, based on ASTM G99 and ASTM G 77 for BOD and BOR techniques.





**Figure 3.5: (a) tribological specimen geometry, (b) tribological mould and fibre position**

Different Vfs of graphite were used (zero, one, three, five and seven weight per cent). The graphite particles were mixed with the epoxy resin and the hardener kept for a while in jelly form. The 92% pure graphite filler size used in the current study is 45  $\mu\text{m}$  as supplied by Chem-Supply Pty Ltd, Australia. Zhang et al. (2008a) reported that the bigger sizes ( $>45 \mu\text{m}$ ) of graphite may assist in reducing the weight loss of the material under tribological loading conditions. However, in the recent year, Hou et al. (2013) reported the opposite for the mechanical properties of the composites. The late findings are highly supported with the deterioration in the microstructure of the composite with bigger sized of graphite. Therefore, the current study focuses on the graphite size of 45  $\mu\text{m}$  as to maintain good mechanical and tribological properties. At this stage, a similar procedure to the previous one was followed to fabricate the composite.

### **3.4 Experimental procedure**

There were three sorts of composites, in addition to the ECs (see Figure 3.6):

- graphite-ECs (GEC)
- date fibre-reinforced ECs (FEC)
- graphite-date fibre-reinforced ECs (GFEC).

The GEC, FEC and GFEC were designed according to results in previous paragraphs: the optimum fibre diameter, the optimum NaOH treatment and the optimum graphite ratio. Mechanical and tribological testing was performed to study the mechanical and tribological behaviour of composites, such as tensile properties, specific wear rate and friction coefficient. Comparison with the EC behaviour followed. Moreover, these four composites were studied and compared thoroughly to attain evidence-based scientific understanding of these composites' tribological behaviour.

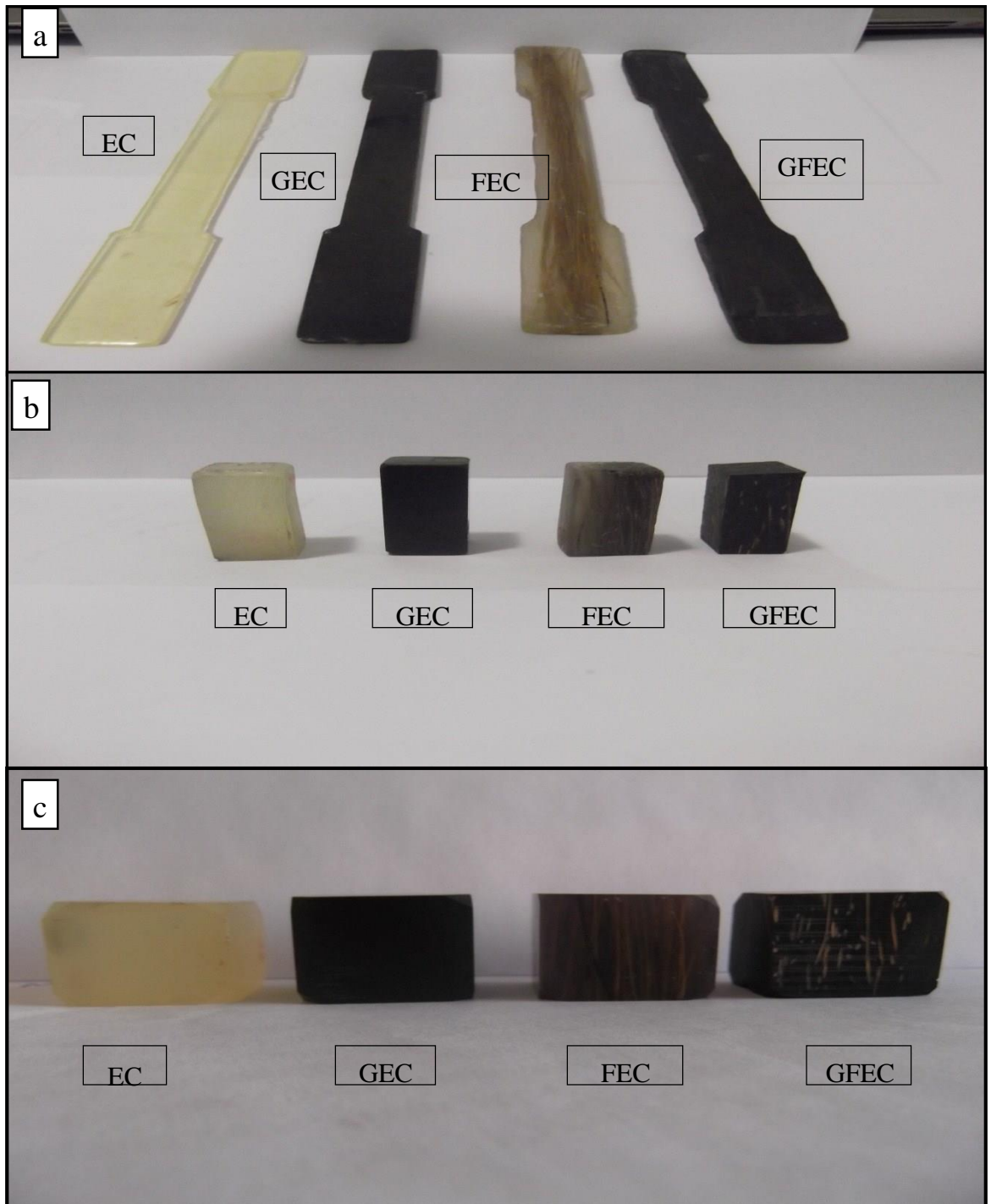
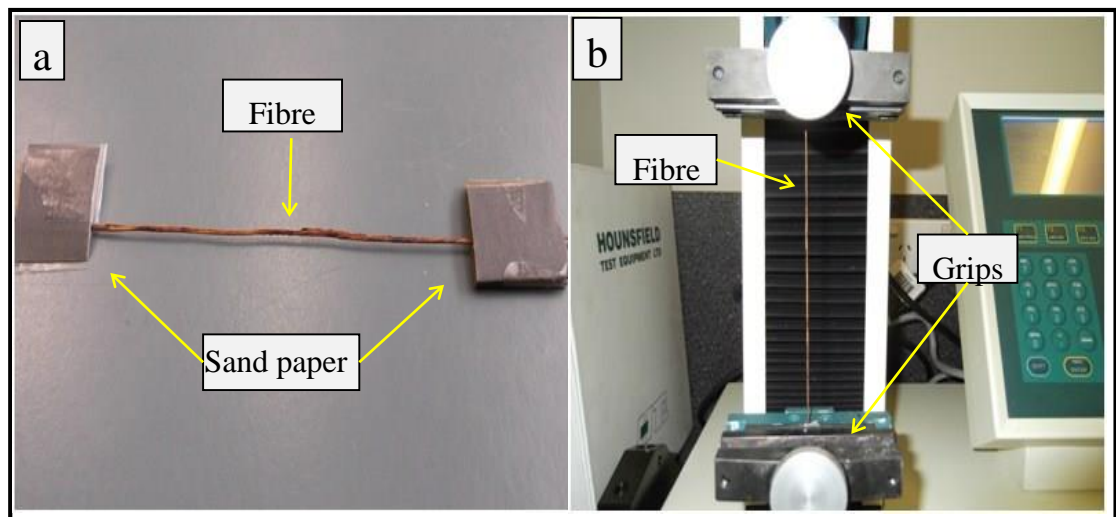


Figure 3.6: a) tensile specimens, b) BOD-tribological specimen, c) BOR-tribological test

### 3.4.1 Mechanical properties

#### 3.4.1.1 Single fibre tensile test

The mechanical characteristics (TS, Young's modulus and elongation to break) of single DPF were determined with a universal testing machine: the Hounsfield tensometer (250 N–2500 N) system. Specimens were prepared by fitting both fibre ends (about 20 mm) between the grip arms, using fine sand paper to prevent slipping of fibre and crosshead speed (one millimetre minimum was employed, as shown in Figure 3.7). Calibration was achieved by conducting three samples in each set and taking the average reading of the diameter at the fracture point by stereo zoom microscope (Motic-SMZ 168 series) for each set.



**Figure 3.7:** (a) single fibre specimen, (b) fixing single fibre specimen in tensile test machine

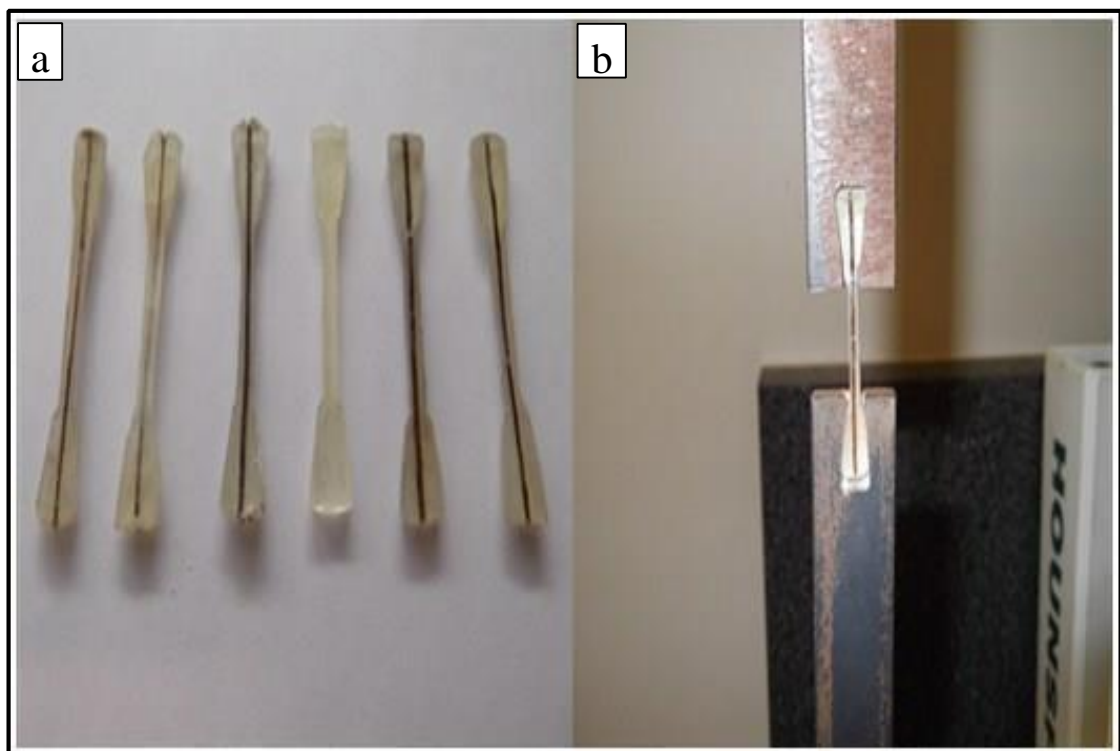
#### 3.4.1.2 Single fibre fragment test

The interfacial shear strength of polymer fibre composites could be measured using the SFFT. Nine sets of SFFT specimens, according to the diameter of fibre and percentage of treatment, were carried out by applying a sustained tensile load using Hounsfield tensometer (250 N–2500 N). Figure 3.8 shows some specimens and demonstrates how to fix specimen in the grips of the tensile machine using two steel

pieces with suitable grooves for specimen ends, avoiding any compression load that may lead to micro-cracks on the specimen. The average interfacial shear could be calculated with the following equation and the test was conducted three times for each set.

$$\tau = \frac{F}{L \cdot D} \quad (1)$$

where  $\tau$  = the shear stress,  $F$  = the applied force,  $L$  = length of the fibre and  $D$  = the diameter of fibre.



**Figure 3.8: (a) some of SFFT specimens, (b) fixing specimen in tensile machine**

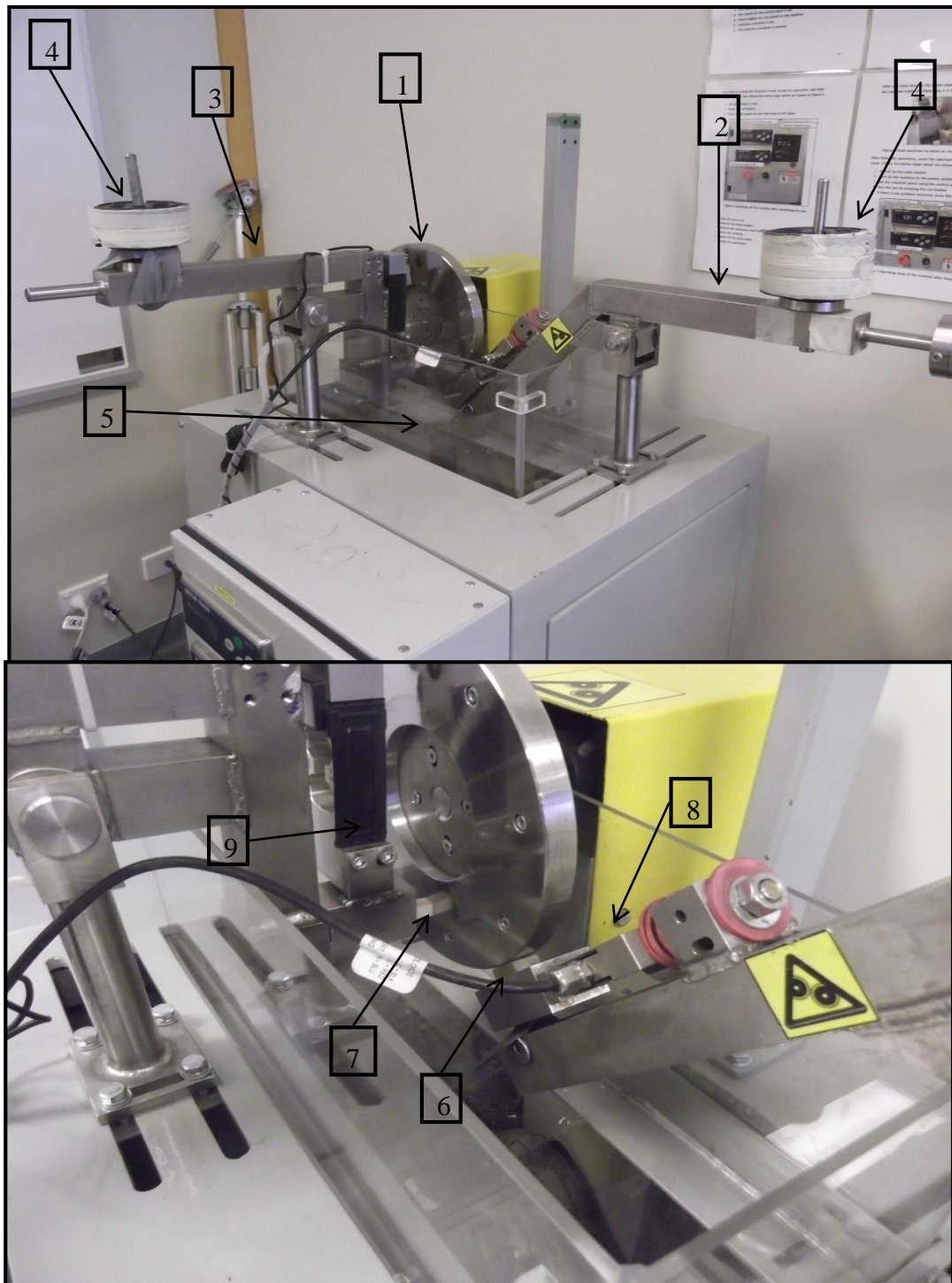
#### *3.4.1.3 Tensile experiments of the composites*

TS, tensile modulus (E) and elongation at break ( $\epsilon$ ) are determined according to ASTM D638–99, under ambient conditions, using MTS 810 TestStar Material Testing

System. The hardness is measured using a Durometer type D in accordance with ASTM D2240. Six sets of specimens are tested, according to compositions of graphite modified epoxy resin with the optimum diameter of fibres. Three tests are repeated for each sample set and the average values are calculated.

### **3.4.2 Tribological experiments**

In this work, the friction and wear characteristics of DPFE composite are investigated under dry contact and ambient conditions (temperature = 25° C, humidity = 50% ± 5) against stainless steel (AISI 304, hardness = 1250 HB, roughness average (Ra) = 0.1 µm) counterface. The experiments are conducted using BOD and BOR techniques, a newly developed machine designed to conduct these techniques. A three-dimensional view of the machine is displayed in Figure 3.9. Some of the machine specifications are given in Table 4. More details of the machine are given in Yousif (2012).



**Figure 3.9: The tribo-test machine.**

**1 = Counterface, 2 = BOR load lever, 3 = BOD load lever, 4 = Dead weights, 5 = Lubricant container, 6 = BOR-specimen, 7 = BOD-specimens, 8 = BOR-load cell, 9 = BOR-load cell Table**

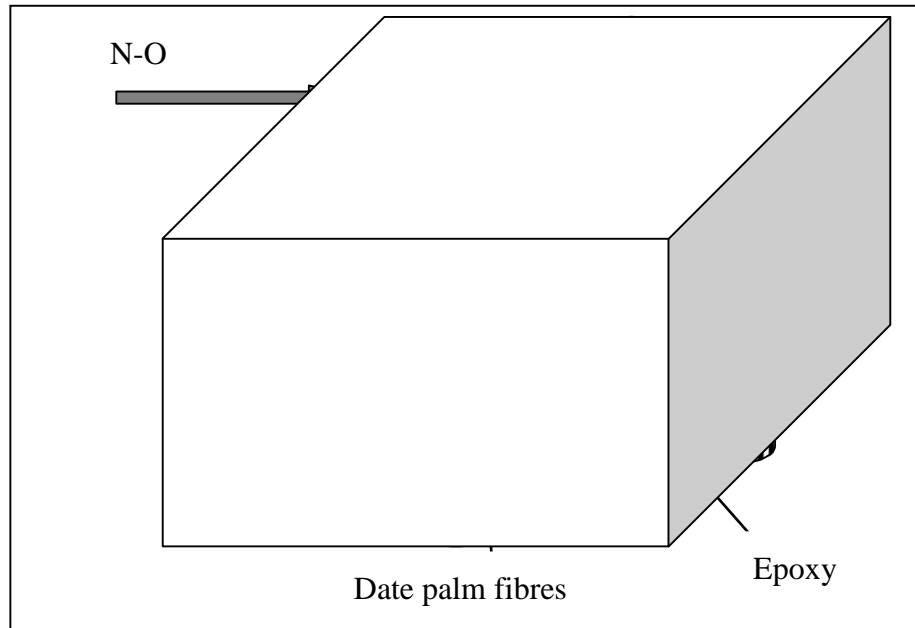
**3.2: Technical specifications of the newly developed machine (Yousif 2012)**

Part	Specification
------	---------------

Wheel speed	5–2000 rpm
Wheel types	6.65” steel wheel, as per ASTM B 611
	9” rubber wheel, as per ASTM G 65
Load	5–500 N
Motor type	AC motor with frequency inverter drive
Specimen size	25 mm × 58 mm for BOR
	10 mm × 10 mm for BOD
Specimen thickness	6 mm–20 mm
Test types	ASTM (G 65, G 105, B 611, G 137–95 and G 77)

Before each test, the surfaces of each specimen and counterpart ring were polished with 600 grit paper and cleaned with ethanol. DPFE composite was tested in normal orientation, as shown schematically in Figure 3.10, which was recommended in the literature (Yousif and El-Tayeb, 2008b, Yousif et al., 2010a, Yousif and Nirmal, 2011). The sliding test is performed at sliding velocities (1.1–3.9 m/s), applied loads (30–100 N) and sliding distances (0–5 km).





**Figure 3.10: Fibre orientations with respect to the sliding direction**

The friction force, measured with load bending beam and coefficient friction, is determined by Equation 2. The wear volume loss is calculated from the loss of each specimen's weight using a  $\pm 0.1$  mg weight scale. Specific wear rates calculation used Equation 3. Each test is repeated three times and the average of the measurements is determined. The morphology of the worn composite surfaces is examined using the SEM to categorise the damage features and analyse the results.

$$\mu = F_M / F_N \quad (2)$$

$$W_s = \Delta V / F_N D \quad (3)$$

where  $\mu$  = friction coefficient,  $F_M$  = measured frictional force and  $F_N$  = normal applied load

and  $W_s$  = specific wear rate [ $\text{mm}^3/\text{N m}$ ],  $\Delta V$  = volume difference [ $\text{mm}^3$ ],  $F_N$  = normal applied load and  $D$  = sliding distance [m].

The volume difference was determined by dividing the weight loss from weight scale by the density of material.

Roughness of a counterface made of stainless steel (AISI 304, hardness = 1250 HB, Ra = 0.1  $\mu\text{m}$ ) and the surface of specimens was determined before and after each test using Mahr (MarSuf PS1). SEM (Philip XL-30) categorises the damage features and fracture mechanisms of both tribological and mechanical samples after each test. Before taking the micrographs, the surface was coated with a thin layer of gold through ion sputtering. During the running tribology test, a thermo camera (Testo) determined the distribution of temperature on the surface of counterface and specimen.

### 3.4.3 Calibration and measurement technique of friction coefficient

To obtain the correct frictional force, the load cell was calibrated in each set of experiments to ensure precision in the collected data. In the calibration process, the load cell was applied with different standard weights, while the captured forces were recorded through the data acquisition system. Fitting liner lines between the measured and actual forces were plotted, as shown in Figure 3.11. Calibration equations were then obtained and used.

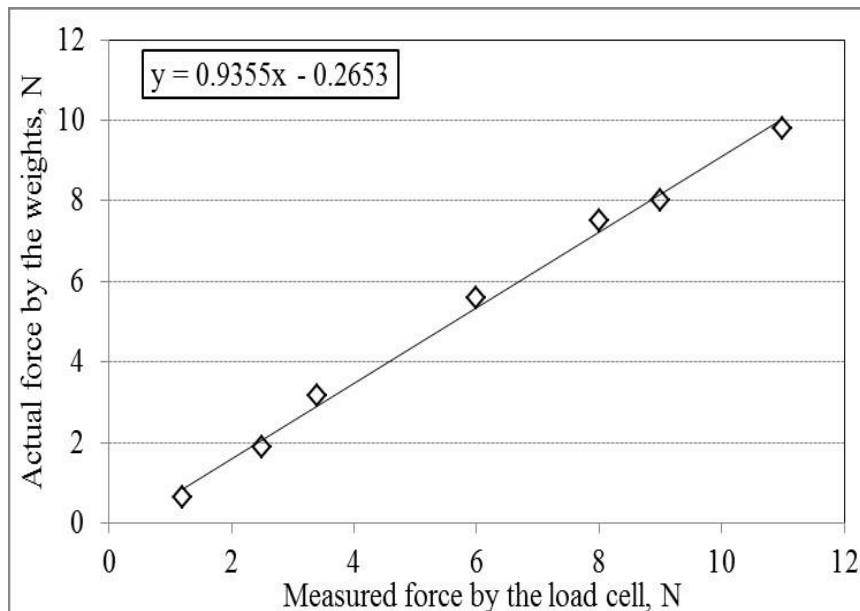


Figure 3.11: Calibration chart for measuring friction force



## **Chapter 4: Interfacial adhesion of date palm/epoxy using fragmentation technique**

### **4.1 Introduction**

Natural fibres have become an attractive alternative for synthetic reinforcements of polymeric composites from both economic and ecological perspectives (Holmberg et al., 2012, Fontaras and Samaras, 2010). This is mainly due to the advantages of natural fibres over synthetics, including their low cost, low weight, renewability, non-toxicity, lack of harm to skin and eyes and good relative mechanical properties (Joshi et al., 2004, Corbière-Nicollier et al., 2001, Wötzel et al., 1999, Alawar et al., 2009b). Conversely, natural fibres lack good interfacial adhesion with synthetic matrices. Many researchers have reported that the mechanical efficiency of the fibre-reinforced polymer composites depends on the fibre-matrix interface and the ability to transfer stress from the matrix to fibre (Venkateshwaran et al., 2012, Rokbi et al., 2011, Shalwan and Yousif). The interface bonding between the fibres and the polymer matrix is a key factor in determining the mechanical behaviour of natural fibre-reinforced polymer composites (Haque et al., 2009, Chin and Yousif, 2009, Shalwan and Yousif).

Natural fibres tend to be strong polar and hydrophilic materials because of their high content of cellulose, hemicelluloses, pectins and lignin, which have hydroxyl groups (Shalwan and Yousif), while polymers exhibit significant hydrophobicity. In other words, there is a significant issue regarding the compatibility of natural fibres and synthetic matrices. Chemical treatments, such as bleaching, acetylation and alkali treatment, may improve the fibre-matrix interfacial adhesion (Alawar et al., 2009a, Saha et al., 2010). Conversely, a high concentration of chemical treatment could attack the main fibre construction components and weaken it (Alawar et al., 2009a, Saha et al., 2010, Shalwan and Yousif).

Study of the interfacial adhesion characteristics of fibre-reinforced polymer composites could discover the interactions between fibre and matrix, offering

significant information about the interactions. For instance, many researchers have studied the interfacial adhesion characteristics of fibre-reinforced polymer composites using the single fibre pull out technique (Joseph et al., 2002, Joseph et al., 1996, Sydenstricker et al., 2003, García-Hernández et al., 2004). The weakness of the single fibre pull out test is that the thermal stresses and polymer morphology around the fibre are not the same as in a real composite; this places the fibre under direct tensile stress. In contrast, using fragmentation test avoids placing the fibre under any direct tensile stress, giving similar conditions to those occurring in a fibre-reinforced composite.

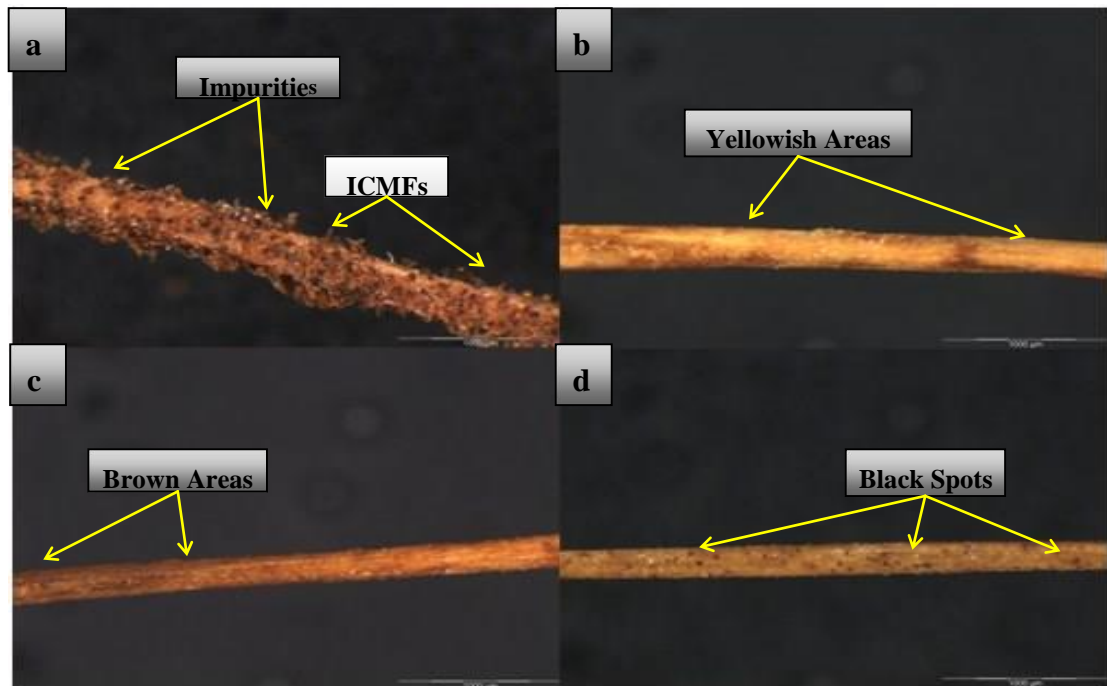
A few researchers have investigated the relationship between fibre diameter and fibre strength, irrespective of fibre gauge length. These studies have found that the decreasing fibre diameter has a positive improvement on the mechanical properties of fibre/polymeric composites. Prasad and Sain (Prasad and Sain, 2003) reported that the TS and the modulus of hemp fibres have increased with decreased fibre diameters. This could be because of a high probability of decreasing numbers of natural defects in the small diameter. In the same context, Virk et al. (Virk et al., 2010) studied the relationship between the jute fibre diameter and its strength, irrespective of fibre gauge length. It was found that, as the fibre diameter increases, the fibre strength value decreases.

This work aims to investigate the influences of alkali treatment and fibre diameter on fibre strength and the interfacial adhesion behaviour of date palm/EC. Different alkali treatment concentrations (zero, three, six and nine weight per cent NaOH) and fibre diameters (0.3, 0.5 and  $0.7 \pm 0.05$  mm) were considered. For achieving high interfacial adhesion and fibre strength with the matrix, the optimum alkali concentration and DPF diameter were addressed. Tensile behaviour of single fibre and single fibre/ECs were investigated using the SFTT and SFFT, respectively. Optical microscope micrographs and SEM were used to examine the fibre after treatment and the damage features on the surface of fibre/epoxy samples.

## **4.2 Influence of fibre treatment on surface morphology**

### **4.2.1 Optical microscope micrographs morphology**

Figure 4.1 presents optical images of natural DPF with diameter 0.3 mm before and after immersion in different concentrations of alkaline solution for 24 hours. As shown in Figure 4.1a, there is a high number of impurities and incomplete maturation fibres (ICMF). Figure 4.1b shows a very clean surface and absence of surface impurities and ICMFs with the assistance of three per cent NaOH treatment. As alkali concentration increases to six per cent, as shown in Figure 4.1c, it was clear that the solution attacked the construction of fibre surface and turned the surface colour from yellowish to brown. This could be attributed to the high ability of alkali solution at six per cent to remove, clean and attack the fibre. In other words, the alkali solution treatment at six per cent could be the boundary that converts the alkali solution from a positive effect on DPF to a negative effect.



**Figure 4.1: Optical images of fibre surface (D = 0.3 mm)—(a) untreated, (b) at 3% NaOH, (c) at 6% NaOH (d) at 9% NaOH**

Figure 4.1d clarified the fibre damage from an increase in alkali solution concentration to nine per cent, with changes to the fibre surface colour and the appearance of deep black spots. All signs could be indicative of damage to the fibre surface from burning or charring, deeply attacking the main fibre structure, which in turn could weaken the fibre. In contrast, Figure 4.2 presents different fibre diameters (0.3, 0.5 and  $0.7 \pm 0.05$  mm) under three per cent alkali treatments. In this figure, the highest deterioration was at the largest diameter. This deterioration existed as a change in the fibre colour to brown, with the emergence of grooves on the fibre surface. This could be attributed to large diameter fibres degrading with age or the fibre being affected by too many changes in surrounding factors, such as temperature and humidity. It was evident that fibre damage at diameter 0.5 mm and 0.3 mm was slight, particularly at diameter 0.3 mm, as fibre surface colour was still yellowish and no grooves or deep holes were present on the surface.

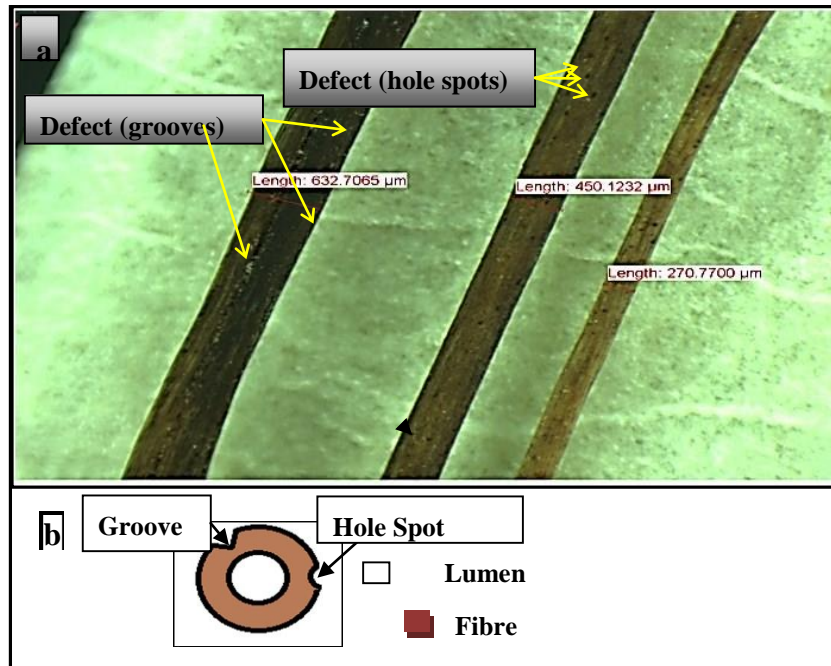
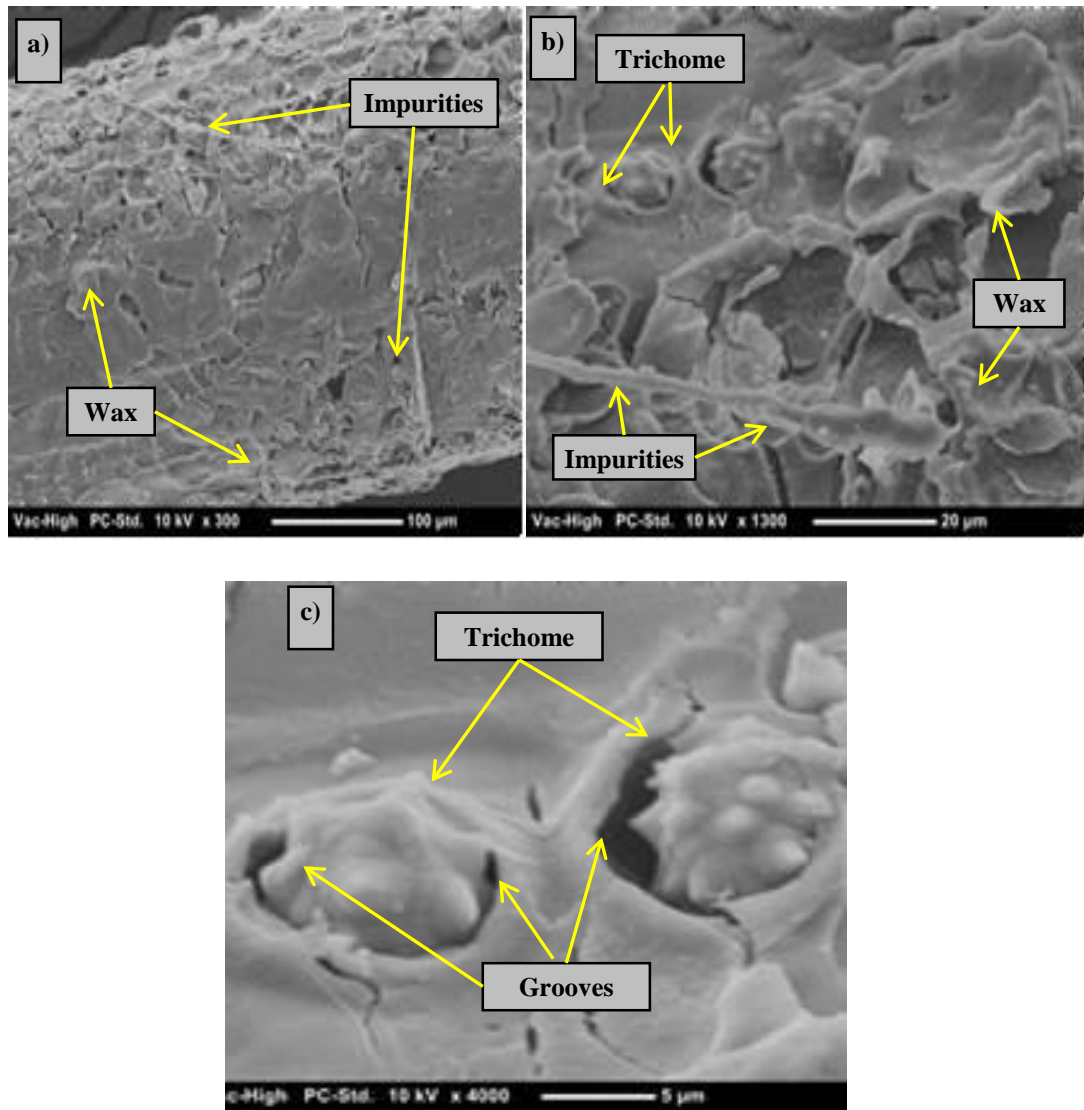


Figure 4.2: (a) optical microscope micrographs for three different diameters of fibre with defects, (b) scheme of cross-section of fibre with lumen and defects

#### 4.2.2 Scanning electron microscope morphology

Examination of surface morphology of fibres before and after alkali treatment using SEM was conducted, observing the effect of alkali treatment on the fibre surface. Figures 4.3 and 4.4 present the micrographs of natural DPF before and after treatment in different concentrations of alkaline solution. The impurities and wax were observed on the surface of the untreated fibre, as shown in Figure 4.3a. Further, Figure 4.3b shows the presence of a waxy layer and impurities on the surface, providing an insulation layer to the fibre. This has been observed on different types of natural fibres, such as date palm, coir, betelnut and kenaf (Yousif et al., 2012, Rokbi et al., 2011, Gassan and Bledzki, 1999). Conversely, the existence of a number of trichomes on the surface fibre could lead to an increase in the surface roughness and the fibre interlock with the matrix during the fabrication process (Nirmal et al., 2010). However, the structure of trichome contains grooves and rough surfaces that can act as an area of wax and impurities collation (see Figure 4.3c). Figure 4.4 displays the SEM images of the DPFs after treatment with different concentrations of alkali solution (three, six and nine per cent NaOH).





**Figure 4.3: Micrographs of the untreated DPF**

In general, the surface morphology of the treated fibres was improved, compared to the surfaces observed on untreated fibres. It can be noticed that the surface smoothness of fibre increases when the concentration of NaOH in the treatment increases. In other words, the treated fibre with nine per cent NaOH solution exhibits the smoothest surface compared to other percentages of NaOH. At a low NaOH concentration of three per cent, the chemical treatment cleaned and removed some of the waxy layer and the impurities observed on the surface of the untreated fibres (Figure 4.4a). There were still some traces of trichomes on the surface of the treated fibre with three per cent NaOH, while there was no sign of trichomes on other treated surfaces with high

NaOH concentrations (six and nine per cent NaOH), as shown in Figures 4.4b & 4.4c. With the nine per cent NaOH treatment, there was no sign of trichomes on the fibre surface. However, the high concentration may attack the fibre structure, which, in turn, may worsen the strength of the fibres.

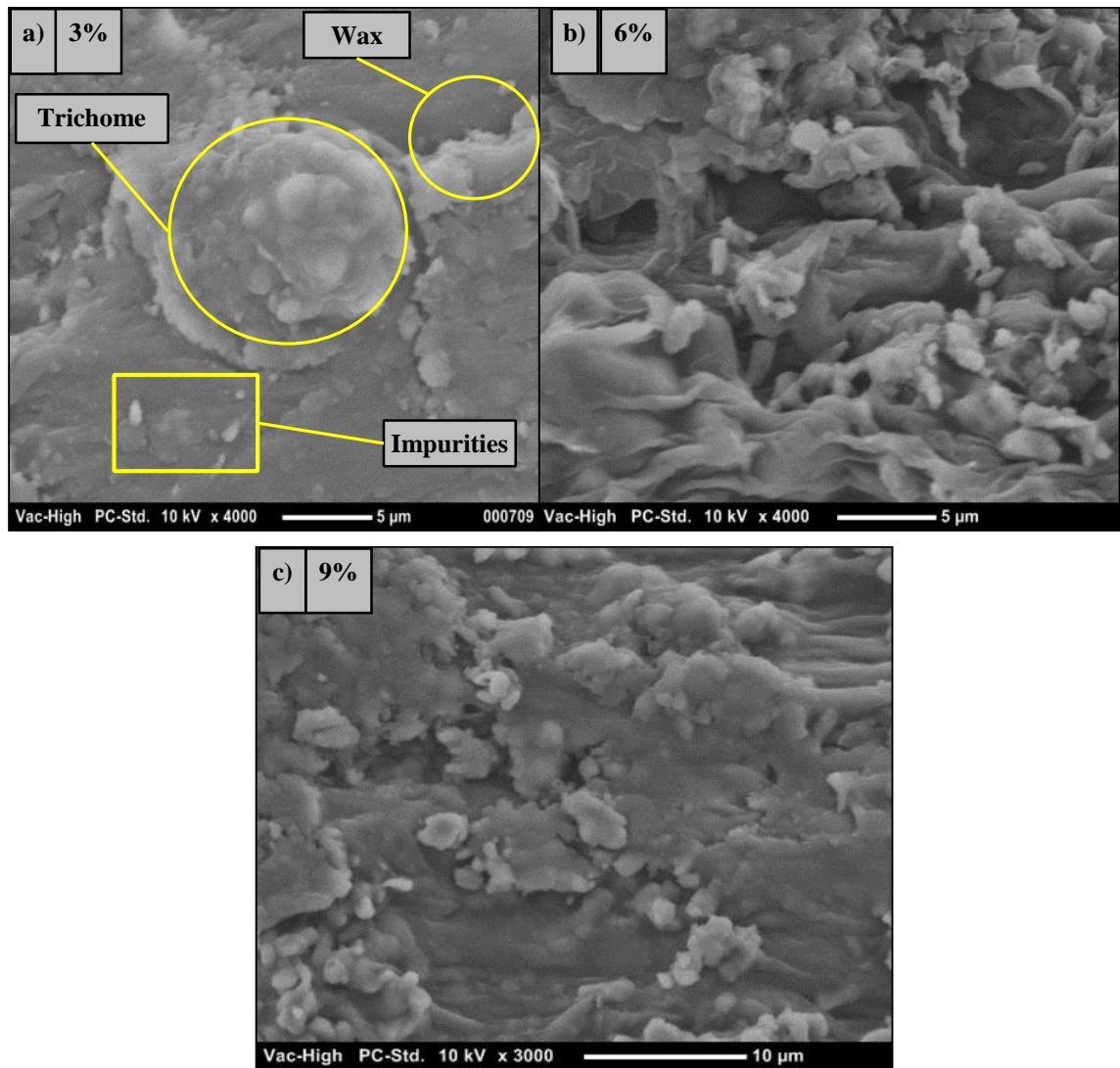


Figure 4.4: Treated DPF with different NaOH concentrations

### 4.3 Single fibre tensile test

The SFFT measured the tensile properties, such as TS, modulus of elasticity and elongation at fracture (fracture strain), for synthetic/natural single fibre. SFFT could attain useful knowledge of fibres and their potential future applications. In other words, SFFT could help to estimate and determine the fibre usages. This present study aims to research the effect of both the DPF diameter sizes and the degree of chemical treatment on the mechanical properties of DPF. The fibre diameters ( $0.3, 0.5$  and  $0.7 \pm 0.05$  mm) and NaOH treatment percentages (zero, 3, 6, 9 wt%) adopted during this test were in accordance with literature reviewed in Chapter Two. Figures 4.5, 4.6 and 4.7 show the stress strain curve for each set. Each set has three samples, according to the diameter size and NaOH treatment percentage.

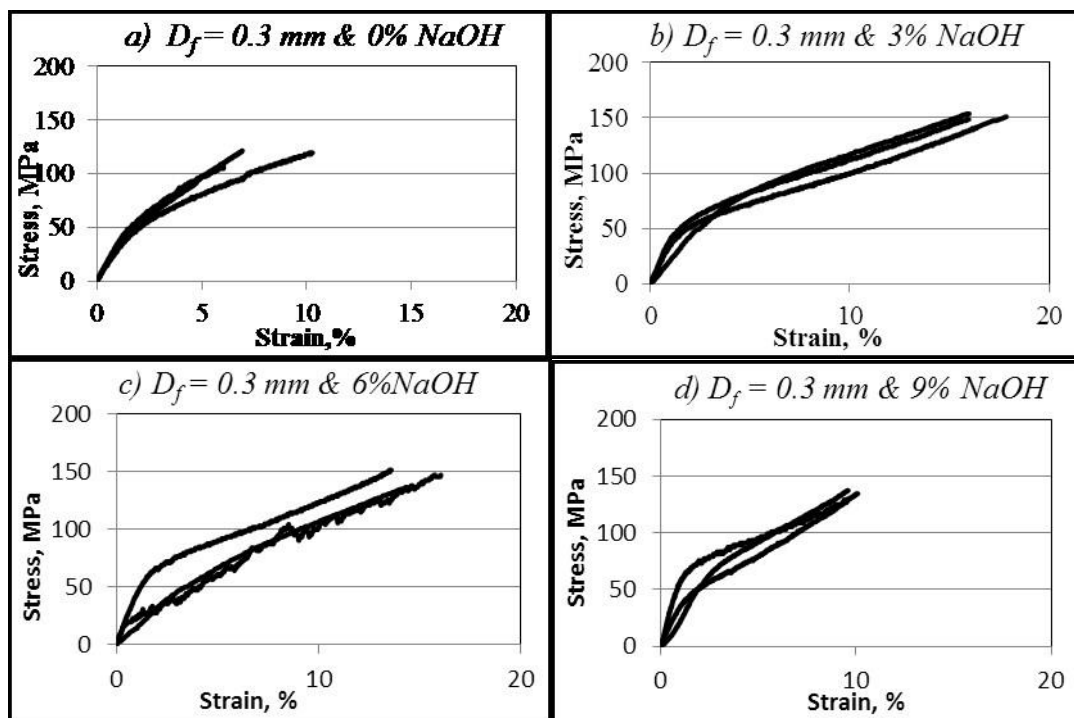


Figure 4.5: Tensile behaviour of the single DPF (0.3 mm diameter) treated with different NaOH concentrations

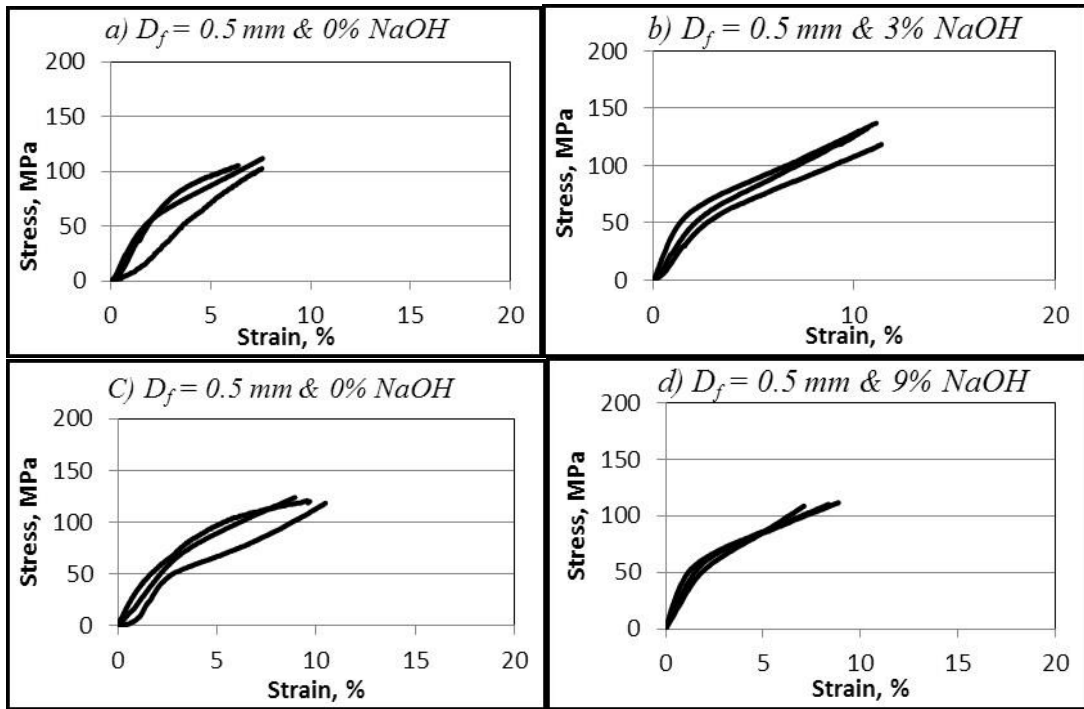


Figure 4.6: Tensile behaviour of the single DPF (0.5 mm diameter) treated with different NaOH concentration

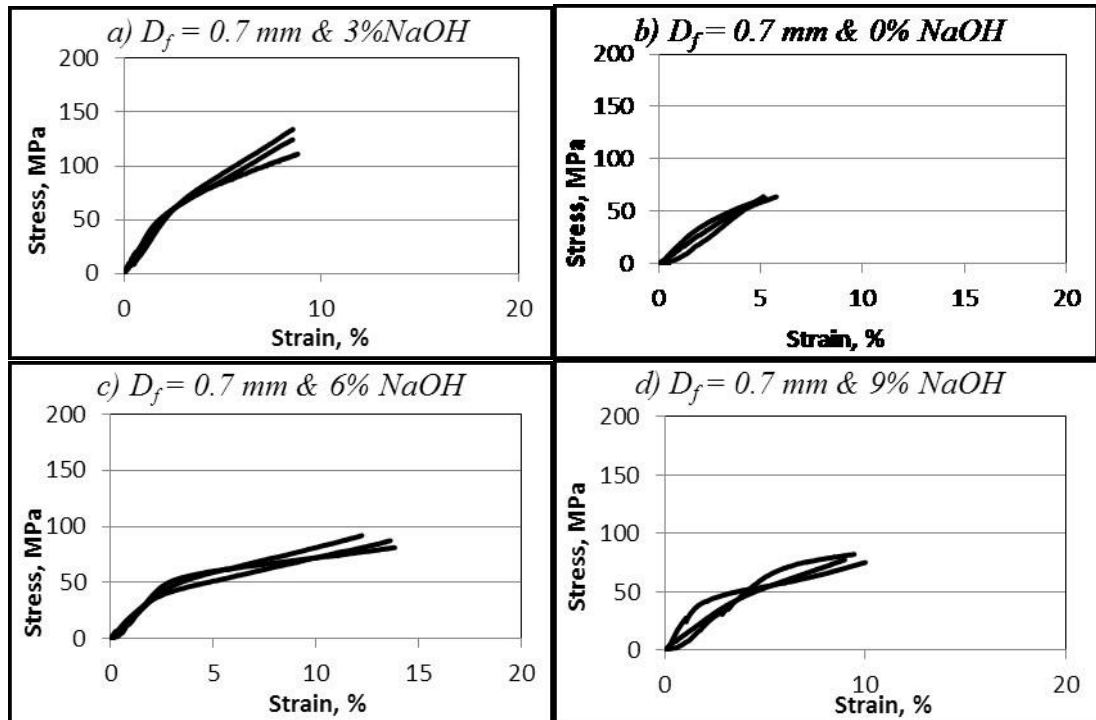


Figure 4.7: Tensile behaviour of the single DPF (0.7 mm diameter) treated with different NaOH concentrations

For clarification, the summary of the SFTT results, ultimate tensile stress, modulus of elasticity and strain at fracture of the fibre before and after treatment with different concentrations (three, six and nine per cent NaOH) are shown in Figures 4.8, 4.9 and 4.10 for different diameters of fibres (0.3 mm, 0.5 mm and 0.7 mm). It is obvious that the ultimate tensile stress of DPF was improved when alkali treatment was applied and the maximum TS and strain at fracture were reported at three per cent NaOH, as shown in Figures 4.8 and 4.9.

At alkali concentration 3 wt%, the fibre became cleansed of its impurities and waxes, which led to the fibrillation of micro fibres. This then improves the TS and strain fracture at about 23% and 48%, compared to the receptivity of untreated fibre. In other words, removing impurities and some cementing material in the DPFs by alkaline treatments produced a fibrillation of the cellular structure, leading to a better packing of cellulose chains (Rokbi et al., 2011). In contrast, increases in the concentration of alkali treatment (6 % –9 wt%) could drive the solution to attack the main construction of fibre component, which, in turn, weakens the fibre. This can be seen with the cases of six per cent and nine per cent NaOH treatments. However, treated fibre with diameter of 0.3 mm exhibits the maximum TS.

The TS and strain at fracture of the fibre decreases with the increase of the fibre diameter. This agrees with other types of fibre, such as jute and hemp (Virk et al., 2010, Placet et al., 2012). This is mainly due to the nature of the natural fibre at low diameters, where an increase in diameter size could lead to an increase in the porosity of the fibres, weakening the fibre structure (Yousif and El-Tayeb, 2007a).

Further, natural fibres with a large diameter have an irregular cross-section area, structural defects along the fibre length and lumens (central void) within each of the individual cells (Duval et al., 2011, Placet et al., 2012, Hu et al., 2010, Andersons et al., 2005).

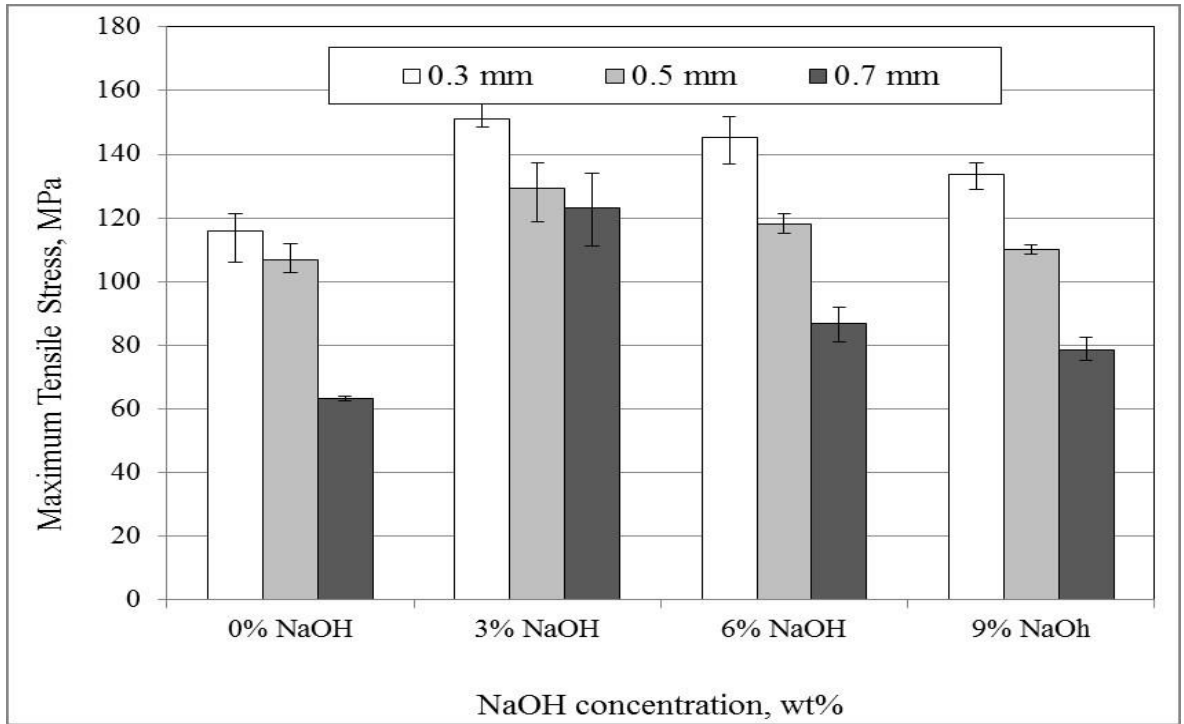


Figure 4.8: Effect of diameter of fibre and NaOH treatment on TS on single fibre

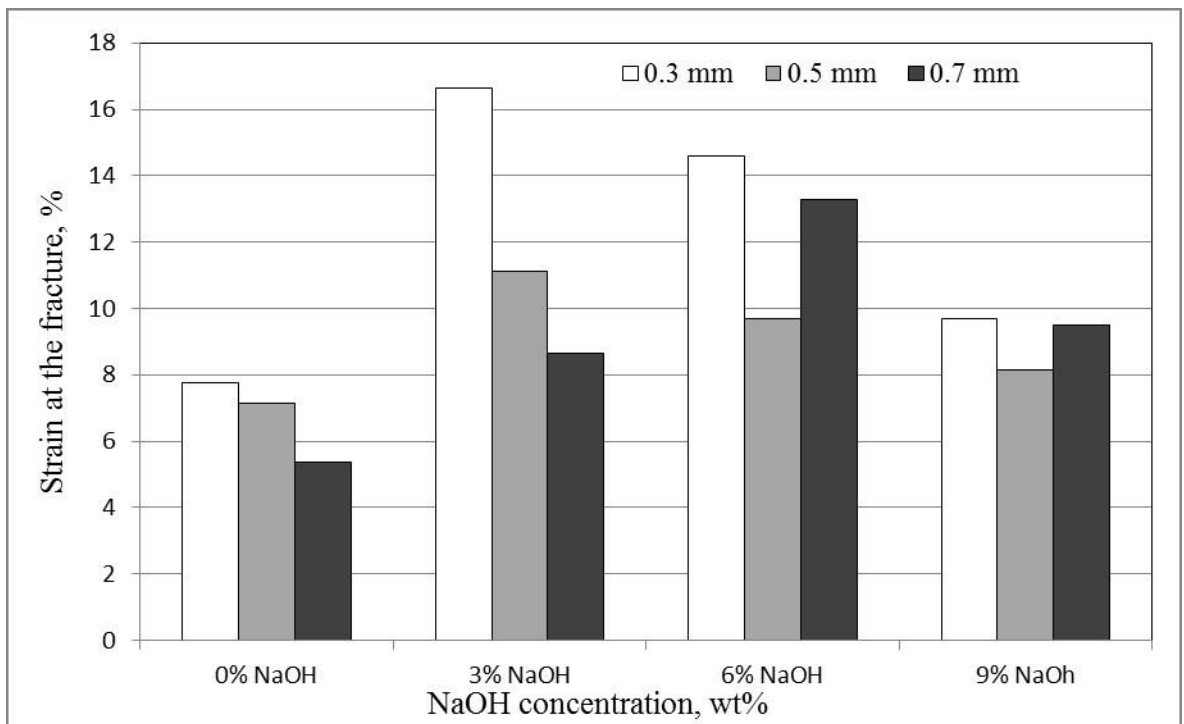
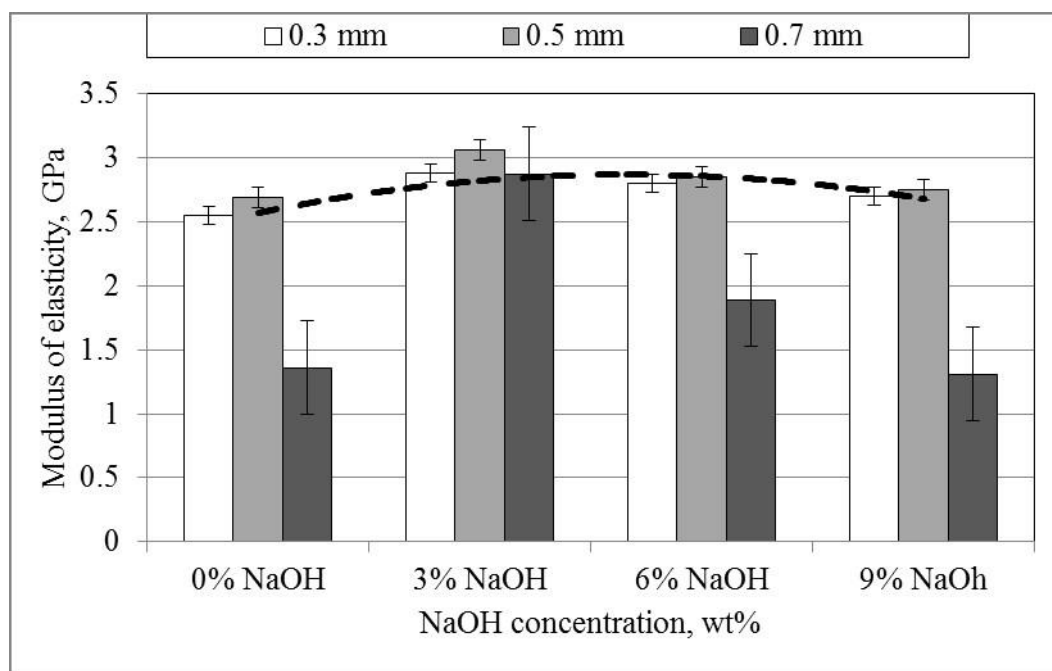


Figure 4.9: Effect of diameter of fibre and NaOH treatment on strain at fracture on single fibre

The optimum fibre diameter size that leads to optimum modulus of elasticity is at a diameter of 0.5 mm and three weight per cent NaOH. This presents an enhancement in the modulus of fibre of approximately 15% compared to untreated fibre.

From reported works, it has been found that the optimum modulus of fibre elasticity can be obtained when there is a balance between the removing of impurities and wax and pectin maintenance (Li et al., 2007, Kabir et al., 2012, Vallo et al., 2004). This equilibrium is mainly dependent on the fibre diameter size and the percentage of chemical treatment.



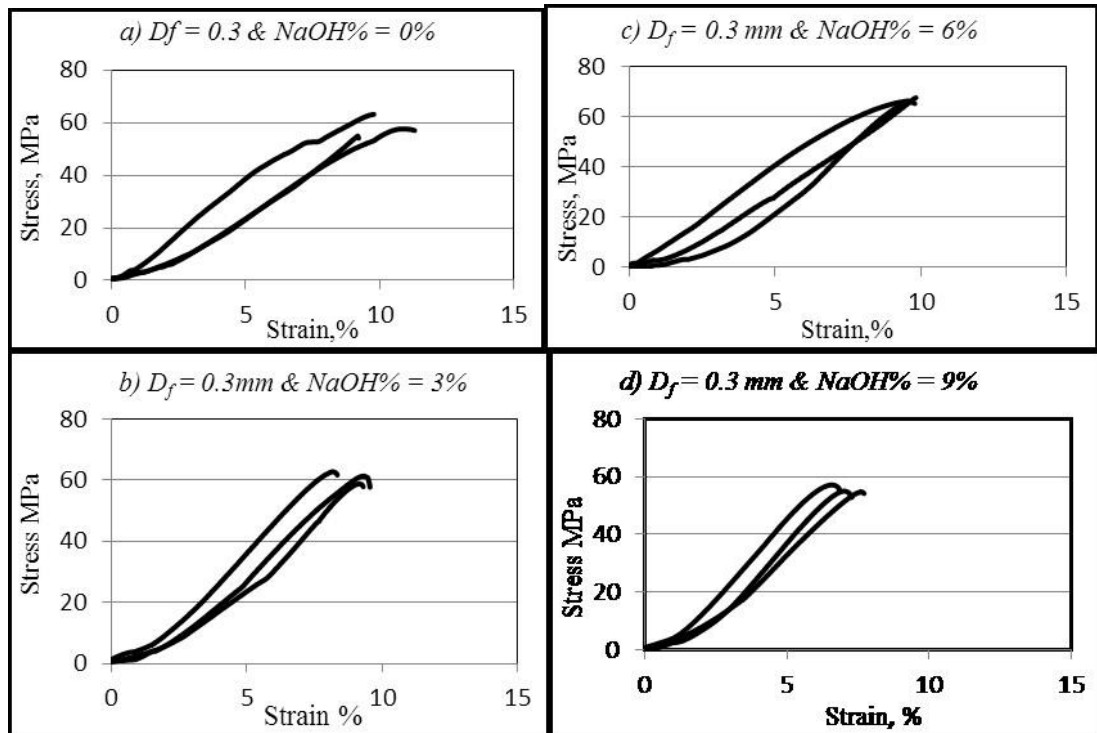
**Figure 4.10: Effect of diameter of fibre and NaOH treatment on modulus of elasticity on single fibre**

#### **4.4 Single fibre fragmentation tensile test**

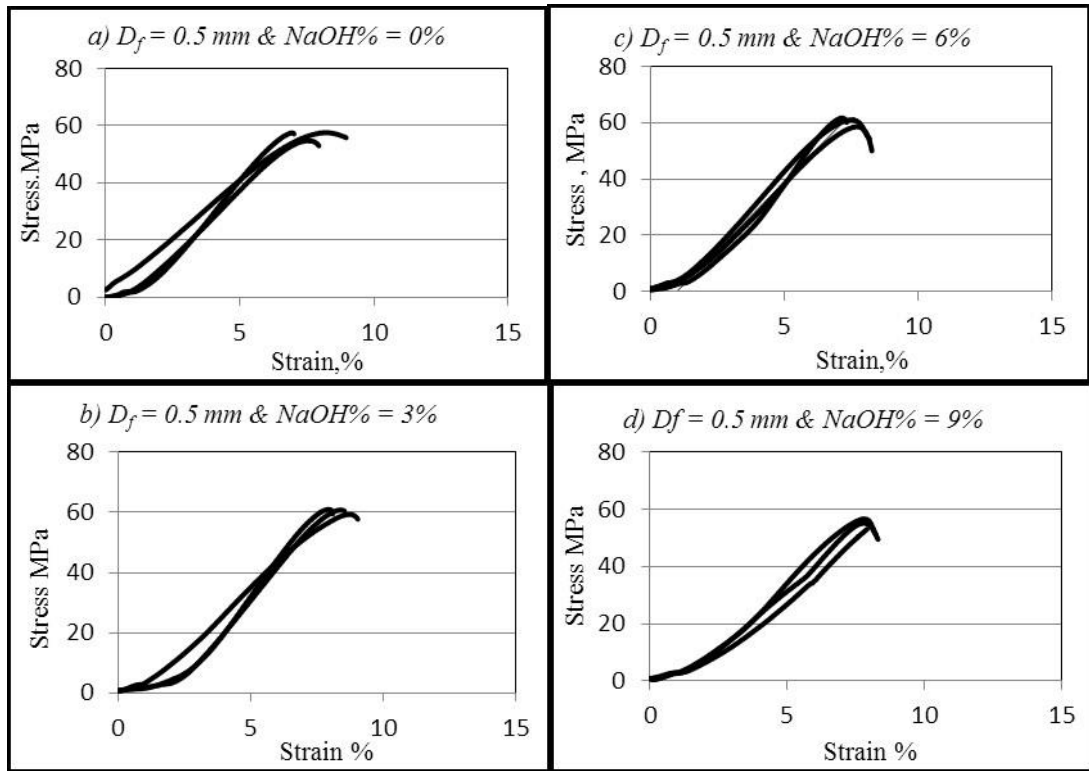
The SFFT is used to measure the interfacial bonding force between the fibre and matrix composite by gauging the tensile stress of the composite and the shear stress between the fibre surface and composite matrix. The importance of SFFT lies in its ability to gauge the compatibility between the fibre and polymer matrix, considered crucial in determining the mechanical behaviour of fibre-reinforced polymer composites.

This present work will study the effect of both DPF diameter sizes, along with the degree of chemical treatment on the interface bonding between the fibre and polymer matrix. The fibre diameters (0.3, 0.5 and  $0.7 \pm 0.05$  mm) and NaOH treatment percentages (zero, 3wt%, 6wt%, 9 wt%) were adopted during this test, according to the literature review in Chapter Two. Figures 4.11, 4.12 and 4.13 show the stress strain curve for each set. In each set, there are three samples, according to the diameter size and NaOH treatment percentage.



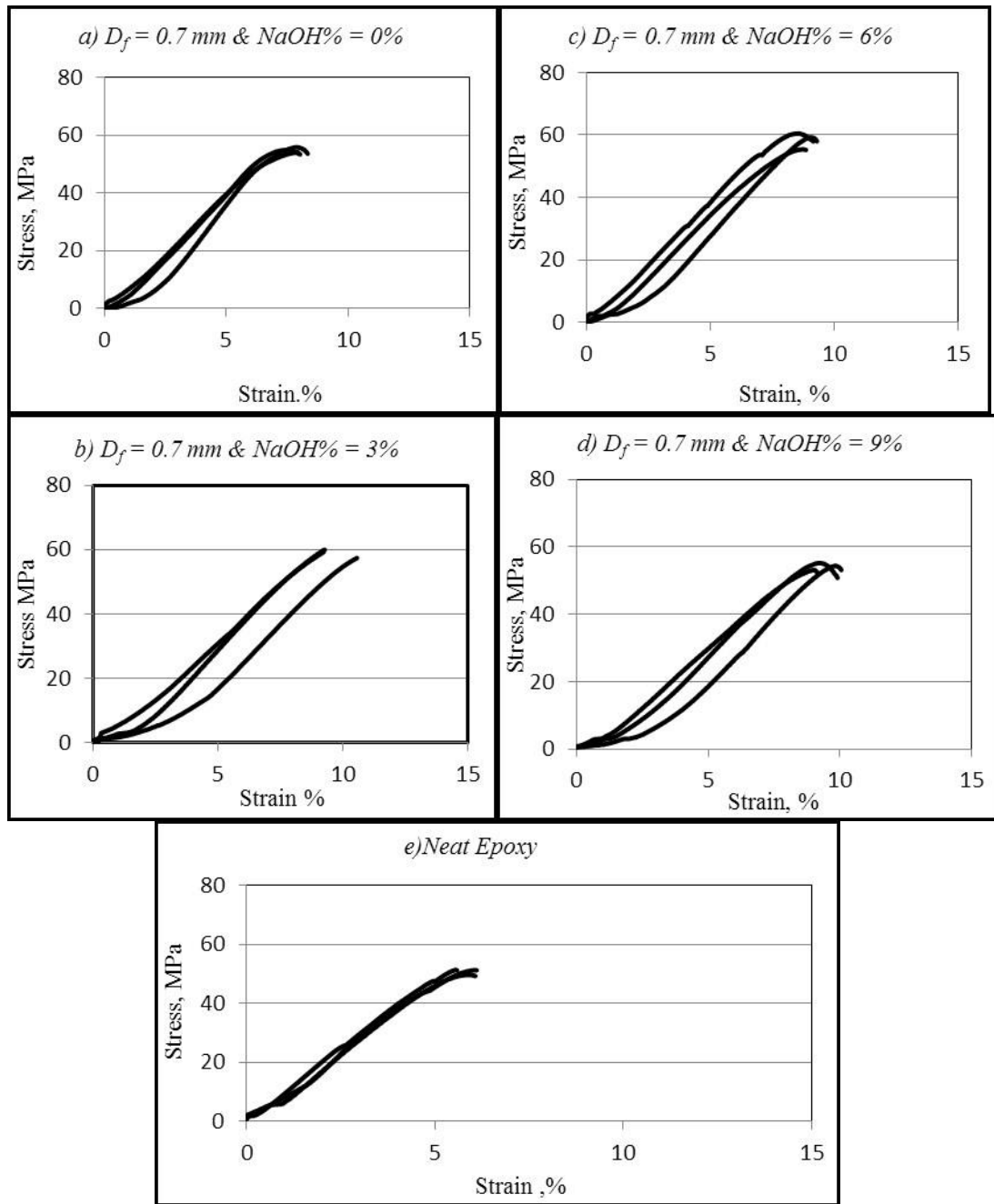


**Figure 4.11: Tensile behaviour of the single DPF fragmentation test (0.3 mm diameter) treated with different NaOH concentrations**



**Figure 1**

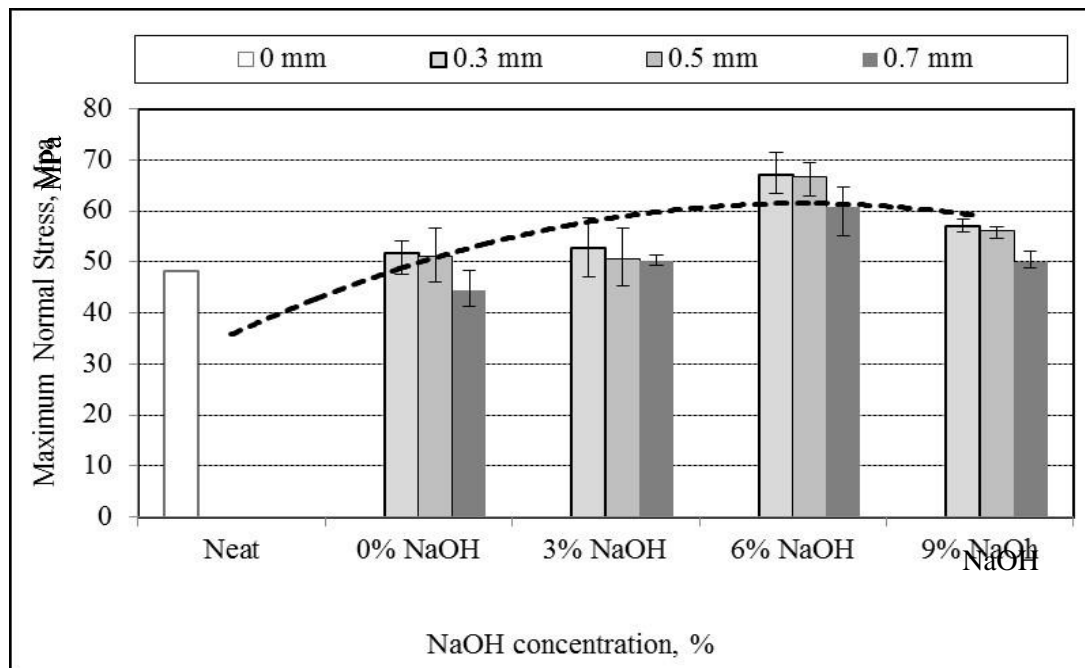
**Figure 4.12: Tensile behaviour of the single DPF fragmentation test (0.5 mm diameter) treated with different NaOH concentrations**



**Figure 4.13: Tensile behaviour of the single DPF fragmentation test (0.7 mm diameter) treated with different NaOH concentrations and NE**

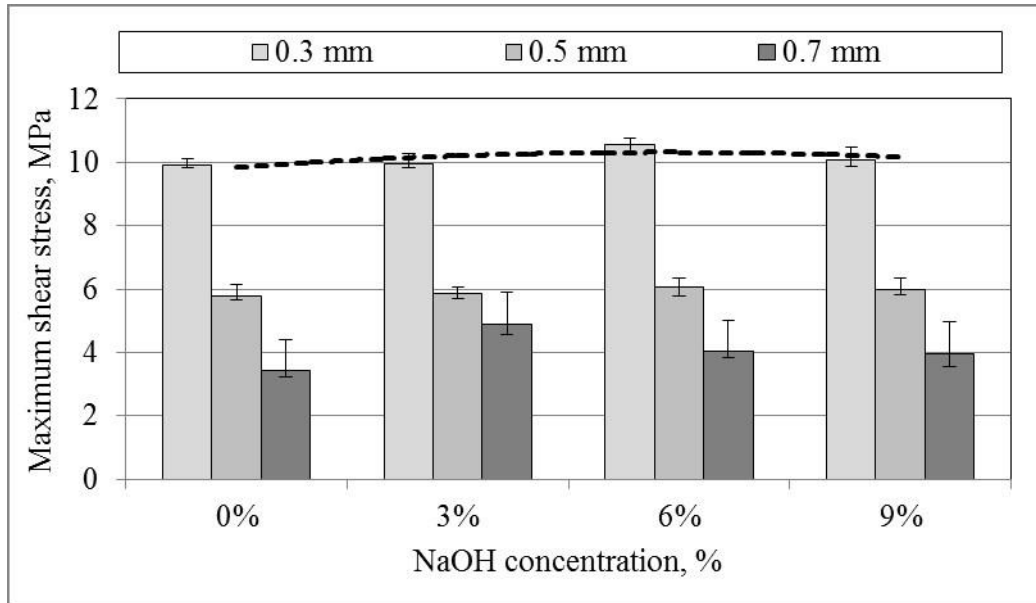
For clarification, the summary of the TS and shear strength of both NE and DPFE composites are shown in Figures 4.14 and 4.15 for different fibre treatments and diameters. In general, adding a fibre to specimen of EC enhances the TS of specimens with all untreated and treated cases (zero to nine per cent NaOH), except at diameter fibres of 0.3 mm at 9% NaOH treatment.

In other words, adding fibres to polymer composites does not always create good results or enhanced effects of the mechanical behaviour of composites. Chemical treatment of natural fibres plays an important role in determining and enhancing the mechanical behaviour of reinforced natural fibre polymer composites (RNFPCs), just as fibre diameter plays an important role.



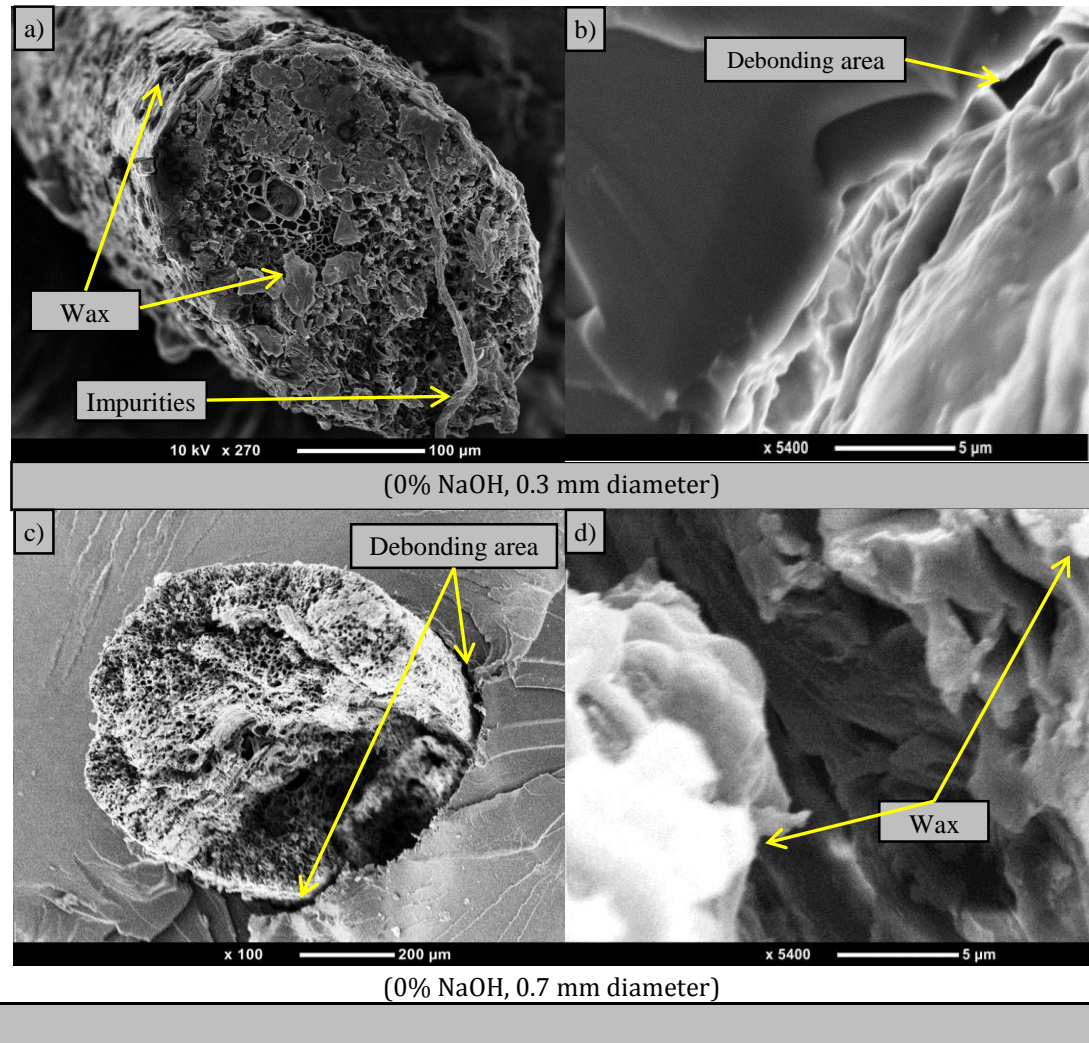
**Figure 4.14:** Effect of diameter of fibre and NaOH treatment on tensile stress of date palm/EC

Conversely, Figure 4.15 shows the effect of chemical treatment on the shear strength (interfacial interaction) between fibre surface and matrix. This highlights that the correct selection of diameter dimensions and chemical treatment proportions for natural fibre leads to optimum results and mechanical behaviour of RNFPCs. In general, the maximum enhancement in mechanical behaviour of RNFPCs was 36% at a fibre diameter of 0.3 mm and 6% NaOH treatment (see Figures 4.11 and 4.12). The worst mechanical behaviour of RNFPCs was -8.5% at fibre diameter and 9% NaOH treatment, compared to mechanical behaviour of NE.



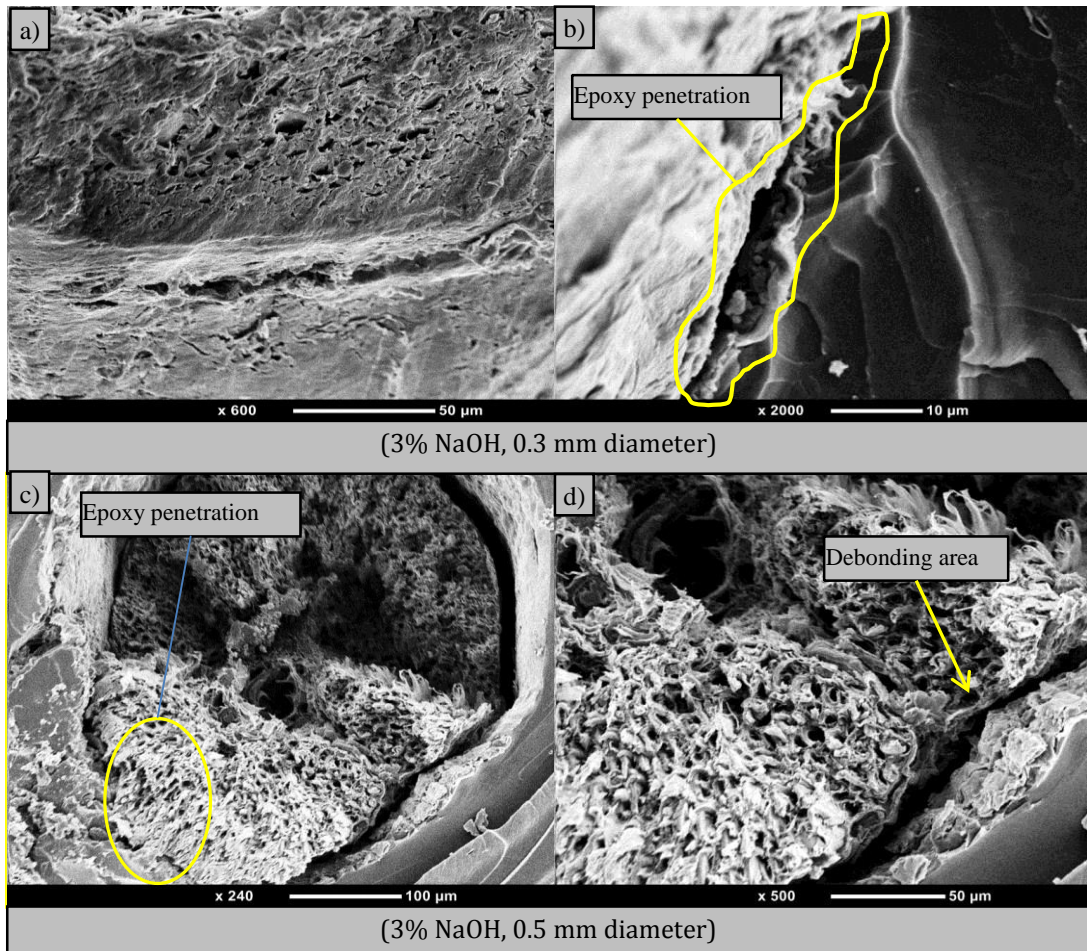
**Figure 4.15: Effect of fibre diameter and NaOH treatment on shear stress on fibre of date palm/EC**

At zero per cent NaOH concentration (untreated), the presence of impurities and an insulating layer of wax on the fibre surface created a debonding region between the fibre and the matrix. This was evident in the micrographs of the sample after the test, as shown in Figure 4.16. Moreover, Figure 4.16 suggests there is no sign of epoxy penetration in the fibre core (Figures 4.16a & 4.16c), which aligns with the notion that the waxy layer insulated the fibre. Further, the fibre's nature (hydrophilic) has a compatibility issue with epoxy nature (hydrophobicity), leading to poor interface bonding between fibre and matrix. Conversely, the date palm/epoxy at the smallest diameter displayed the maximum strength and shear stress, compared to fibre diameters of 0.5 and 0.7 mm. This confirms two concepts: the suitability of solution concentration with the diameter of fibre, and the diameter and probability of increase of fibre impurities or degradation (ageing).



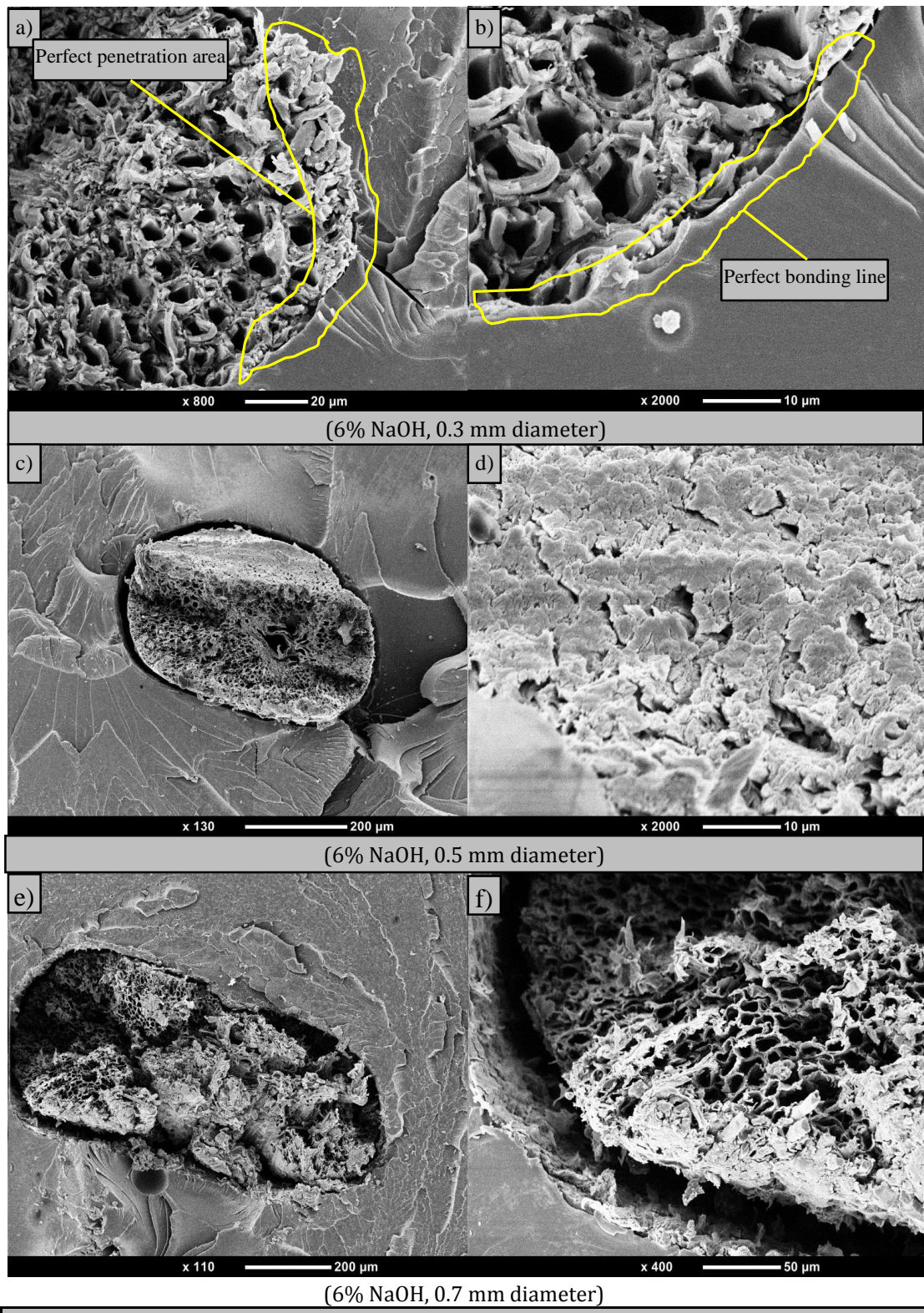
**Figure 4.16: Microscopy of fragmentation samples after testing the untreated DPFE**

Compatible with the previous view, DPFE composites treated with three per cent NaOH exhibit higher TS than the untreated DPFE by about seven per cent. This is not a high increase in the TS; it seems that the three per cent NaOH assisted in removal of some impurities and waxes, resulting in an increased contact area between the fibre core and the epoxy resin. Figure 4.17 shows the enhanced interfacial bonding. However, Figure 4.17c shows incomplete adhesion of the fibre with the matrix, and a small part of the fibre core is filled with the resin.



**Figure 4.17: Microscopy of fragmentation samples after testing the treated DPF (3% NaOH)/epoxy**

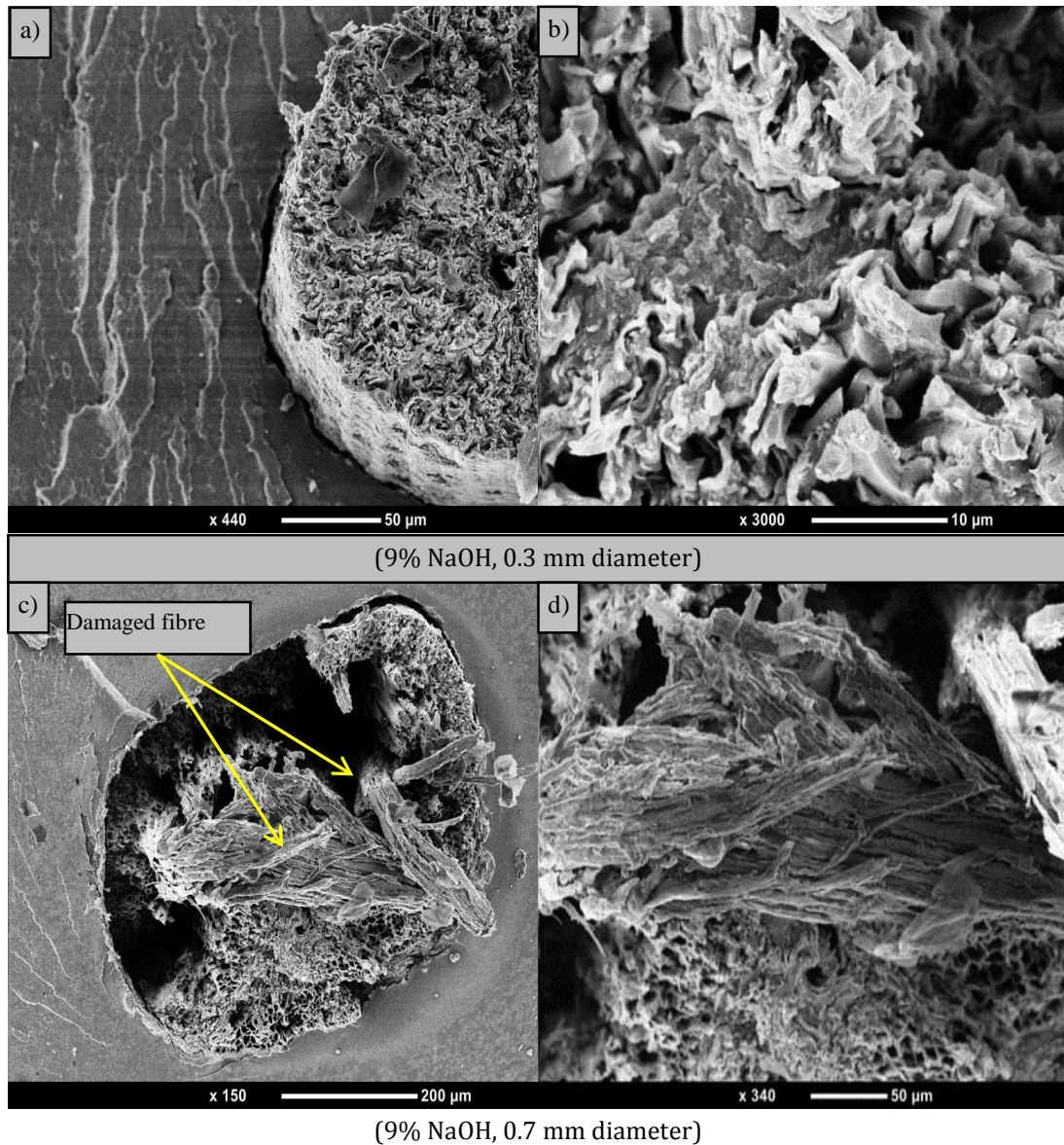
In contrast, the DPFE composite treated with six per cent NaOH shows the maximum TS in all cases. This could clarify that the amount of NaOH solution was enough to achieve equilibrium between removing and cleaning impurities and wax from the fibre and the fibre strength, through reducing the power of NaOH solution to attack the fibre structure. As shown in Figure 4.18, there are perfect bonding lines between fibre and matrix with maintenance of the internal fibre structure.



**Figure 4.18: Microscopy of fragmentation sample after testing the treated DPF (6% NaOH)/epoxy**



At high NaOH concentration of nine per cent, it is clear there is a reduction in the value of the tensile stress; this reduction is not a consequence of the weak interfacial adhesion between the fibre and matrix. Rather, it is due to the weakened fibre structure from the attack and damage of NaOH solution, as mentioned in the fibre surface morphology section and shown in Figure 4.19.



**Figure 4.19: Microscopy of fragmentation sample after testing the treated DPF (9% NaOH)/epoxy**

In general, applying chemical treatment on natural fibres has two main goals: to decrease the fibre moisture to increase compatibility between natural fibre

(hydrophilic) and polymer matrix (hydrophobicity) natures, and to clean the fibre surfaces from impurities that lead to enhancement of the interfacial adhesion between fibre and polymeric matrix.

In contrast, excess treatment could lead to adverse results because of chemical solutions attacking and damaging the fibre structure, then weakening the structure, or highly smoothing or polishing the fibre surface, which leads to a reduction in the interfacial adhesion between fibre and polymeric matrix. Particularly with untreated fibre, remaining impurities created a thick bending area as an insulated layer between fibre and matrix, shown in Figure 4.20a. Conversely, application of three per cent NaOH treated on fibres was not enough to clean the fibre surface of all impurities and waxes. However, it did increase the direct contact between fibre and matrix, which allowed for slight epoxy penetration, as shown in Figure 4.20b. At six per cent NaOH treatment, it was enough to clean the fibre surface from impurities, leading to perfect direct contact between fibre and matrix and increasing the epoxy penetration.

Moreover, this treatment has maintained fibre strength, as shown in Figure 4.20c.

In contrast, the rise of NaOH concentration to nine per cent cleaned the fibre of impurities but also resulted in the NaOH solution attacking the fibre structure and smoothing the fibre surface, which decreased the composite strength, as shown in Figure 4.20d.

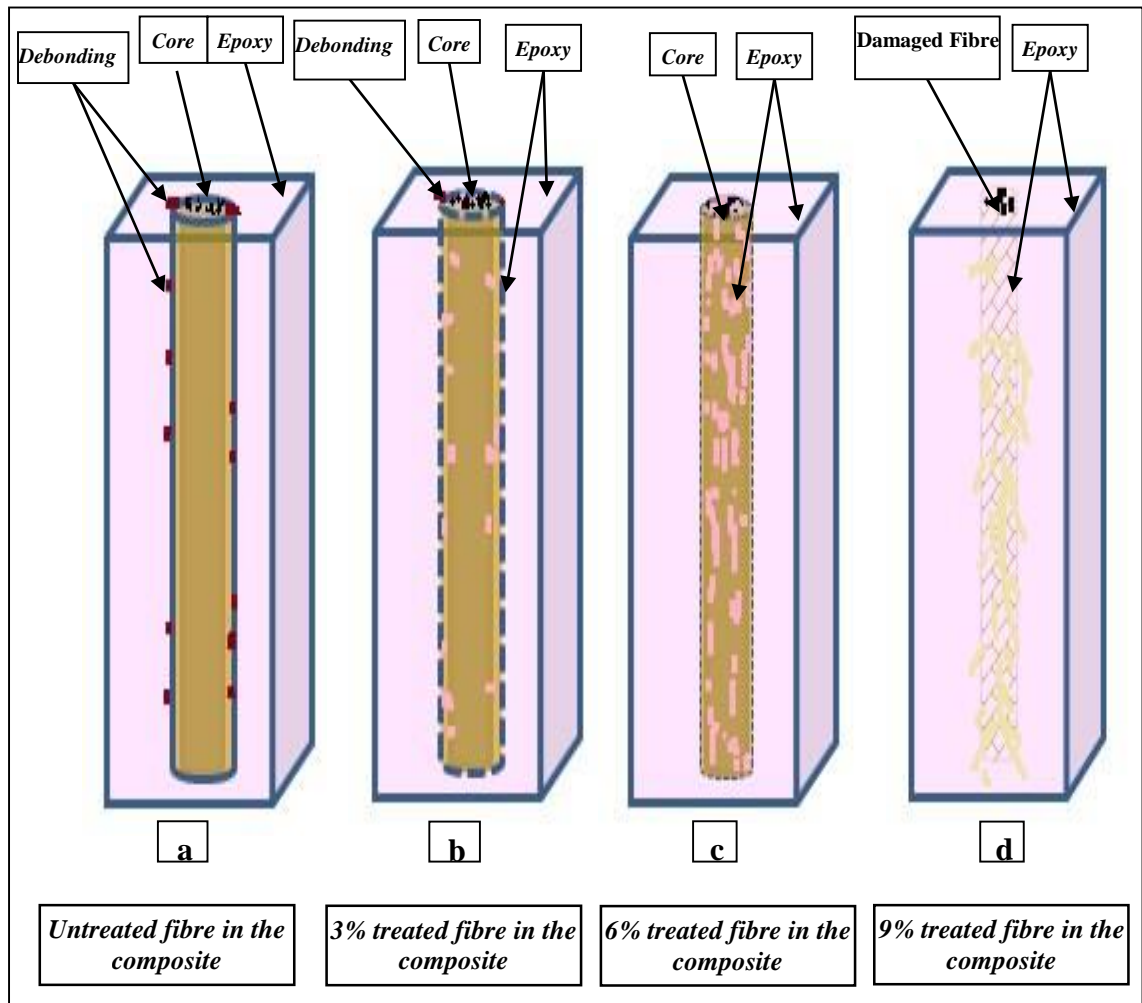


Figure 4.20: Schematic drawing showing the treatment effect of different concentration (0%, 3%, 6% and 9%) on surface and structure fibre

#### 4.5 Comparison to other published works

It is interesting to compare the current results with previous works and examine the compatibility with previous results. Table 4.1 summarises some of the most recent works that study the influence of fibre diameter and chemical treatment on the fibre strength and/or fibre/polymer composite strength. In these previous works, it was obvious that the fibre diameter was considered the key design criterion for natural fibre composite strength. Moreover, the fibre/polymer composites have shown the optimum mechanical behaviour at the smallest diameter, which was congruent with the results of this study (Andersons et al., 2011, Virk et al., 2010). The table shows a compatibility

between the chemical treatment and the enhancement of fibre strength and/or interfacial adhesion between fibre and polymer (Alsaeed et al., 2013, Edeerozey et al., 2007, Haque et al., 2009, Rong et al., 2001). The chemical treatment could result in a reduction of the fibre/polymer composite strength (Arrakhiz et al., 2012). Moreover, this conclusion corresponds with the current results of this study, which show that six per cent NaOH was the optimum alkali concentration, with nine per cent NaOH leading to a negative effect on the mechanical behaviour of the fibre/polymer composite.

**Table 4.1: Summary of the previous works on optimum diameter and chemical treatment concentration on mechanical behaviour of fibre/polymer composites**

Fibre	Matrix	Treatment	Remarks
Jute (Virk et al., 2010)			The optimum TS of fibre was at the smallest fibre diameter.
Flax (Andersons et al., 2011)			The optimum TS of fibre was at the smallest fibre diameter.
Date palm (Alsaeed et al., 2013)	epoxy	NaOH (0%–9%)	The optimum TS of fibre was at 3% NaOH. The optimum TS of composite was at 6% NaOH.
Kenaf (Edeerozey et al., 2007)		NaOH (0%–9%).	The optimum TS of fibre was at 6% NaOH.
Palm (Haque et al., 2009)	polypropylene	The standard diazotization method.	15% enhancement in TS of composite compared to untreated fibre.
Coir (Haque et al., 2009)	polypropylene	The standard diazotization method	10% enhancement in TS of composite compared to untreated fibre.
Sisal (Rong et al., 2001)	epoxy	2% NaOH.	18% enhancement in TS of composite compared to untreated fibre.
Coir (Arrakhiz et al., 2012)	polyester	NaOH (1.6 mol/L).	4% reduction in TS of composite compared to untreated fibre.



## 4.6 Chapter summary

The main findings of the current work are:

- The strength of the single fibre increased with the decrease of the fibre diameter and/or the NaOH concentration. The NaOH treatment has many effects on the fibre and interfacial adhesion between fibre and matrix, such as surface morphology, elimination of impurities, fibre fibrillation and lowering of the polarity between fibre and matrix, which should determine the optimum concentration treatment.
- The smooth surface of the fibre and the degree of polymer penetration of the fibre play an intrinsic role in determining the strength of fibre/polymer composite material.
- Low concentration of alkali treatment leads to slight enhancement of mechanical behaviour of composite because of the inability of treatment to make high modifications in fibre surface and decrease the polarity of fibre.
- High concentration of alkali treatment could lead to the attrition of the fibre's main structure, which leads to a weaker fibre and composite.





## **Chapter 5: Influence of graphite content on mechanical and wear characteristics of epoxy composites**

### **5.1 Introduction**

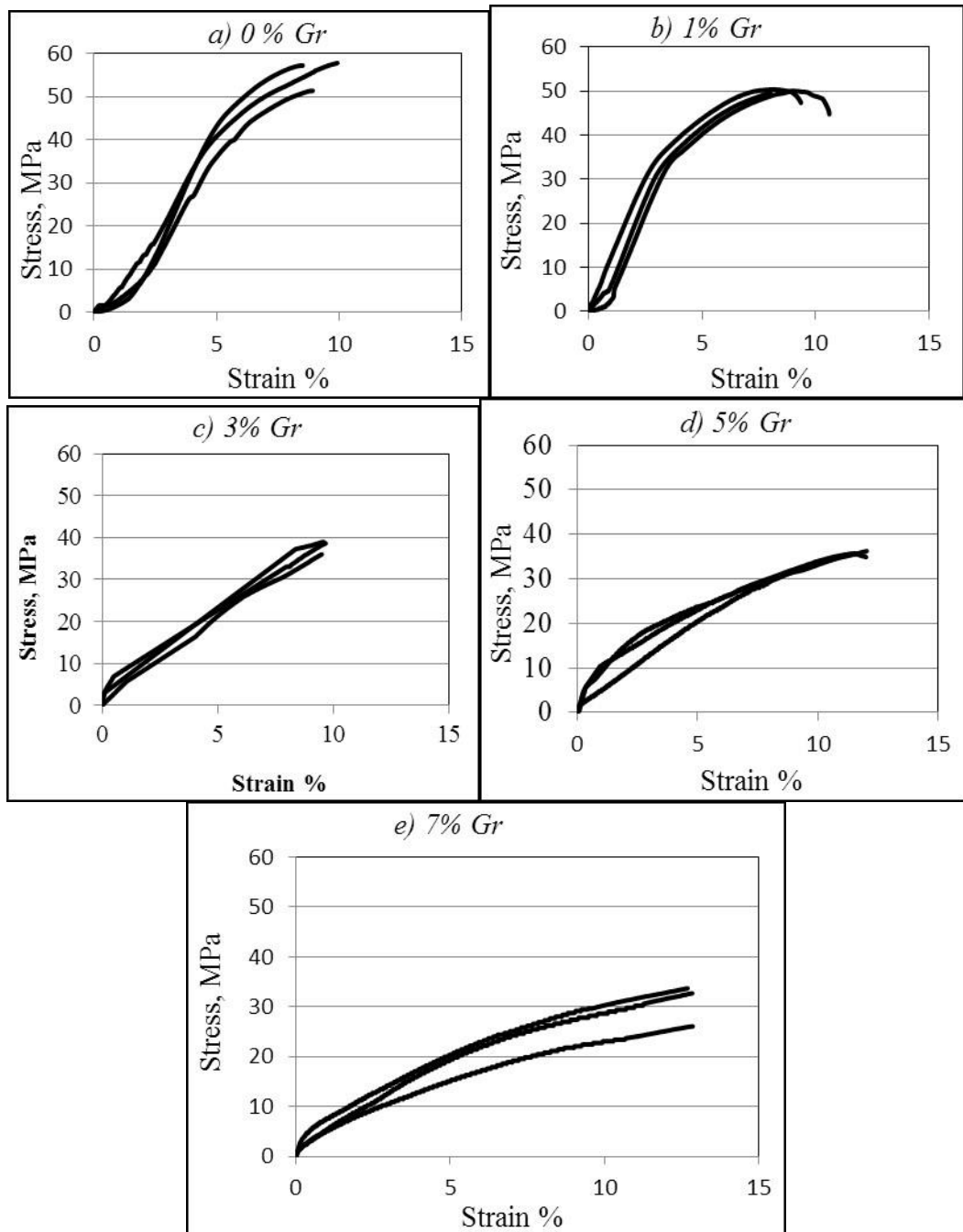
In this chapter, the influence of the graphite weight presence in ECs is evaluated from mechanical and tribological perspectives. Different weight percentages were used in the sample preparation (zero to seven per cent) for tensile, hardness and adhesive wear experiments. The optimum percentage of the graphite addition to the epoxy is determined, which will be used in the DPF/graphite/ECs to gain optimum mechanical and tribological properties for the ECs. In the first part of this chapter, ultimate TS and modulus of elasticity values and fracture morphology are determined. In the second part, specific wear rate, friction coefficient, interface temperature and surface morphology of the composites are determined. Then the results are discussed to gain the optimum mixing ratio of graphite with the epoxy. At the end of this chapter, the main findings are discussed with the previous related works and the findings are summarised.

### **5.2 Tensile properties of graphite/epoxy composites**

#### **5.2.1 Stress strain diagram, ultimate TS and modulus of elasticity**

The tensile testing was performed on more than five samples. The closest three trends are presented in this study. Figures 5.1a–e show the stress strain diagram of the ECs with different graphite percentages: zero, one, three, five and seven weight per cent, respectively. In general, the trend of the stress is almost the same for all the composites, since there is a clear region of elastic deformation and a slight area of plastic deformation. The composites exhibit brittle failure with all the percentages of graphite. This is due to both materials being brittle, since the epoxy is thermoset material and the graphite is considered to be brittle as reported by Berto et al. (2013). Therefore, such behaviour is expected. It should be mentioned here that the main idea behind

graphite addition is to be a solid lubricant, not to be a reinforcement to improve the mechanical properties. However, regarding strain, there is no remarkable difference between the composites. In contrast, there is deterioration in the maximum TS with the addition of the graphite fillers. The deterioration could be because of the low interaction between the epoxy matrix and the graphite fillers.



**Figure 5.1: Stress strain diagrams of graphite/ECs**

Sengupta et al. Sengupta et al. (2011) comprehensively reviewed the mechanical properties of different polymer composites based on graphite fillers and confirmed that the addition of more than four per cent graphite significantly reduces the TS of different polymer composites, such as PPE (Celik and Warner, 2007), EVA (George and Bhowmick, 2008), PMMA (Ramanathan et al., 2008), HDPE (Zheng et al., 2004) and PLA (Narimissa et al., 2012). In those studies, the interaction, distribution, size and orientation of the graphite have a great effect on mechanical properties. Despite these studies attempting different techniques to improve the tensile properties of the composites by graphite, all the reported research showed no improvement. Conversely, such a decrease has been reported with metal alloys as well. The TS of grey cast iron alloy has decreased with the increased amount of the graphite addition up to eight per cent (Wang et al. Wang et al. (2007)). This can be further clarified with the micrographs of the fractured samples in the following sections.

The summary of the tensile data is given in Figure 5.2, displaying the ultimate TS (maximum) and the modulus of elasticity (Young's modulus). The figure clearly shows a reduction in the TS of the ECs, since there is a reduction of about 90% with a large amount of graphite (seven weight per cent). Such a reduction is not desirable from mechanical and tribological perspectives. Therefore, a slight reduction in the TS could be considered in the design. At one and three weight per cent of graphite, there is a reduction in the TS of about 10% and 20%, respectively, since the TS reduces from 55 MPa to 50 MPa and 47 MPa, respectively. This reduction can be improved with the addition of the natural fibres and will be explained in Chapter Six. Moreover, the tribological behaviour of the ECs, based on different weight fractions of graphite, will determine the optimum weight percentage of the graphite. This will be discussed in the following sections.

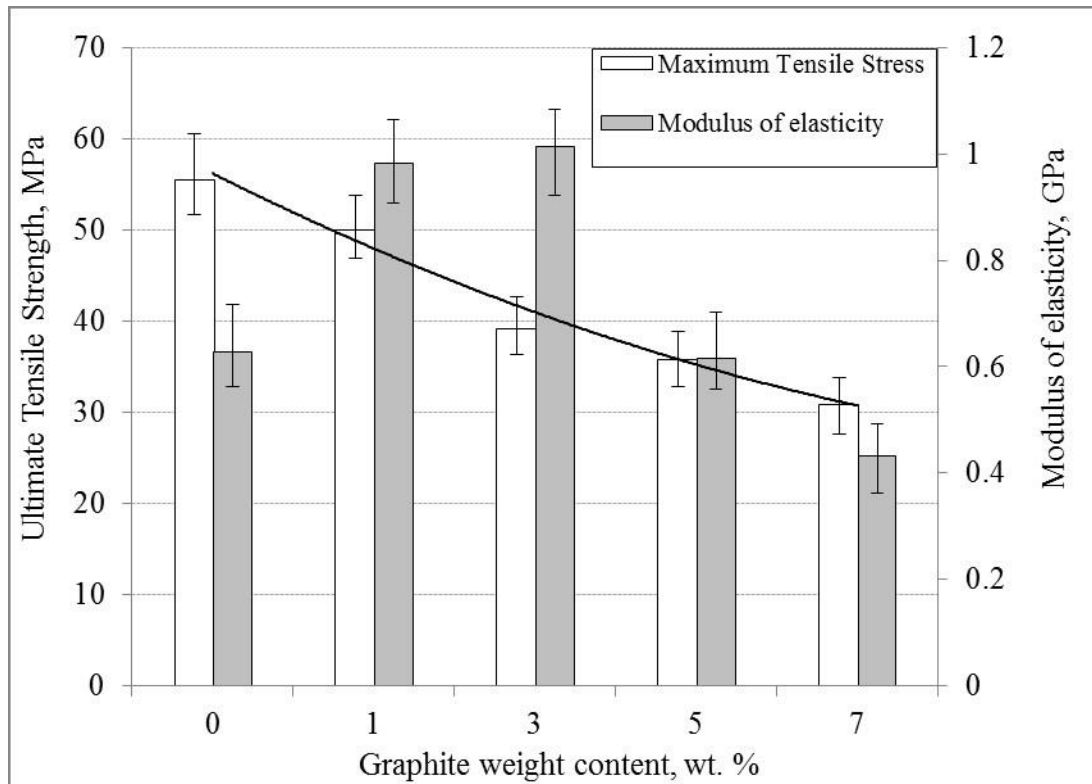
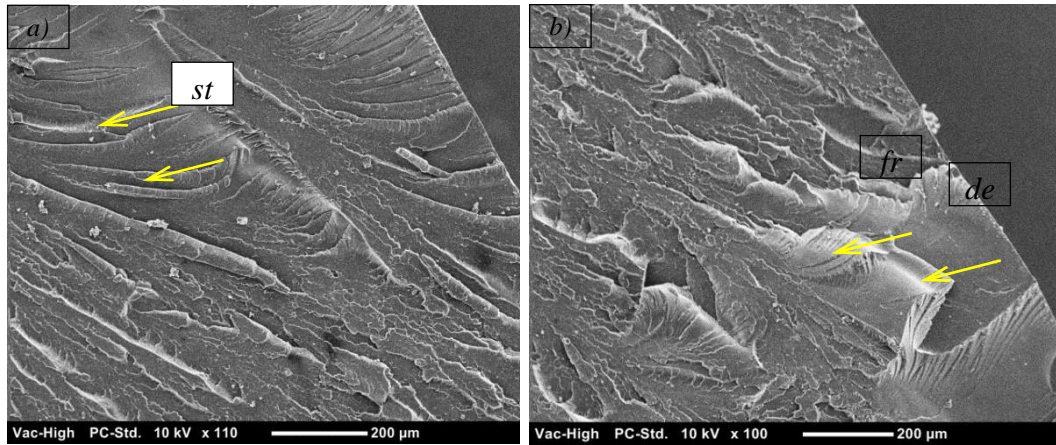


Figure 5.2: Ultimate TS and modulus of elasticity of graphite/ECs

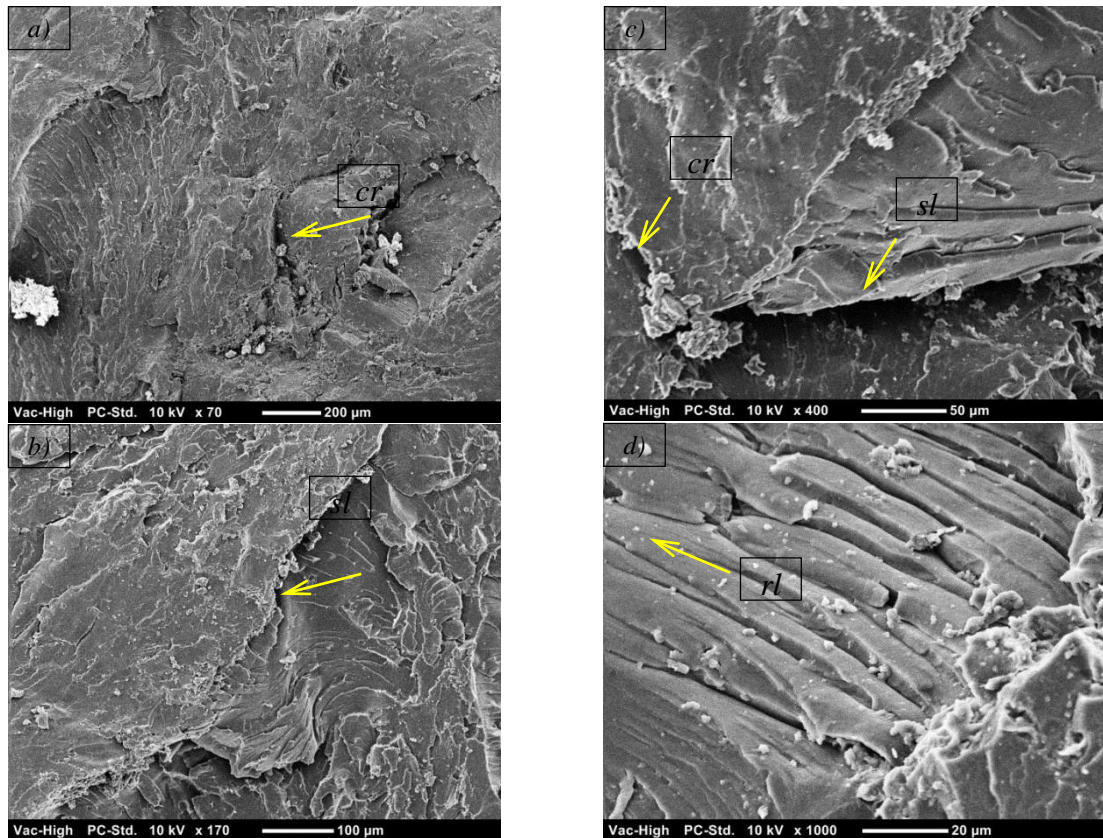
### 5.2.2 Fracture behaviour of the epoxy composites

The micrographs of the failed NE samples after the test are given in Figure 5.3. Since the micrographs are for the NE, there are no obstacles or initiators for the cracks. There are irregular fracture features. The figure clearly shows a cleavage failure, which represents the nature of the thermoset epoxy. The fractured surface does not look smooth. This means that the material resisted the shear loading and detachments in the molecules occurred. Such failure has been reported by some published works (Kanchanomai and Thammaruechuc, 2009) in which plain strain fracture mechanism was evident.



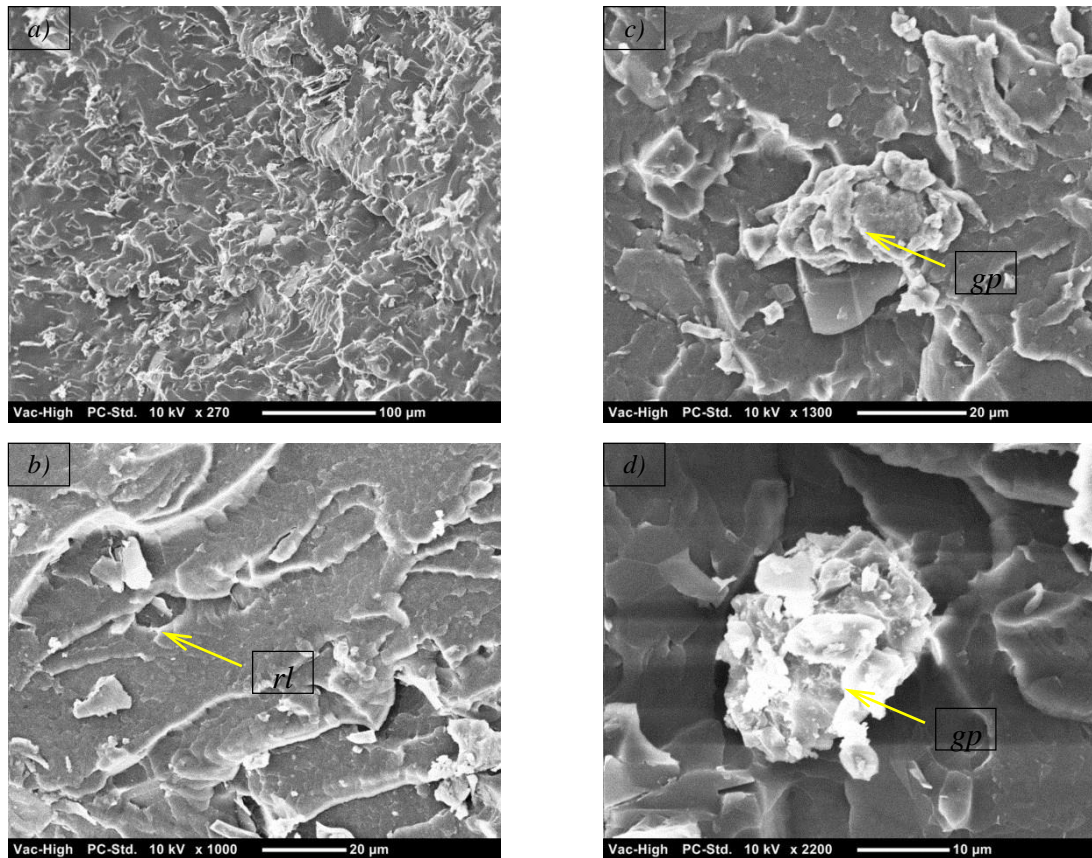
**Figure 5.3: Micrographs of the NE after tensile testing—st = stretching, de = detachment, fr = fracture**

The micrographs of the one weight per cent graphite/EC are shown in Figure 5.4 with different magnifications. There are obvious differences between the micrographs of the NE and the EC with one per cent, since the brittle failure features are less than the NE, that is, there is no sharp fracture on the surface. In Figure 5.4d, there is a river-like pattern and stretching, indicating resistance to the load. Shear lips are very clear in Figures 5.4b and 5.4c. From this figure, it is clear that the graphite interface with the epoxy seems to be acceptable compared to the literature on the graphite pallet (Sengupta et al., 2011) and nano-clay (Jawahar et al., 2006, Alamri and Low, 2012), since there are no voids (Tang et al., 2013) and/or debonding (Kim and Khamis, 2001) of fillers at this weight fraction of graphite. However, some researchers have reported that such fillers can be crack initiators (see Delucchi, Ricotti & Cerisola Delucchi et al. (2011) Tang et al. Tang et al. (2013)). In the current work, at this low fraction of graphite, there is no sign of crack initiation.



**Figure 5.4: Micrographs of the 1% graphite/ECs after tensile testing—cr = cracks, sl = shear lips, rl = river-like pattern**

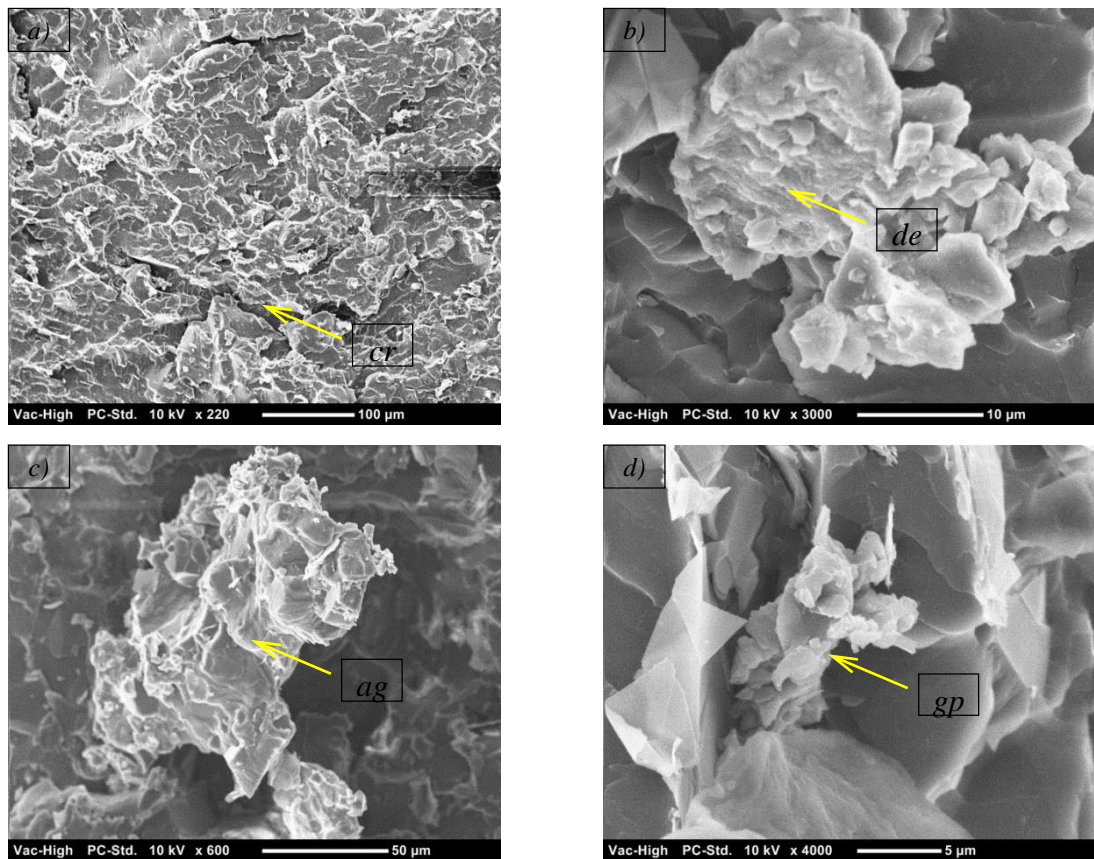
For three weight per cent graphite in ECs, the micrographs of the fractured samples are displayed in Figure 5.5. The figure shows sign of shear lips surrounded by debris, which seems to be the graphite fillers. At a higher magnification, Figures 5.5b and 5.5d display the graphite with a size of 10–20  $\mu\text{m}$ . The filler size used in the current study is 45  $\mu\text{m}$ . Figure 5.5c shows a sign of stretching, indicating a good resistance to the load. Further, there is no evidence of voids and no detachments of fillers can be seen. This represents a good interfacial adhesion of the filler with the matrix at such low weight content of the graphite. It should be mentioned here that, in the fabrication process of the graphite/ECs, an ultrasonic machine was used for 1 hour before the solidification process occurs to assist the dispersion of the graphite and get out of the bubbles. This technique could contribute to better homogenisation of composites compared to the other composites in the literature.



**Figure 5.5: Micrographs of 3% graphite/ECs after tensile testing—rl = river-like pattern, gp = graphite particle**

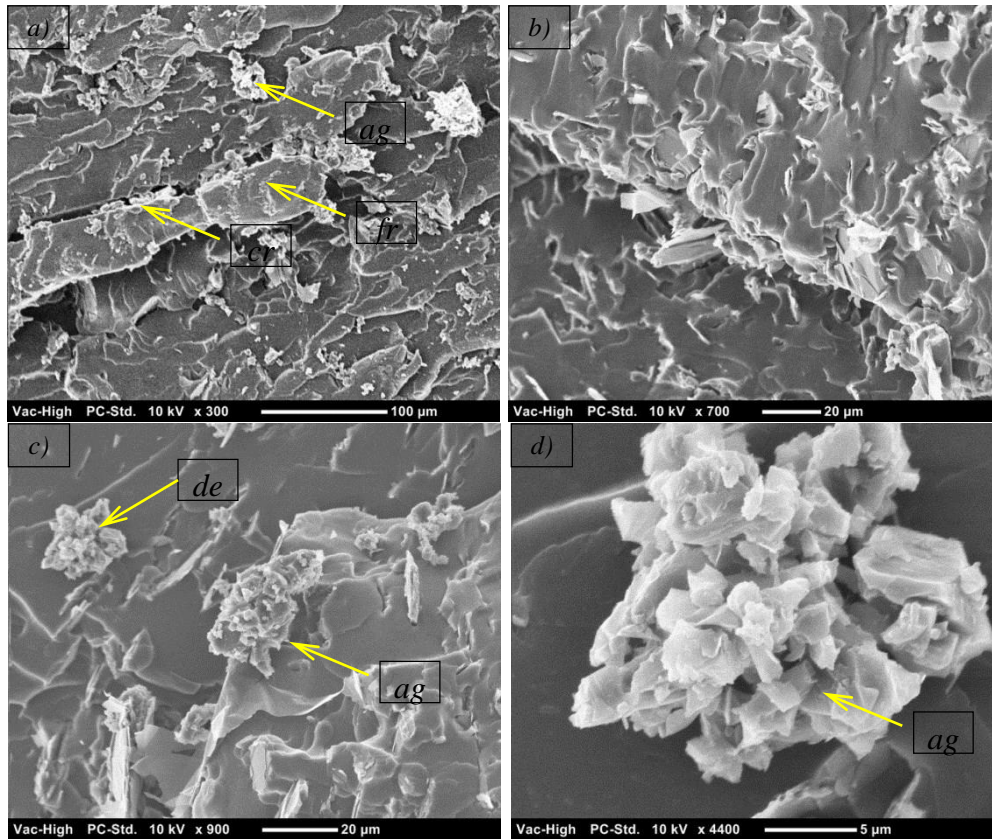
At the very high weight percentage of graphite in the ECs (five weight per cent), the micrographs (Figure 5.6 ) of the fractured samples display clusters and aggregation of graphite. It seems a large amount of aggregated graphite significantly deteriorates the microstructure of the composites, leading to debonding and a fragmentation process taking place, (see Figure 5.6c). Despite ultrasonic usage in the fabrication process, the large percentage of graphite in the composites influenced the quality of the composite mixing and integration between the fillers and the resin during the curing process. This correlates with published works on nano-clay/epoxy (Alamri and Low, 2012), graphite pallet/epoxy (Sengupta et al., 2011) and graphite/polyester composites (Sengupta et al., 2011). This is highly pronounced at seven weight per cent of graphite in the ECs, as shown in Figure 5.7. In this figure, micro and macrocracks can be seen. These could have been initiated by the poor interface between the large aggregated amount of

graphite and the resinous regions. In addition, there are signs of filler detachment in Figures 5.7b and 5.7c.



**Figure 5.6: Micrographs of 5% graphite/ECs after tensile testing—rl = river-like pattern, gp = graphite particle, de = debonding, ag = aggregation**





**Figure 5.7: Micrographs of 7% graphite/ECs after tensile testing—de = debonding, ag = aggregation, cr = cracks, fr = fracture**

For the influence of graphite on the hardness of the epoxy, considering different weight percentage of graphite, Figure 5.8 indicates that an increase in graphite percentage increases the composite hardness. It seems that the hardness of graphite is greater than epoxy (82.25). Jana and Zhong (2009) and Shivamurthy et al. (2013) worked on glass fibre reinforced epoxy composites filled with different volume fraction of graphite. In those works, the tribological performance was enhanced with the increase percentage of the graphite up to 9 %. It is known that under adhesive wear loading, when the hardness of the surfaces increases, the adhesive wear enhanced. In other words, the current results are in agreement with the published works. This is promising for the tribological performance of epoxy for adhesive wear applications, since greater hardness is desirable for low surface deformation during rubbing. However, from the results of the tensile experiments and the surface observations, one can recommend that three weight per cent of the graphite is the maximum amount for reasonable and acceptable mechanical and microstructure ECs characteristics.

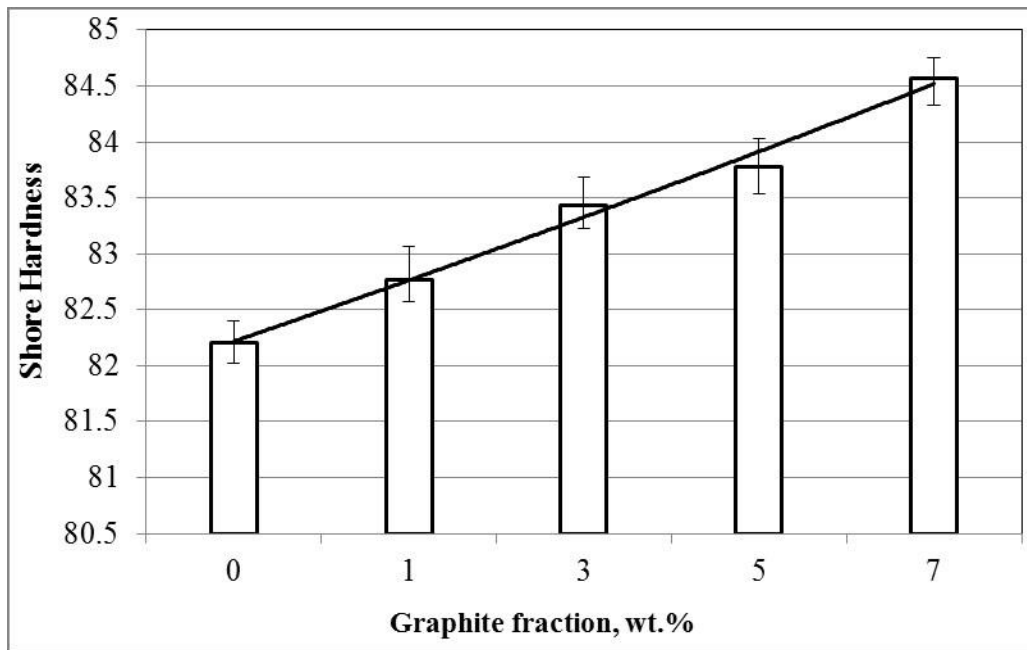


Figure 5.8: Shore D hardness of graphite/ECs

## **5.3 Tribological performance of the epoxy composites based on different graphite contents**

### **5.3.1 Running in and steady state of the adhesive wear**

Specific wear rates of the ECs, based on different weight fractions of graphite, are presented in Figure 5.9 for different sliding distances. At the initial rubbing process (before three kilometres sliding distance), the value of the specific wear rate is relatively high compared to those after three kilometres sliding distance. This is a well-known phenomenon, known as the running in process. At this stage, the asperities in contact are at the first stage of the interaction process leading to high mass removal from the soft rubbed body. In the current process, the rubbing takes place between the epoxy and the stainless steel. Since the stainless steel is much harder and tougher than the epoxy, it is expected that the epoxy will lose surface tips to adhere on the stainless steel counterface. This is illustrated in Figure 5.10. This proposal may be confirmed with the assistance of micrographs of the worn surfaces. Moreover, the roughness profile of the counterface may be influenced by the rubbing process, since modification could occur (Narish et al., 2011, Chin and Yousif, 2010, Chand et al., 2010, Chand and Sharma, 2008). The modifications on the counterface wear track played an important part in controlling the wear performance of some polymeric composites, such as kenaf/epoxy, glass/polyester and carbon/ECs, (Narish et al., 2011, Chin and Yousif, 2010, Chand et al., 2010, Chand and Sharma, 2008, Hao et al., 2011).

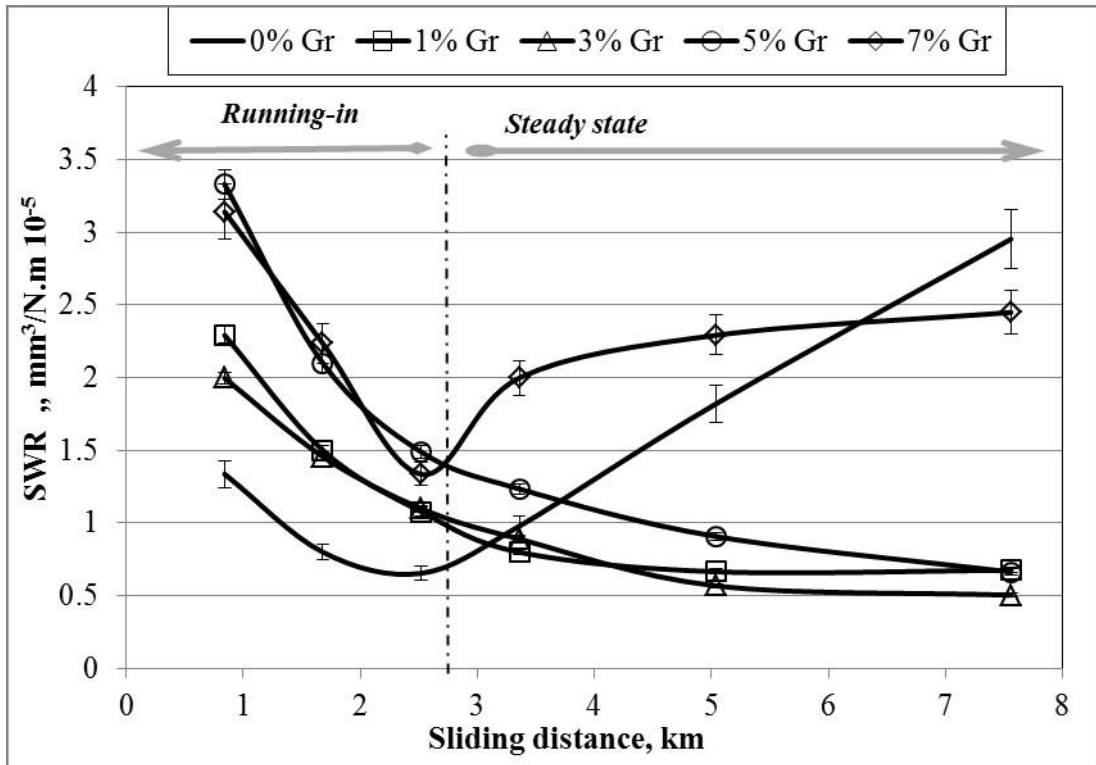


Figure 5.9: Specific wear rate v. sliding distance of graphite/ECs

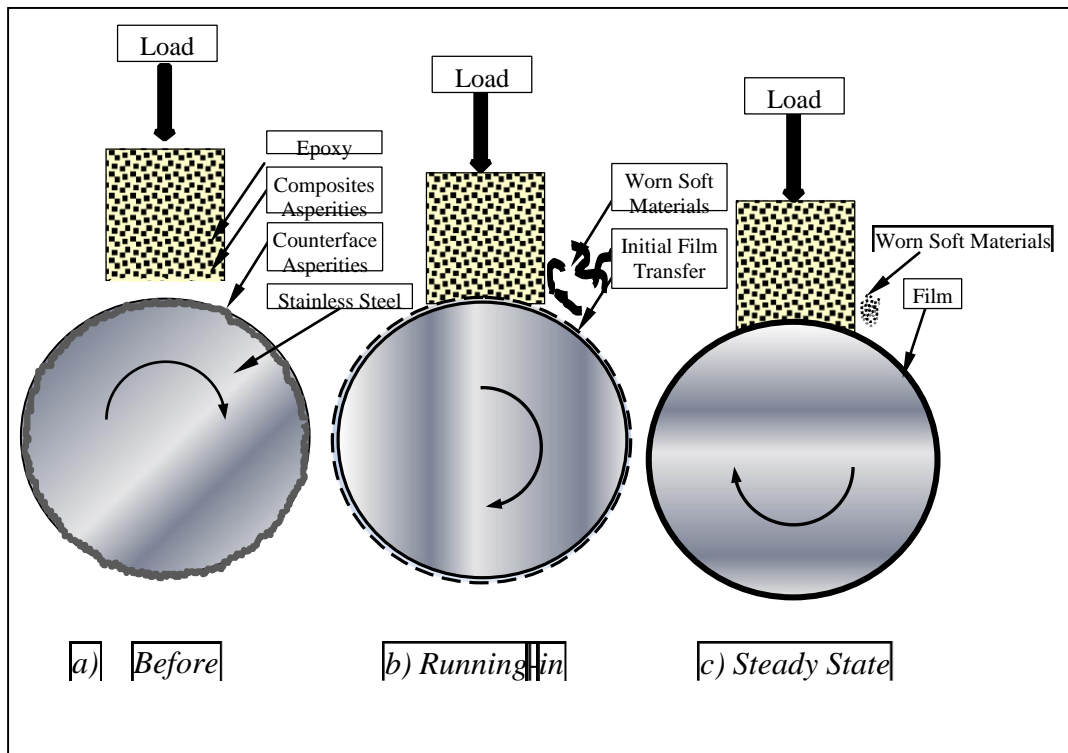


Figure 5.10: Schematic drawing representing the running in and steady state

In the current study, it is important to find out the optimum graphite content percentage in the ECs to assist in the next stage of the project. In the next stage, the ECs will be

based on the graphite and the DPFs. The current study revealed that the optimum graphite percentage is about three per cent, which leads to the lowest specific wear rate at the steady state, as in Figure 5.11. To understand the reasons for better wear performance of the epoxy at this percentage, SEM and the roughness profile of the composite and the counterface may assist.

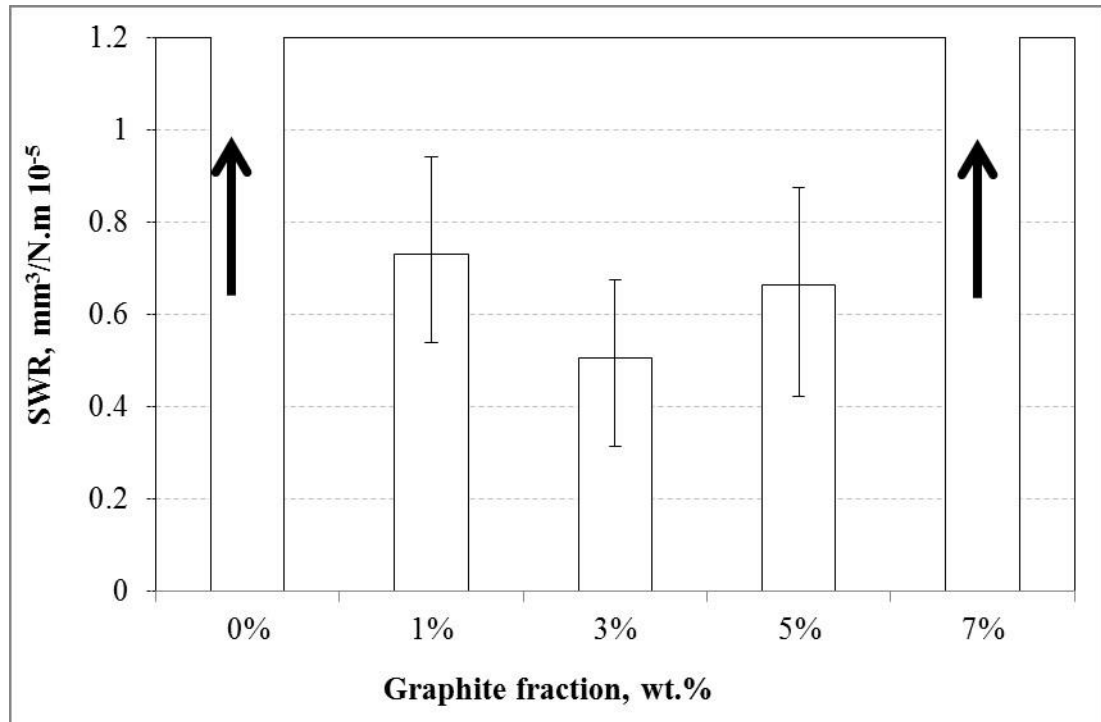


Figure 5.11: Specific wear rate at the steady state of the graphite/ECs after 7.5 km sliding distance

### 5.3.2 Running in and steady state of the coefficient of friction

The friction coefficient of the ECs, as a function of the sliding distance, is shown in Figure 5.12 for different graphite contents in the ECs. The figure shows that the running in stage for the friction coefficient is not obvious, since a clear steady state of the friction coefficient appeared within a few seconds of the sliding. However, some fluctuation remained in the friction coefficient values with the sliding distance for almost all the composites. This indicates that some modification is occurring on the counterface wear track during the sliding. Further, the NE exhibits high friction coefficient values compared to its composites. Such high friction should reflect high wear resistance since the friction is the resistance in the interface. In other words, when the resistance is high, the weight loss is less with high frictional force.

However, in this research, the NE exhibits poor wear resistance associated with high friction coefficient. In the thermosets, such as epoxy and polyester, there is a phenomenon called ‘stick slip’, which occurs between the polymer surface and the counterface. This has been reported in the literature with pure thermosets, such as polyester (Samyn et al., 2005, Eiss and Hanchi, 1998, Zhang and Li, 2003). In such a phenomenon, there is a generation of weak film transfer of pure polymer on the counterface. Film detachment takes place during the rubbing process because of the high shear associated with high temperatures in the interface, which leads to high mass removal from the surface and high friction.

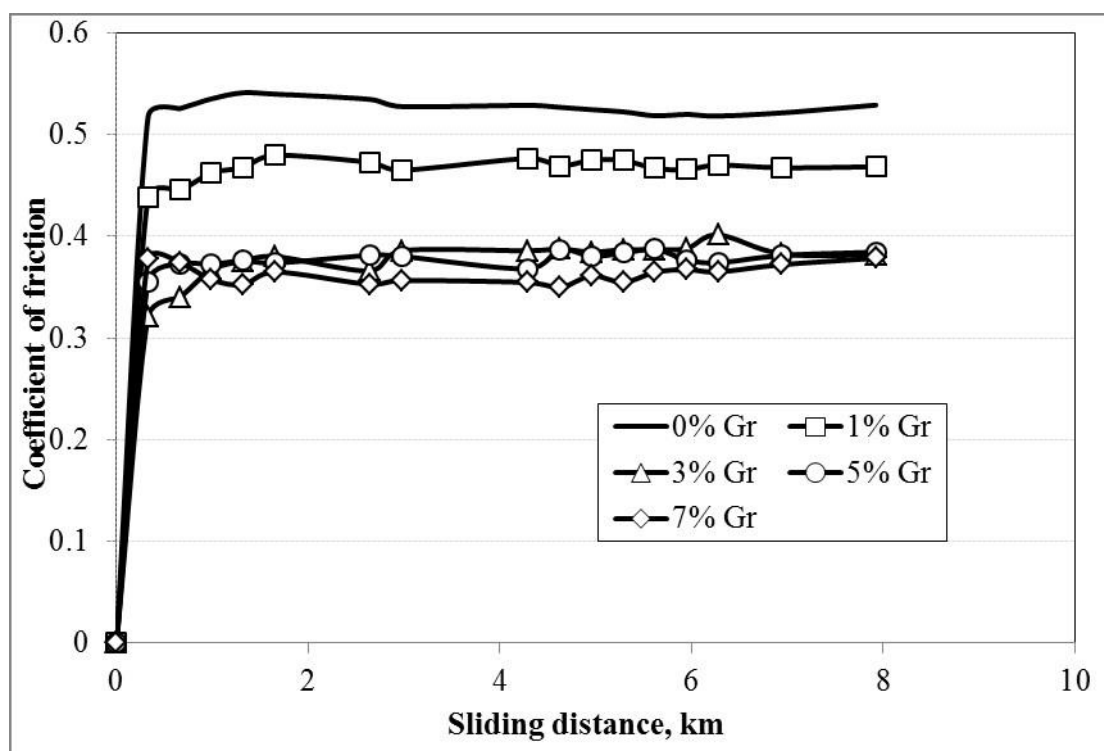


Figure 5.12: Coefficient of friction v. sliding distance of the composites

The presence of graphite in the composites assists in reducing the friction coefficient, since graphite is well known as a solid lubricant material. This is the main reason it was selected as a filler in the current study. In Figure 5.12, it seems the addition of the one weight per cent of graphite reduces the friction coefficient of the composites by about 12%. A higher amount of graphite (more or equal to three weight per cent) in the ECs resulted in a friction coefficient reduction of about 31%. Basically, this reduction in the friction coefficient is because of the generation of lubricant graphite film on the counterface. It should be mentioned here that a very visible black film is

generated on the counterface during the sliding of the ECs containing more or equal to three weight per cent of graphite. In other words, more or equal to three weight per cent graphite in EC is considered a promising filler for the DPFE composites. From the mechanical and adhesive wear characteristics of the graphite/ECs, considering different contents of graphite, three weight per cent of graphite exhibited the optimum weight fraction that achieved acceptable mechanical and adhesive wear performance for the composites. From a frictional perspective (see Figure 5.13), three per cent of graphite or above introduces similar frictional performance. Based on this, three per cent graphite can be considered the optimum weight fraction for the ECs from tribological and mechanical perspectives. This weight percentage is used to fabricate and test the DPF/graphite/ECs, achieving good mechanical and tribological performance.

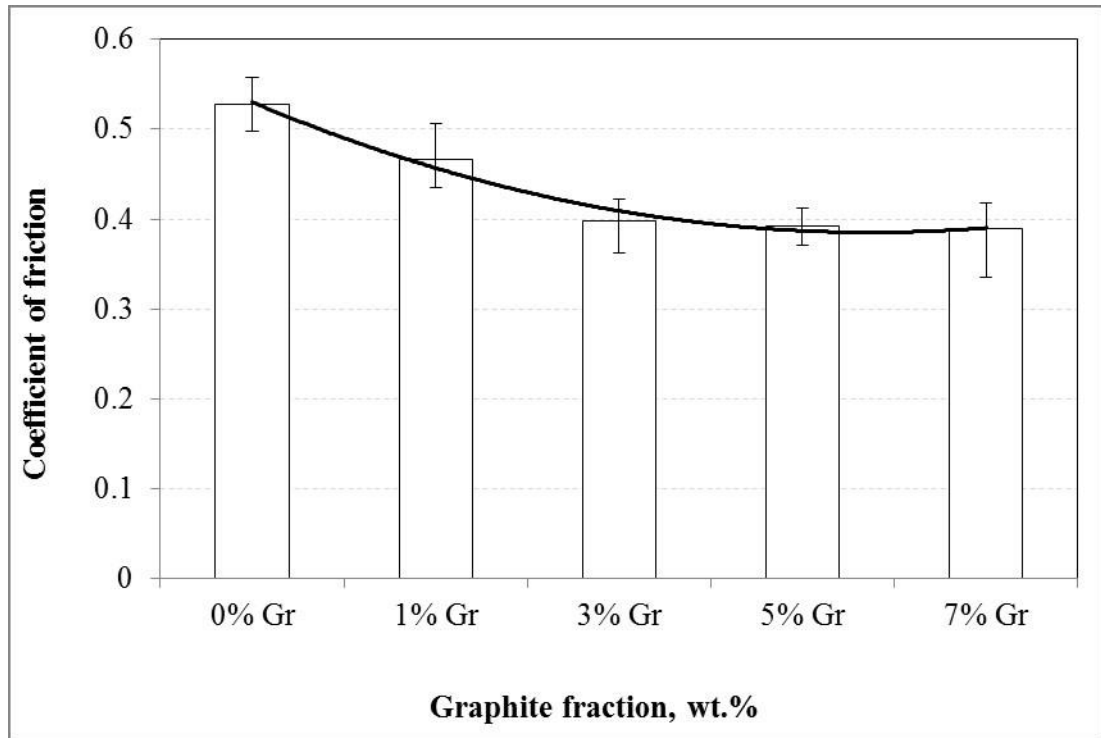


Figure 5.13: Coefficient of friction at the steady state of the composites after 7 km sliding distance

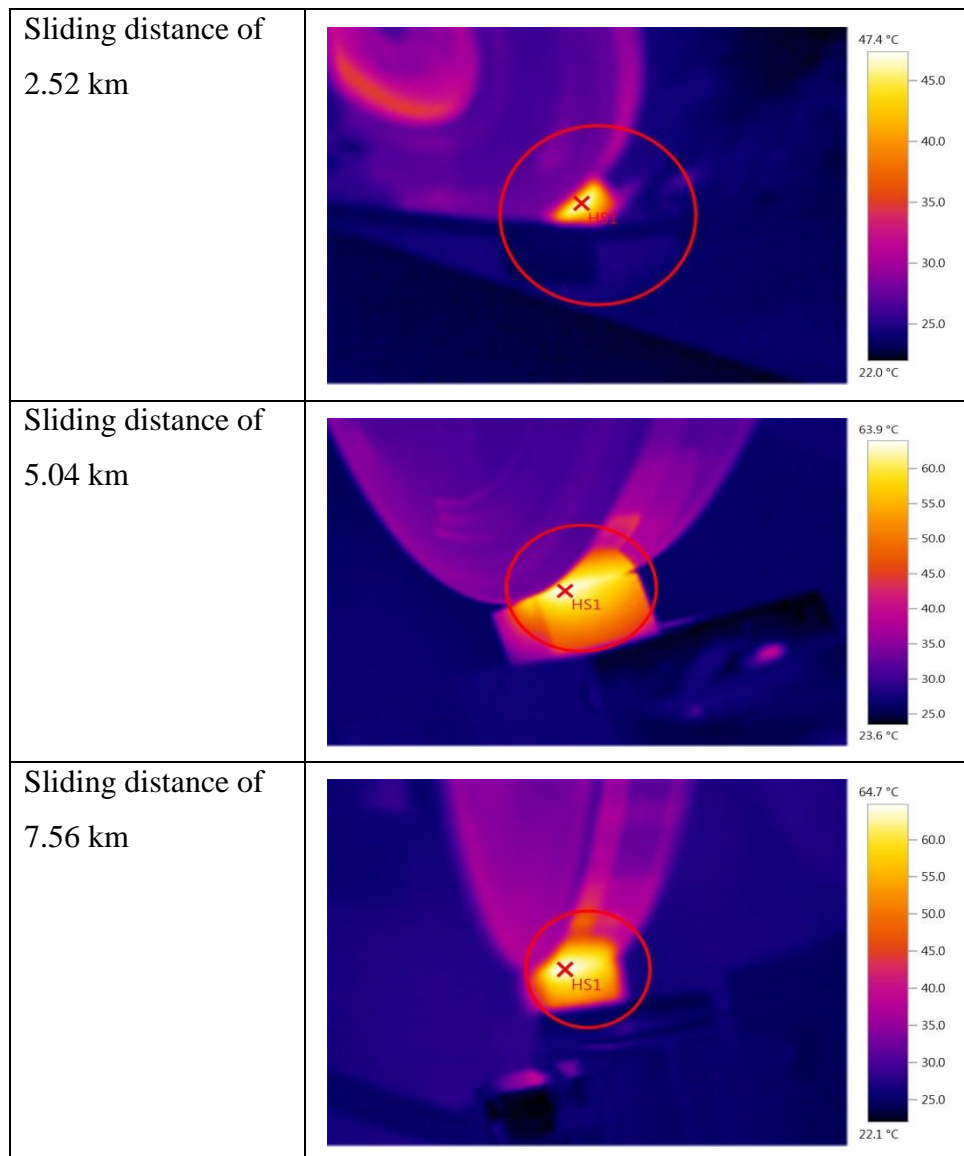
### 5.3.3 Frictional heat in the interface of graphite/epoxy composites

Thermosets are very sensitive to heat, since they soften at high temperatures. The glass transition temperature of the selected epoxy is about 120° C; it is very important not to reach the level of temperature at which the epoxy transfers from a hard to a rubbery phase. At this temperature, the epoxy becomes soft and the removal of materials increases greatly because of the thermo-mechanical loading in the rubbing area. In this research, a thermo-imager camera monitors the interface temperature, which was found to be more accurate than the infrared thermometer. After collecting the images, the maximum temperature (in the interface) is extracted for each operating parameter. Samples of the thermo-images are given in Figure 5.14 for the NE at different sliding distances.

The collected interface temperature at different sliding distances for all the composites are extracted and represented in Figure 5.15. For all the material types, interface temperature increases with the increase of the sliding distance; the relationship is proportional and seems to be linear relation. From a theoretical perspective, a longer sliding distance produces more heat in the interface. Therefore, the experimental data



are in agreement with the theoretical data. At this operating parameter, NE exhibits a higher interface temperatures compared to its composites. The neat polyester showed similar high interface temperatures compared to its glass and natural fibre polyester composites (Basavarajappa and Ellangovan, 2012, Yousif and Nirmal, 2011). The association of a high interface temperature with the shear force in the interface deteriorates the surface of the neat thermoset, which results in high mass removal from the surface.



**Figure 5.14: Heat distribution in the interface and both rubbed surfaces of the NE after 2.52, 5.04 and 7.56 km sliding distances at sliding velocity of 2.8 m/s and applied load of 50 N**

This can explain the specific high wear rate of the NE compared to its composites (see Figure 5.11). For the ECs based on different graphite content, the interface temperature

is lower at the higher graphite content. This concurs with the frictional results in Figure 5.13, since the higher the friction the higher the interface temperature. The reduction in the friction coefficient is explained based on the graphite film generated on the counterface. It is interesting to confirm this with the roughness profile of the wear track and the composite surfaces after each test. This will be explained in the next section. In addition, worn surface micrographs may offer supporting evidence.

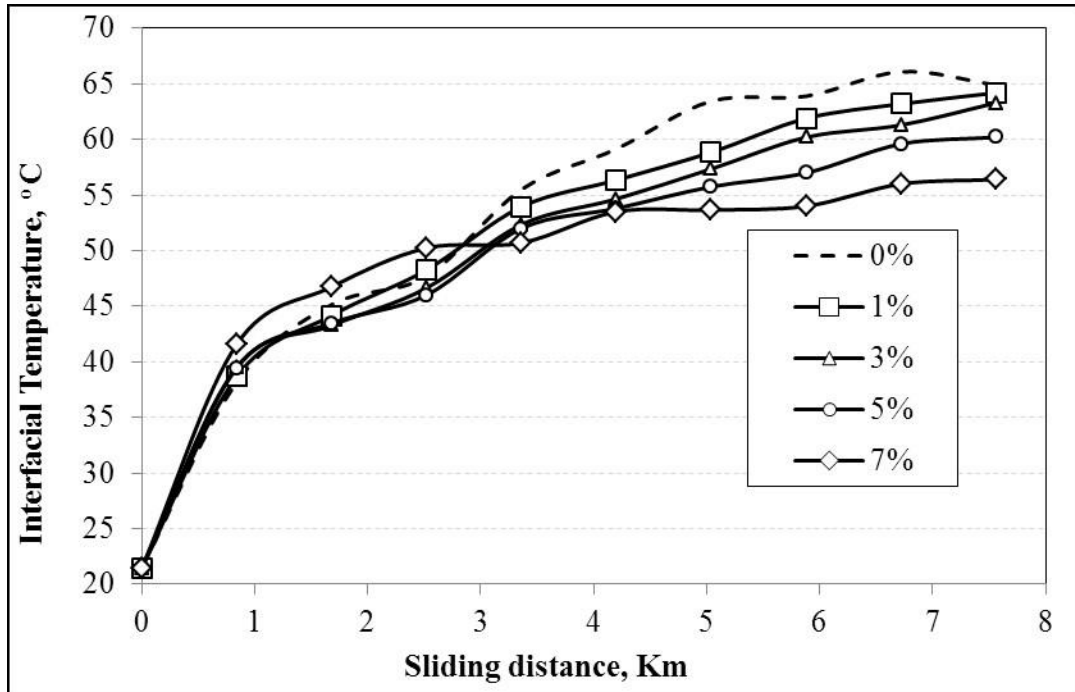


Figure 5.15: Interface temperature of graphite/ECs surface at the end of the adhesive loadings

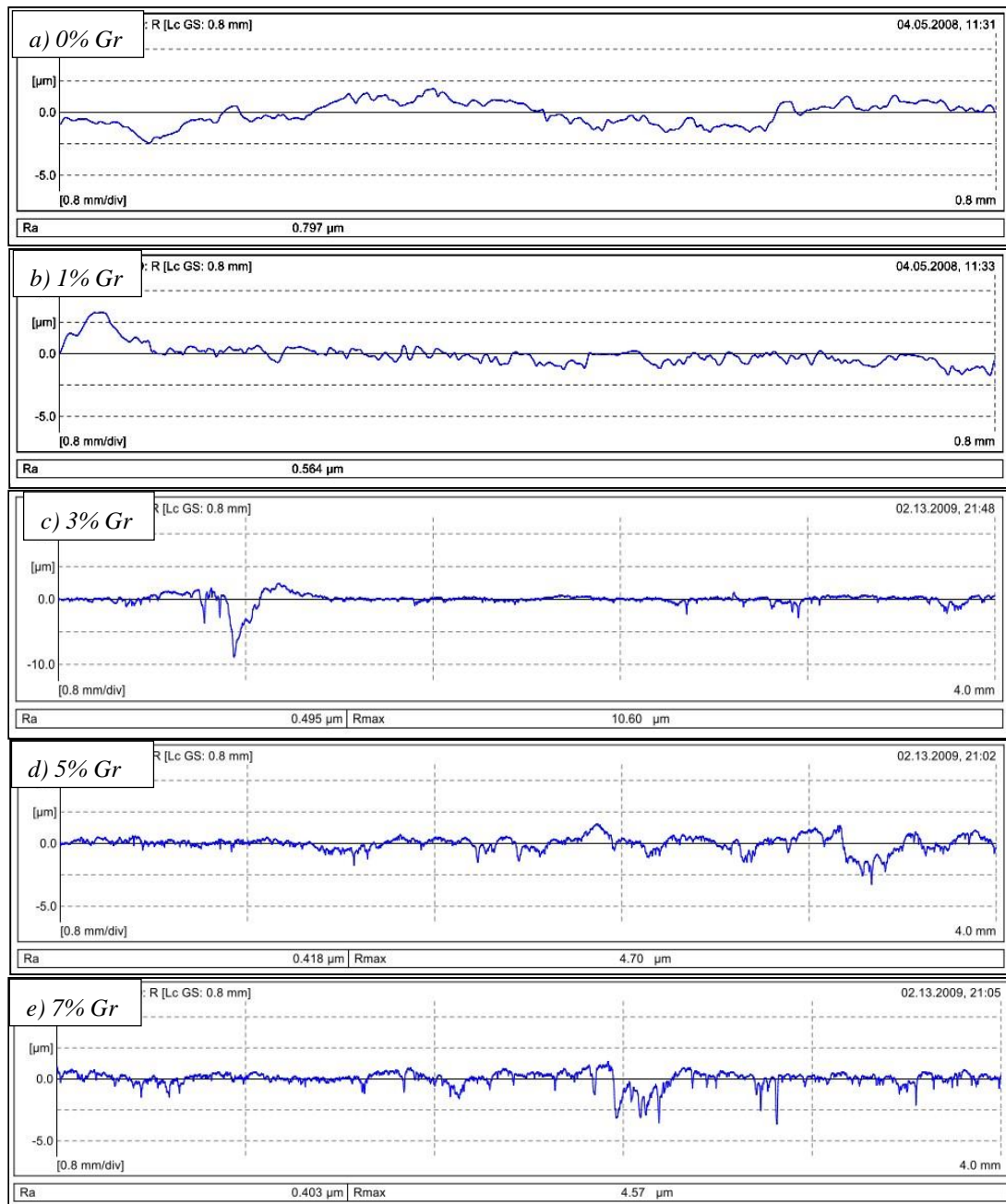
## 5.4 Surface observations

### 5.4.1 Roughness modifications of the wear track

Wear track roughness profile is measured after each test for each operating parameters at least three times. Samples of the wear track roughness profile after testing the EC

with different graphite contents are displayed in Figure 5.16a–d. The average of the readings after the sliding distance of 7.5 km associated with the maximum and minimum readings are determined and presented in Figure 5.17. Information from Chapter Three regarding the roughness of the counterface before the test, for instance stainless steel (AISI 304, hardness = 1250 HB, Ra = 0.1  $\mu\text{m}$ ) counterface, is relevant here (see Section 3.4.2). Further, wear track roughness is measured at two conditions: measurement with the presence of the film transfer and measurement after cleaning the counterface following each test, using acetone then wet cloths and drying with an air dryer. In the second condition measurement, the roughness value did not show remarkable changes compared to the original surface, whereas the Ra roughness values were in range of 0.085  $\mu\text{m}$ –0.16  $\mu\text{m}$ .

With regards to the value of the Ra after each test with the presence of the film transfer, Figure 5.17 shows increases in the roughness value compared to the surface roughness before the test. The significant effect of the material's sliding on the counterface roughness can be seen when the NE is sliding against it. There is about a 700% increase in the roughness of the stainless steel counterface. Such an increase is illustrated in Figure 5.10, considering the rough film transfer of the NE on the counterface. Similar findings have been reported when the neat polyester rubbed against the steel counterface (Albdiry and Yousif, 2013, Nirmal et al., 2010, Pihtili, 2009). It seems the mass transfer of the epoxy debris covered the counterface wear track, which resulted in significant modification of the roughness of the stainless steel counterface. This could be another reason for the high specific wear rate of the NE compared to its composites, since the higher the counterface roughness the higher the mass removal from the epoxy surface. Moreover, this could explain the high friction coefficient of the NE, since there could be interlocking between the asperities, resisting movement.



**Figure 5.16: Samples of the roughness profile of the counterface**

For the graphite/ECs, Figure 5.17 shows that the roughness of the counterface relatively reduces with the increase of the graphite content. This means the sliding has a lower effect on the roughness of the counterface. It seems the graphite generated a smooth and stable film transfer on the counterface, which resulted in a relatively smooth surface compared to the NE. However, there is an increase in the roughness of the counterface compared to the condition before sliding. This is expected, since there

is modification on the counterface during the sliding because of the removal of materials; there may be debris movement in the interface. The smooth surface of the graphite/EC wear track is the reason for the less specific wear rate of the composites compared to the NE.

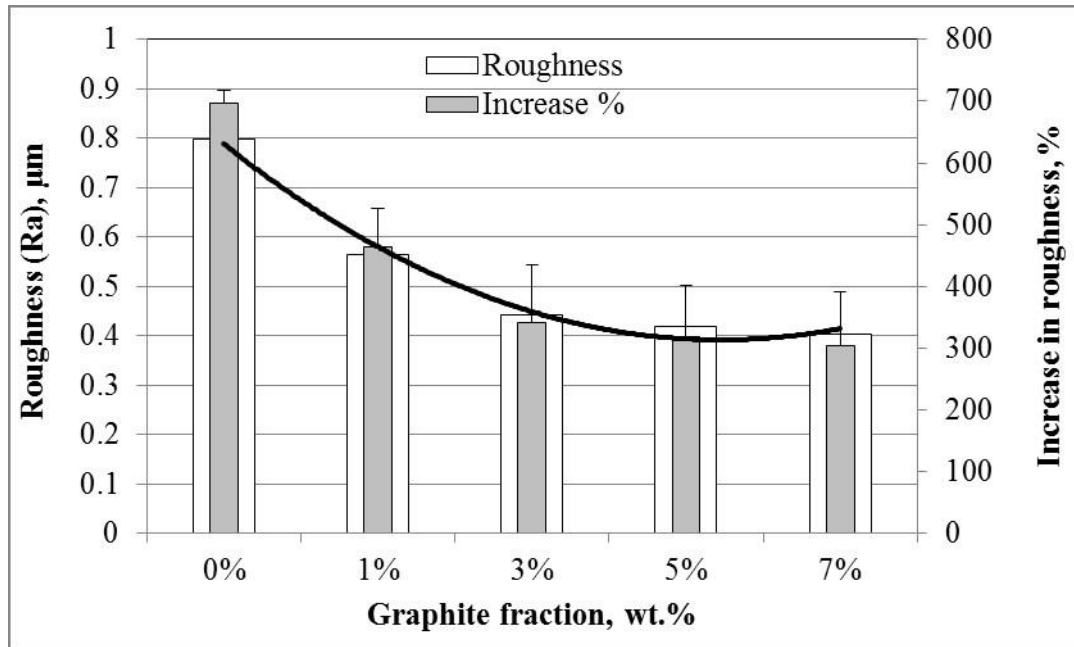
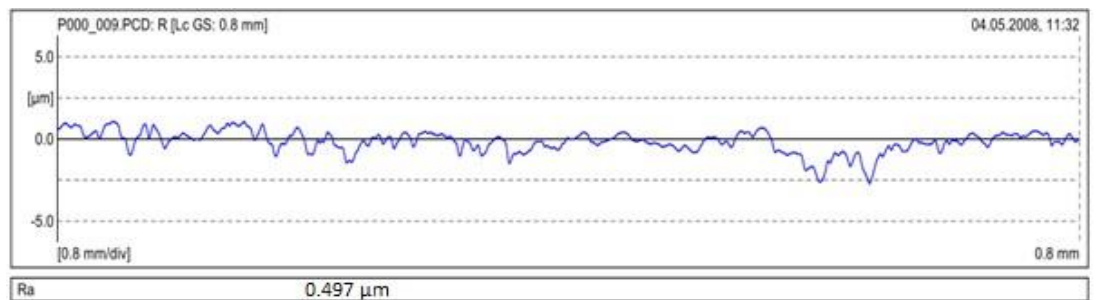
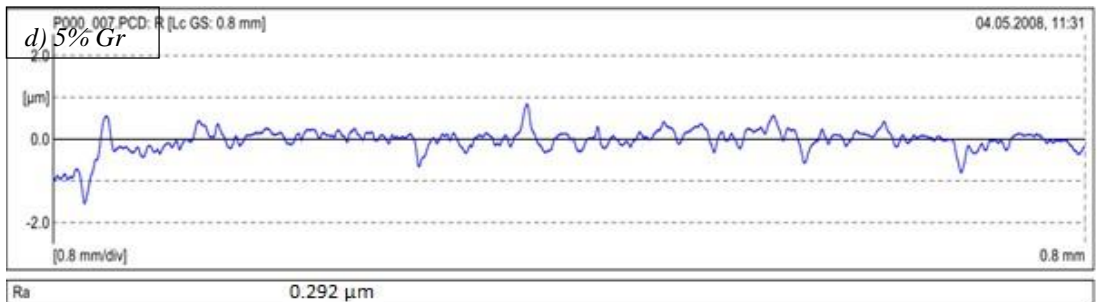
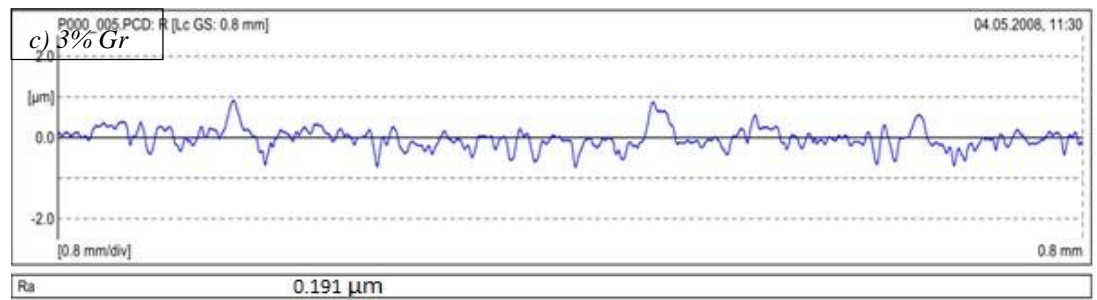
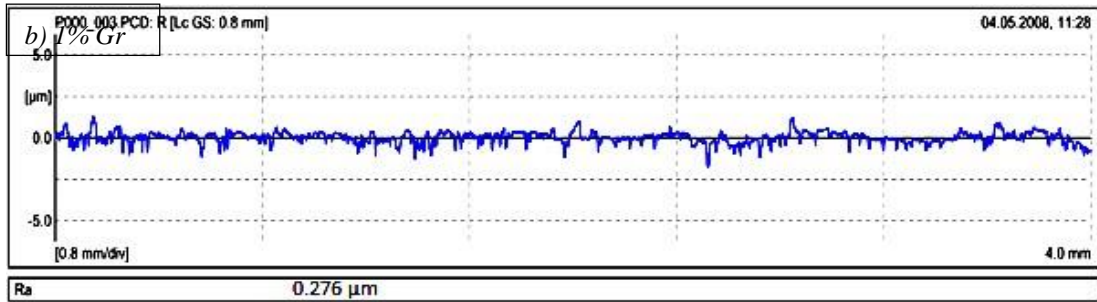
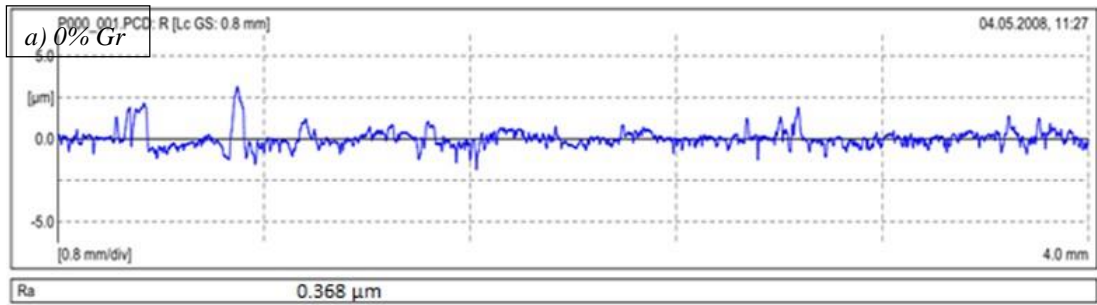


Figure 5.17: Ra roughness values of the counterface surface after adhesive loadings for 7.56 km sliding distance

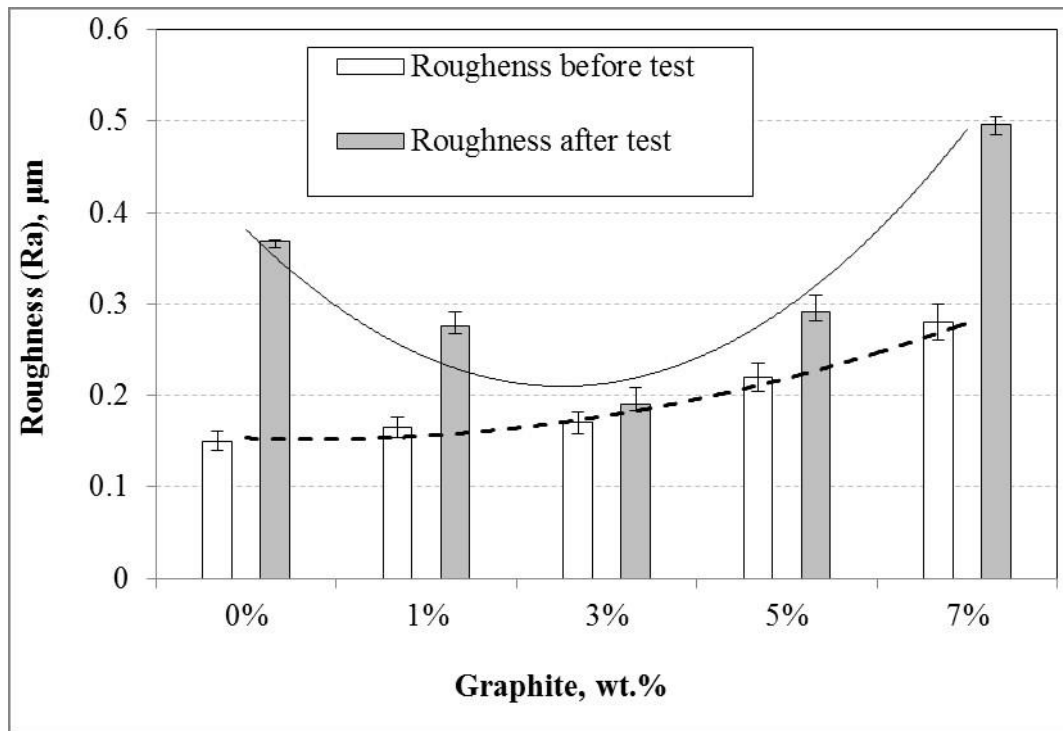
#### 5.4.2 Roughness of the composite surface

Samples of the composite surface roughness after the test are given in Figure 5.18. The average of the roughness readings associated with the maximum and minimum values for the surface before and after the test is introduced in Figure 5.19. The roughness of the sample before the test showed a slight increase with the percentage increase of the graphite, despite all samples being polished with a sand paper of 1500–2000 grade. It seems the presence of the filler on the surface influences the roughness. Conversely, it can be seen that the roughness after the test decreases at a lower and intermediate percentage of graphite (one to five weight per cent). Increase occurs at seven weight per cent. The way that the asperities adapt in the contact zone influences the roughness of the composite surface. From the roughness of the wear track on the counterface, there is a clear reduction in the roughness of the wear track with the presence of the graphite greater than three weight per cent in the EC, as in Figure 5.17. It seems the

counterface reaches the stable roughness surface condition when the three weight per cent graphite/EC is rubbed. There is not as much influence with the extra addition of graphite in the composites, since the film is already transferred and adhered well. As such, the optimum graphite content in the EC is three per cent to maintain low roughness surfaces for both the epoxy composites and the wear track of the stainless steel counterface. Further, three weight per cent graphite/EC exhibited better wear and frictional performance than others.



**Figure 5.18: Samples of the roughness profile of the composite surfaces after 7.56 km sliding distance at sliding velocity of 2.8 m/s and applied load of 50 N**



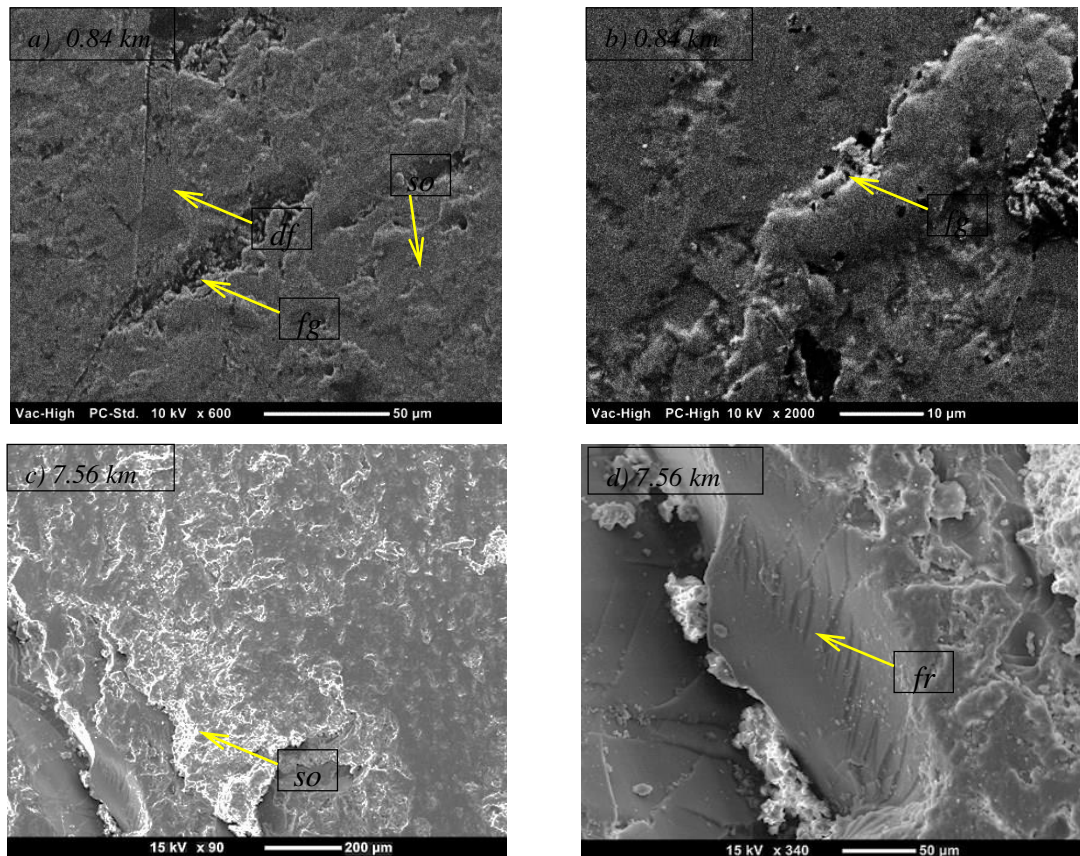
**Figure 5.19: Ra roughness values of graphite/ECs surface after adhesive loadings for 7.56 km sliding distance**

### 5.4.3 Scanning electron microscopy observation

#### 5.4.3.1 Micrographs of NE worn surface

Micrographs of the NE worn surface after sliding against stainless steel counterface under 50 N applied load and 2.8 m/s sliding velocity for different sliding distances are presented in Figure 5.20. For the short distance of 0.84 km, the surface of the NE suffers from fragmentation (marked as 'fg') and deformation (marked as 'df'), as shown in Figures 5.20a and 5.20b. Despite the short distance of the rubbing process of the NE against the stainless steel, a deformation process occurred. This is mainly due to the influence of the thermo-mechanical loading in the rubbing region.





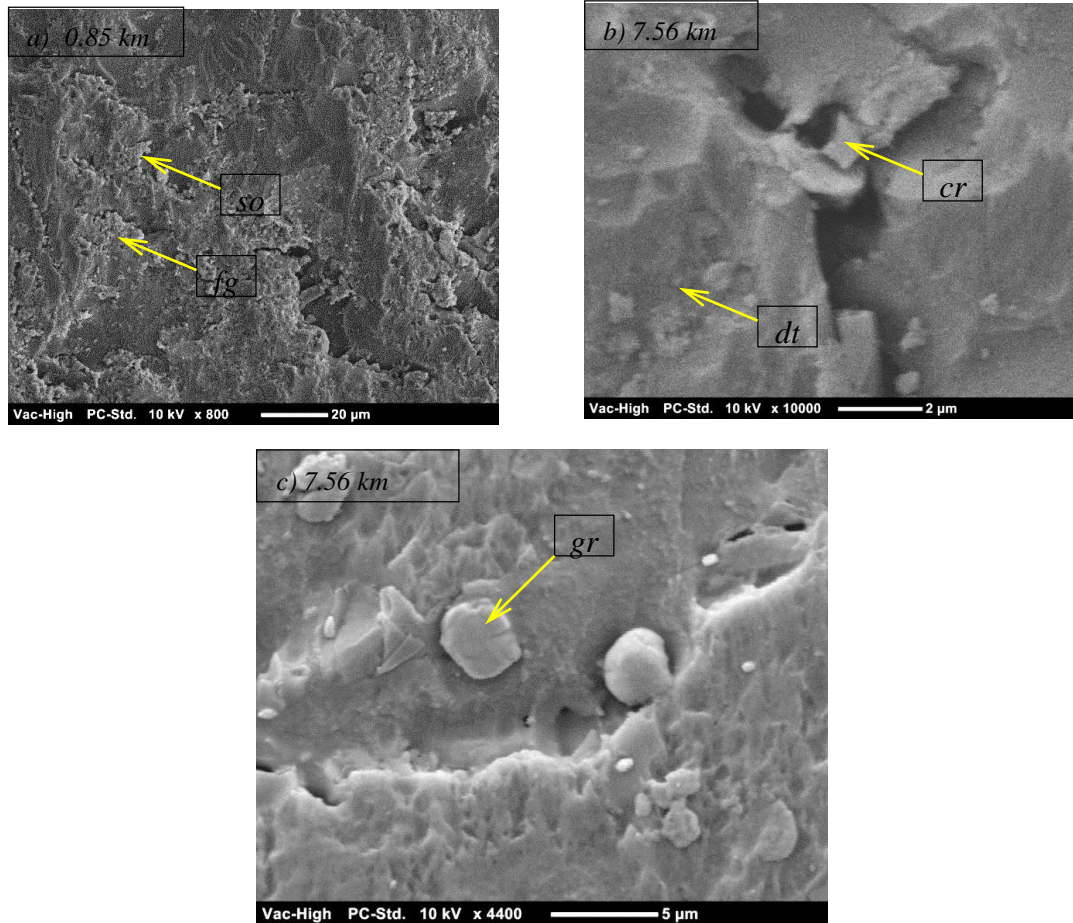
**Figure 5.20: Micrographs of NE after adhesive testing—fg = fragmentation, so = softening, fr = fracture, df= deformation**

This is highly pronounced in the NE slide for the further distance of 7.56 km, as seen in Figure 5.20c. A softening process (marked as ‘so’) was taking place. At this long sliding distance, there is a fractured appearance on the surface because of the high shear loading in the interface associated with the high temperature. At this sliding distance, the temperature reached up to 67° C (see Figure 5.15), and the frictional force in the interface was approximately three kiloNewton (see Figure 5.12). Such behaviour has been reported elsewhere when vinyl ester (Suresha et al., 2010) and polyester (Albdiry and Yousif, 2013, Pihtili, 2009) have been tested under adhesive wear loading. Further to this, the increase in the roughness of the counterface (wear track) is another reason contributing to the high removal of materials from the NE surface. This can explain the poor performance of the NE sliding against stainless steel counterface.

#### *5.4.3.2 Micrographs of one weight per cent graphite/epoxy worn surface*

The micrographs of the worn surface of the one weight per cent graphite/EC are displayed in Figure 5.21 for different sliding distances. At the short sliding distance, the composite surface suffers from the same symptoms observed on the worn surface of the NE, since there is a softening process and fragmentation because of the high interface temperature associated with the shear force.

Moreover, the presence of the graphite at low contact of one weight per cent could not reduce the heat and/or the friction in the interface. This led to macro-cracks associated with detachments of the fillers on the surface, as shown in Figure 5.21b. In contrast, on some regions of the composite worn surfaces, graphite particles adhered well on the composite surface, indicating a good adhesion of the fillers in some regions. For this composite, it can be suggested that the high friction (Figure 5.12) in the interface with the high temperature (Figure 5.15), along with the absence of the stable film transfer (high roughness of the wear track, Figure 5.17) is the main reason for the relatively high specific wear rate of the composites at this content of graphite, compared to the three weight per cent graphite/EC (see Figure 5.11).

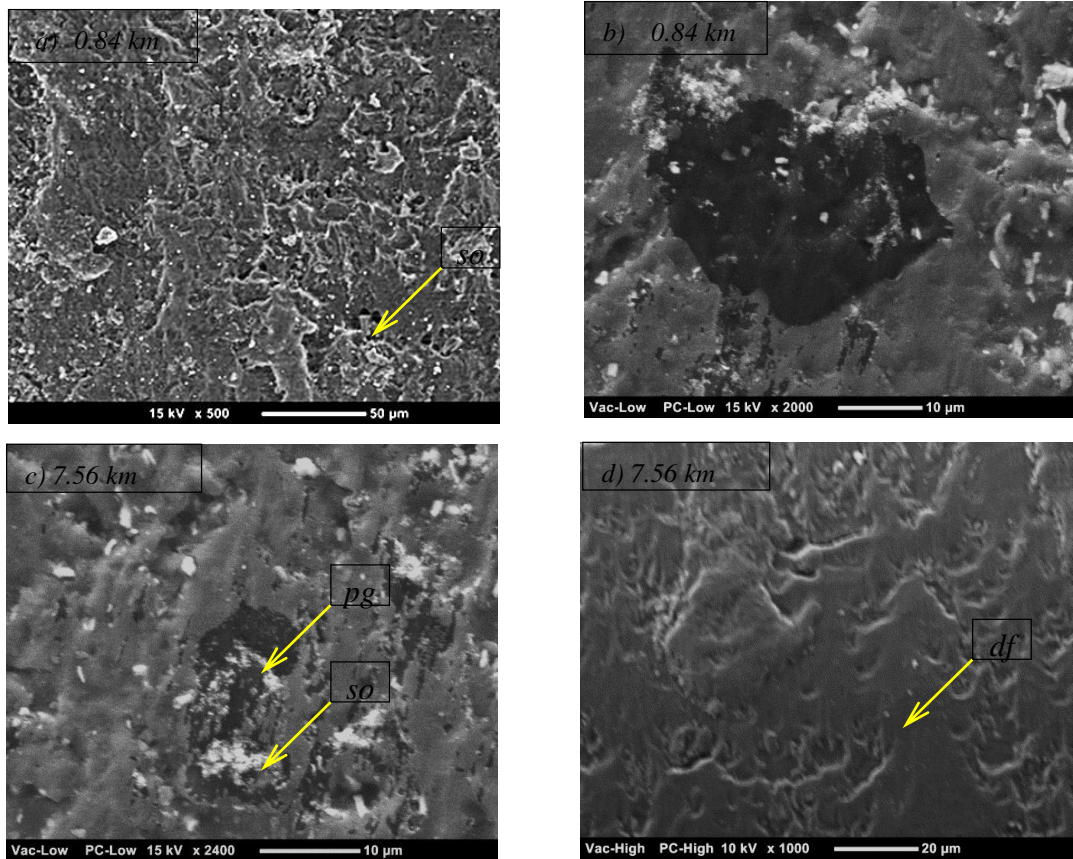


**Figure 5.21: Micrographs of 1% graphite/ECs after adhesive testing—fg = fragmentation, so = softening, fr = fracture, gr = graphite, dt = detachment, cr = crack**

#### 5.4.3.3 Micrographs of three weight per cent graphite/epoxy worn surface

Figure 5.22 displays the micrographs of the three weight per cent graphite/epoxy worn surfaces. At the short sliding distance of 0.84 km, there are clear signs of the softening process associated with plastic deformation. The deformation associated with the black patch on the surface represents the generation of the film transfer on the counterface. It may transfer to the composite surface at the initial stage of the rubbing. At the longer sliding distance of 7.56 km, Figures 5.22c and 5.22d show dark places of graphite, which indicate the generation of the film transfer. There is a clear stretching on the composite surface, representing the high resistance in the interface in some regions. The high resistance in the interface reflects the good wear resistance of the composite and the high friction coefficient. There is agreement with the wear results, since three weight per cent graphite exhibited the lowest specific wear rate compared to other wear rates. However, from a frictional perspective, the three weight per cent graphite showed

a low friction coefficient. This is mainly due to the presence of the film transfer on the wear track, which acted as a solid lubricant, leading to relatively low friction coefficient (Figure 5.12) and good wear resistance (Figure 5.11). Further, there is no sign of filler detachment, poor dispersion of the fillers on the surface and/or aggregation of the fillers. This could represent another important factor in controlling the tribological performance of the graphite/ECs.

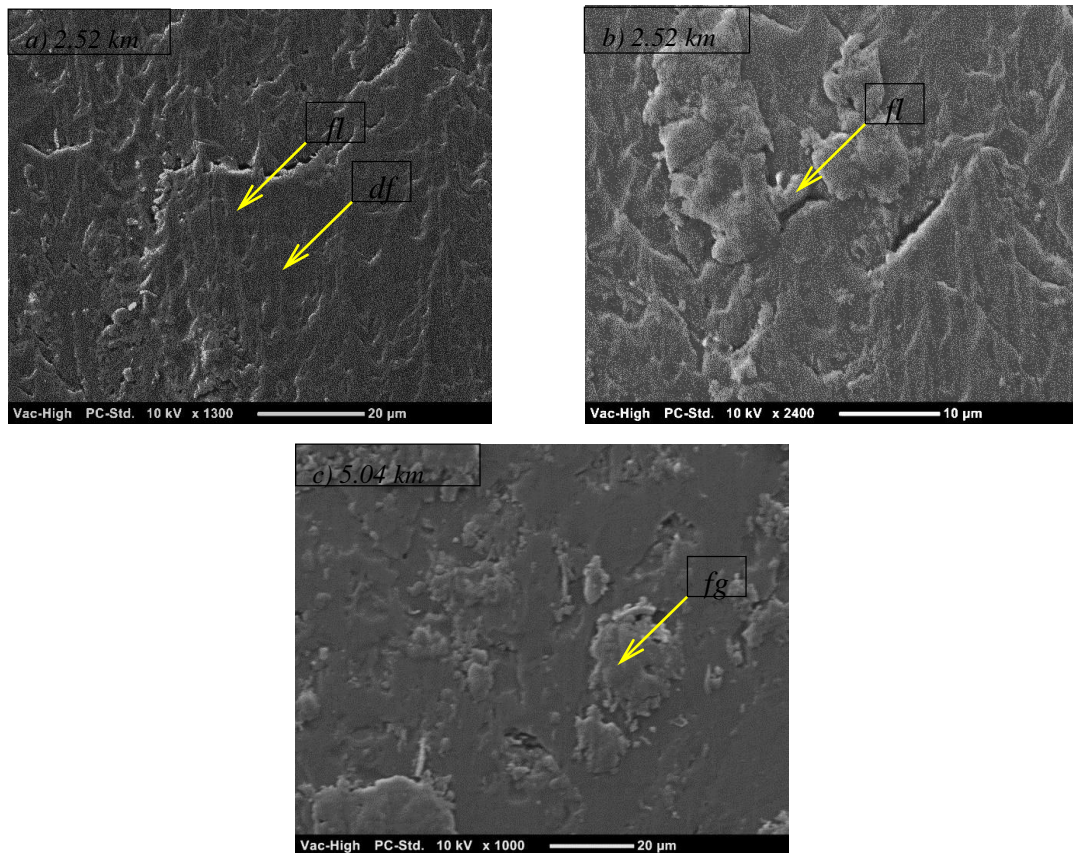


**Figure 5.22: Micrographs of 3% graphite/ECs after adhesive testing—so = softening, fr = fracture, pg = patch of graphite, df = deformation**

#### 5.4.3.4 Micrographs of five weight per cent graphite/epoxy worn surface

At the high weight content of the graphite (five weight per cent) in the epoxy, Figure 5.23 shows the micrographs of the worn surfaces, indicating that clear deformation, film transfer, fragmentation and softening were taking place for different sliding distances. Further, micro-cracks can be seen on the micrograph (Figure 5.23a) after 2.52 km sliding distance. According to the literature, the high content of the fillers in

the composite may act as a crack initiator and indicate a weak area on the composite surface (Bahadur et al., 1996, Friedrich et al., 2005).



**Figure 5.23: Micrographs of 5% graphite/ECs after adhesive testing—so = softening, fr = fracture, fl = film transfer, df = deformation**

Further, it seems the film transfer on the counterface is unstable; there is a presence of film adhered to the composite surface with the presence of the aggregated graphite particle. In comparison with previous micrographs of the three weight per cent graphite, the extra addition of the graphite into the EC starts to lessen the quality of the composite surface. In other words, the maximum amount of graphite should not exceed three weight per cent to maintain a good quality surface and tribological performance. This will be confirmed in the next section on the surface observation of the seven weight per cent graphite/EC.

#### 5.4.3.5 Micrographs of seven weight per cent graphite/epoxy worn surface

The micrographs of the EC based on the large amount of seven weight per cent graphite are presented in Figure 5.24 for different sliding distances. At the short distance of

2.52 km, the micrographs show a clear fragmentation, softening and film transfer on the surface. The patch of the film transfer seems to be carrying the load during the sliding, which could be the reason for the high roughness of the composites after the test, as shown in Figure 5.19. Therefore, there is not a good integration between the two surfaces because of the large amount of graphite on the surface of the composites. Further, Figure 5.24c shows a clear aggregation of the fillers associated with cracks near those groups of fillers. Also, signs of a fracture could be a crack propagation leading to fractures on the surface of the composites. In Figure 5.24d, the aggregation of the fillers resulted in a weak surface, since there is a patch of fillers removed, indicating a weak surface with the presence of a large amount of graphite. The easy removal of the material from the surface is the reason for the poor wear resistance (Figure 5.11) of the composites and the low friction coefficient (Figure 5.13).

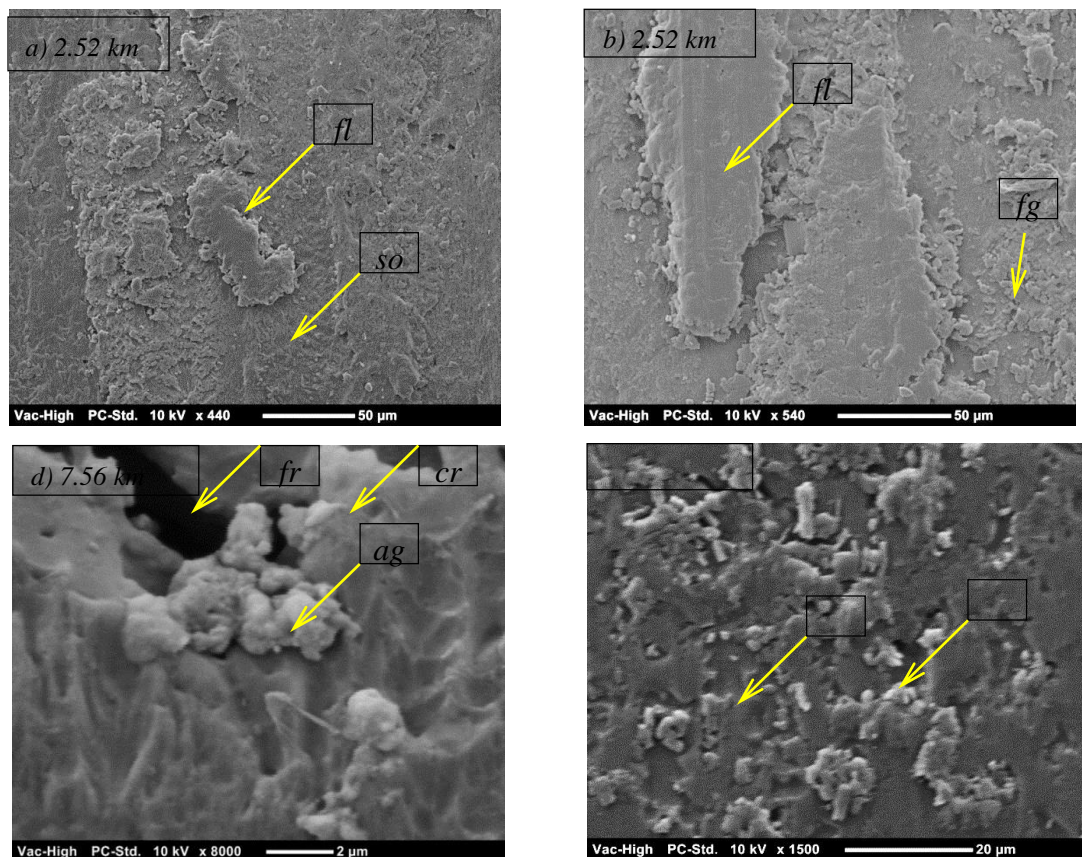


Figure 5.24: Micrographs of 7% graphite/ECs after adhesive testing—so = softening, fr = fracture, fl = film transfer, df = deformation, fg = fragmentation, cr = cracks

## 5.5 Comparison with previous works

For comparison, the current study's main findings are discussed with the literature. Table 5.1 briefly introduces some of the related works on thermoset epoxy and polyester composites based on fillers additives. The current investigation in this chapter concluded that three weight per cent graphite is the optimum for good adhesive wear and frictional performance and was chosen for this comparison. In general, epoxy thermoset performs much better than polyester with all types of fillers (i.e., the specific wear rate of the polyester  $\gg$  epoxy). This promotes epoxy further compared to polyester.

With regard to the influence of fillers, clay fillers are potential reinforcements. However, the main limitations of these fillers are the poor interfacial adhesion with the matrix and their abrasive nature. The presence of clay filler on the composite surface acts as a third body and/or rough hard surface, which leads to high mass removal from both resinous and wear track regions. However, the presence of graphite showed good improvement in the adhesive wear performance of the epoxy (Basavarajappa & Ellangovan 2012), despite the presence of the SiC fillers and/or glass fibres, which are both considered very abrasive materials. With regard to the content of the fillers, the reported works agreed that the high content of the filler in the composite deteriorates the composite. Some selected five per cent (Basavarajappa and Ellangovan, 2012) as the optimum and some three per cent (Jawahar et al., 2006). In other words, the current findings concur with the published related works.

**Table 5.1: Summary of the previous works on effect of adding filler tribological behaviour of polymer composite**

Matrix	Filler	SWR, 10 <sup>-5</sup> mm <sup>3</sup> /N.m	μ	References and remarks
Current epoxy	3 wt% graphite	0.5	0.4	
Polyester		19	0.9	Yousif Yousif (2013a) reported high friction because of the stick slip phenomenon, softening and fragmentation due to the high interface temperature due to the large amount of heat generated in the interface. High wear rate because of the thermomechanical loading.
Epoxy	GF	1.3		In Basavarajappa and Ellangovan (Basavarajappa and Ellangovan, 2012), the presence of the graphite with the glass fibres enhanced the wear performance. The addition of the SiC additives worsened the surface, since it acted as a third body in the interface. Micrographs showed poor interface between the fibres, graphite and SiC with the epoxy.
Epoxy	GF, 5 wt% Gr and 5 wt% SiC	0.79		
Epoxy	GF-5% Gr-10% SiC	0.92		



Polyester	1% organoclay	110	0.5	Jawahar et al. (Jawahar et al., 2006) reported that the coefficient of friction and wear loss decreases significantly on addition of organoclay. Synthetic clay filled composites exhibited high wear loss and coefficient of friction with the increase in clay content. The highest wear resistant and least coefficient of friction is observed in the nanocomposite with a clay content of 3 wt%.
Polyester	3% organoclay	140	0.6	
Polyester	5% organoclay	158	0.6 2	

## 5.6 Chapter summary

The chapter can be summarised in a few points:

- There is a significant influence of the weight fraction of the graphite on both mechanical and tribological performance of the composites. At a low percentage of the graphite (one weight per cent), there is not much influence on the tensile behaviour and there is slight improvement to the wear performance of the ECs. Intermediate weigh percentage of the graphite in the EC is considered optimum for both mechanical and tribological performance, since there is a slight reduction in the tensile properties and significant improvement to the hardness, wear and frictional characteristics.
- A higher amount of the graphite in the composites (greater than or equal to five weight per cent) greatly deteriorated the tensile and tribological properties of the composites, despite an increase in the hardness.
- The modification on wear track roughness significantly controlled the wear and frictional behaviour of the composites. Further, the shear force associated with the interface heat (thermo-mechanical loading) played a role in the wear mechanism of the composites.
- Micrographs of the worn surface showed different wear mechanisms, depending on the content of the graphite in the composites. Softening and fragmentation were seen with a low content of graphite presence in the composite, since there was no sign of aggregation or detachments of fillers.

- At the graphite amount greater than or equal to five weight per cent, aggregation and poor dispersion of the filler seen on the surface indicated a deteriorated wear performance of the composites. This was the main reason for the poor performance of the composites with large amounts of graphite.

# **Chapter 6: Mechanical and wear characteristics of DPF and graphite filler/ECS**

## **6.1 Introduction**

Chapter Five concluded that three weight per cent of graphite in the ECs represented the optimum content from mechanical and tribological perspectives. In this chapter, the mechanical and tribological performance of the ECs, as based on three weight per cent graphite, DPF and three weight per cent graphite plus DPF, are discussed and compared with the NE. Further, the tribological performance of the composites is discussed considering two different adhesive wear techniques: BOR and BOD. At the end of this chapter, the main findings are discussed with the previous related works and the findings are summarised.

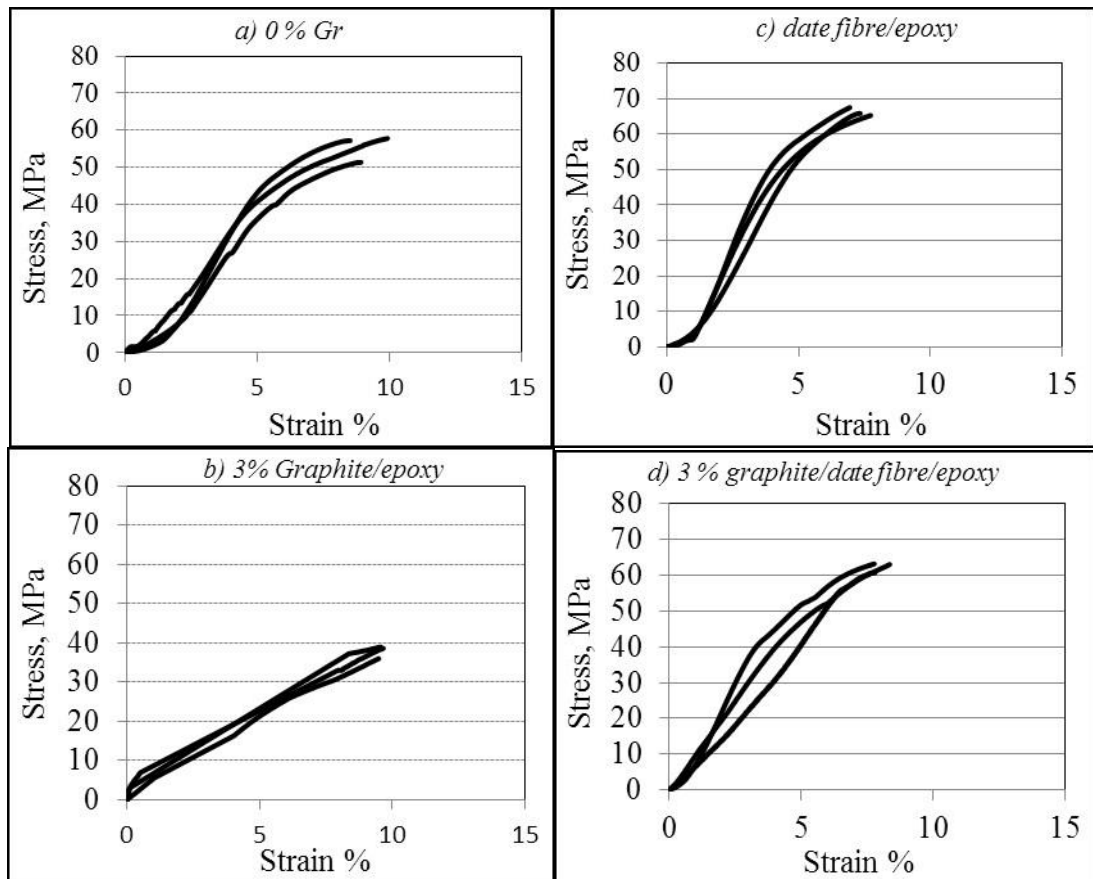
## **6.2 Tensile properties of date palm/graphite/epoxy composites**

Mechanical properties of the composites are presented in Figure 6.1–6.5, showing the stress strain diagrams, modulus of elasticity, hardness and the micrographs of the fractured samples for the selected ECs, NE three weight per cent graphite (GE), DPF (FE) and three weight per cent graphite plus DPF (GFE).

### **6.2.1 Stress strain diagram, ultimate tensile stress and modulus of elasticity of date palm/graphite/epoxy composites**

In section 5.2.1, it was revealed that the addition of the graphite worsens the tensile properties of the ECs, which can be represented for the three weight per cent of graphite with the addition of the fibres, as displayed in Figure 6.1. From this figure, the addition of the fibre enhances the tensile properties of the epoxy, since there is an increase in the TS from 58 MPa to approximately 68 MPa. This represents a 17% increment in the

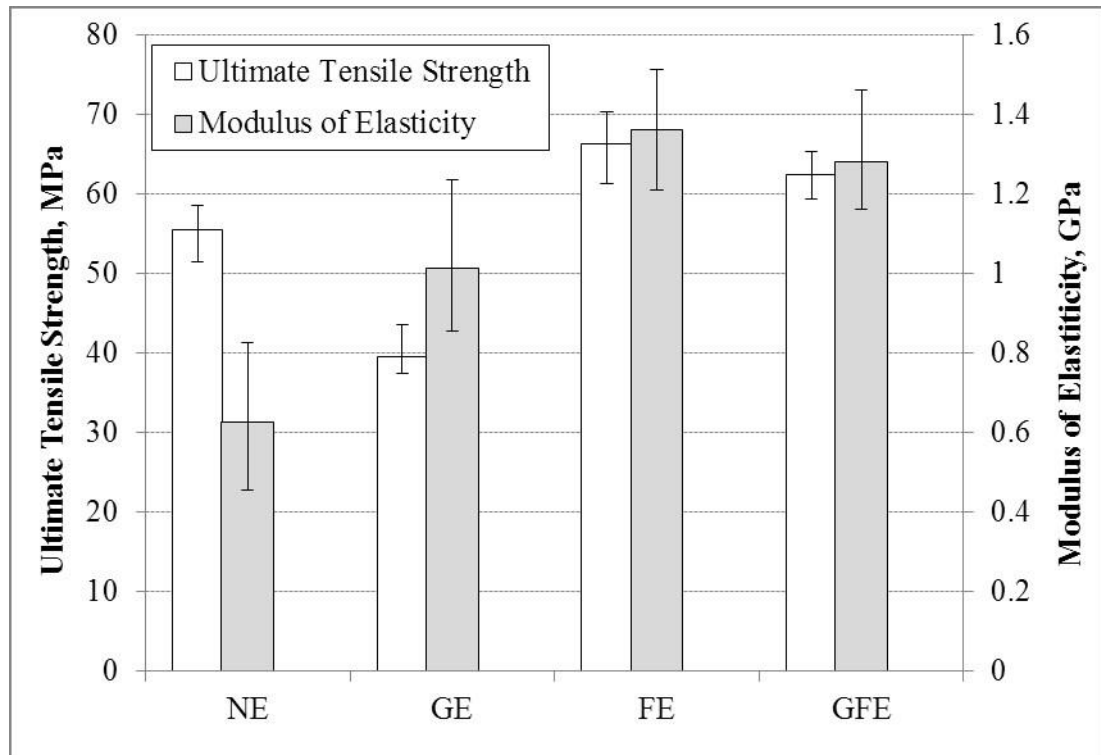
TS when the epoxy is reinforced with the DPF. With regards to the ductility of materials, it seems the addition of the ductile DPF (see Section 4.3, Figure 4.5) to the brittle ECs exhibits no significant influence. To show the influence of both graphite and DPF on the tensile properties of the EC, the ultimate TS and the modulus of elasticity are extracted from the stress strain diagrams and represented in Figure 6.2.



**Figure 6.1: Stress strain diagram of different ECs based on graphite and/or DPFs**

From Figure 6.2, it is clear that the addition of the graphite worsens the tensile and the modulus of elasticity of the epoxy. Interestingly, the addition of the date palm alone and/or three weight per cent graphite showed improvement to the ultimate TS and the modulus of the elasticity of the ECs. From Chapter Four (Figure 4.15), the TS of the selected DPF (0.3 mm diameter and six per cent NaOH treatment) was about 150 MPa. Meanwhile, the NE has a TS of approximately 55 MPa, (see Chapter 5, Figure 5.2). Since the Vf of the fibre in the composite is approximately 35% (see Section 3.3.3 in

Chapter 3), a TS of approximately 88 MPa can be expected (Berto et al., 2013). That is, there is a 22% difference between the theoretical and the experimental value of the TS. Such a difference is expected, since the theoretical concept assumes the interfacial adhesion of the fibre with the matrix is 100% bonded; this cannot be guaranteed, especially with natural fibres. This will be clarified with the aid of surface observation by the SEM, which will be introduced in the next section.



**Figure 6.2: Ultimate TS and modulus of elasticity of different ECs based on graphite and/or DPF. NE = neat epoxy, GE = 3% graphite/epoxy, FE = DPF, GFE = 3 wt% graphite/date palm fibre/epoxy**

Further to the above, it can be seen that the addition of the three weight per cent to the DPF reinforced ECs reduces the TS of the composites, since there is seven per cent reduction. From Chapter Five, it was agreed that the addition of the graphite worsens the TS of the epoxy because of the interfacial adhesion of the graphite with the epoxy. From a mechanical perspective, graphite should be used to reinforce the ECs. However, three weight per cent of graphite should be considered to maintain good wear and frictional performance of the composites because of the requirement of fillers as solid lubricant (see Figures 5.1 & 5.13 in Chapter 5).

The current findings compare well with the most recent published works, which are extracted and listed in Table 6.1. All of these reported works confirmed that the addition of the natural fibres greatly improves the tensile properties of the synthetic composites. These are promising results, which encourages the replacement of synthetic with natural fibres for both environmental and economic reasons.

**Table 6.1: Published works on tensile properties of natural fibre reinforce epoxy or polyester composites**

Ref	Materials	Findings	Remarks
(Berto et al., 2013)	Grass/polyester	In most cases, added grass to polyester has enhanced the tensile of grass/polyester composite. High Vf of fibre could lead to deterioration mechanical behaviour of fibre/polymer composite.	98% enhancement in tensile stress of grass/polyester composite at Vf = 25%. 22% decrease in the tensile stress grass/polyester composite at Vf = 30%. SEM of tensile fracture specimen shows good interfacial properties and poor intra fibre delamination.
(Zhang et al., 2008a)	Alfa/polyester	The fibre orientation played a remarkable role in improving the tensile stress of alfa/polyester composite.	733% enhancement in tensile stress of composite at longitude direction compare to tensile stress of composite at transverse direction. 146% enhancement in Young modulus of composite at longitude direction compare to Young modulus of composite at transverse direction.

(Hou et al., 2013)	Palmyra/jute/ polyester	Jute fibre was able, individually or with other PPLS fibres, to enhance the mechanical properties of jute/PPLS/polyester.	7.5 P/22.5 jute/70 ECs shows the best mechanical behaviour compared to others.  SEM photos show that the failure was because of fibre fracture and part fibres pull out from the
--------------------	----------------------------	---	--

			matrix more than the matrix interfacial failure.
(Ratna Prasad and Mohana Rao, 2011)	Jowar/polyester	Reinforcement polyester polymer by jowar fibre has enhanced the mechanical behaviour of jowar/polyester composite.	Jowar content has improved the TS and Young modulus of jowar/polyester composite by 293% and 336%, respectively.
(Ratna Prasad and Mohana Rao, 2011)	Sisal/polyester	Reinforcement polyester polymer by jowar fibre has enhanced the mechanical behaviour of jowar/polyester composite.	Sisal content has improved the TS and Young modulus of jowar/polyester composite by 107% and 201%, respectively.
(Ratna Prasad and Mohana Rao, 2011)	Bamboo/polyester	Reinforcement polyester polymer by jowar fibre has enhanced the mechanical behaviour of jowar/polyester composite.	Bamboo content has improved the TS and Young modulus of jowar/polyester composite by 300% and 293%, respectively.



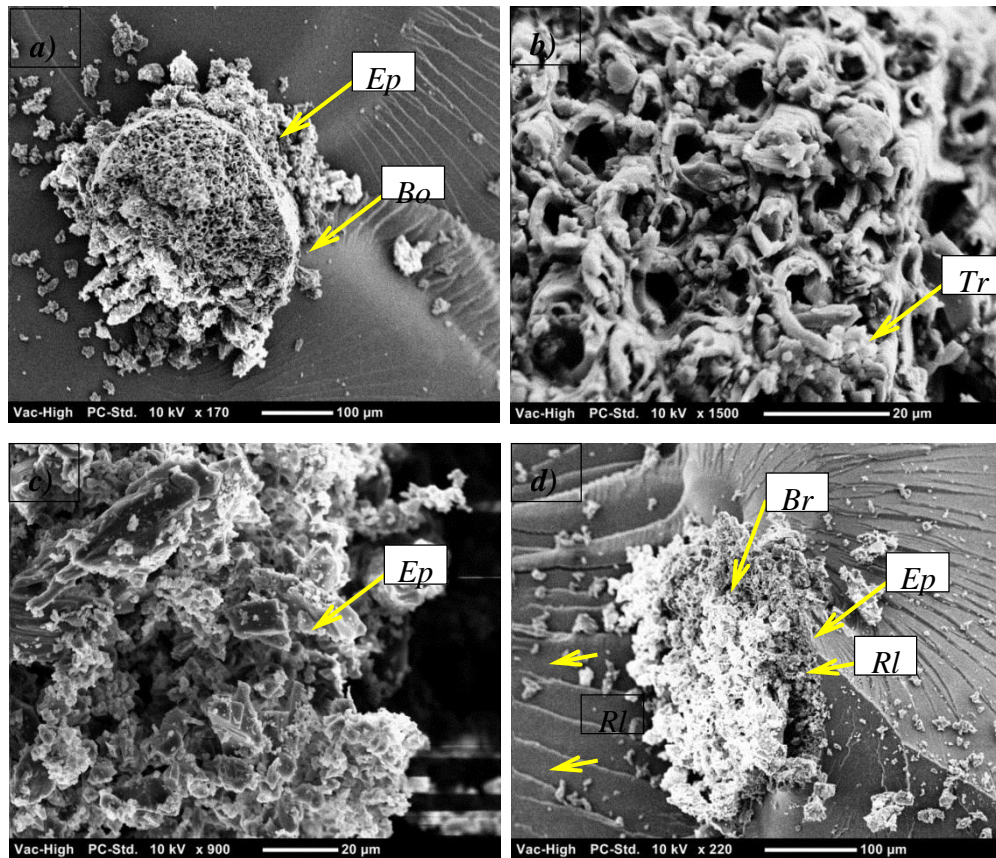
(Shivamurthy et al., 2013)	Coir/epoxy	Curing time, Vf and compression load at fabrication have significance influence on tensile properties of fibre/polymer composite.	The maximum TS was at 48 hrs, 0.5 kg and Vf = 15%
(Sapuan et al., 2006)	Banana/epoxy	The geometry of woven banana fibre composite has insignificant effect on	

		the mechanical behaviour of composite.	
(Coroller et al., 2013)	Flax/epoxy	The study revealed that the elementary fibre properties significantly influenced the mechanical behaviour of fibre/polymer composite.	Epoxy/hermes flax shows the best mechanical behaviour compared to epoxy/andrea flax and epoxy/marylin flax.
(Zhang et al., 2008a)	Sugar/epoxy	The concentration time of treatment is a significant factor in determining the mechanical behaviour of sugar/EC.	0.25 M NaOH shows better results than 0.5 M NaOH. 4 hrs soaking time showed better results than others (1 and 8 hrs.)

Current work	Graphite/Date palm/epoxy	The study revealed that date palm highly improved the tensile properties. However, high fraction of graphite deteriorated the tensile properties	6% NaOH treatment to the date palm fibres introduced the best mechanical properties since it is significantly improved the interfacial adhesion of the fibre with the matrix
--------------	--------------------------	--	--

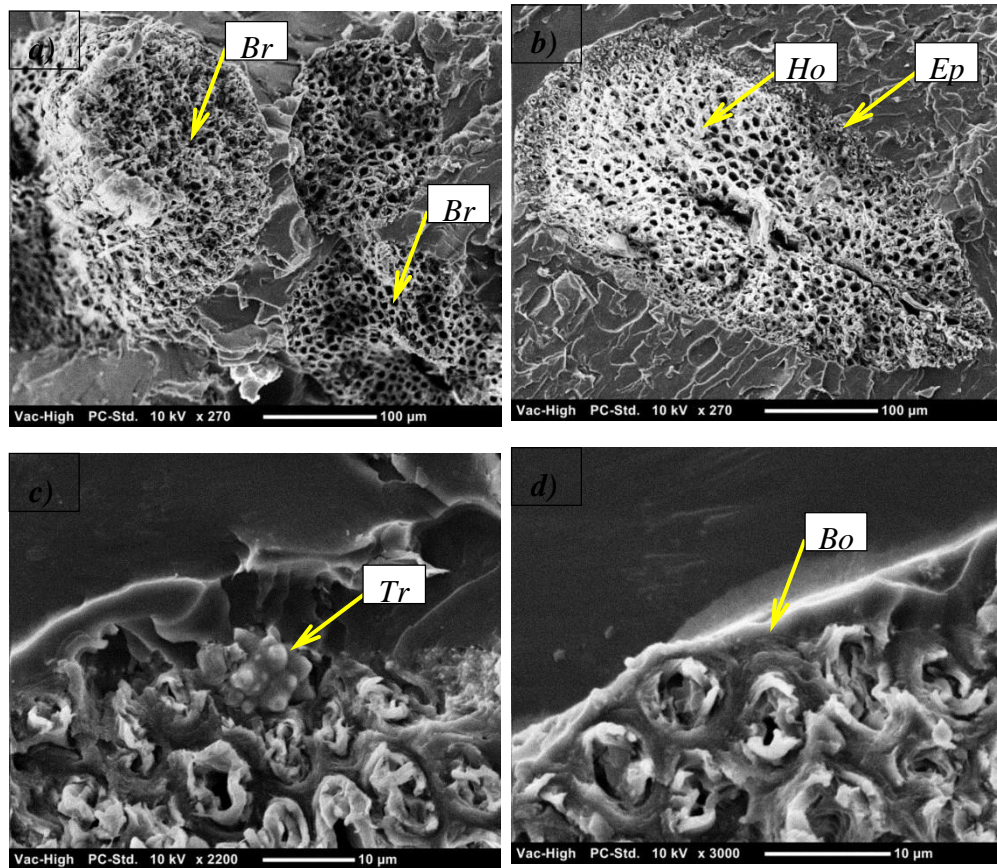
### 6.2.2 Fracture behaviour date palm/graphite/epoxy composites

In the previous chapter, the micrographs of the ECs based on different content of graphite were discussed, and it was mentioned that the three weight per cent of graphite has less effect on the microstructure of the composites compared to higher percentages. Further, the main fracture mechanism was the cleavage failure and some river-like patterns were observed, which were associated with stretching. This indicated resistance to the applied load. In this section, the micrographs of fractured samples of the EC based on DPF(s) with three weight per cent graphite are displayed in Figure 6.3 and 6.4, respectively. Where the epoxy is based only on DPF, Figure 6.3 shows a very strong bonding between the fibre and the matrix, which indicates the high interfacial adhesion of the fibre with the matrix under tensile loading conditions. This is mainly due to the six per cent NaOH treatment in improving the integrity of the two fibrous and resinous surfaces (see Figure 4.1 and Section 4.4 in Chapter 4.) This good bonding between the fibre and the matrix can be seen in Figure 6.3 and is marked as 'Bo'. Further to this surface treatment, there are some debris and partial epoxy particles in the core of the fibres. This indicates that, during the curing process, the resin was able to penetrate the fibre, with the fibre partially filling with epoxy resin (marked as 'Ep' in Figure 6.3). The micrographs show a breakage in the fibrous regions (marked as 'Br'), with no pull out process during the tensile loading. These are the main contributors to improvements in the TS of the epoxy, when reinforced with the six per cent NaOH treated DPFs.



**Figure 6.3: Micrographs of DPFE composite after tensile test.**  
**Bo = bonded, Ep = Epoxy, Br = breakage, Rl = river-like, Tr = Trichome**

For the influence of the three weight per cent of graphite to the DPF reinforced ECs on the fracture and the microstructure of the composite, the fracture surface of the tensile samples were observed and the micrographs are displayed in Figure 6.4. Similar to the micrographs of the DPF reinforced epoxy (Figure 6.3), the micrographs of the composites with the three weight per cent graphite show fibre breakage and strong interfacial adhesion of the fibre with the matrix. This indicates the high interaction between the surface of the fibre and the epoxy resin. However, there is a clear warning regarding the composite porosity. It seems the addition of the graphite fillers blocked the penetration of the epoxy resin into the core of the fibres during the curing process, despite the six per cent NaOH treatment. In Figure 6.4, it seems the core of the fibres is empty, indicating the high porosity of the composite, which could be a weak region in the composites. Despite this, there is no any sign of debonding of fibres and/or pull out.



**Figure 6.4: Micrographs of 3% graphite/DPFE after tensile test.**  
**Bo = bonded, Ep = Epoxy, Br = breakage, Tr = Trichome, Ho= holes**

### 6.2.3 Shore D hardness of the selected composites

The shore D hardness of different ECs is given in Figure 6.5. From the figure, the addition of either graphite, DPF and/or both improves the hardness of the composite. The highest increase in the hardness is exhibited when both fillers and fibres reinforce the ECs; for instance, the hardness increased from 82.3 to 84.8. Such an increase in the hardness will greatly influence the adhesive wear and frictional behaviour of the composites. The correlation between the mechanical properties and the wear and frictional performance of the composites will be discussed at the end of this chapter.

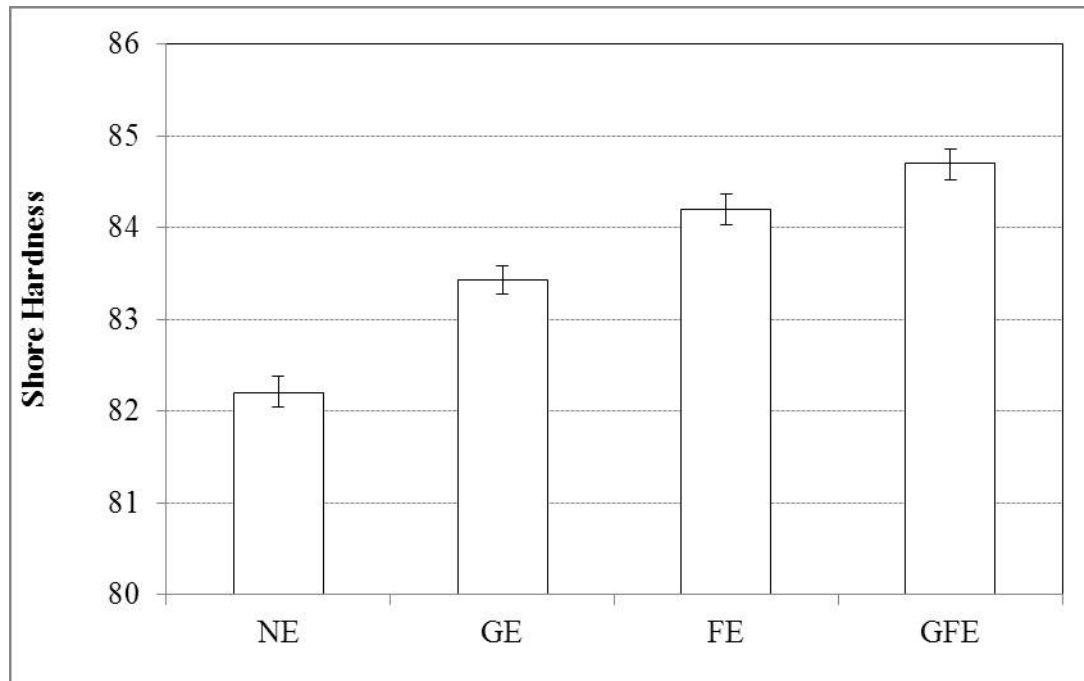


Figure 6.5: Shore D hardness of different ECs based on graphite and/or DPF. NE = neat epoxy, GE = 3% graphite/epoxy, FE = DPFE, GFE = 3 wt% graphite/date palm fibre/ epoxy

### 6.3 Tribological performance of date palm/graphite/epoxy composites under BOR technique

Wear and frictional results of various ECs based on DPFs and graphite are presented in Figures 6.6–6.14, including images showing modification on the rubbed surfaces.

#### 6.3.1 Wear behaviour of date palm/graphite/epoxy composites

The influences of the applied load on the wear performance of the composites are displayed in Figure 6.6. This shows the relationship between the specific wear rate of the composites and the applied load. In general, the specific wear rate values are scattered and there is no clear trend for the influence of the applied load. However, at an applied load of more than 40 N, there is no remarkable effect of the applied load on the specific wear rate. Such behaviour has been reported in the literature for both natural fibre/epoxy (Nirmal et al., 2012a, Yousif and Chin, 2012) or synthetic fibre/ECs (Arhaim et al., 2013). It seems that there is high integration between the asperities in

contact and steady weight loss from the surface, which results in a low effect of the applied load on the specific wear rate. It should be mentioned here that the weight loss increases with the increase of the applied load. However, specific wear rates give a general understanding of the wear performance of the materials and are comparable with results reported in the literature.

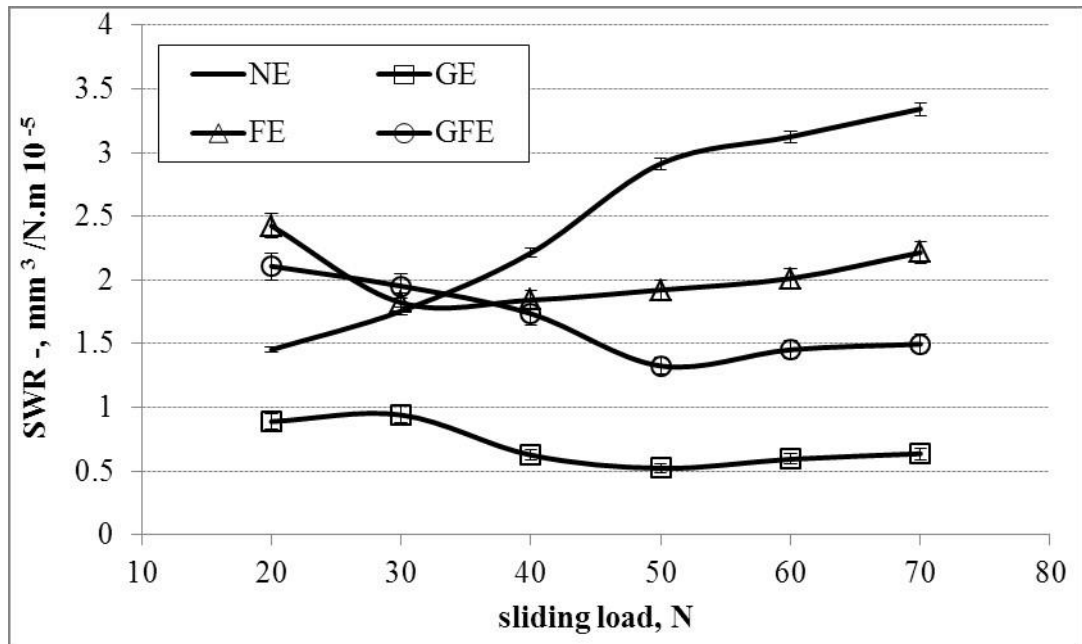
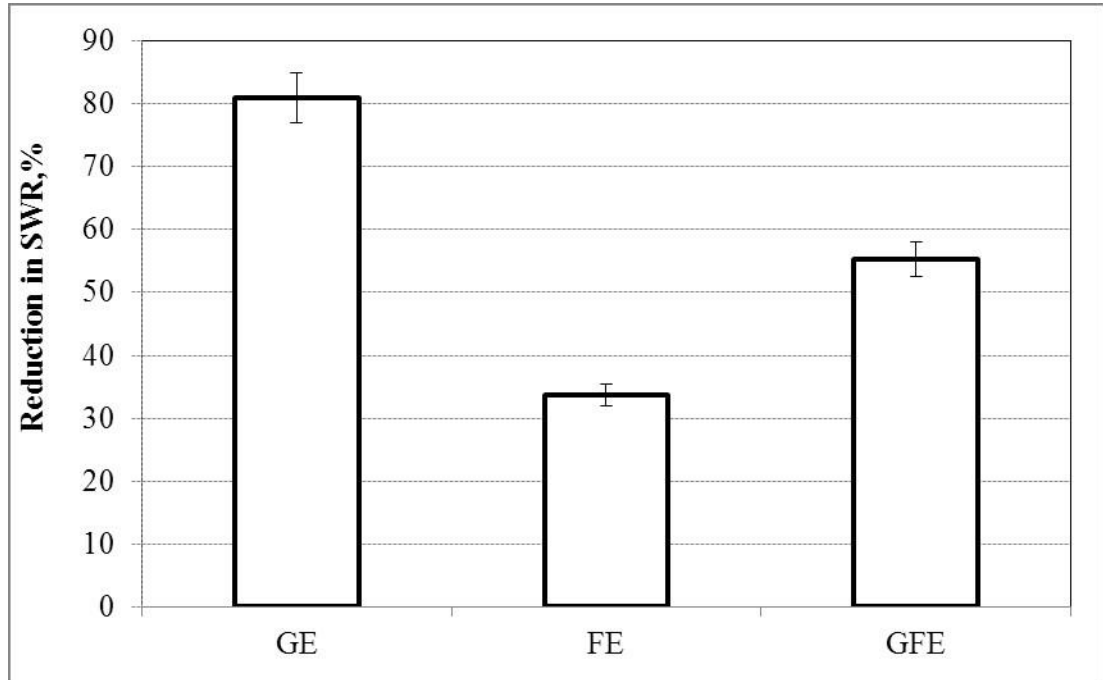


Figure 6.6: Specific wear rate v. applied load of different ECs based on graphite and/or DPF after 5.04 km sliding distance using BOR technique at sliding speed of 2.8m/s.

With regards to the influence of the DPF on the specific wear rate of the ECs, the results of Figure 6.6 are summarised in Figure 6.7, showing the reduction percentage of the selected composites compared to the NE. The figure clearly shows that the highest reduction in the specific wear rate is seen when the epoxy is reinforced with three weight per cent graphite without the addition of the DPFs. Despite that, DPF assists the epoxy to reduce the specific wear rate by about 30%. The combination of both graphite and DPF in the epoxy achieved more than 50% reduction in the specific wear rate. Note that the presence of the DPF is necessary from a mechanical perspective, since there is good enhancement of the TS (Figure 6. 1). Meanwhile, the addition of graphite alone caused deterioration of the mechanical properties. It seems the combination of both DPF and the graphite results in optimum composites in terms of wear performance and TS. This outcome could be a result of the influence of composite porosity, graphite

film transfer and the modifications on both rubbed surfaces on the wear performance of the composites. Further discussion and clarification will be given in the surface observation section.



**Figure 6.7: Reduction in specific wear rate at the steady state of different ECs based on graphite and/or DPF at 70 N applied load using BOR technique**

### **6.3.2 Frictional behaviour of date palm/graphite/epoxy composites**

The friction coefficients of the ECs with different reinforcements under different applied loads are presented in Figure 6.8. The value of the friction coefficient for each composite was obtained at the steady state conditions after five kilometres sliding distance for three sets of tests. The friction coefficient seems to decrease with the increase of the applied load. Further, there is no significant influence on the friction coefficient by the higher values of applied loads. The friction force in the interface also increases with the increase of the applied load.



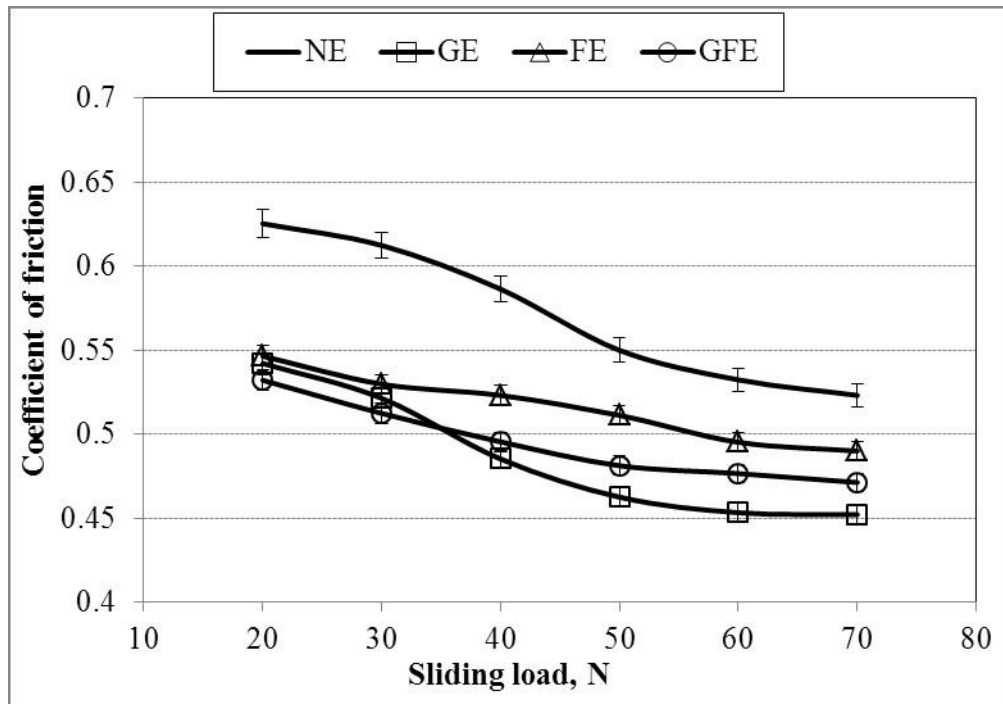


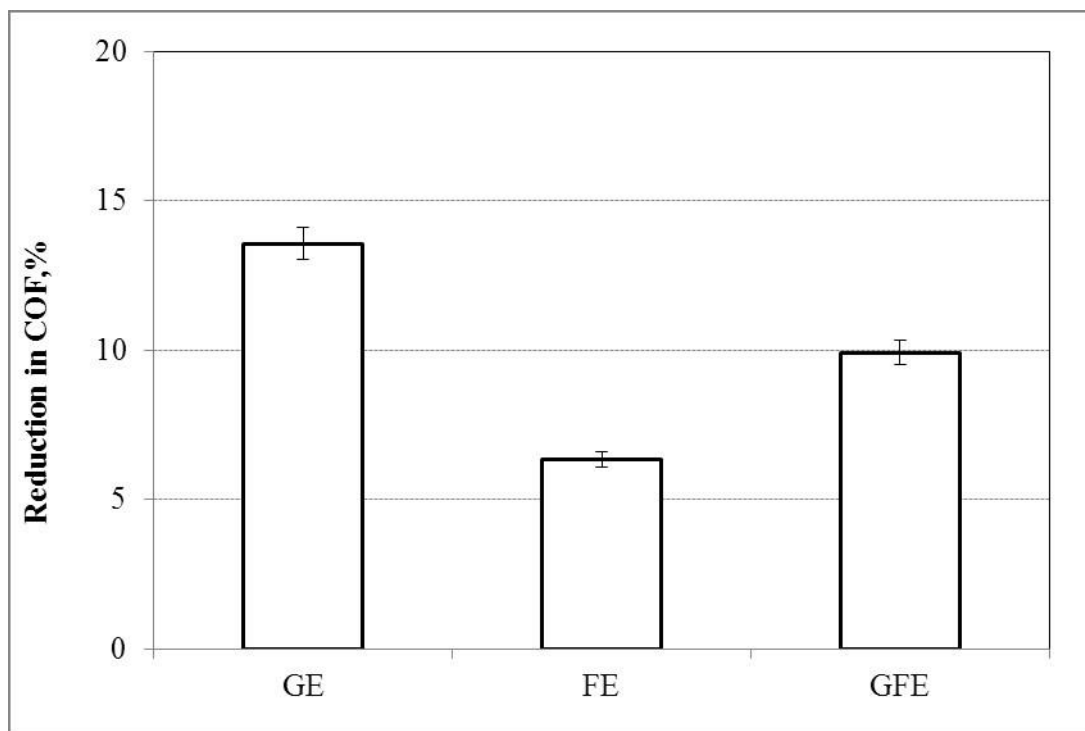
Figure 6.8: Coefficient of friction v. sliding load of different ECs based on graphite and/or DPF using BOR technique

The reason for the stability of the friction coefficient with the increase of the applied load is the film generation on the stainless steel counterface for all the materials. Similar trends have been reported on polyester and ECs, based on either synthetic or natural fibres, such as glass fibre/polyester or ECs (Pihtili, 2009, Yousif, 2013a), cotton/polyester (Hashmi et al., 2007a) and coir/polyester (Yousif, 2009). Further discussion will be presented in the section that examines the roughness modification of the rubbed surfaces during the sliding process.

Regarding the influence of the reinforcement on the friction performance of the ECs, the reduction percentage of the friction coefficient of the epoxy from the reinforcements are determined and presented in Figure 6.9. It seems all the reinforcements assist in reducing the friction coefficient of the epoxy. The highest reduction in the friction coefficient can be seen when the epoxy is reinforced with the graphite solid lubricant only. This is expected and was explained in detail in Chapter Five. For the influence of the DPF, there is approximately seven per cent reduction in the friction coefficient, which is a low reduction. The insignificant influence of the DPF on the friction coefficient could be because of high resistance in the interface to

the material removal from the surface. From the literature, it has been reported that the addition of oil palm (Yousif, 2008), betelnut (Nirmal et al., 2012a), coir (Yousif, 2009), sugarcane (El-Tayeb, 2008) or cotton (Hashmi et al., 2007b) fibres into polyester composites increases the friction coefficient.

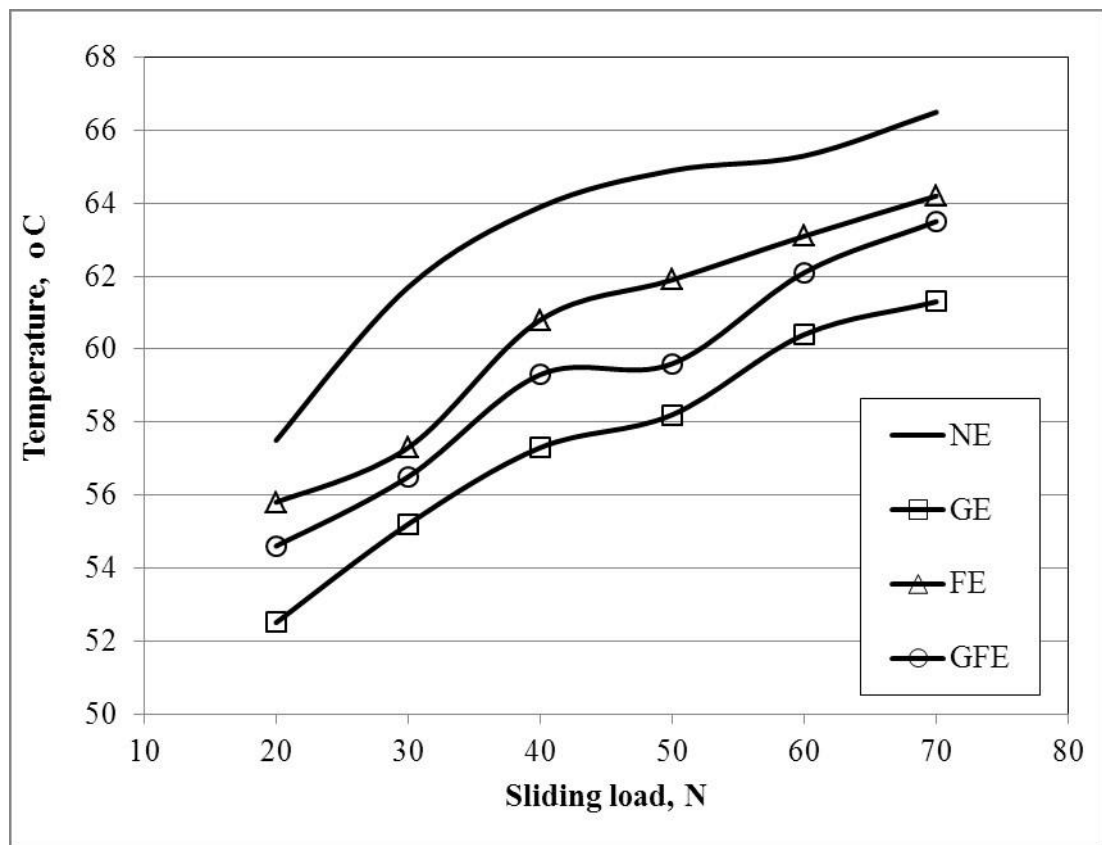
It can be seen that there is very high integration between the asperities of the natural fibres with the smooth metal surface. The presence of a solid lubricant, such as graphite, supports its role in the reduction of the friction coefficient. In the current study, the addition of the three weight per cent of graphite into the date palm/ECs increases the reduction in the friction coefficient to 10%, compared to the DPF alone, which shows about seven per cent reduction only, that is,  $\mu = 0.57 \text{ NE} \rightarrow 0.49 \text{ epoxy} + \text{DPF} \rightarrow 0.47 \text{ epoxy} + \text{DPF} + 3 \text{ wt. \% graphite}$ .



**Figure 6.9: Reduction in COF at the steady state of different ECs based on graphite and/or DPF at 70 N sliding load using BOR technique**

Heat generates and raises the interface temperature because of the friction in the interface, which is monitored using the thermo-imager. The maximum temperature

reached the maximum sliding distance for each material under each applied load, since heat is generated with the sliding. The maximum recorded temperature for each material under each applied load is presented in Figure 6.10. There is an obvious increase in the interface temperature with the increase of the applied load. This is expected from a theoretical perspective, since the frictional force increases with the increase of the applied load. NE exhibits the highest interface temperature compared to others and the lowest is achieved when the graphite is added into the epoxy. The presence of the DPF in the ECs shows an intermediate effect on the interface temperature. In contrast, there is not much increase in the temperature up to the level of temperature gradient of the resin ( $120^{\circ}\text{C}$ ).



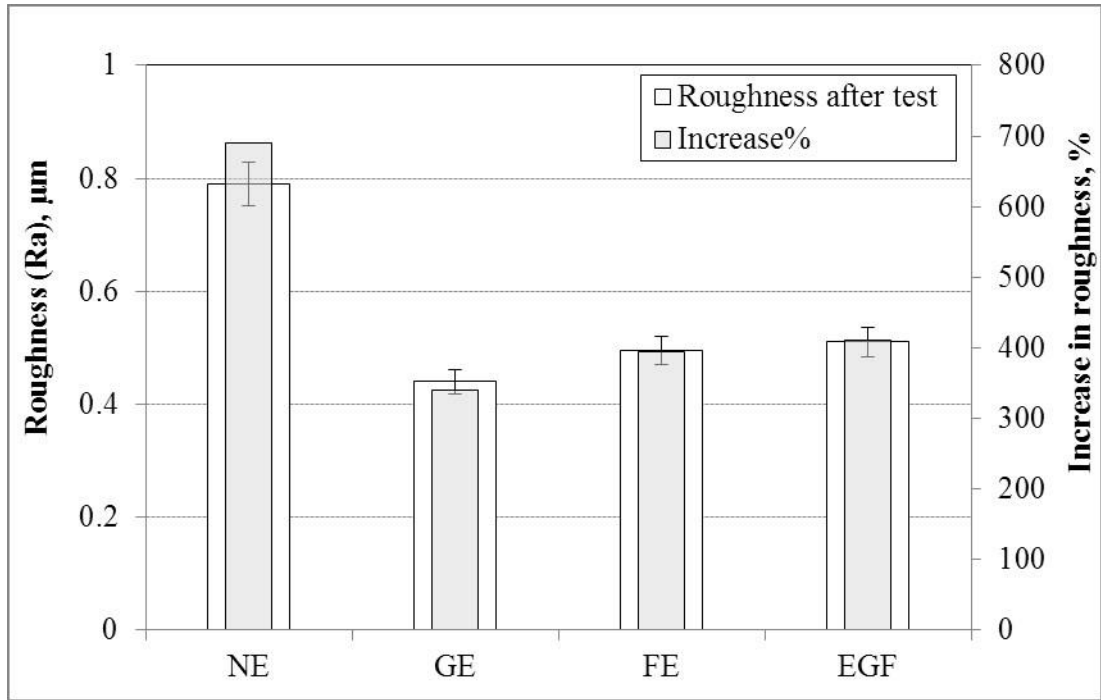
**Figure 6.10: Interface temperature of different ECs based on graphite and/or DPF at different applied loads after 5.04 km sliding distance using BOR technique**

### 6.3.3 Observation on the worn surfaces after BOR tests

This section is divided into three sub-sections to discuss the modifications on the roughness of both the composite surface and the wear track on the stainless steel counterface. The last section covers the SEM observation of the worn surface of the composites after the BOR tests.

#### *6.3.3.1 Roughness modifications of the wear track*

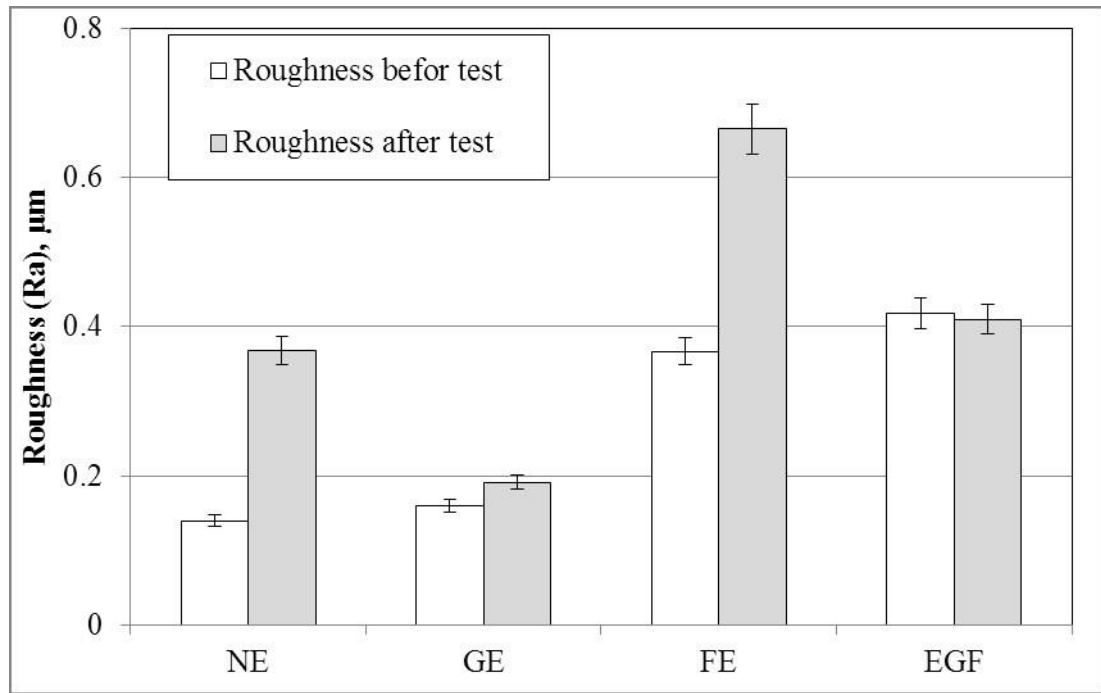
Before each test, the roughness of the stainless steel (AISI 304, hardness = 1250 HB) was maintained at  $R_a = 0.1 \pm 0.05 \mu\text{m}$ . After the composite rubbed against the stainless steel counterface, the wear track formed. The roughness of the wear track after testing is presented in Figure 6.11 for the 50 N applied load. All the materials caused increases in roughness, as shown in Figure 6.11. The greatest increase is exhibited when the NE is tested. The addition of the graphite alone has the least effect on the roughness of the counterface, which could indicate the presence of the film transfer on the wear track. DPF alone, or combined with the three weight per cent graphite, showed a similar effect to the three weight per cent of graphite/ECs. That is, the DPF has a smaller effect on the roughness of the counterface. This is promising compared to synthetic fibres, which always reported high abrasive fibres and damaged the counterface. This was reported with glass fibres (Nirmal et al., 2012a).



**Figure 6.11: Roughness values of the counterface surface after adhesive loadings of different ECs based on graphite and/or DPF at 50 N applied load using BOR technique**

### 6.3.3.2 Roughness of the composite surface

The modifications of the roughness of composite surfaces after the test are displayed in Figure 6.12 after the test under 50 N applied load for five kilometre sliding distance. Significant changes can be seen in the case of the NE and the EC based on DPFs. However, the addition of the three weight per cent graphite to the DPF reinforced ECs maintains a stable roughness to the composite surface, since there is little change to the surface roughness of the date palm/three weight per cent graphite/EC.



**Figure 6.12: Roughness values of the specimen surface of different ECs based on graphite and/or DPF after adhesive loadings at 50 N using BOR technique for 5 km sliding distance**

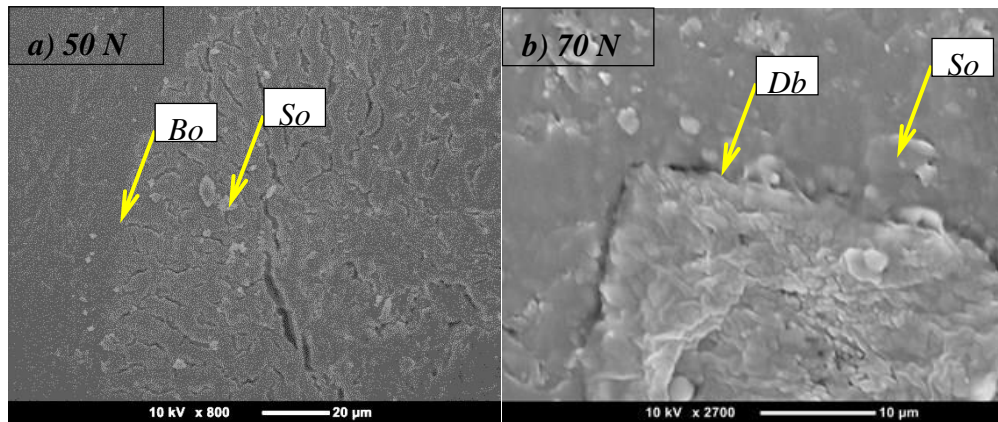
### 6.3.3.3 SEM observation

#### Date palm FECs

The micrographs of the worn surface of the DPF reinforced ECs are presented in Figure 6.13 at 50 N and 70 N applied loads. The micrographs show that the resinous regions are exposed to a softening process. Meanwhile, at 50 N applied load, the fibres are still well adhered in the matrix and are well bonded (marked as 'Bo' in Figure 6.13a). At the higher applied load of 70 N, it seems the fibres suffer from slight debonding because of the shear force (marked as 'Db' in Figure 6.13b). Interestingly, there is no pull out for the fibres and they are still in the bulk of the composite. In addition, at higher applied loads, it seems the DPF are partially coated by particles of epoxy because of the thermo-mechanical loading.

For the graphite epoxy, Chapter Five, Section 5.4.3.3 (Figure 5.22) showed that the composites suffered from different wear mechanisms. The main ones are so = softening, fr = fracture, pg = patch of graphite and df = deformation. When comparing

both materials under the same condition of 50 N applied load, the DPF/composite surface is not highly damaged compared to the ones seen on the graphite/EC surfaces.



**Figure 6.13: Micrographs of DPF/ECs after testing under 50 N applied load using BOR technique Bo = bonded, So =Softening, Db =debonding**

DPFE combined with three weight per cent graphite composites.

The micrographs of the worn surfaces of the ECs based on DPF with the three weight per cent graphite are displayed in Figure 6.14 for two different applied loads, after five kilometre sliding distance. At the 50 N applied load, the micrographs show a very good quality surface, since there is no sign of debonding, pull out or high porosity. However, micro-cracks (marked as 'Cr') appear on the end of the fibres, indicating the high resistance to shear in the rubbing process. At the 70 N applied load, a very small micro-gap can be seen between the fibre end and the resinous region, indicating a very minor debonding process. In comparison to the date palm/EC (see Figure 6.13), the presence of the graphite seems to be very effective in reducing the damage on both resinous and fibrous regions. This is mainly due to the high reduction in the frictional heat in the interface with the presence of the solid lubricant graphite. In other published works, oil palm (Yousif, 2008), betelnut (Nirmal et al., 2012a) and sugarcane (El-Tayeb, 2008) reinforced polyester composites exhibited very poor surface quality, since the surface was suffering from fibre pull out, breakage and tear, as well as a very high softening process because of the high frictional force in the interface. Further, it seems the addition of the three weight per cent of graphite makes the date palm/EC very competitive with other natural fibres/polymer composites. Nevertheless, polymer

composites based on synthetic fibres, such as glass/epoxy (Basavarajappa and Ellangovan, 2012), carbon fabric/phenolic (Fei et al., 2012) and carbon/epoxy (Subbaya et al., 2012) exhibited high deterioration in the bonding region between the fibre and the matrix under dry adhesive wear loading conditions. For glass/epoxy (Basavarajappa and Ellangovan, 2012), the abrasive nature of the glass fibre and the presence of the debris in the interface damaged the composite surface and roughened the counterface surface simultaneously. Since the glass debris acted as a third body in the interface and transferred the adhesive wear into three body abrasion, leading to high removal of materials. Similar issues have been reported with the case of carbon fibre/polymer composites, with relatively less damage compared to glass, since carbon fibre is considered one of the lubricant materials in the interface, carbon/epoxy (Subbaya et al., 2012). In other words, natural fibres have a high potential to replace synthetic fibres, since they have a smaller effect on rubbed surfaces.



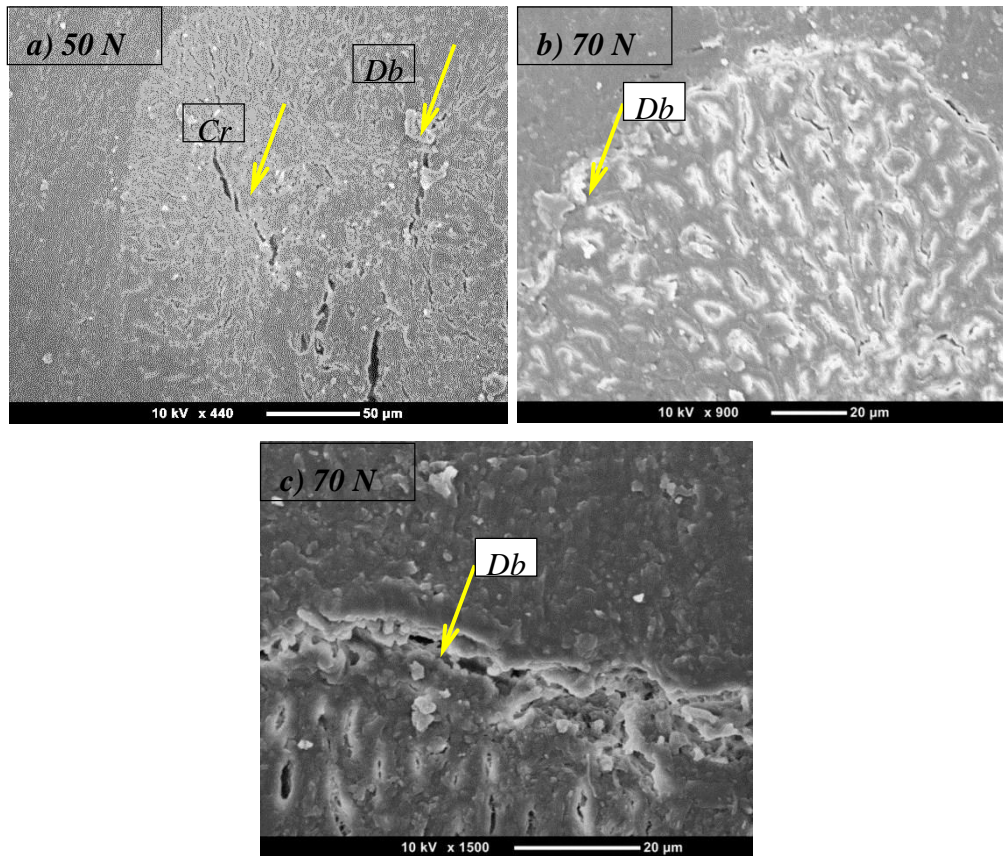


Figure 6.14: Micrographs of date palm/3 wt% graphite/ECs after testing at 50 N using BOR technique Cr= cracks, Db =debonding

#### 6.4 Tribological performance of date palm/graphite/epoxy composites under BOD technique

In the majority of reported studies, the experiments were performed individually on BOD, BOR, ball-on-block or roller-on-block tests. However, no material displayed a universal tribo-performance on different test techniques. Recently, an attempt was made by Zhang et al. (2007) to investigate the effect of short length carbon fibres on the tribo-performance of ECs sliding against steel, using the BOD and BOR techniques. The longer fibres in the composites exhibited a better wear resistance in comparison to the shorter fibres for both the BOD and BOR methods. However, there was a variation in the wear results from the two techniques at the same conditions of contact pressure. The composites showed higher wear resistance in the case of BOD compared to BOR. In other words, the wear properties were not intrinsic material parameters but were

sensitive to the applied conditions. There seemed to be significant effects of the test techniques on the wear performance of polymeric composites. Similar findings have been reported with glass fibre/polyester composites under both dry/wet adhesive wear contact conditions using BOR and BOD (Yousif and El-Tayeb, 2008b). In the current study, some of the promising materials were selected to be tested with the BOD technique and compared with the BOR (NE, three weight per cent graphite/EC, date fibre/EC and three weight per cent graphite/date fibre/EC). The results appear in Figures 6.15 to 6.24, covering the wear and frictional results combined with observation of the worn surfaces.

#### **6.4.1 Wear and frictional behaviour of date palm/graphite/epoxy composites**

The specific wear rates of the composites under different applied loads are presented in Figure 6.15 after a sliding distance of five kilometres, using the BOD technique. It seems the increase of the applied load generally increases the specific wear rate of all the materials. In the previous section on the BOR technique, there was no significant influence of the applied load on the specific wear rate, especially at high range of applied load ( $\geq 50$  N). It seems the contact between the asperities is formed and connected to control the wear behaviour of materials. In the BOD, the contact starts with an area of 10 mm x 10 mm and continues to the end of the sliding. Meanwhile, in the BOR, the contact starts with a small curved area and gradually increases. Such findings have been reported by Zhang et al. Zhang et al. (2007), whose work investigated the effect of short length carbon fibres on the tribo-performance of ECs sliding against steel using the BOD and BOR. Similar findings have been reported with the glass/polyester composites (Yousif and El-Tayeb, 2008b).

With regard to the influence of the DPF and graphite filler on the wear performance of the ECs under BOD, the reduction in the specific wear rate compared to the NE is given in Figure 6.16 for each selected material. This figure clearly shows that the addition of the graphite alone to the ECs exhibits the highest reduction in the specific wear rate, followed by graphite and date palm and then date palm alone. This is similar to the BOR trends given in Figure 6.7.

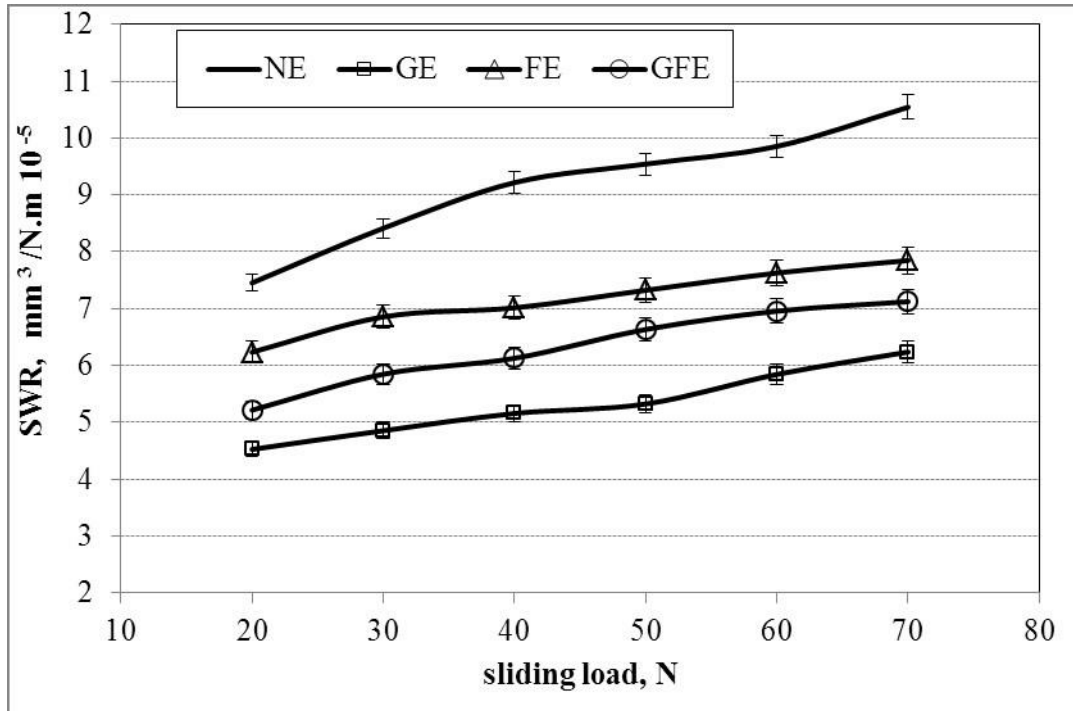


Figure 6.15: Specific wear rate v. applied loads of different ECs based on graphite and/or DPF using BOD technique

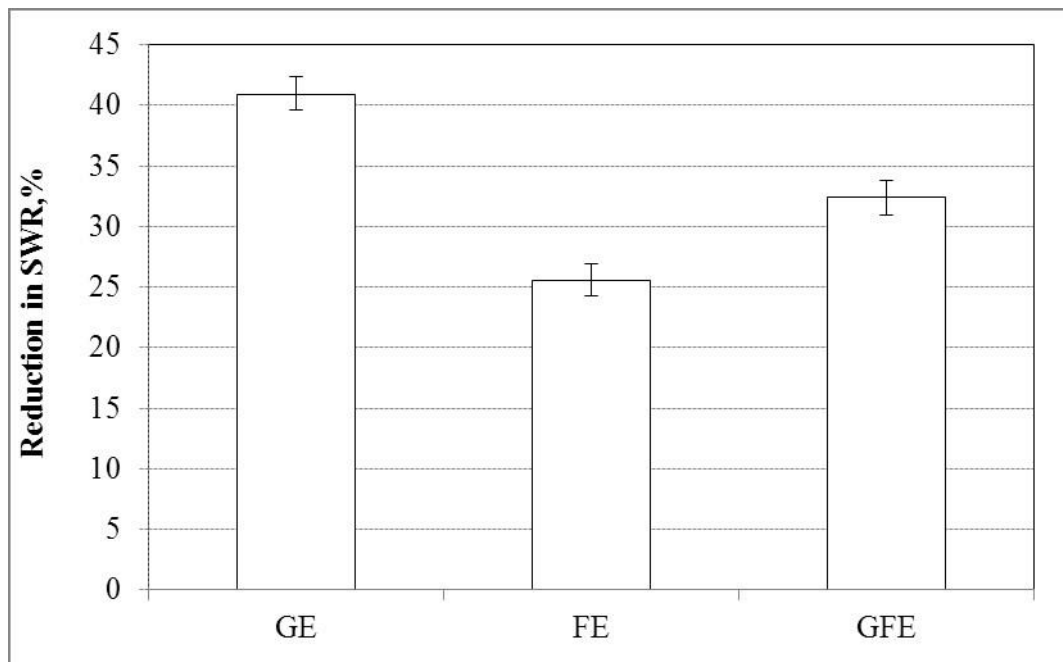
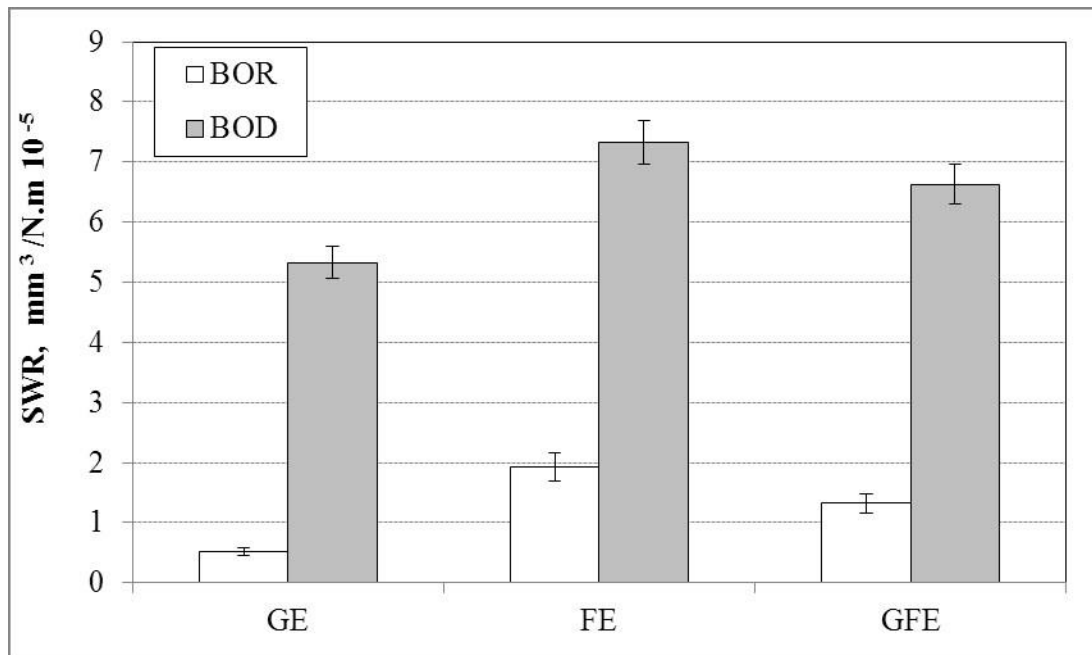


Figure 6.16: Reduction in specific wear rate at the steady state of different ECs based on graphite and/or DPF at 70 N sliding load using BOD technique

To show the influence of the testing technique on the wear performance of the composites, specific wear data were extracted for both techniques at 50 N applied load

after five kilometre sliding distance and plotted in Figure 6.17. All the composites show similar behaviour in terms of the techniques, since they show higher specific wear rate when they have been tested on the BOD than the BOR. This has been reported with synthetic fibres/polymer composites, glass/polyester (Yousif and El-Tayeb, 2008b) and carbon/epoxy (Zhang et al. (2007).



**Figure 6.17: Specific wear rate of the selected composites using BOR and BOD techniques after applied load 50 N and 5 km sliding distance.**

This can be clarified when the frictional results are presented. In Figures 6.18 and 6.19, the frictional and the interface temperature of the composites tested using the BOD techniques are presented. Obviously, the friction coefficient of the composites is very high for all the applied loads, which increases the interface temperature. Accordingly, the high thermo-mechanical loading in the interface is the main reason for the poor wear performance of the BOD composite, compared to the BOR, which showed less and shear forces (Figure 6.8). With the BOR, the friction coefficient of date palm/graphite/ECs is 0.47, equivalent to friction force = 23.5 N at the 50 N applied load. Under the same operating conditions for the same material using BOD, the friction coefficient is 0.84, equivalent to a frictional force of 42 N. In other words, the shear force in the BOD is greater than the BOR by about 46%. In comparing the

interface temperature of both techniques, there is not much difference between them, despite BOD (Figure 6.10) exhibiting slightly higher temperatures than the BOR.

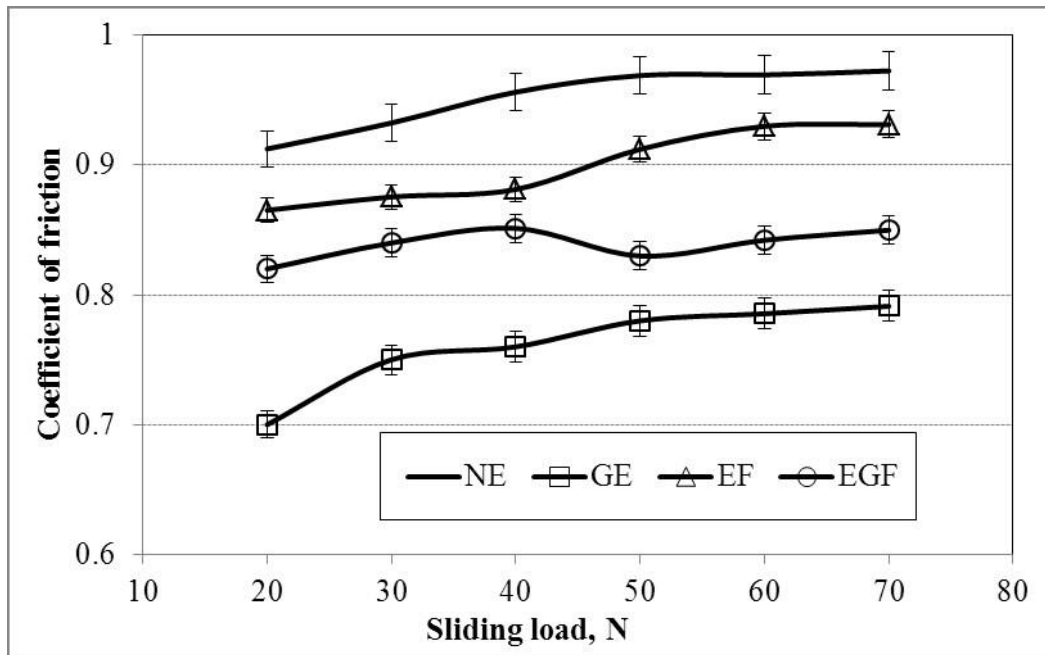


Figure 6.18: Coefficient of friction v. sliding load of different ECs based on graphite and/or DPF using BOD technique

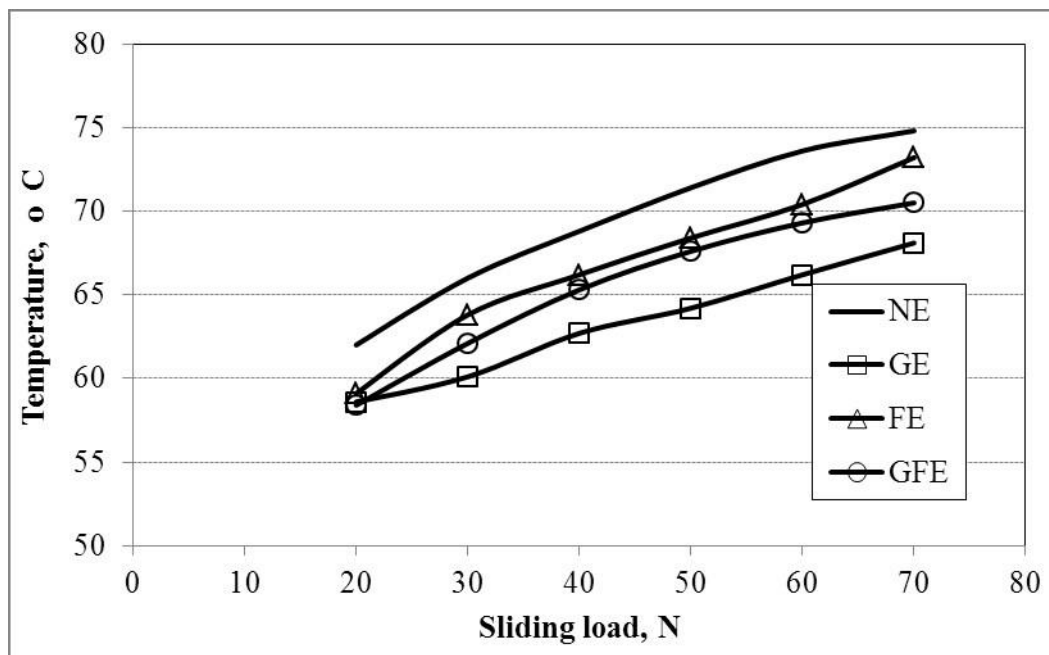
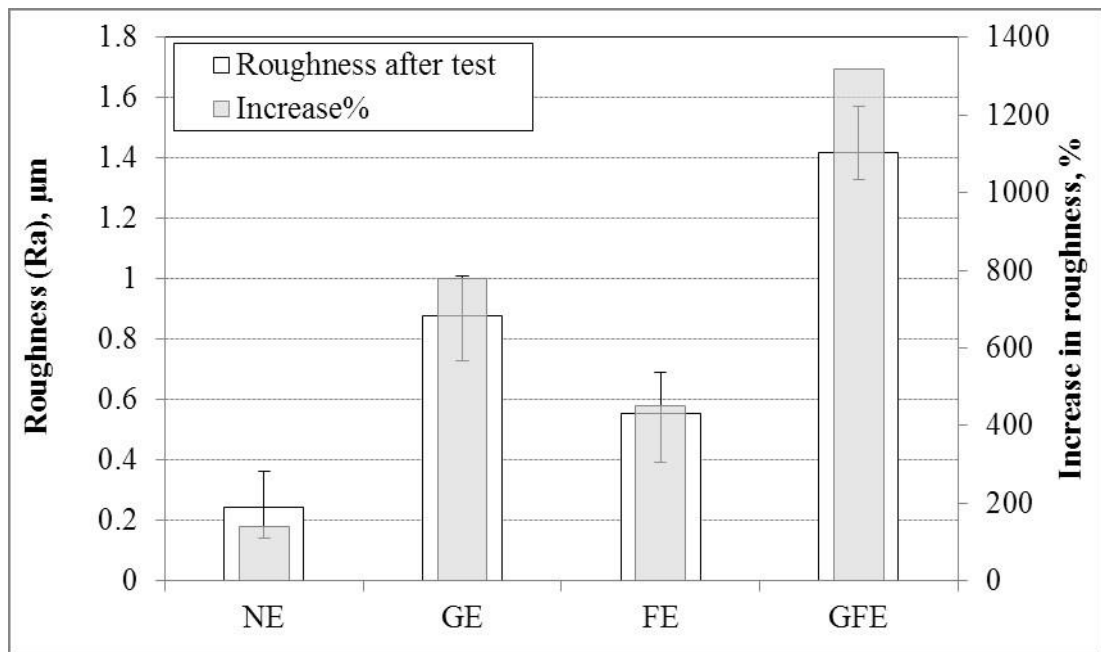


Figure 6.19: Interface temperature of different ECs based on graphite and/or DPF at different applied loads using BOD technique

Further to the clarification given through the thermo-mechanical loading, the counterface roughness increased dramatically when the composites were tested using

BOD, as shown in Figure 6.20. Comparing this figure with Figure 6.11 of the counterface roughness using BOR, there is a significant difference in which the wear track of the BOD becomes very abrasive compared to the BOR. Accordingly, with the BOD technique, there is an increase in the shear force and roughness of the wear track, leading to high material removal from the composite surface and deterioration of the composite wear performance. This may be confirmed by the SEM observations in the next section.

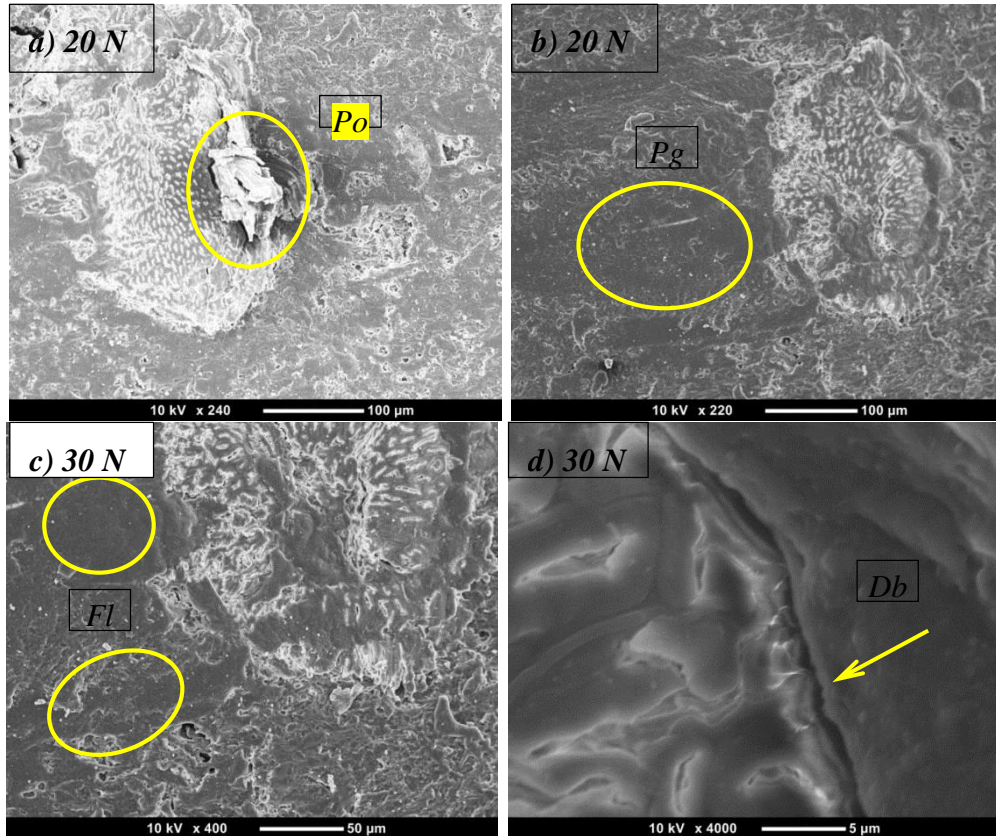


**Figure 6.20: Roughness values of the counterface surface after adhesive of different ECs based on graphite and/or DPF loadings at 50 N using BOD technique**

#### **6.4.2 Observation on the worn surfaces of date palm/graphite/ECs after BOR testing**

From the tribological and mechanical experimental data, we can suggest that date palm/three weight per cent graphite/EC is the optimum composition for mechanical and tribological performance. Therefore, only the micrographs of the worn surface of the selected date palm/three weight per cent graphite/ECs will be discussed in this section. Under low applied loads of 20 N and 30 N, the micrographs of the worn surfaces are presented in Figure 6.21. Under such loads, the micrographs show there is a pull out process on the fibrous regions (Figure 6.21a), which is not seen with the

BOR. This is due to the rougher surface of the counterface associated with the high thermo-mechanical loading, as explained in the previous section. Further, there is a ploughing process occurring on the resinous region, as shown in Figure 6.21b. At the 30 N applied load, debonding of the fibres took place and pitting or fragmentation appeared with plastic deformation, despite the presence of film transfer.

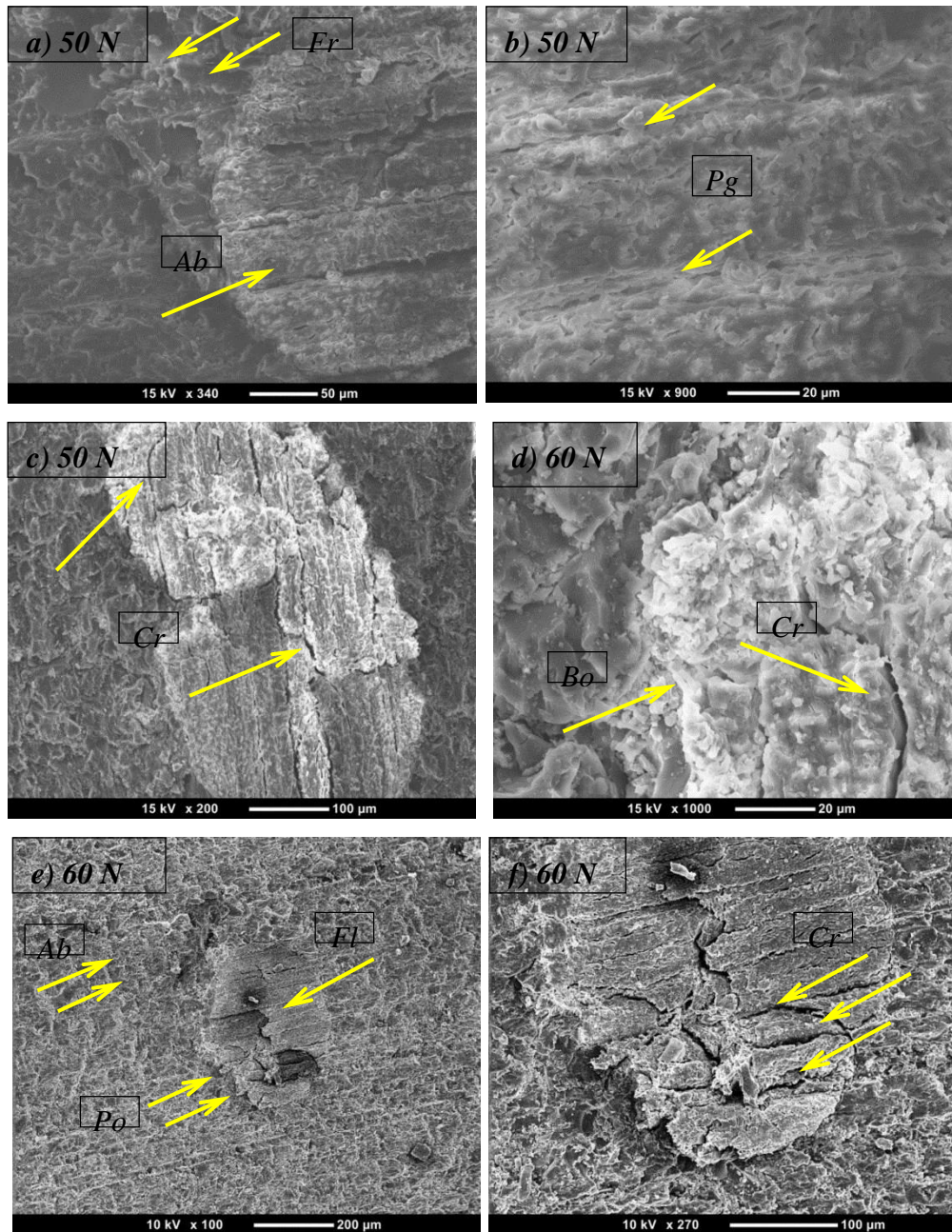


**Figure 6.21: Micrographs of the date palm/3 wt% graphite/ECs after the experiments using BOD under low applied loads. Fr = fragmentation, Ab = abrasive, Pg = ploughing, Cr = crack, Bo = bonded, Po = pull out, Fl = film transfer**

Under the high applied load of 50 and 60 N, Figure 6.22 displays the micrographs of the worn surface of the selected optimum composite. The abrasive nature of the surface of the composites and on both resinous and fibrous regions is very clear. The abrasive nature is mainly due to the high roughness of the counterface from the modification on the wear track. It is clear now that the contact technique controlled the asperities' interaction. Such a massive abrasive nature was not seen when the same composite was tested using BOR under the same operating conditions. The wear mechanism

dominated by abrasive wear, ploughing, crack and pulls out of fine fibres forms the fibre bundle, as shown in Figure 6.22. Unfortunately, there is no sign of film transfer or plastic deformation on the surface. It seems, during the sliding, a roughening process occurs on the counterface, associated with high removal of the material from the composite surface. This can clarify and explain the poor wear performance of the composite, despite the presence of the solid lubricant as graphite.





**Figure 6.22: Micrographs of the date palm/3 wt% graphite/ECs after the experiments using BOD under high applied loads. Pl = pull out fibre, Pg = ploughing, Fl = film transfer, Db = debonding, Ab= Abrasive wear, Fr= Fracture, Cr, Cracks**

## 6.5 Discussion and arguments with previous works

Some of the related and recent published works are listed in Table 6.2. The collected data are selected based on the operating parameters being closer to the current operating parameters of 2.8 m/s sliding velocity, the specific wear rate and friction coefficient at the steady state. The applied load is about 50 N using the BOR technique. Moreover, the participant candidate attempted to study the tribological performance of the EC based on synthetic glass fibre with the research group at the University of Southern Queensland (USQ) (Arhaim et al., 2013). The research findings are included in Table 6.2. It is interesting to compare the polymeric performance of the ECs based on natural fibres (current reported results) and synthetic fibres (published work by the USQ group).

Both results found that DPFs have a high potential to replace synthetic fibres; the specific wear rate of the glass fibres and data palm fibres were still in the same order (10 to five), with glass fibre presenting lower specific wear rates. In addition, the comparison of the friction coefficient values of glass (0.2), kenaf fibre (0.4) and DPF (with/without graphite) (0.5–0.47) was supportive, encouraging natural fibres as an alternative to synthetic fibres in ECs.

From this table, it can be seen that the DPFE composite is a very competitive candidate, especially with the addition of the graphite fillers. Based on the given information in this table, a few important points can be made:

- Interfacial adhesion of the fibre with the matrix is the key of the wear performance of natural fibre/polymer composites.
- The addition of the graphite is highly recommended for the natural fibre/polymer composites, which can assist in reducing the friction that, in turn, enhances the wear characteristics of the polymer composites.
- Natural fibres are very competitive candidates for replacing synthetic fibre, such as glass, since they can support the composite and lower the wear rate and the friction coefficient more than the synthetic fibres.

**Table 6.3: Summary of previous works on effect of natural fibres and fillers on tribological behaviour of polymer composite**

Matrix	Reinforcements	SWR, 10 <sup>-5</sup> mm <sup>3</sup> /N.m	$\mu$	Remarks
Current	Date palm/epoxy	1.9	0.51	
Current	Gr/date/palm epoxy	1.35	0.47	
(Arhaim et al., 2013)	GF/epoxy	0.6	0.2	The lowest specific wear rate is represented with the anti-parallel orientation at 30 N applied load.
(Arhaim et al., 2013)	Kenaf/epoxy	1	0.4	The lowest specific wear rate was found at the normal orientation at 30 N.
(Nirmal et al., 2012b)	Bamboo/epoxy	6.5	0.6	Adhesive tribological performance of Bamboo/EC was found to be superior for AP-O.
(Basavarajappa and Ellangovan, 2012)	GF/epoxy	1.3	NA	The fillers have contributed to improving the wear performance of composites.
(Basavarajappa and Ellangovan, 2012)	GF/Gr/SiCp/epoxy	0.92	NA	The applied load has highly effected SWR compared to the others parameters. SEM showed a thin dark film on the surface of GEC.

(Yousif, 2009)	Coir/polyester	1.7	0.66	<p>Deformation, micro-ploughing and debonding of fibre appear clearly on the worn surface of composite.</p> <p>All test parameters have a considerable effect on the tribological behaviour of the materials.</p>
(El-Tayeb et al., 2006)	Chopped glass/polyester	2.85	0.68	<p>The wear mechanism was controlled by debonding of fibres, matrix deformation and polyester debris transfer.</p> <p>The orientations of CSM glass fibre had a significant influence on the tribological performance of polyester composite.</p>
(Xin et al., 2007)	Sisal/polyester	1	0.65	<p>Chemical treatment has enhanced wear performance of untreated sisal fibre-reinforced polyester composite.</p> <p>Coefficient of friction was directly proportional to increase of fibre content and inversely decreased with increase of load.</p>
(Hashmi et al., 2007b)	Cotton/polyester	3.5	> 1	<p>The graphite content significantly reduced the SWR and COF of cotton/polyester.</p>
(Hashmi et al., 2007b)	Cotton-5%Gr/polyester	1.2	0.62	<p>Addition of graphite in cotton-polyester composite has minimised the contact surface's temperature.</p>

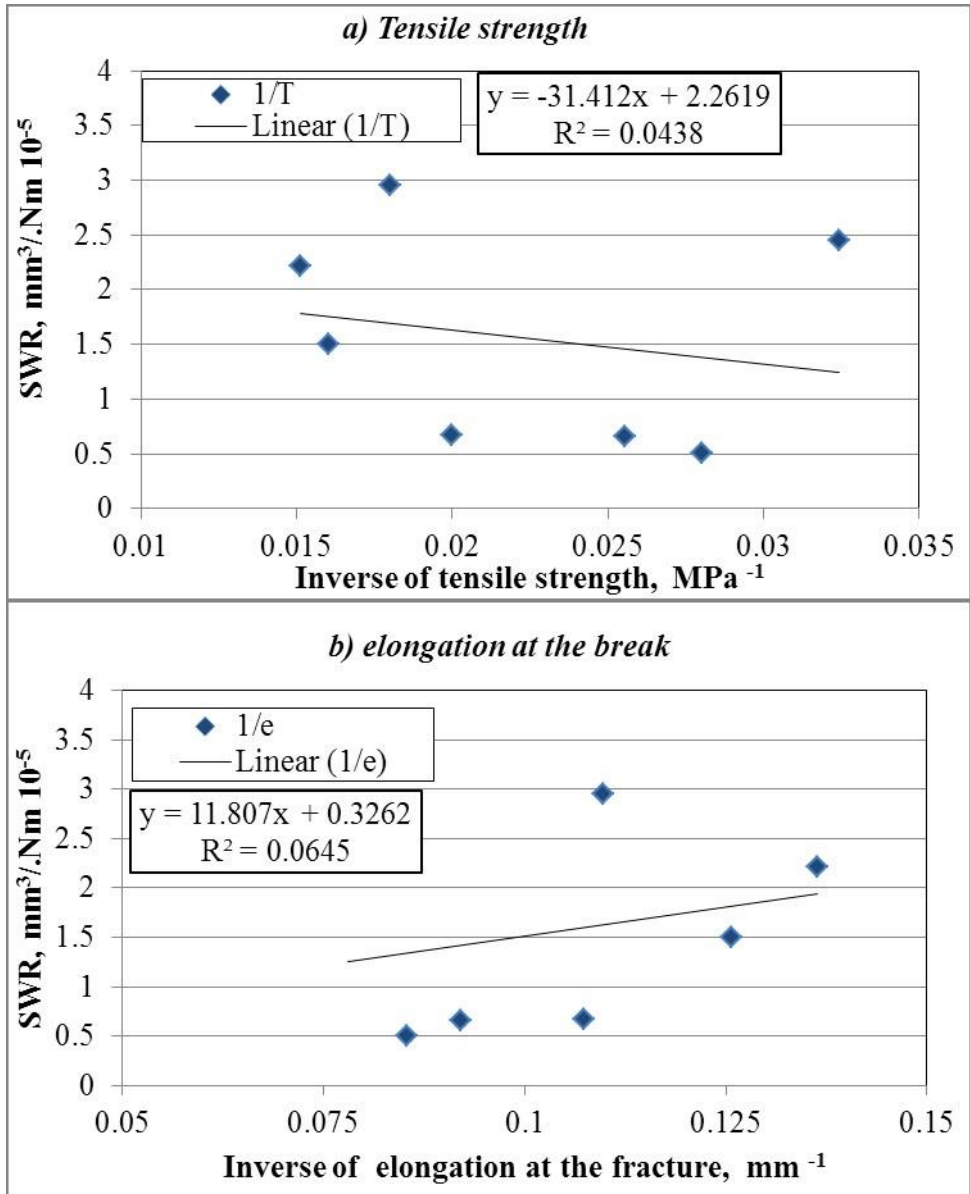
(Hashmi et al., 2007b)	Cotton-10%Gr/polyester	1	0.6
------------------------	------------------------	---	-----

## 6.6 Correlation between mechanical and tribological properties

There is great debate in the literature regarding the relationship or correlation between the mechanical and the tribological performance of materials, as reported by many scholars. The main reason for reinforcing the polymers is to improve their mechanical properties, while the wear performance of the composites is not consistently considered (Harsha et al., 2003). Arguments and contradictions have been reported. For instance, studies by some researchers (Shipway and Ngao, 2003) showed a poor relationship between the mechanical properties (T, e and H) with the 3B-A wear rate of twenty polymeric materials, where T = ultimate strength, e = elongation at the break and H = hardness). In considering the properties individually, some studies found that hardness plays a major role in controlling the abrasive wear (Shipway and Ngao, 2003); however, some found otherwise (Budinski and Ives, 2005); (Larsen et al., 2008). For the current work on NE and its composites based on different graphite percentage and date palm fibres, the mechanical and wear properties of the materials were extracted and plotted to study the correlation between the adhesive wear performance and the mechanical properties. The correlation between the mechanical properties and the tribological performance of materials have been attempted by (Budinski and Ives, 2005); (Larsen et al., 2008) (Shipway and Ngao, 2003); and (Yousif and El-Tayeb, 2010). In those works, linear correlation was established associated with the error square. Accordingly, the current study establishes the correlation based on the same technique with different materials. This will assist in the arguments with the published works as well.

For the current work, several attempts were made to find any correlation between individual mechanical properties with the steady state of the specific wear rate under 50 N applied load after five kilometres sliding distance, using the BOR technique. The completed figures are given in **Appendix C**. Samples of the plotted figures are given in Figure 6.23, showing the inverse of the TS and the elongation at the break against the specific wear rate of the studied materials. Considering individual mechanical property, there is no remarkable and significant correlation between the mechanical properties and the specific wear rate. In other words, hardness, TS, modulus of elasticity and elongation at the break have no correlation with the specific wear rate of the materials. This confirms the concept of wear being the response to the interaction between the asperities. It does not depend on the mechanical properties of materials (Stachowiak, 2006).

The combination of more than one mechanical property may give a better correlation with the specific wear rate. Figure 6.24 displays some of the mechanical properties combined together against the specific wear rate. Despite the fact that there is a slight increase in the error square (36%) compared to the individual properties (< 10%), there is no strong confirmation of a correlation between the mechanical and the tribological properties. Therefore, this work concurs with the literature that states no correlation exists especially with regards of the specific wear rate and the mechanical properties, (Yamaguchi (Yamaguchi, 1990); Budinski (Budinski, 1997); Bakumov et al. (Bakumov et al., 2012) & Pöllänen et al. (Pöllänen et al., 2011).



**Figure 6.23: Correlation between the individual mechanical properties and specific wear rate of the studied materials**



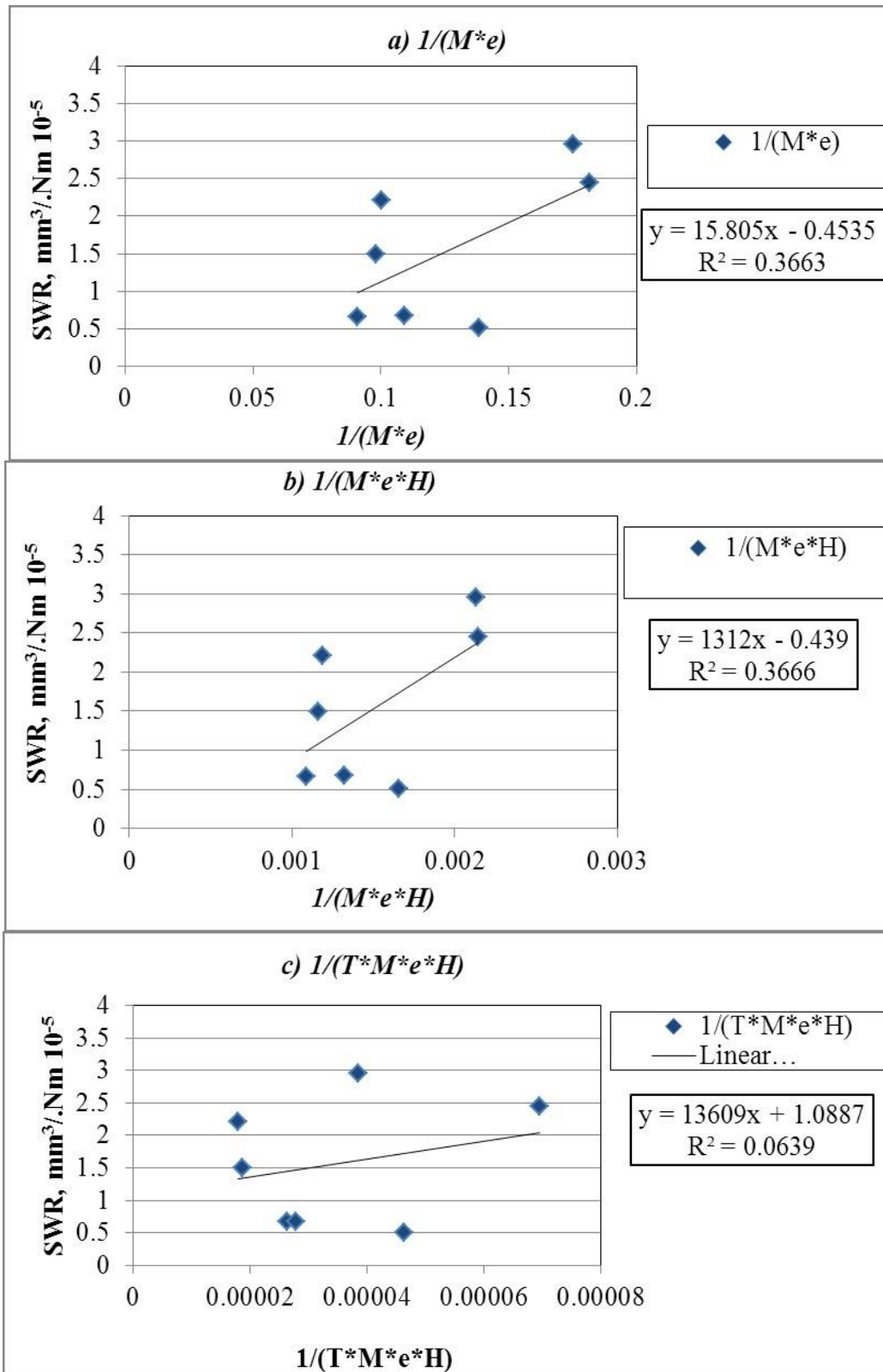


Figure 6.24: Correlation between selective combined mechanical properties and specific wear rate of the studied materials

There is another measurement to determine the relation between the mechanical properties and the tribology by considering the correlation coefficient. It can be defined as a measure of linear association between the variables. The values of the coefficient are between -1 to +1. The closer the value the boundary (+1 or -1) the significant is the relation, while, a correlation coefficient of 0 indicates that there is no relationship between the variables.

The equation for the correlation coefficient is:

$$Correl(X, Y) = \frac{\sum (x - \bar{x})(y - \bar{y})}{\sqrt{\sum (x - \bar{x})^2 \sum (y - \bar{y})^2}} \quad (6.1)$$

where

$\bar{x}$  and  $\bar{y}$  are the sample means AVERAGE(array1) and AVERAGE(array2).

The correlation coefficient between different combination of mechanical properties and tribological output parameters (specific wear rate and friction coefficient) are given in the below **Tables 6.4-6.6**.

Table 6.4 suggests that the most influenced mechanical property on the friction coefficient behaviour of the composites is the tensile strength followed by the elongation of the materials. Moreover, it seems there is no significant effect of individual mechanical property on the specific wear rate. The combination of two

mechanical properties did not show significant relation with the specific wear rate, **Table 6.5**. On the other hand, the combination of the tensile strength with the elongation at the break is the main key in controlling the frictional performance of the composites. Table 6.6 shows that the combination of the elongation and the hardness of properties of the composites has an influence of about 88% on the friction coefficient the addition of the tensile strength to this combination increases the correlation coefficient to 94%.

Modulus of elasticity and the elongation with the hardness are the most affected mechanical properties on the specific wear performance of the composites. 61% correlation coefficient can be seen between the combination of modulus elongation and the hardness with the specific wear rate.

**Table 6.4 correlation coefficient of individual mechanical properties with coefficient of friction and specific wear rate.**

	<i>1/T</i>	<i>1/M</i>	<i>1/e</i>	<i>1/H</i>	<i>COF</i>	<i>SWR</i>
<i>1/T</i>	1.00					
<i>1/M</i>	0.78	1.00				
<i>1/e</i>	-0.96	-0.78	1.00			
<i>1/H</i>	-0.19	0.00	-0.04	1.00		
<i>COF</i>	<b>-0.91</b>	-0.48	<b>0.86</b>	0.35	1.00	
<i>SWR</i>	-0.21	0.34	0.25	0.02	0.53	1.00

**Table 6.5 Correlation coefficient of two mechanical properties combined with coefficient of friction and specific wear rate.**

	$1/(T*M)$	$1(T*M*e)$	$1/(T*M*e*H)$	$1/(T*e)$	$1/(T*H)$	<i>COF</i>	<i>SWR</i>
$1/(T*M)$	1.00						
$1(T*M*e)$	0.99	1.00					
$1/(T*M*e*H)$	0.99	1.00	1.00				
$1/(T*e)$	0.82	0.75	0.75	1.00			
$1/(T*H)$	0.90	0.86	0.86	0.96	1.00		
<i>COF</i>	-0.67	-0.60	-0.59	<b>-0.95</b>	-0.91	1.00	
<i>SWR</i>	0.18	0.25	0.25	-0.31	-0.22	0.53	1.00

**Table 6. 6 Correlation coefficient of two or more than two mechanical properties combined with coefficient of friction and specific wear rate.**

	$1/(M*e)$	$1/(M*H)$	$1/(e*H)$	$1/(T*M*e)$	$1/(T*M*e*H)$	$1/(M*e*H)$	$1/(H*e*T)$	COF	SWR
$1/(M*e)$	1.00								
$1/(M*H)$	0.92	1.00							
$1/(e*H)$	-0.50	-0.78	1.00						
$1/(T*M*e)$	0.84	0.98	-0.83	1.00					
$1/(T*M*e*H)$	0.84	0.98	-0.83	1.00	1.00				
$1/(M*e*H)$	1.00	0.91	-0.49	0.82	0.83	1.00			
$1/(H*e*T)$	0.31	0.64	-0.92	0.76	0.75	0.29	1.00		
COF	-0.09	-0.46	<b>0.88</b>	-0.60	-0.59	-0.07	<b>-0.94</b>	1.00	
SWR	<b>0.61</b>	0.35	0.26	0.25	0.25	<b>0.61</b>	-0.32	0.53	1.00



## 6.7 Chapter summary

This chapter focused on the mechanical and tribological behaviour of ECs based on DPF associated with the graphite fillers. Based on the findings and the discussion, a few points can be summarised as follows:

- From a mechanical perspective, DPF improves the mechanical properties of the ECs with no sign of pull out and/or debonding of the fibres. However, the addition of graphite worsens the tensile properties of the composite. Both date palm and graphite were able to improve the hardness of the composite. The main fracture mechanisms were breakage in the fibre, fracture in the resinous regions and micro-cracks with graphite presence in the composites. The six per cent NaOH treatment highly contributed to the improvement of the mechanical properties. It assisted in enhancing the interfacial adhesion and reducing the porosity of the composites by allowing the resin to penetrate inside the core of the fibres through holes in the surface, which were created by the NaOH treatment.
- From a tribological perspective, the addition of the DPF enhanced the wear and frictional characteristics of the ECs. Further, the addition of the three weight per cent of the graphite into the date fibre/ECs contributed to the improvement of the ECs. The fibres assisted in strengthening the surface, while the graphite generated the lubricant film transfer. This combination was the optimum material when compared to others.
- Tribological experimental configuration significantly influenced the wear performance of the composite, since the wear performance worsened when the composites were tested using the BOD configuration, compared to the BOR. This is mainly due to the high thermo-mechanical loading in the BOD compared to the BOR.

This chapter confirmed there is no correlation between the adhesive wear performances of the composites and their mechanical properties, since wear is a response to the action between asperities.

## Chapter 7: Conclusions and recommendations



## 7.1 Conclusion

The current study focused mainly on the possibility of using DPF for ECs. The study was divided into three parts. The first part aimed to find the optimum fibre diameter and NaOH concentration for the ECs. The second part covered the influence of the graphite content on the mechanical and tribological performance of the ECs. The last part included the influence of both DPF and graphite on the mechanical and tribological performance of the ECs. Several significant findings have been reported at the end of each result chapter. Some of the important findings are further concluded in this section as follows:

- NaOH concentration in the chemical treatment significantly influences both the fibre strength and the fibre interfacial adhesion properties; that is, it smoothens the surface of the fibre. The degree of polymer penetration in the fibre plays an intrinsic role in determining the strength of fibre/polymer composite material. Intermediate concentration of the NaOH (six per cent) is optimum and is recommended, since low concentrations of alkali treatment lead to slight enhancement of mechanical behaviour of composite, and high concentrations of alkali treatment attack the main structure of fibre and deteriorate the strength of the fibre.
- There is a significant influence of the weight fraction of the graphite on both mechanical and tribological performance of the composites. Intermediate weight percentage of the graphite (three per cent) in the EC is considered the optimum for both mechanical and tribological performance, since there is a slight reduction in the tensile properties and significant improvement to the hardness, wear and frictional characteristics.
- The modification on the wear track roughness significantly controlled the wear and frictional behaviour of the graphite/ECs, since the film transfer of the graphite assisted reduction of the friction coefficient and the thermomechanical loading in the interface. For each percentage of graphite, micrographs of the worn surface showed different wear mechanism, with softening and fragmentation seen with a low content of graphite presence in the composite.

Meanwhile, at the graphite amount greater than or equal to five weight per cent, aggregation and poor dispersion of the filler was seen on the surface.

- DPF was able to improve the mechanical properties of the ECs, with no signs of pull out or debonding of fibres. The main fracture mechanisms were breakage in the fibre, fracture in the resinous regions and micro-cracks with graphite presence in the composites. From a tribological perspective, the addition of the DPF with the three weight per cent graphite significantly enhanced the wear and frictional characteristics of the ECs, with fibres assisting in strengthening the surface and the graphite generating the lubricant film transfer.
- Tribological experimental configuration significantly influenced the wear performance of the composite. The results revealed that the composites performed better with the BOR technique compared to the BOD. This was mainly due to the high thermo-mechanical loading in the BOD compared to the BOR.

The study confirmed that there is no correlation between the adhesive wear performances of the composites with their mechanical properties, since wear is a response to the action between asperities.

## **7.2 Recommendations**

Much work remains to be done because of time limits in the current study. The findings of this study can be improved and some areas that deserve further investigation are listed below. Since date palm fibres were found to be a good candidate and may replace synthetic fibres, it is strongly recommended to conduct a cost analysis, which could assist in the commercialisation process.

- In some applications, composites may be subjected to adhesive wear with the presence of liquids (such as water) at the interface. Consequently, adhesive wear under wet contact conditions should be studied to investigate the behaviour of composites under these conditions.
- Many recent works have been published or will be published in 2013 and 2014, which recommend the combination of synthetic fibres and natural fibres for

better mechanical properties. No work is reported on tribology. This could be another study area for postgraduate students.

## References

- ABU-SHARKH, B. F. & HAMID, H. 2004. Degradation study of date palm fibre/polypropylene composites in natural and artificial weathering: mechanical and thermal analysis. *Polymer Degradation and Stability*, 85, 967-973.
- ALAMRI, H. & LOW, I. M. 2012. Effect of water absorption on the mechanical properties of nano-filler reinforced epoxy nanocomposites. *Materials & Design*, 42, 214-222.
- ALAWAR, A., HAMED, A. M. & AL-KAABI, K. 2009a. Characterization of treated date palm tree fiber as composite reinforcement. *Composites Part B: Engineering*, 40, 601-606.
- ALAWAR, A., HAMED, A. M. & AL-KAABI, K. 2009b. Characterization of treated date palm tree fiber as composite reinforcement. *Composites Part B: Engineering*.
- ALBDIRY, M. T. & YOUSIF, B. F. 2013. Morphological structures and tribological performance of unsaturated polyester based untreated/silane-treated halloysite nanotubes. *Materials & Design*, 48, 68-76.
- ALSAEED, T., YOUSIF, B. F. & KU, H. 2013. The potential of using date palm fibres as reinforcement for polymeric composites. *Materials & Design*, 43, 177-184.
- ANDERSONS, J., PORIKE, E. & SPARNINS, E. 2011. Modeling strength scatter of elementary flax fibers: The effect of mechanical damage and geometrical characteristics. *Composites Part A: Applied Science and Manufacturing*, 42, 543-549.
- ANDERSONS, J., SPĀRNIŅŠ, E., JOFFE, R. & WALLSTRÖM, L. 2005. Strength distribution of elementary flax fibres. *Composites Science and Technology*, 65, 693-702.
- ARHAIM, Y. H., SHALWAN, A. & YOUSIF, B. F. 2013. Correlation between frictional force, interface temperature and specific wear rate of fibre polymer composites.
- ARRAKHIZ, F. Z., EL ACHABY, M., KAKOU, A. C., VAUDREUIL, S., BENMOUSSA, K., BOUHFID, R., FASSI-FEHRI, O. & QAISS, A. 2012. Mechanical properties of high density polyethylene reinforced with chemically modified coir fibers: Impact of chemical treatments. *Materials & Design*, 37, 379-383.
- ASTM 2000. D638-99 .Standard test method for tensile properties of plastics. *American Society for Testing Materials*
- ATHIJAYAMANI, A., THIRUCHITRAMBALAM, M., NATARAJAN, U. & PAZHANIVEL, B. 2009. Effect of moisture absorption on the mechanical properties of randomly oriented natural fibers/polyester hybrid composite. *Materials Science and Engineering: A*, 517, 344-353.

- AWAL, A., CESCUTTI, G., GHOSH, S. B. & MÜSSIG, J. 2011. Interfacial studies of natural fibre/polypropylene composites using single fibre fragmentation test (SFFT). *Composites Part A: Applied Science and Manufacturing*, 42, 5056.
- AZIZ, S. H. & ANSELL, M. P. 2004. The effect of alkalization and fibre alignment on the mechanical and thermal properties of kenaf and hemp bast fibre composites: part 2 – cashew nut shell liquid matrix. *Composites Science and Technology*, 64, 1231-1238.
- AZWA, Z. N., YOUSIF, B. F., MANALO, A. C. & KARUNASENA, W. 2013. A review on the degradability of polymeric composites based on natural fibres. *Materials & Design*, 47, 424-442.
- BAHADUR, S., GONG, D. & ANDEREGG, J. 1996. Investigation of the influence of CaS, CaO and CaF<sub>2</sub> fillers on the transfer and wear of nylon by microscopy and XPS analysis. *Wear*, 197, 271-279.
- BAKUMOV, V., BLUGAN, G., ROOS, S., GRAULE, T., FAKHFOURI, V., GROSSENBACHER, J., GULLO, M., KIEFER, T., BRUGGER, J. & PARLINSKA, M. 2012. Mechanical and tribological properties of polymer-derived Si/C/N sub-millimetre thick miniaturized components fabricated by direct casting. *Journal of the European Ceramic Society*, 32, 1759-1767.
- BALEY, C. 2002. Analysis of the flax fibres tensile behaviour and analysis of the tensile stiffness increase. *Composites Part A: Applied Science and Manufacturing*, 33, 939-948.
- BASAVARAJAPPA, S. & ELLANGO VAN, S. 2012. Dry sliding wear characteristics of glass-epoxy composite filled with silicon carbide and graphite particles. *Wear*, 296, 491-496.
- BEG, M. D. H. & PICKERING, K. L. 2008. Mechanical performance of Kraft fibre reinforced polypropylene composites: Influence of fibre length, fibre beating and hygrothermal ageing. *Composites Part A: Applied Science and Manufacturing*, 39, 1748-1755.
- BEN DIFALLAH, B., KHARRAT, M., DAMMAK, M. & MONTEIL, G. 2012a. Mechanical and tribological response of ABS polymer matrix filled with graphite powder. *Materials & Design*, 34, 782-787.
- BEN DIFALLAH, B., KHARRAT, M., DAMMAK, M. & MONTEIL, G. 2012b. Mechanical and tribological response of ABS polymer matrix filled with graphite powder. *Materials & Design*, 34, 782-787.
- BERTO, F., LAZZARIN, P. & AYATOLLAHI, M. R. 2013. Brittle fracture of sharp and blunt V-notches in isostatic graphite under pure compression loading. *Carbon*, 63, 101-116.
- BIJWE, J. & INDUMATHI, J. 2004. Influence of fibers and solid lubricants on low amplitude oscillating wear of polyetherimide composites. *Wear*, 257, 562-572.
- BLEDZKI, A. K. & GASSAN, J. 1999. Composites reinforced with cellulose based fibres. *Progress in Polymer Science*, 24, 221-274.
- BORRUTO, A., CRIVELLONE, G. & MARANI, F. 1998. Influence of surface wettability on friction and wear tests. *Wear*, 222, 57-65.
- BUDINSKI, K. G. 1997. Resistance to particle abrasion of selected plastics. *Wear*, 203, 302-309.

- BUDINSKI, K. G. & IVES, L. K. 2005. Measuring abrasion resistance with a fixed abrasive loop. *Wear*, 258, 133-140.
- CANTERO, G., ARBELAIZ, A., LLANO-PONTE, R. & MONDRAGON, I. 2003. Effects of fibre treatment on wettability and mechanical behaviour of flax/polypropylene composites. *Composites Science and Technology*, 63, 1247-1254.
- CAULFIELD, D. F., FENG, D., PRABAWA, S., YOUNG, R. A. & SANADI, A. R. 1999. Interphase effects on the mechanical and physical aspects of natural fiber composites. *Die Angewandte Makromolekulare Chemie*, 272, 57-64.
- CELIK, C. & WARNER, S. B. 2007. Analysis of the structure and properties of expanded graphite-filled poly(phenylene ether)/atactic polystyrene nanocomposite fibers. *Journal of Applied Polymer Science*, 103, 645-652.
- CHAND, N. & DWIVEDI, U. K. 2006. Effect of coupling agent on abrasive wear behaviour of chopped jute fibre-reinforced polypropylene composites. *Wear*, 261, 1057-1063.
- CHAND, N. & DWIVEDI, U. K. 2007. High stress abrasive wear study on bamboo. *Journal of Materials Processing Technology*, 183, 155-159.
- CHAND, N. & DWIVEDI, U. K. 2008. Sliding wear and friction characteristics of sisal fibre reinforced polyester composites: Effect of silane coupling agent and applied load. *Polymer Composites*, 29, 280-284.
- CHAND, N. & SHARMA, M. K. 2008. Development and sliding wear behaviour of milled carbon fibre reinforced epoxy gradient composites. *Wear*, 264, 69-74.
- CHAND, N., SHARMA, P. & FAHIM, M. 2010. Tribology of maleic anhydride modified rice-husk filled polyvinylchloride. *Wear*, 269, 847-853.
- CHEUNG, H.-Y., HO, M.-P., LAU, K.-T., CARDONA, F. & HUI, D. 2009. Natural fibre-reinforced composites for bioengineering and environmental engineering applications. *Composites Part B: Engineering*, 40, 655-663.
- CHIN, C. W. & YOUSIF, B. F. 2009. Potential of kenaf fibres as reinforcement for tribological applications. *Wear*, 267, 1550-1557.
- CHIN, C. W. & YOUSIF, B. F. 2010. Tribological behaviour of KFRE composite. *International Journal of Modern Physics B*, 24, 5589-5599.
- CHO, M. H., JU, J., KIM, S. J. & JANG, H. 2006. Tribological properties of solid lubricants (graphite, Sb<sub>2</sub>S<sub>3</sub>, MoS<sub>2</sub>) for automotive brake friction materials. *Wear*, 260, 855-860.
- CHOW, C. P. L., XING, X. S. & LI, R. K. Y. 2007. Moisture absorption studies of sisal fibre reinforced polypropylene composites. *Composites Science and Technology*, 67, 306-313.
- CORBIÈRE-NICOLLIÈRE, T., GFELLER LABAN, B., LUNDQUIST, L., LETERRIER, Y., MÅNSON, J. A. E. & JOLLIET, O. 2001. Life cycle assessment of biofibres replacing glass fibres as reinforcement in plastics. *Resources, Conservation and Recycling*, 33, 267-287.
- COROLLER, G., LEFEUVRE, A., LE DUIGOU, A., BOURMAUD, A., AUSIAS, G., GAUDRY, T. & BALEY, C. 2013. Effect of flax fibres individualisation on tensile failure of flax/epoxy unidirectional composite. *Composites Part A: Applied Science and Manufacturing*, 51, 62-70.

- DELUCCHI, M., RICOTTI, R. & CERISOLA, G. 2011. Influence of micro- and nano-fillers on chemico-physical properties of epoxy-based materials. *Progress in Organic Coatings*, 72, 58-64.
- DHAKAL, H. N., ZHANG, Z. Y. & RICHARDSON, M. O. W. 2007. Effect of water absorption on the mechanical properties of hemp fibre reinforced unsaturated polyester composites. *Composites Science and Technology*, 67, 1674-1683.
- DUVAL, A., BOURMAUD, A., AUGIER, L. & BALEY, C. 2011. Influence of the sampling area of the stem on the mechanical properties of hemp fibers. *Materials Letters*, 65, 797-800.
- EDEEROZEY, A. M. M., AKIL, H. M., AZHAR, A. B. & ARIFFIN, M. I. Z. 2007. Chemical modification of kenaf fibers. *Materials Letters*, 61, 2023-2025.
- EISS, N. S. & HANCHI, J. 1998. Stick-slip friction in dissimilar polymer pairs used in automobile interiors. *Tribology International*, 31, 653-659.
- EL-SAYED, A. A., EL-SHERBINY, M. G., ABO-EL-EZZ, A. S. & AGGAG, G. A. 1995. Friction and wear properties of polymeric composite materials for bearing applications. *Wear*, 184, 45-53.
- EL-TAYEB, N., YOUSIF, B. & YAP, T. 2006. Tribological studies of polyester reinforced with CSM 450-R-glass fiber sliding against smooth stainless steel counterface. *Wear*, 261, 443-452.
- EL-TAYEB, N. S. M. 2008. A study on the potential of sugarcane fibers/polyester composite for tribological applications. *Wear*, 265, 223-235.
- FEI, J., LI, H.-J., HUANG, J.-F. & FU, Y.-W. 2012. Study on the friction and wear performance of carbon fabric/phenolic composites under oil lubricated conditions. *Tribology International*, 56, 30-37.
- FONTARAS, G. & SAMARAS, Z. 2010. On the way to 130 g/km—Estimating the future characteristics of the average European passenger car. *Energy Policy*, 38, 1826-1833.
- FRIEDRICH, K., ZHANG, Z. & SCHLARB, A. K. 2005. Effects of various fillers on the sliding wear of polymer composites. *Composites Science and Technology*, 65, 2329-2343.
- FU, S.-Y. & LAUKE, B. 1996. Effects of fiber length and fiber orientation distributions on the tensile strength of short-fiber-reinforced polymers. *Composites Science and Technology*, 56, 1179-1190.
- GARCÍA-HERNÁNDEZ, E., LICEA-CLAVERÍE, A., ZIZUMBO, A., ALVAREZCASTILLO, A. & HERRERA-FRANCO, P. J. 2004. Improvement of the interfacial compatibility between sugar cane bagasse fibers and polystyrene for composites. *Polymer Composites*, 25, 134-145.
- GASSAN, J. & BLEDZKI, A. K. 1999. Possibilities for improving the mechanical properties of jute/epoxy composites by alkali treatment of fibres. *Composites Science and Technology*, 59, 1303-1309.
- GEORGE, J. J. & BHOWMICK, A. K. 2008. Ethylene vinyl acetate/expanded graphite nanocomposites by solution intercalation: Preparation, characterization and properties. *Journal of Materials Science*, 43, 702-708.
- H. WELLS, D. H. B., I. MACPHAIL, P.K. PAL, PROC. 35TH ANNUAL TECHNICAL CONF., SOCIETY OF THE PLASTIC INDUSTRY, SECTION 1-F (1980) 1. 1980.

- HAO, Y., LIU, F., SHI, H., HAN, E. & WANG, Z. 2011. The influence of ultra-fine glass fibers on the mechanical and anticorrosion properties of epoxy coatings. *Progress in Organic Coatings*, 71, 188-197.
- HAQUE, M. M., HASAN, M., ISLAM, M. S. & ALI, M. E. 2009. Physico-mechanical properties of chemically treated palm and coir fiber reinforced polypropylene composites. *Bioresource Technology*, 100, 4903-4906.
- HARGITAI, H., RÁCZ, I. & ANANDJIWALA, R. D. 2008. Development of HEMP Fiber Reinforced Polypropylene Composites. *Journal of Thermoplastic Composite Materials*, 21, 165-174.
- HARSHA, A. P., TEWARI, U. S. & VENKATRAMAN, B. 2003. Three-body abrasive wear behaviour of polyaryletherketone composites. *Wear*, 254, 680692.
- HASHMI, S. A. R., DWIVEDI, U. K. & CHAND, N. 2007a. Graphite modified cotton fibre reinforced polyester composites under sliding wear conditions. *Wear*, 262, 1426-1432.
- HASHMI, S. A. R., DWIVEDI, U. K. & CHAND, N. 2007b. Graphite modified cotton fibre reinforced polyester composites under sliding wear conditions. *Wear*, 262, 1426-1432.
- HEPWORTH, D. G., VINCENT, J. F. V., JERONIMIDIS, G. & BRUCE, D. M. 2000. The penetration of epoxy resin into plant fibre cell walls increases the stiffness of plant fibre composites. *Composites Part A: Applied Science and Manufacturing*, 31, 599-601.
- HERRERA-FRANCO, P. J. & VALADEZ-GONZÁLEZ, A. 2004. Mechanical properties of continuous natural fibre-reinforced polymer composites. *Composites Part A: Applied Science and Manufacturing*, 35, 339-345.
- HOLMBERG, K., ANDERSSON, P. & ERDEMIR, A. 2012. Global energy consumption due to friction in passenger cars. *Tribology International*, 47, 221-234.
- HOU, Y., HU, P., ZHANG, X. & GUI, K. 2013. Effects of graphite flake diameter on mechanical properties and thermal shock behavior of ZrB<sub>2</sub>-nanoSiC-graphite ceramics. *International Journal of Refractory Metals and Hard Materials*, 41, 133-137.
- HU, R. & LIM, J.-K. 2007. Fabrication and Mechanical Properties of Completely Biodegradable Hemp Fiber Reinforced Polylactic Acid Composites. *Journal of Composite Materials*, 41, 1655-1669.
- HU, W., TON-THAT, M.-T., PERRIN-SARAZIN, F. & DENAULT, J. 2010. An improved method for single fiber tensile test of natural fibers. *Polymer Engineering & Science*, 50, 819-825.
- JACOB, M., THOMAS, S. & VARUGHESE, K. T. 2004. Mechanical properties of sisal/oil palm hybrid fiber reinforced natural rubber composites. *Composites Science and Technology*, 64, 955-965.
- JANA, S. & ZHONG, W.-H. 2009. Graphite particles with a “puffed” structure and enhancement in mechanical performance of their epoxy composites. *Materials Science and Engineering: A*, 525, 138-146.
- JAWAHAR, P., GNANAMOORTHY, R. & BALASUBRAMANIAN, M. 2006. Tribological behaviour of clay – thermoset polyester nanocomposites. *Wear*, 261, 835-840.
- JOSEPH, K., VARGHESE, S., KALAPRASAD, G., THOMAS, S.,



- PRASANNAKUMARI, L., KOSHY, P. & PAVITHRAN, C. 1996. Influence of interfacial adhesion on the mechanical properties and fracture behaviour of short sisal fibre reinforced polymer composites. *European Polymer Journal*, 32, 1243-1250.
- JOSEPH, P. V., JOSEPH, K. & THOMAS, S. 1999. Effect of processing variables on the mechanical properties of sisal-fiber-reinforced polypropylene composites. *Composites Science and Technology*, 59, 1625-1640.
- JOSEPH, S., SREEKALA, M. S., OOMMEN, Z., KOSHY, P. & THOMAS, S. 2002. A comparison of the mechanical properties of phenol formaldehyde composites reinforced with banana fibres and glass fibres. *Composites Science and Technology*, 62, 1857-1868.
- JOSHI, S. V., DRZAL, L. T., MOHANTY, A. K. & ARORA, S. 2004. Are natural fiber composites environmentally superior to glass fiber reinforced composites? *Composites Part A: Applied Science and Manufacturing*, 35, 371-376.
- KABIR, M. M., WANG, H., LAU, K. T. & CARDONA, F. 2012. Chemical treatments on plant-based natural fibre reinforced polymer composites: An overview. *Composites Part B: Engineering*, 43, 2883-2892.
- KADDAMI, H., DUFRESNE, A., KHELIFI, B., BENDAHO, A., TAOURIRTE, M., RAIHANE, M., ISSARTEL, N., SAUTEREAU, H., GÉRARD, J.-F. & SAMI, N. 2006. Short palm tree fibers – Thermoset matrices composites. *Composites Part A: Applied Science and Manufacturing*, 37, 1413-1422.
- KANCHANOMAI, C. & THAMMARUECHUC, A. 2009. Effects of stress ratio on fatigue crack growth of thermoset epoxy resin. *Polymer Degradation and Stability*, 94, 1772-1778.
- KELLY, A. & TYSON, W. R. 1965. Tensile properties of fibre-reinforced metals: Copper/tungsten and copper/molybdenum. *Journal of the Mechanics and Physics of Solids*, 13, 329-350.
- KIM, H. S. & KHAMIS, M. A. 2001. Fracture and impact behaviours of hollow microsphere/epoxy resin composites. *Composites Part A: Applied Science and Manufacturing*, 32, 1311-1317.
- KIM, S.-J., MOON, J.-B., KIM, G.-H. & HA, C.-S. 2008. Mechanical properties of polypropylene/natural fiber composites: Comparison of wood fiber and cotton fiber. *Polymer Testing*, 27, 801-806.
- KU, H., WANG, H., PATTARACHAIYAKOOP, N. & TRADA, M. 2011. A review on the tensile properties of natural fiber reinforced polymer composites. *Composites Part B: Engineering*, 42, 856-873.
- LARSEN, T. Ø., ANDERSEN, T. L., THORNING, B. & VIGILD, M. E. 2008. The effect of particle addition and fibrous reinforcement on epoxy-matrix composites for severe sliding conditions. *Wear*, 264, 857-868.
- LEE, B.-H., KIM, H.-J. & YU, W.-R. 2009. Fabrication of long and discontinuous natural fiber reinforced polypropylene biocomposites and their mechanical properties. *Fibers and Polymers*, 10, 83-90.
- LEI, W., LEI, W.-G. & REN, C. 2006. Effect of volume fraction of ramie cloth on physical and mechanical properties of ramie cloth/UP resin composite. *Transactions of Nonferrous Metals Society of China*, 16, Supplement 2, s474s477.

- LI, X., TABIL, L. & PANIGRAHI, S. 2007. Chemical Treatments of Natural Fiber for Use in Natural Fiber-Reinforced Composites: A Review. *Journal of Polymers and the Environment*, 15, 25-33.
- LIU, L., YU, J., CHENG, L. & QU, W. 2009. Mechanical properties of poly(butylene succinate) (PBS) biocomposites reinforced with surface modified jute fibre. *Composites Part A: Applied Science and Manufacturing*, 40, 669-674.
- LIU, W., DRZAL, L. T., MOHANTY, A. K. & MISRA, M. 2007. Influence of processing methods and fiber length on physical properties of kenaf fiber reinforced soy based biocomposites. *Composites Part B: Engineering*, 38, 352-359.
- MYLSAMY, K. & RAJENDRAN, I. 2011. Influence of alkali treatment and fibre length on mechanical properties of short Agave fibre reinforced epoxy composites. *Materials & Design*, 32, 4629-4640.
- N.S.M, E.-T. 2008. Abrasive wear performance of untreated SCF reinforced polymer composite. *Journal of Materials Processing Technology*, 206, 305-314.
- NARIMISSA, E., GUPTA, R., BHASKARAN, M. & SRIRAM, S. 2012. Influence of nano-graphite platelet concentration on onset of crystalline degradation in polylactide composites. *Polymer Degradation and Stability*, 97, 829-832.
- NARISH, S., YOUSIF, B. F. & RILLING, D. 2011. Adhesive wear of thermoplastic composite based on kenaf fibres. *Proceedings of the Institution of Mechanical Engineers, Part J: Journal of Engineering Tribology*, 225, 101-109.
- NGUYEN TRI PHUONG, SOLLOGOUB, C. & GUINAULT, A. 2010. Relationship between fiber chemical treatment and properties of recycled pp/bamboo fiber composites. *Journal of Reinforced Plastics and Composites*, 29, 3244-3256.
- NIRMAL, U., HASHIM, J., LAU, S. T. W., MY, Y. & YOUSIF, B. F. 2012a. Betelnut fibres as an alternative to glass fibres to reinforce thermoset composites: A comparative study. *Textile Research Journal*, 82, 1107-1120.
- NIRMAL, U., HASHIM, J. & LOW, K. O. 2012b. Adhesive wear and frictional performance of bamboo fibres reinforced epoxy composite. *Tribology International*, 47, 122-133.
- NIRMAL, U., YOUSIF, B. F., RILLING, D. & BREVERN, P. V. 2010. Effect of betelnut fibres treatment and contact conditions on adhesive wear and frictional performance of polyester composites. *Wear*, 268, 1354-1370.
- PARK, J.-M., QUANG, S. T., HWANG, B.-S. & DEVRIES, K. L. 2006. Interfacial evaluation of modified Jute and Hemp fibers/polypropylene (PP)-maleic anhydride polypropylene copolymers (PP-MAPP) composites using micromechanical technique and nondestructive acoustic emission. *Composites Science and Technology*, 66, 2686-2699.
- PICKERING, K. L., INSTITUTE OF MATERIALS, M. & MINING 2008. *Properties and Performance of Natural Fibre Composites*, Woodhead Publishing.
- PIHTILI, H. 2009. An experimental investigation of wear of glass fibre–epoxy resin and glass fibre–polyester resin composite materials. *European Polymer Journal*, 45, 149-154.
- PLACET, V., TRIVAUDEY, F., CISSE, O., GUCHERET-RETEL, V. & BOUBAKAR, M. L. 2012. Diameter dependence of the apparent tensile

- modulus of hemp fibres: A morphological, structural or ultrastructural effect? *Composites Part A: Applied Science and Manufacturing*, 43, 275-287.
- PLACKETT, D., LØGSTRUP ANDERSEN, T., BATSBERG PEDERSEN, W. & NIELSEN, L. 2003. Biodegradable composites based on l-poly lactide and jute fibres. *Composites Science and Technology*, 63, 1287-1296.
- PÖLLÄNEN, M., PIRINEN, S., SUVANTO, M. & PAKKANEN, T. T. 2011. Influence of carbon nanotube–polymeric compatibilizer masterbatches on morphological, thermal, mechanical, and tribological properties of polyethylene. *Composites Science and Technology*, 71, 1353-1360.
- PRASAD, B. & SAIN, M. 2003. Mechanical properties of thermally treated hemp fibers in inert atmosphere for potential composite reinforcement. *Materials Research Innovations*, 7, 231-238.
- RAMANATHAN, T., ABDALA, A. A., STANKOVICH, S., DIKIN, D. A., HERRERA-ALONSO, M., PINER, R. D., ADAMSON, D. H., SCHNIEPP, H. C., CHEN, X., RUOFF, R. S., NGUYEN, S. T., AKSAY, I. A., PRUD'HOMME, R. K. & BRINSON, L. C. 2008. Functionalized graphene sheets for polymer nanocomposites. *Nature Nanotechnology*, 3, 327-331.
- RATNA PRASAD, A. V. & MOHANA RAO, K. 2011. Mechanical properties of natural fibre reinforced polyester composites: Jowar, sisal and bamboo. *Materials & Design*, 32, 4658-4663.
- ROKBI, M., OSMANI, H., IMAD, A. & BENSEDDIQ, N. 2011. Effect of Chemical treatment on Flexure Properties of Natural Fiber-reinforced Polyester Composite. *Procedia Engineering*, 10, 2092-2097.
- RONG, M. Z., ZHANG, M. Q., LIU, Y., YANG, G. C. & ZENG, H. M. 2001. The effect of fiber treatment on the mechanical properties of unidirectional sisalreinforced epoxy composites. *Composites Science and Technology*, 61, 14371447.
- ROSA, M. F., CHIOU, B.-S., MEDEIROS, E. S., WOOD, D. F., WILLIAMS, T. G., MATTOSO, L. H. C., ORTS, W. J. & IMAM, S. H. 2009. Effect of fiber treatments on tensile and thermal properties of starch/ethylene vinyl alcohol copolymers/coir biocomposites. *Bioresource Technology*, 100, 5196-5202.
- ROUISSON, D., SAIN, M. & COUTURIER, M. 2006. Resin transfer molding of hemp fiber composites: optimization of the process and mechanical properties of the materials. *Composites Science and Technology*, 66, 895-906.
- SAHA, P., MANNA, S., CHOWDHURY, S. R., SEN, R., ROY, D. & ADHIKARI, B. 2010. Enhancement of tensile strength of lignocellulosic jute fibers by alkali-steam treatment. *Bioresource Technology*, 101, 3182-3187.
- SAMYN, P. & DE BAETS, P. 2005. Friction and wear of acetal: A matter of scale. *Wear*, 259, 697-702.
- SAMYN, P., QUINTELIER, J., OST, W., DE BAETS, P. & SCHOUKENS, G. 2005. Sliding behaviour of pure polyester and polyester-PTFE filled bulk composites in overload conditions. *Polymer Testing*, 24, 588-603.
- SAPUAN, S. M., LEENIE, A., HARIMI, M. & BENG, Y. K. 2006. Mechanical properties of woven banana fibre reinforced epoxy composites. *Materials & Design*, 27, 689-693.
- SAWPAN, M. A., PICKERING, K. L. & FERNYHOUGH, A. 2011. Effect of fibre treatments on interfacial shear strength of hemp fibre reinforced poly lactide

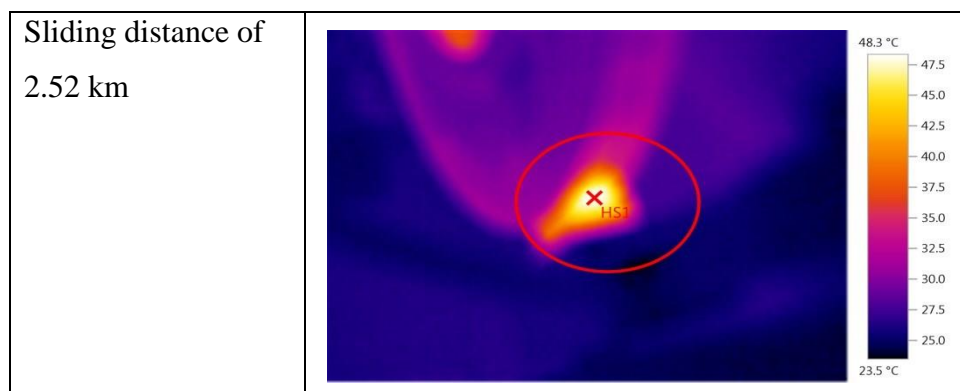
- and unsaturated polyester composites. *Composites Part A: Applied Science and Manufacturing*, 42, 1189-1196.
- SENGUPTA, R., BHATTACHARYA, M., BANDYOPADHYAY, S. & BHOWMICK, A. K. 2011. A review on the mechanical and electrical properties of graphite and modified graphite reinforced polymer composites. *Progress in Polymer Science*, 36, 638-670.
- SHALWAN, A. & YOUSIF, B. F. In State of Art: Mechanical and tribological behaviour of polymeric composites based on natural fibres. *Materials & Design*.
- SHIBATA, S., CAO, Y. & FUKUMOTO, I. 2005. Press forming of short natural fiber-reinforced biodegradable resin: Effects of fiber volume and length on flexural properties. *Polymer Testing*, 24, 1005-1011.
- SHINJI, O. 2008. Mechanical properties of kenaf fibers and kenaf/PLA composites. *Mechanics of Materials*, 40, 446-452.
- SHIPWAY, P. H. & NGAO, N. K. 2003. Microscale abrasive wear of polymeric materials. *Wear*, 255, 742-750.
- SHIVAMURTHY, B., UDAYA BHAT, K. & ANANDHAN, S. 2013. Mechanical and sliding wear properties of multi-layered laminates from glass fabric/graphite/epoxy composites. *Materials & Design*, 44, 136-143.
- SINGH GILL, N. & YOUSIF, B. F. 2009. Wear and frictional performance of betelnut fibre-reinforced polyester composite. *Proceedings of the Institution of Mechanical Engineers, Part J: Journal of Engineering Tribology*, 223, 183-194.
- STACHOWIAK, G. W. 2006. *Wear: materials, mechanisms and practice*, Wiley. com.
- SUBBAYA, K. M., SURESHA, B., RAJENDRA, N. & VARADARAJAN, Y. S. 2012. Grey-based Taguchi approach for wear assessment of SiC filled carbon-epoxy composites. *Materials & Design*, 41, 124-130.
- SURESHA, B., SHIVA KUMAR, K., SEETHARAMU, S. & SAMPATH KUMARAN, P. 2010. Friction and dry sliding wear behavior of carbon and glass fabric reinforced vinyl ester composites. *Tribology International*, 43, 602-609.
- SYDENSTRICKER, T. H. D., MOCHNAZ, S. & AMICO, S. C. 2003. Pull-out and other evaluations in sisal-reinforced polyester biocomposites. *Polymer Testing*, 22, 375-380.
- TANG, L.-C., WAN, Y.-J., YAN, D., PEI, Y.-B., ZHAO, L., LI, Y.-B., WU, L.-B., JIANG, J.-X. & LAI, G.-Q. 2013. The effect of graphene dispersion on the mechanical properties of graphene/epoxy composites. *Carbon*, 60, 16-27.
- THEILER, G. & GRADT, T. 2010. Friction and wear of PEEK composites in vacuum environment. *Wear*, 269, 278-284.
- THOMAS, S. & POTHAN, L. 2009. *Natural Fibre Reinforced Polymer Composites: From Macro to Nanoscale*, Éd. des Archives Contemporaines.
- TORRES, F. G. & CUBILLAS, M. L. 2005. Study of the interfacial properties of natural fibre reinforced polyethylene. *Polymer Testing*, 24, 694-698.
- TUNGJITPORNKULL, S. & SOMBATSOMPOP, N. 2009. Processing technique and fiber orientation angle affecting the mechanical properties of E-glass fiber reinforced wood/PVC composites. *Journal of Materials Processing Technology*, 209, 3079-3088.

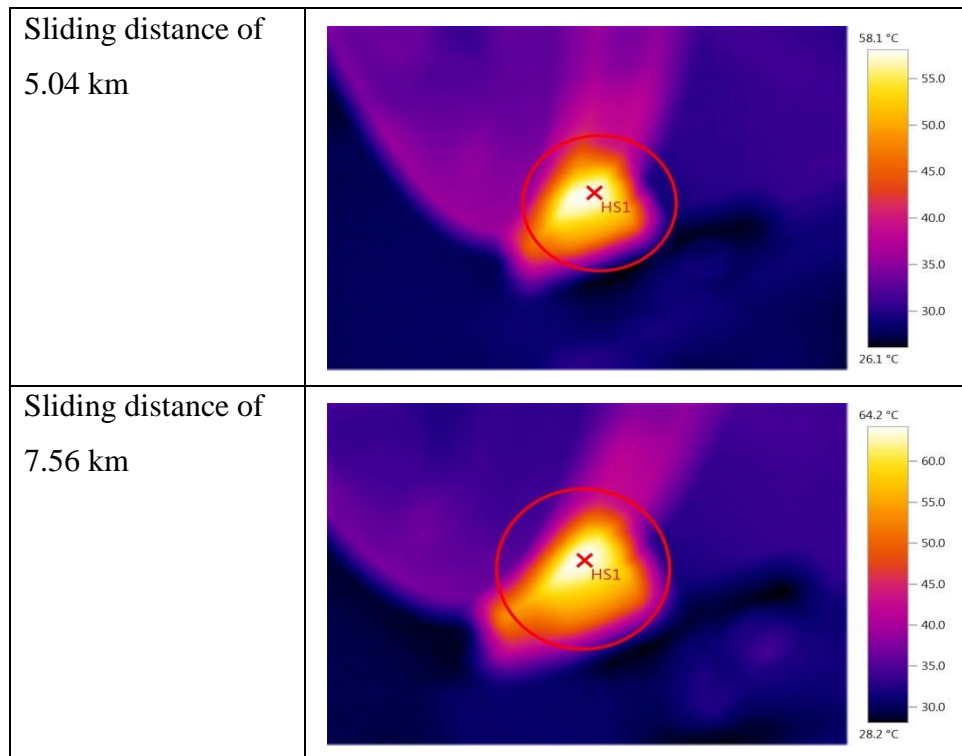
- UMER, R., BICKERTON, S. & FERNYHOUGH, A. 2011. The effect of yarn length and diameter on permeability and compaction response of flax fibre mats. *Composites Part A: Applied Science and Manufacturing*, 42, 723-732.
- VALADEZ-GONZALEZ, A., CERVANTES-UC, J. M., OLAYO, R. & HERRERA-FRANCO, P. J. 1999a. Chemical modification of henequén fibers with an organosilane coupling agent. *Composites Part B: Engineering*, 30, 321-331.
- VALADEZ-GONZALEZ, A., CERVANTES-UC, J. M., OLAYO, R. & HERRERA-FRANCO, P. J. 1999b. Effect of fiber surface treatment on the fiber-matrix bond strength of natural fiber reinforced composites. *Composites Part B: Engineering*, 30, 309-320.
- VALLO, C., KENNY, J. M., VAZQUEZ, A. & CYRAS, V. P. 2004. Effect of Chemical Treatment on the Mechanical Properties of Starch-Based Blends Reinforced with Sisal Fibre. *Journal of Composite Materials*, 38, 1387-1399.
- VENKATESHWARAN, N., ELAYAPERUMAL, A. & SATHIYA, G. K. Prediction of tensile properties of hybrid-natural fiber composites. *Composites Part B: Engineering*.
- VENKATESHWARAN, N., ELAYAPERUMAL, A. & SATHIYA, G. K. 2012. Prediction of tensile properties of hybrid-natural fiber composites. *Composites Part B: Engineering*, 43, 793-796.
- VIRK, A. S., HALL, W. & SUMMERSCALES, J. 2010. Failure strain as the key design criterion for fracture of natural fibre composites. *Composites Science and Technology*, 70, 995-999.
- WAMBUA, P., IVENS, J. & VERPOEST, I. 2003. Natural fibres: can they replace glass in fibre reinforced plastics? *Composites Science and Technology*, 63, 1259-1264.
- WANG, W., JING, T., GAO, Y., QIAO, G. & ZHAO, X. 2007. Properties of a gray cast iron with oriented graphite flakes. *Journal of Materials Processing Technology*, 182, 593-597.
- WÖTZEL, K., WIRTH, R. & FLAKE, M. 1999. Life cycle studies on hemp fibre reinforced components and ABS for automotive parts. *Die Angewandte Makromolekulare Chemie*, 272, 121-127.
- WU, J. & CHENG, X. H. 2006. The tribological properties of Kevlar pulp reinforced epoxy composites under dry sliding and water lubricated condition. *Wear*, 261, 1293-1297.
- XIN, X., XU, C. G. & QING, L. F. 2007. Friction properties of sisal fibre reinforced resin brake composites. *Wear*, 262, 736-741.
- XU, J., ZHOU, Z. R., ZHANG, C. H., ZHU, M. H. & LUO, J. B. 2007. An investigation of fretting wear behaviors of bonded solid lubricant coatings. *Journal of Materials Processing Technology*, 182, 146-151.
- YAMAGUCHI, Y. 1990. *Tribology of plastic materials: their characteristics and applications to sliding components*, Access Online via Elsevier.
- YAMAMOTO, Y. & HASHIMOTO, M. 2004. Friction and wear of water lubricated PEEK and PPS sliding contacts: Part 2. Composites with carbon or glass fibre. *Wear*, 257, 181-189.
- YAMAMOTO, Y. & TAKASHIMA, T. 2002. Friction and wear of water lubricated PEEK and PPS sliding contacts. *Wear*, 253, 820-826.

- YANG, H. & LUO, R. 2011. A novel bronze-impregnated carbon strip containing Al<sub>2</sub>O<sub>3</sub> particles for subway current collectors. *Wear*, 270, 675-681.
- YE, Y., CHEN, J. & ZHOU, H. 2009. An investigation of friction and wear performances of bonded molybdenum disulfide solid film lubricants in fretting conditions. *Wear*, 266, 859-864.
- YOUSIF, B. & EL-TAYEB, N. 2007a. The effect of oil palm fibers as reinforcement on tribological performance of polyester composite. *Surface Review and Letters*, 14, 1095-1102.
- YOUSIF, B. & EL-TAYEB, N. 2007b. Tribological Evaluations of Polyester Composites Considering Three Orientations of CSM Glass Fibres Using BOR Machine. *Applied Composite Materials*, 14, 105-116.
- YOUSIF, B. & EL-TAYEB, N. 2008a. Adhesive Wear Performance of T-OPRP and UT-OPRP Composites. *Tribol Lett*, 32, 199-208.
- YOUSIF, B. & EL-TAYEB, N. 2010. Wear characteristics of thermoset composite under high stress three-body abrasive. *Tribology International*, 43, 2365-2371.
- YOUSIF, B. F. 2008. Replacing of glass fibres with seed oil palm fibres for tribopolymeric composites. *Tribology - Materials, Surfaces and Interfaces*, 2, 99-103.
- YOUSIF, B. F. 2009. Frictional and wear performance of polyester composites based on coir fibres. *Proceedings of the Institution of Mechanical Engineers, Part J: Journal of Engineering Tribology*, 223, 51-59.
- YOUSIF, B. F. 2013a. Design of newly fabricated tribological machine for wear and frictional experiments under dry/wet condition. *Materials & Design*, 48, 2-13.
- YOUSIF, B. F. 2013b. Editorial for SI: Materials, design and tribology. *Materials and Design*.
- YOUSIF, B. F. & CHIN, C. W. 2012. Epoxy composite based on kenaf fibers for tribological applications under wet contact conditions. *Surface Review and Letters*, 19.
- YOUSIF, B. F., EL-TAYEB, N. S. & YUSAF, T. F. The effects of load and velocity on friction and interface temperature of CGRP sliding against smooth stainless steel. 2006.
- YOUSIF, B. F. & EL-TAYEB, N. S. M. 2008b. Wear and friction characteristics of CGRP composite under wet contact condition using two different test techniques. *Wear*, 265, 856-864.
- YOUSIF, B. F. & EL-TAYEB, N. S. M. 2008c. Wear and friction characteristics of CGRP composite under wet contact condition using two different test techniques. *Wear*, 265, 856-864.
- YOUSIF, B. F. & EL-TAYEB, N. S. M. 2009. Mechanical and wear properties of oil palm and glass fibres reinforced polyester composites. *International Journal of Precision Technology*, 1, 213-222.
- YOUSIF, B. F. & KU, H. 2012. Suitability of using coir fiber/polymeric composite for the design of liquid storage tanks. *Materials & Design*, 36, 847-853.
- YOUSIF, B. F., LAU, S. T. W. & MCWILLIAM, S. 2010a. Polyester composite based on betelnut fibre for tribological applications. *Tribology International*, 43, 503-511.
- YOUSIF, B. F. & NIRMAL, U. 2011. Wear and frictional performance of polymeric composites aged in various solutions. *Wear*, 272, 97-104.

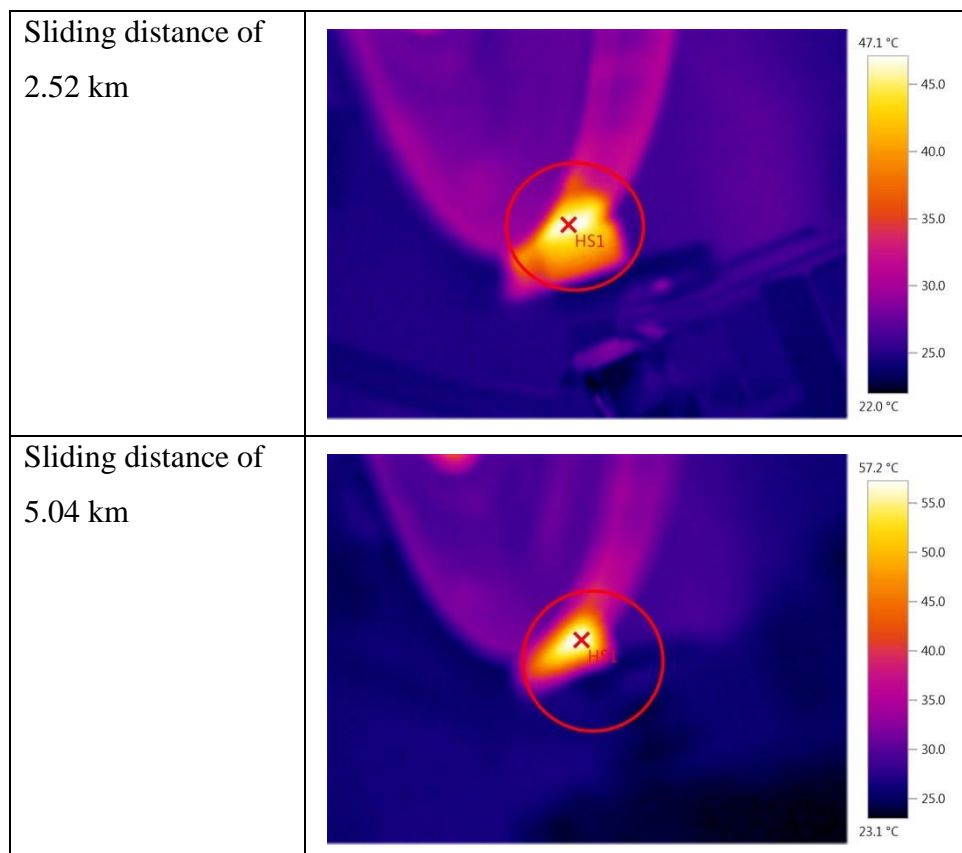
- YOUSIF, B. F., NIRMAL, U. & WONG, K. J. 2010b. Three-body abrasion on wear and frictional performance of treated betelnut fibre reinforced epoxy (TBFRE) composite. *Materials & Design*, 31, 4514-4521.
- YOUSIF, B. F., SHALWAN, A., CHIN, C. W. & MING, K. C. 2012. Flexural properties of treated and untreated kenaf/epoxy composites. *Materials & Design*, 40, 378-385.
- YU, T., REN, J., LI, S., YUAN, H. & LI, Y. 2010. Effect of fiber surface-treatments on the properties of poly(lactic acid)/ramie composites. *Composites Part A: Applied Science and Manufacturing*, 41, 499-505.
- ZHANG, H., ZHANG, Z. & FRIEDRICH, K. 2007. Effect of fiber length on the wear resistance of short carbon fiber reinforced epoxy composites. *Composites Science and Technology*, 67, 222-230.
- ZHANG, M.-J., LIU, Y.-B., YANG, X.-H., AN, J. & LUO, K.-S. 2008a. Effect of graphite particle size on wear property of graphite and Al<sub>2</sub>O<sub>3</sub> reinforced AZ91D-0.8%Ce composites. *Transactions of Nonferrous Metals Society of China*, 18, Supplement 1, s273-s277.
- ZHANG, S. L. & LI, J. C. M. 2003. Slip process of stick–slip motion in the scratching of a polymer. *Materials Science and Engineering: A*, 344, 182189.
- ZHANG, X.-R., PEI, X.-Q. & WANG, Q.-H. 2009. Friction and wear studies of polyimide composites filled with short carbon fibers and graphite and micro SiO<sub>2</sub>. *Materials & Design*, 30, 4414-4420.
- ZHANG, X., LIAO, G., JIN, Q., FENG, X. & JIAN, X. 2008b. On dry sliding friction and wear behavior of PPEsk filled with PTFE and graphite. *Tribology International*, 41, 195-201.
- ZHENG, W., LU, X. & WONG, S. C. 2004. Electrical and mechanical properties of expanded graphite-reinforced high-density polyethylene. *Journal of Applied Polymer Science*, 91, 2781-2788.

## Appendix A: Samples of the collected thermal image for graphite/ECs at different operating parameters and graphite contents

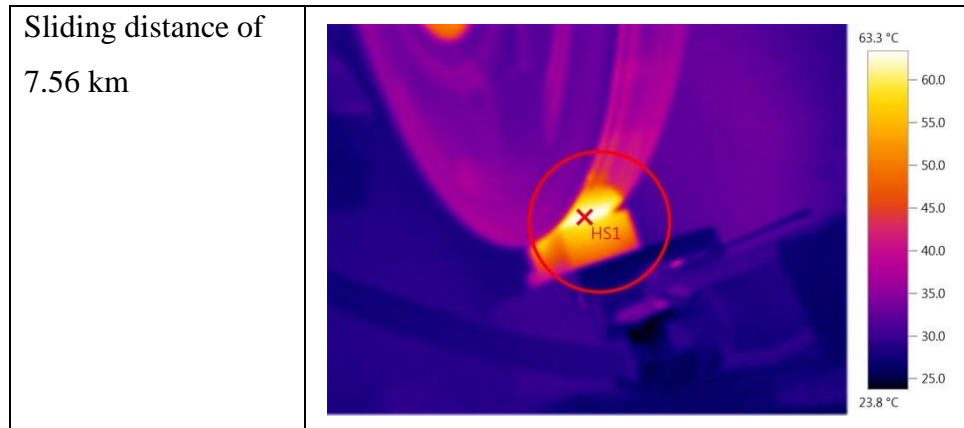




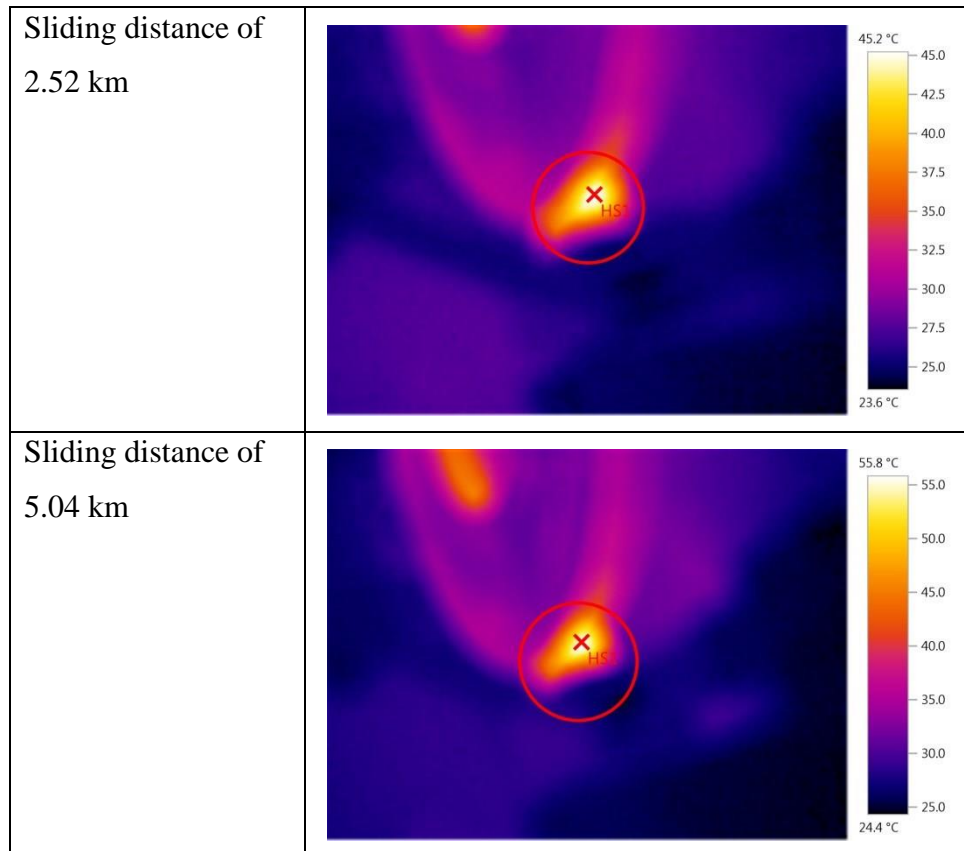
**Figure A.1: Heat distribution in the interface and both rubbed surfaces of the 1%Gr-EC after 2.52, 5.04 and 7.56 km sliding distances at sliding velocity of 2.8 m/s and applied load of 50 N using BOR technique**

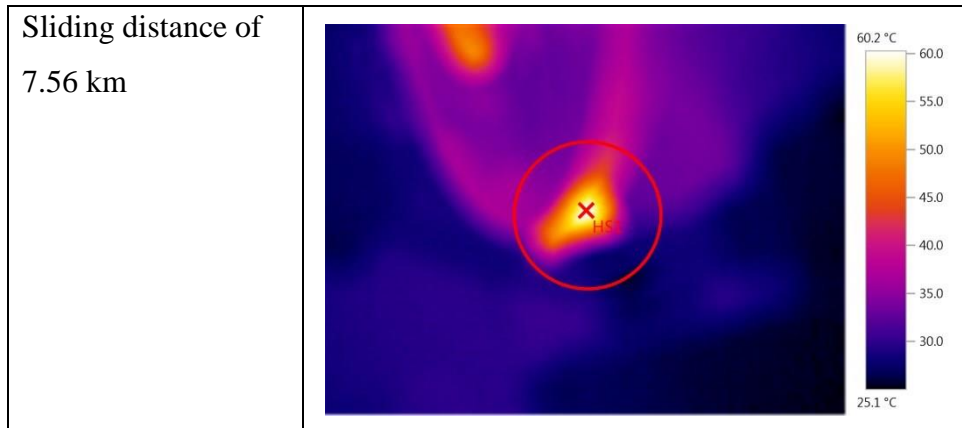




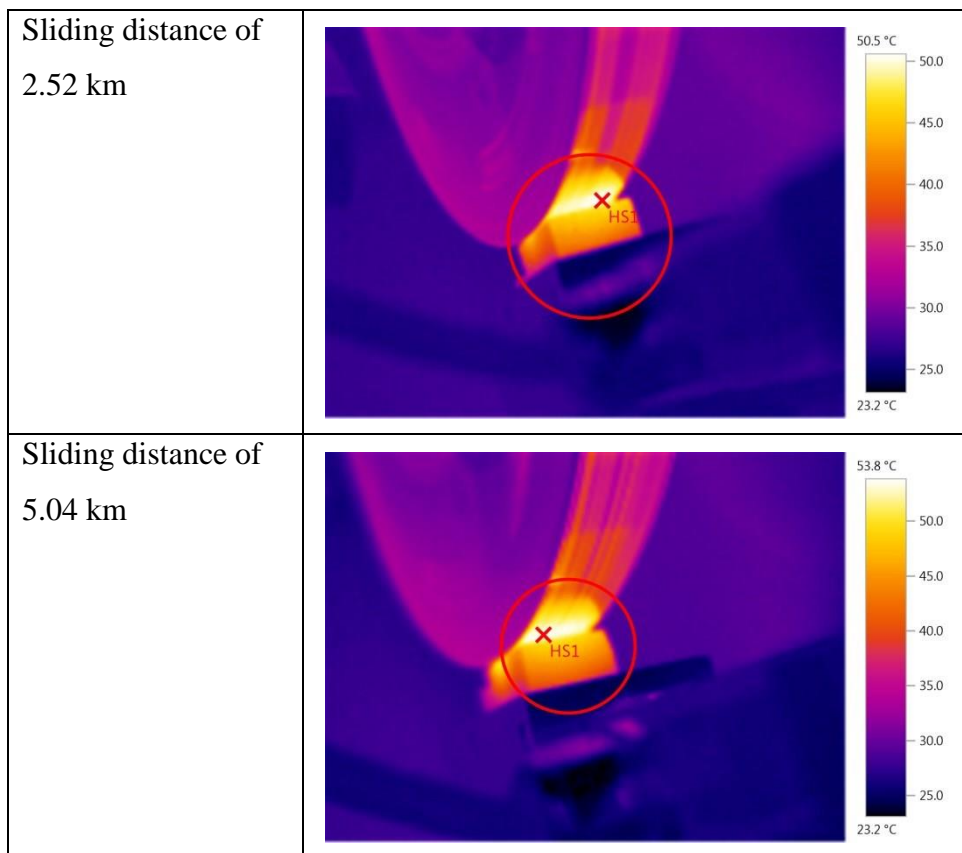


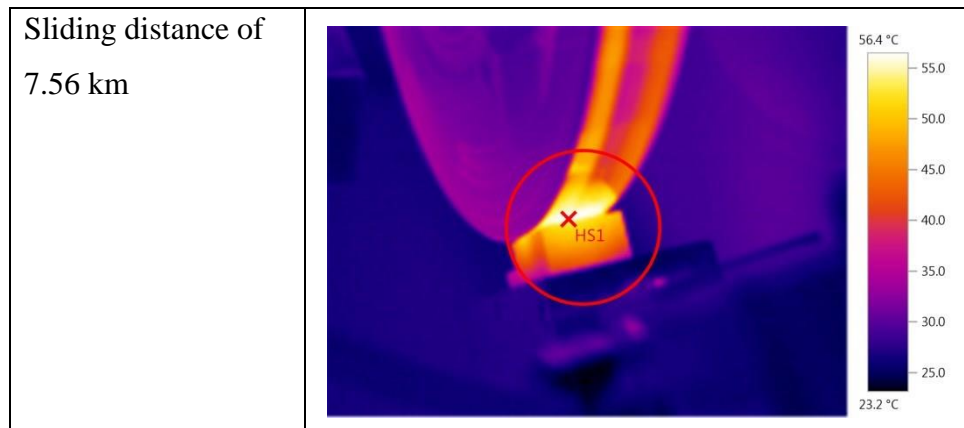
**Figure A.2: Heat distribution in the interface and both rubbed surfaces of the 3%Gr-EC after 2.52, 5.04 and 7.56 km sliding distances at sliding velocity of 2.8 m/s and applied load of 50 N using BOR technique**





**Figure A.3: Heat distribution in the interface and both rubbed surfaces of the 5%Gr-EC after 2.52, 5.04 and 7.56 km sliding distances at sliding velocity of 2.8 m/s and applied load of 50 N using BOR technique**



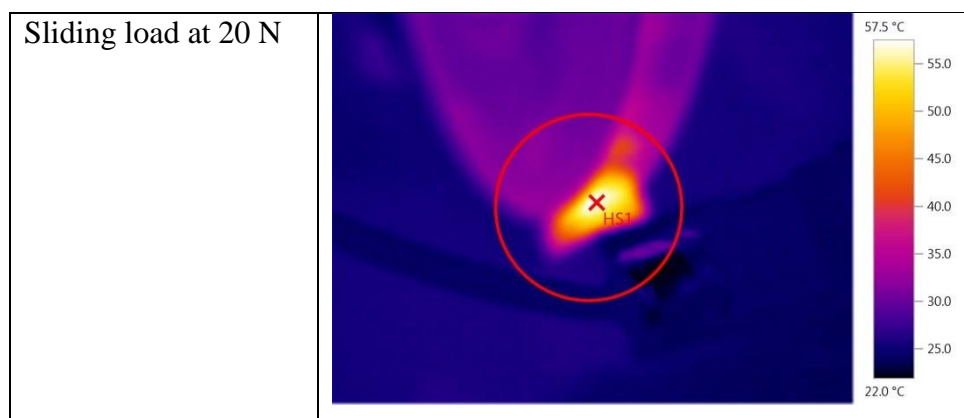


**Figure A.4:** Heat distribution in the interface and both rubbed surfaces of the 7%Gr-EC after 2.52, 5.04 and 7.56 km sliding distances at sliding velocity of 2.8 m/s and applied load of 50 N using BOR technique

## **Appendix B: Samples of the collected thermal image and roughness profile for graphite/date palm fibre/ECs at different operating parameters and test configurations**

### **B.1 Thermal image samples**

#### **B.1.1 Thermal image samples during the sliding of the composites (BOR)**



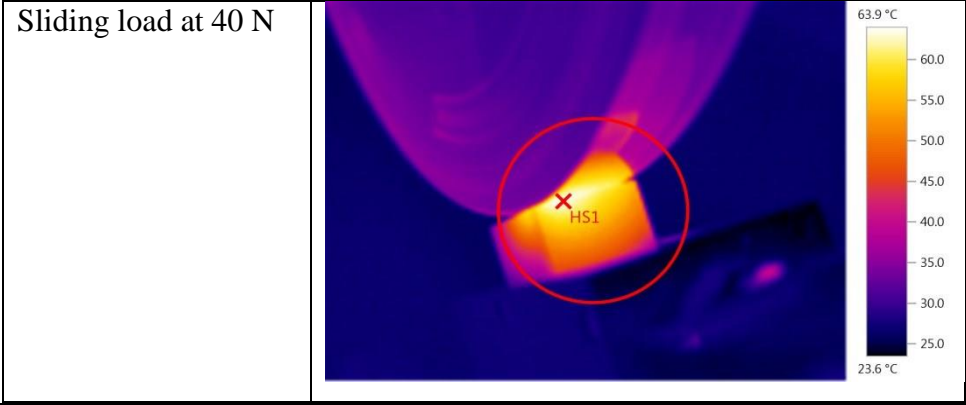
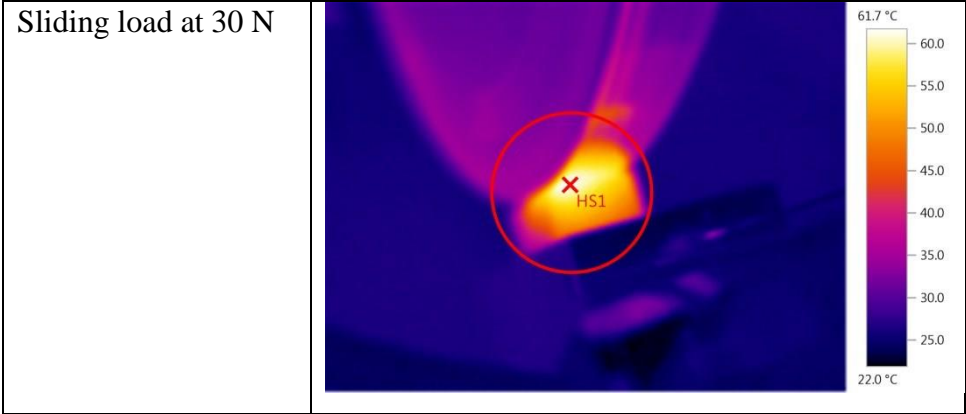
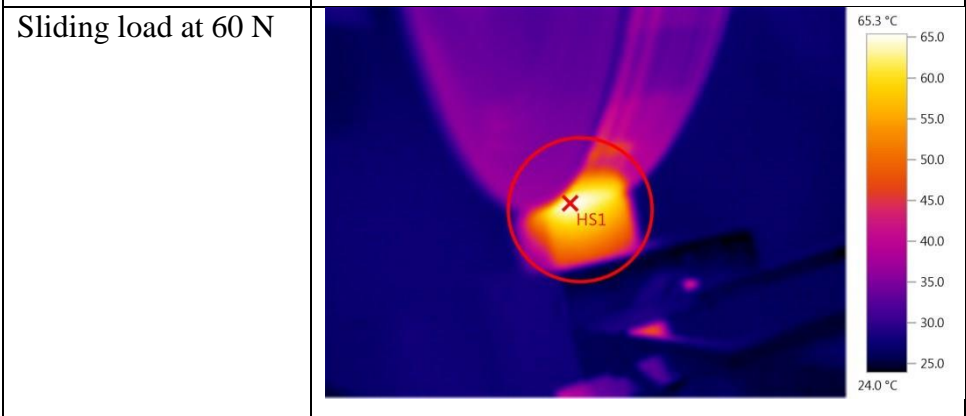
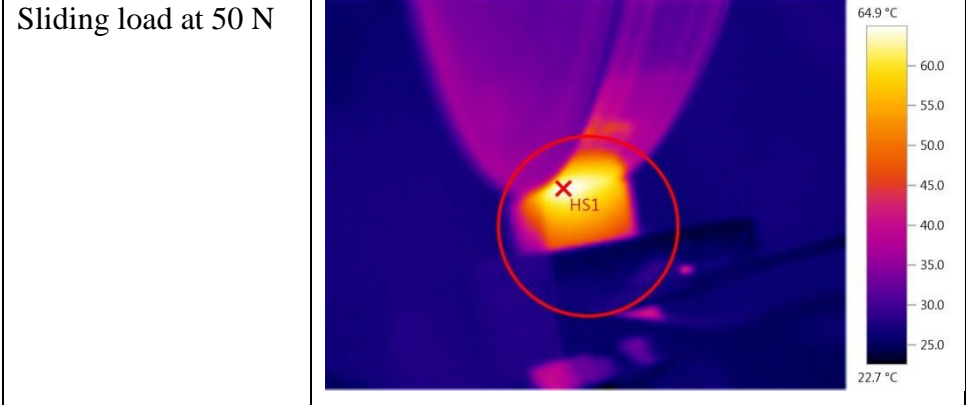
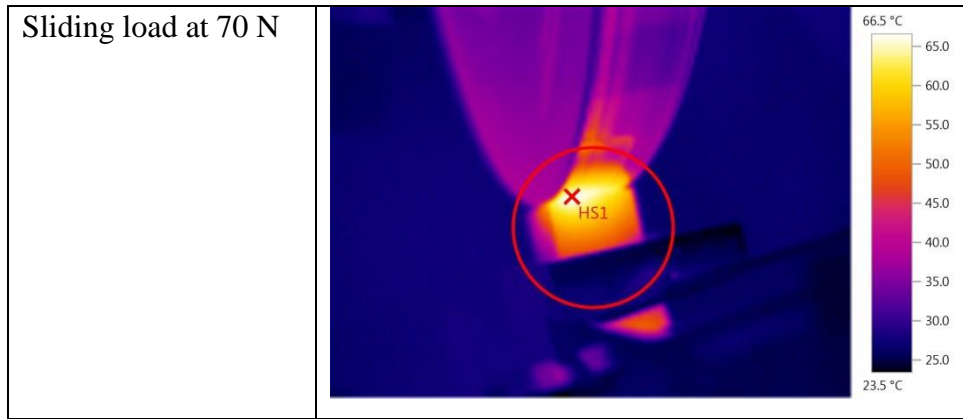
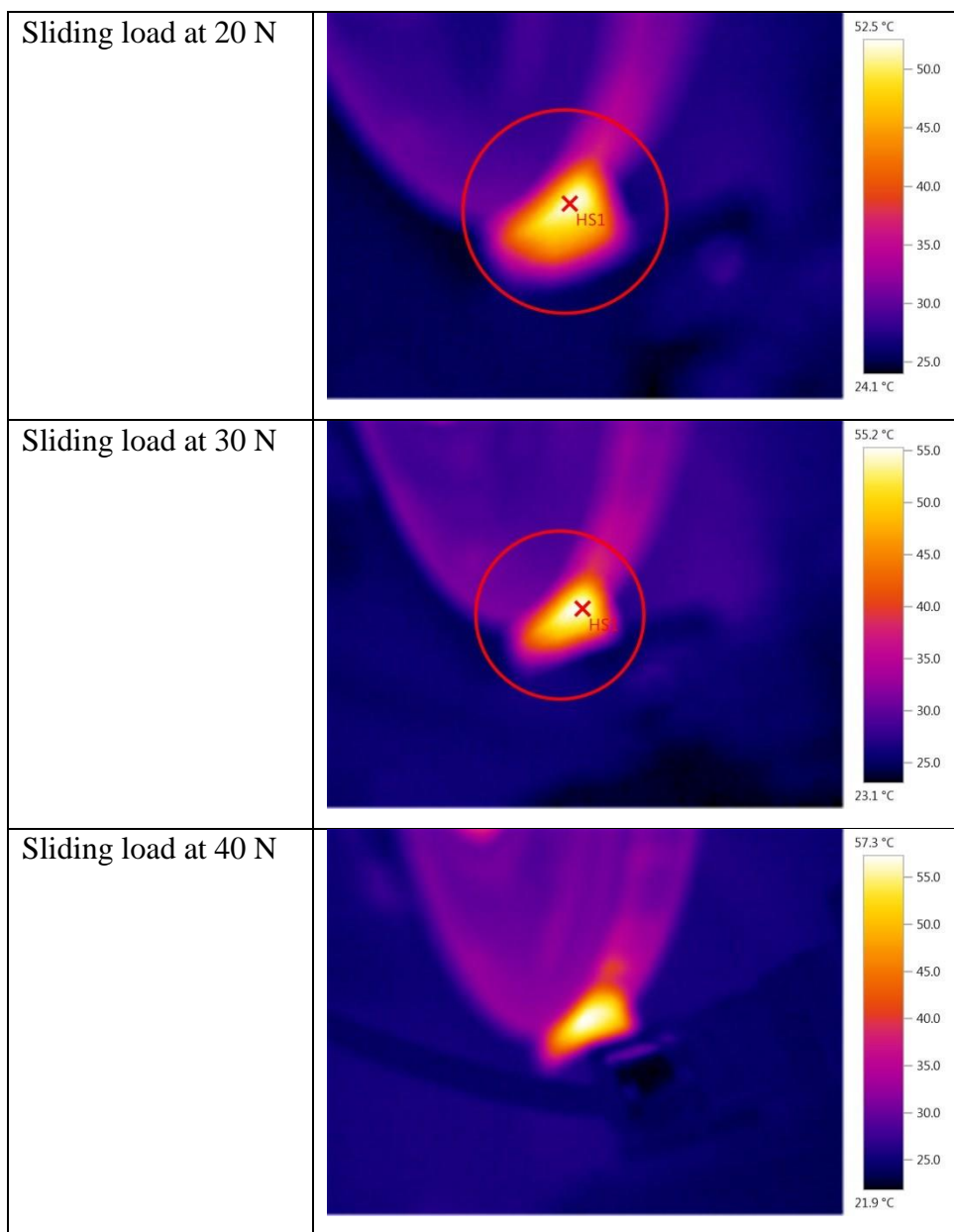


Figure B. 1 continued





**Figure B.1: Heat distribution in the interface and both rubbed surfaces of the NE at 20, 30, 40, 50 N sliding loads at sliding velocity of 2.8 m/s and sliding distance 5.04 km (BOR)**



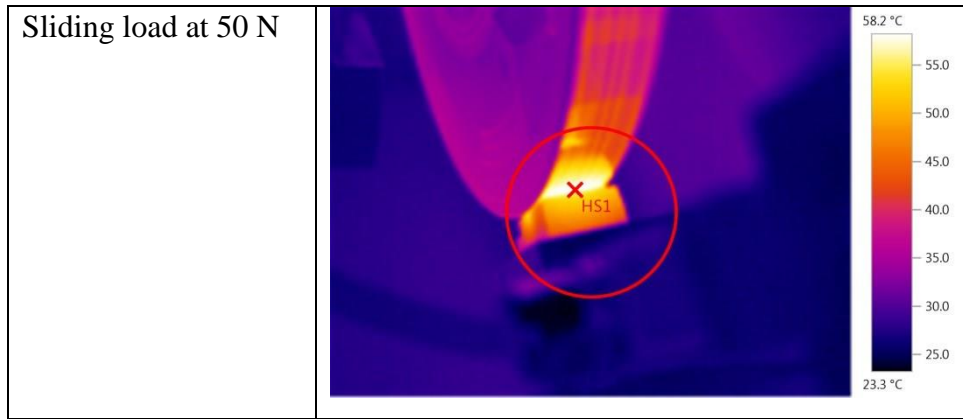


Figure B2 continued

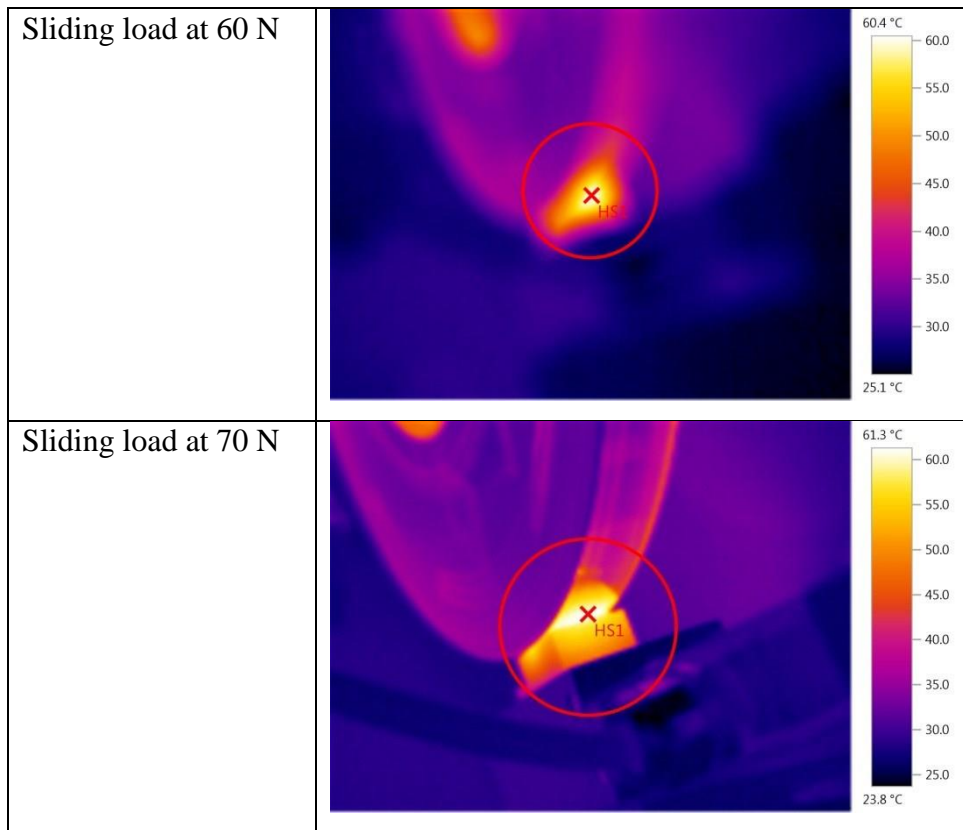


Figure B.2: Heat distribution in the interface and both rubbed surfaces of the GE at 20, 30, 40, 50 N sliding loads at sliding velocity of 2.8 m/s and sliding distance 5.04 km (BOR)

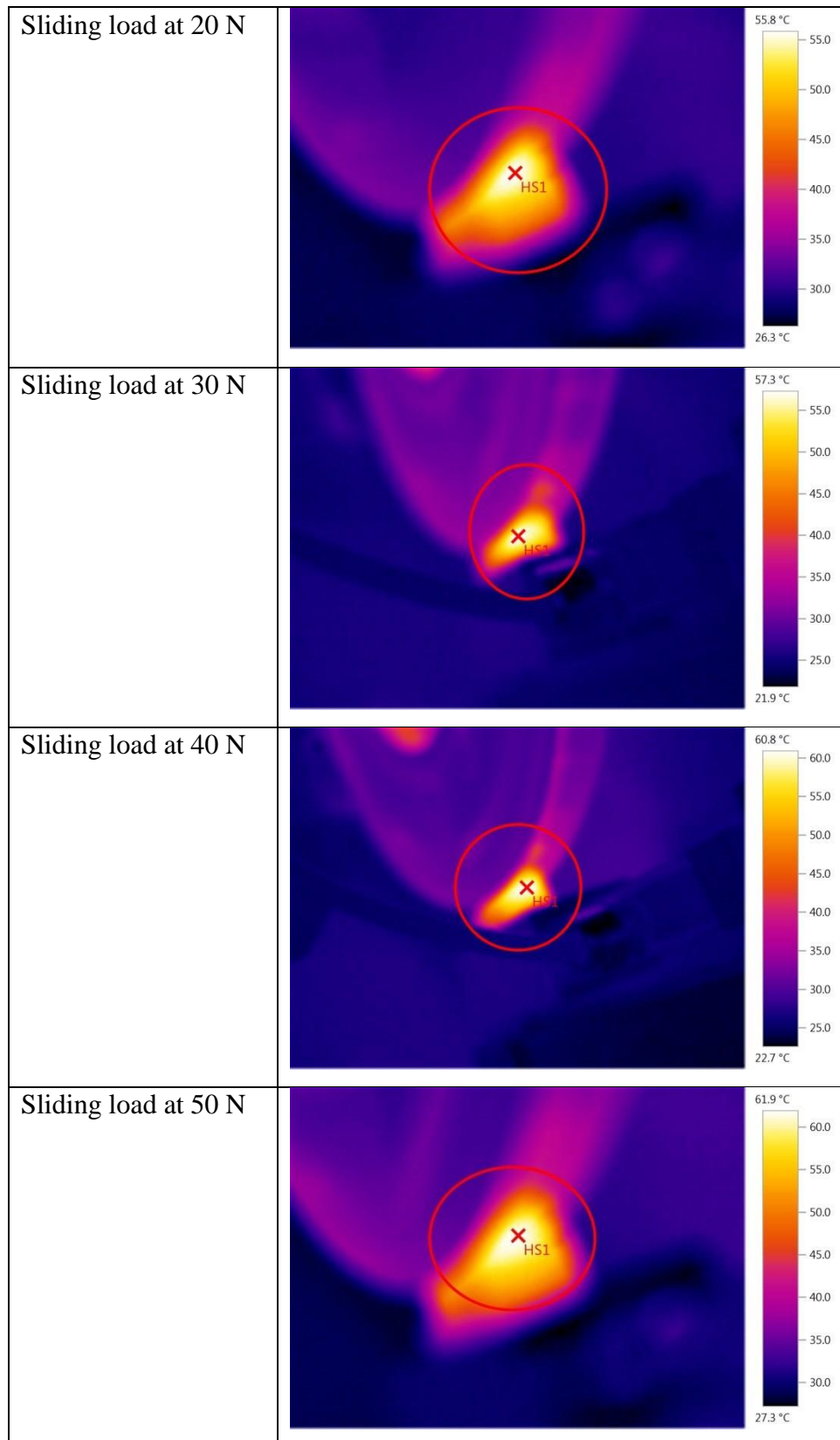
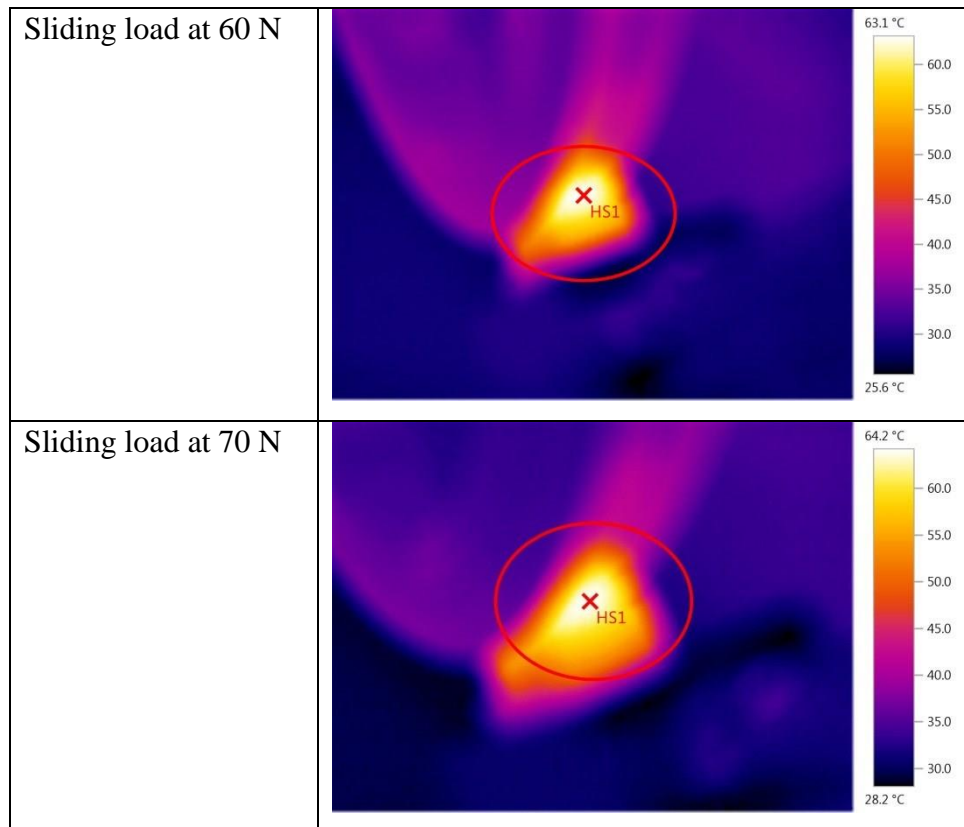


Figure B.3 continued



**Figure B.3: Heat distribution in the interface and both rubbed surfaces of the FE at 20, 30, 40, 50 N sliding loads at sliding velocity of 2.8 m/s and sliding distance 5.04 km (BOR)**



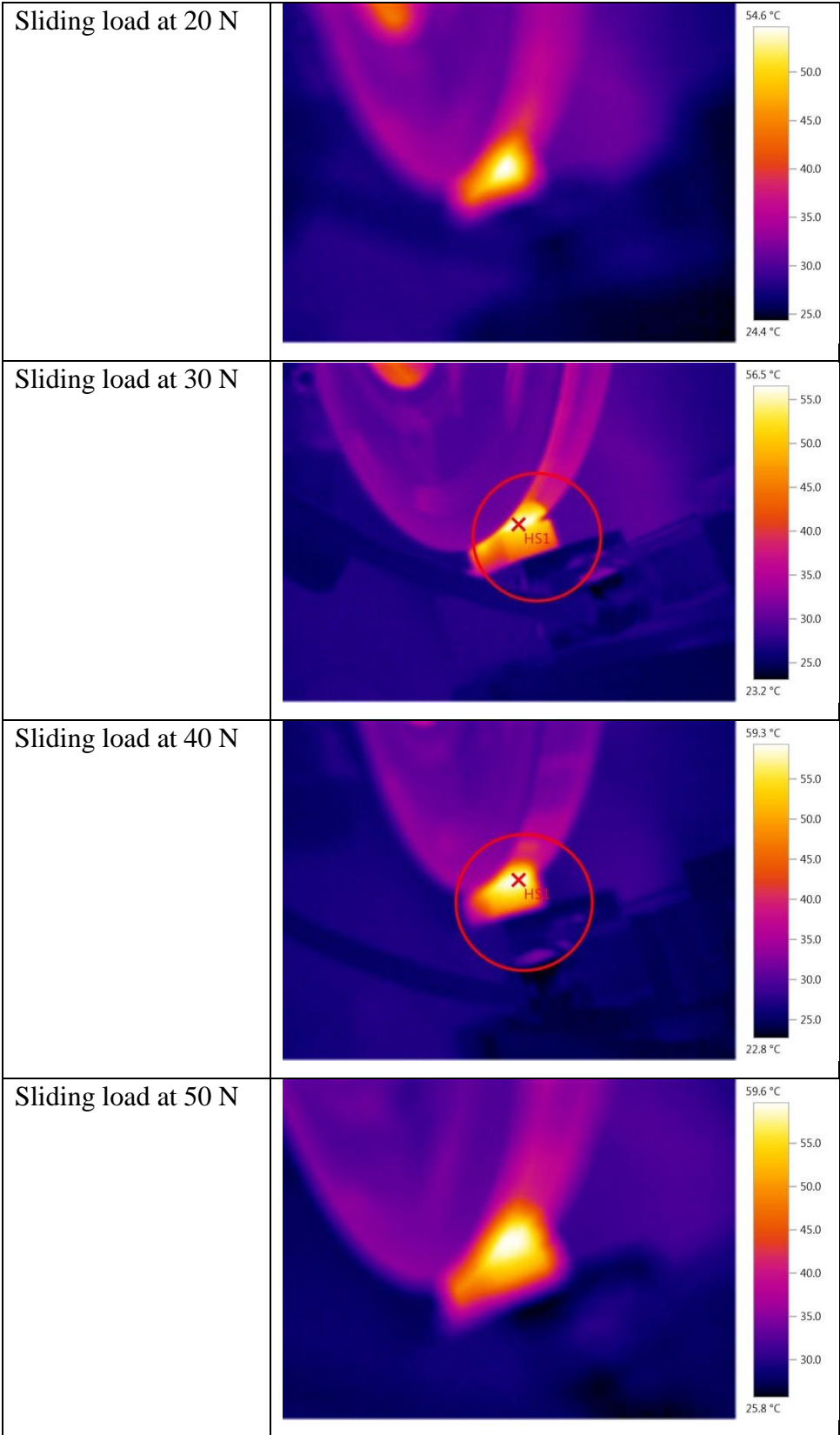
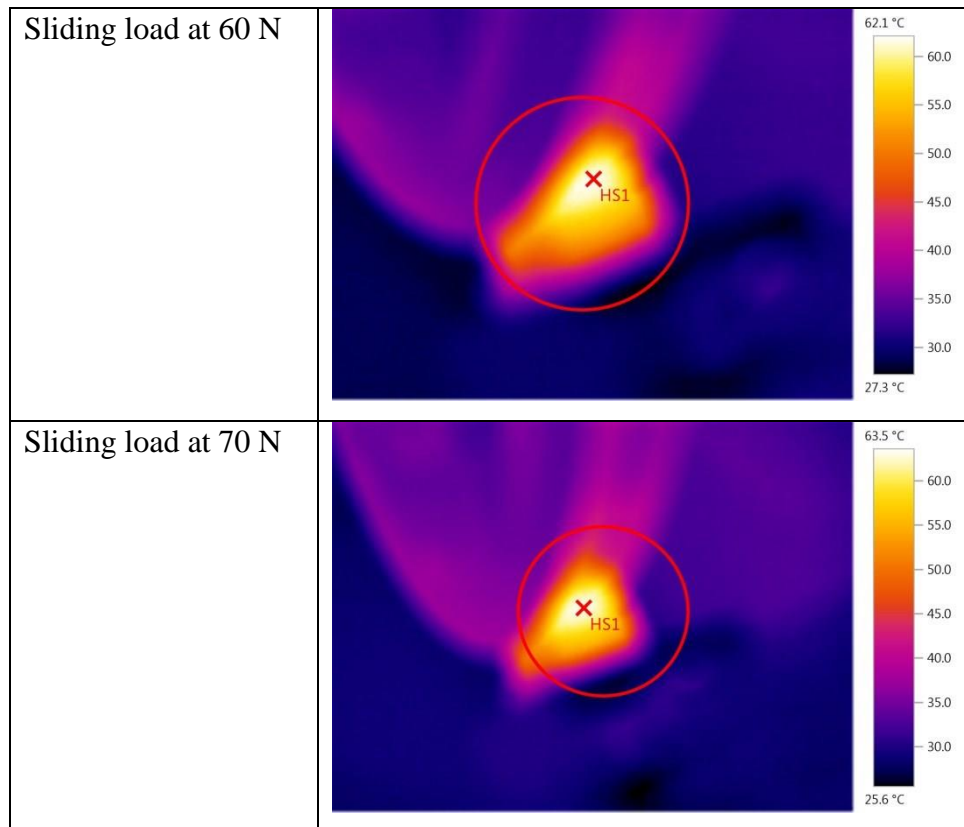


Figure B.4 continued



**Figure B.4: Heat distribution in the interface and both rubbed surfaces of the GFE at 20, 30, 40, 50 N sliding loads at sliding velocity of 2.8 m/s and sliding distance 5.04 km (BOR)**

### B.1.2 Thermal image samples during the sliding of the composites (BOD)

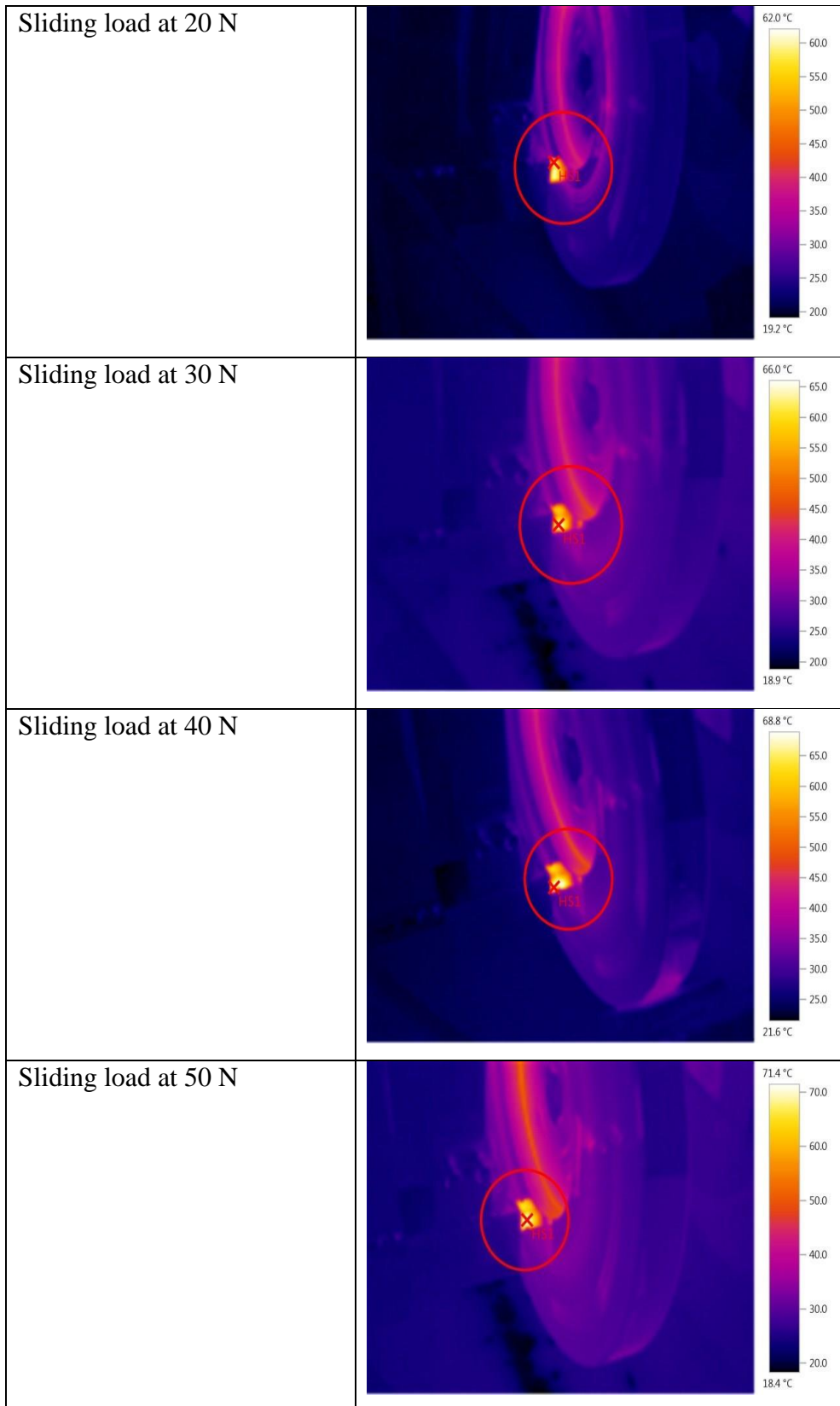
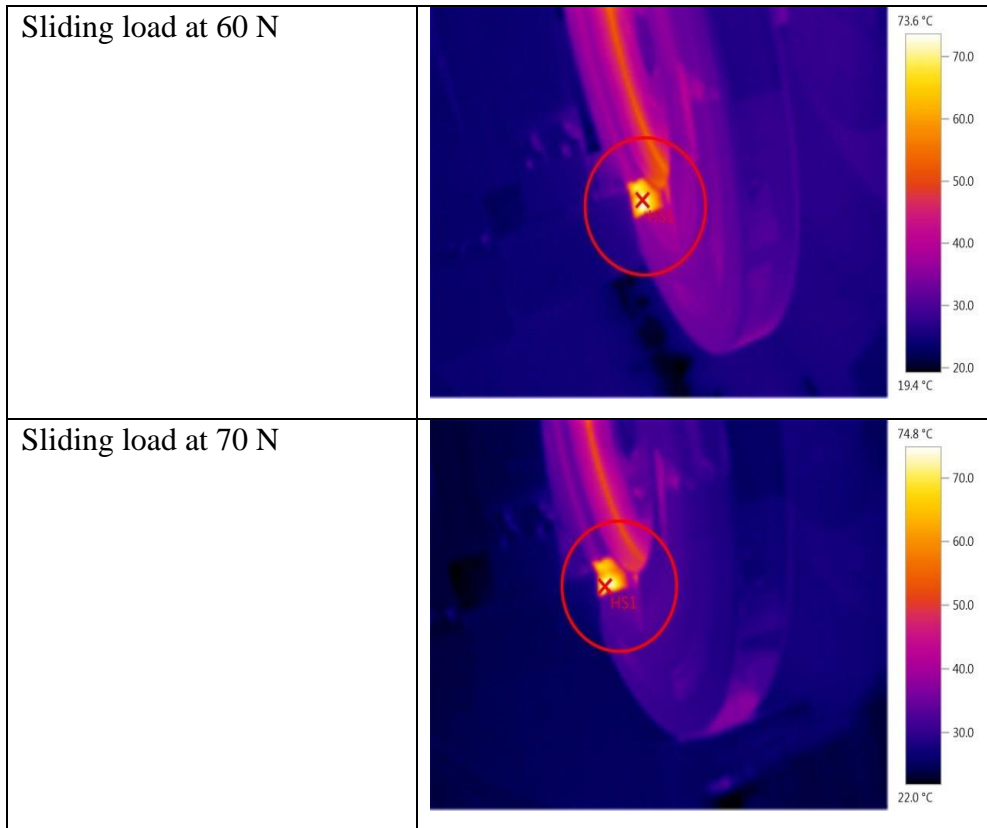
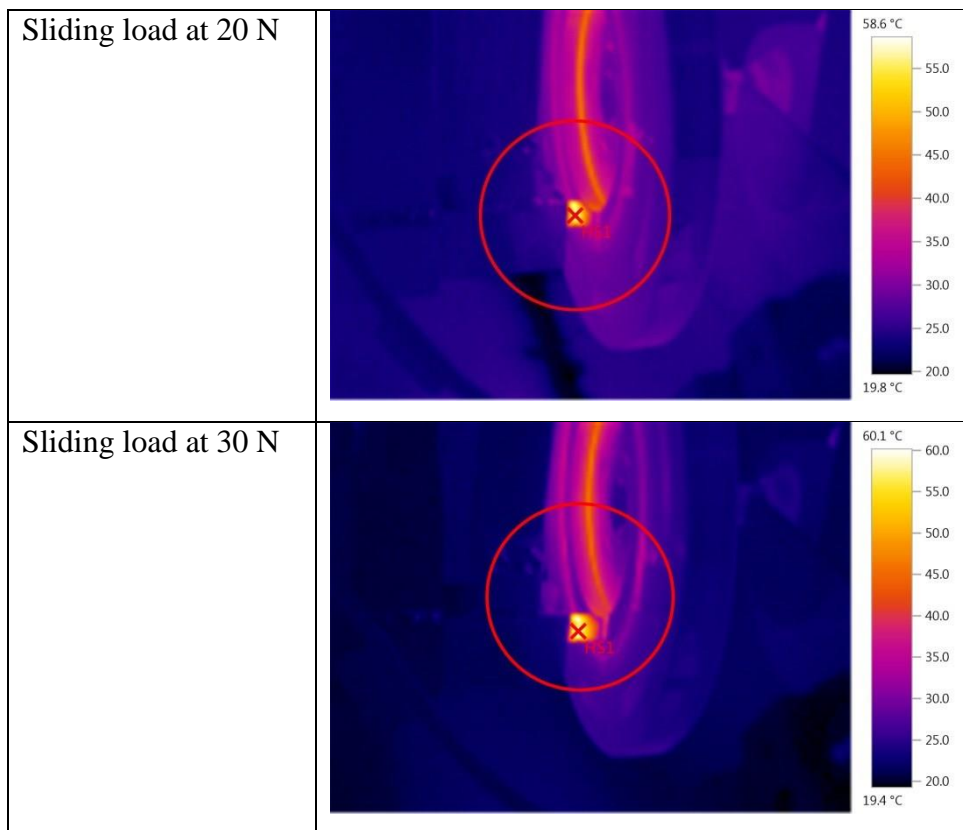


Figure B.5 continued



**Figure B.5: Heat distribution in the interface and both rubbed surfaces of the NE at 20, 30, 40, 50 N sliding loads at sliding velocity of 2.8 m/s and sliding distance 2.52 km (BOD)**



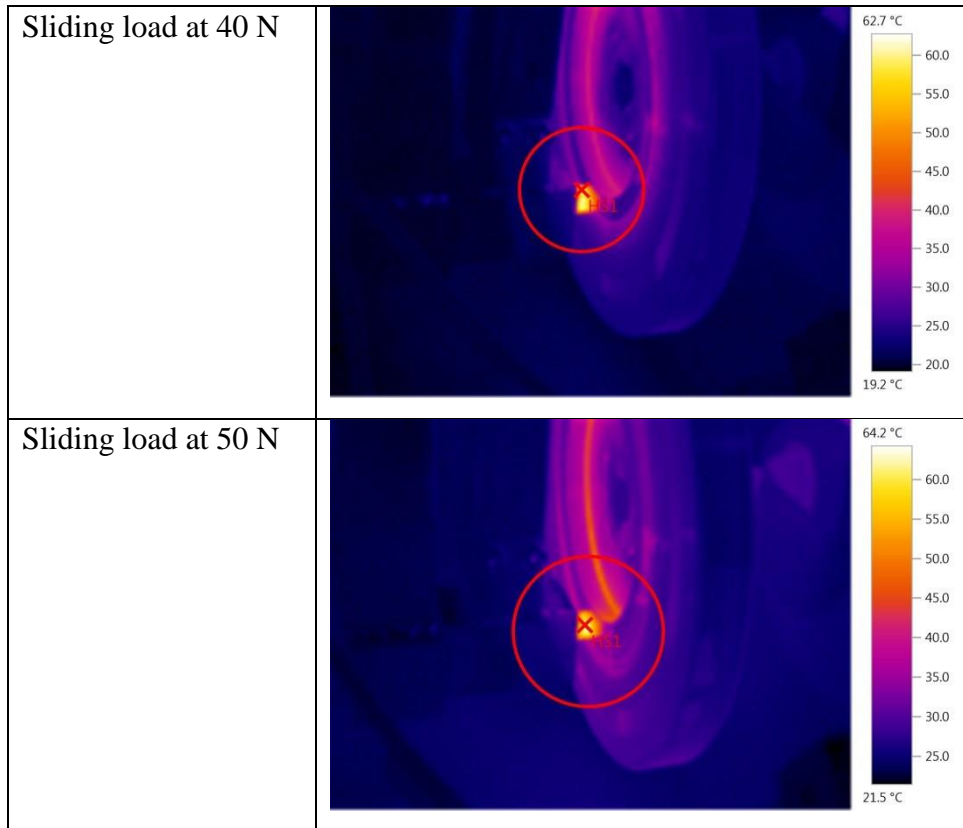


Figure B.6 continued

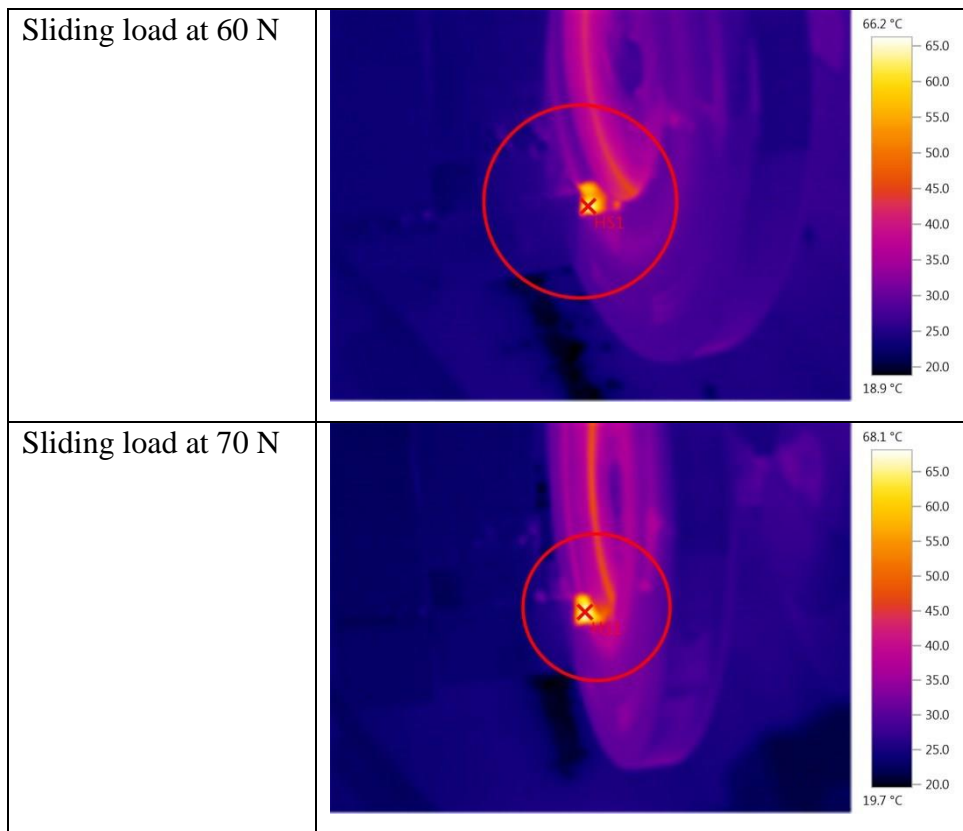


Figure B.6: Heat distribution in the interface and both rubbed surfaces of the GE at 20, 30, 40, 50 N sliding loads at sliding velocity of 2.8 m/s and sliding distance 2.52 km (BOD)

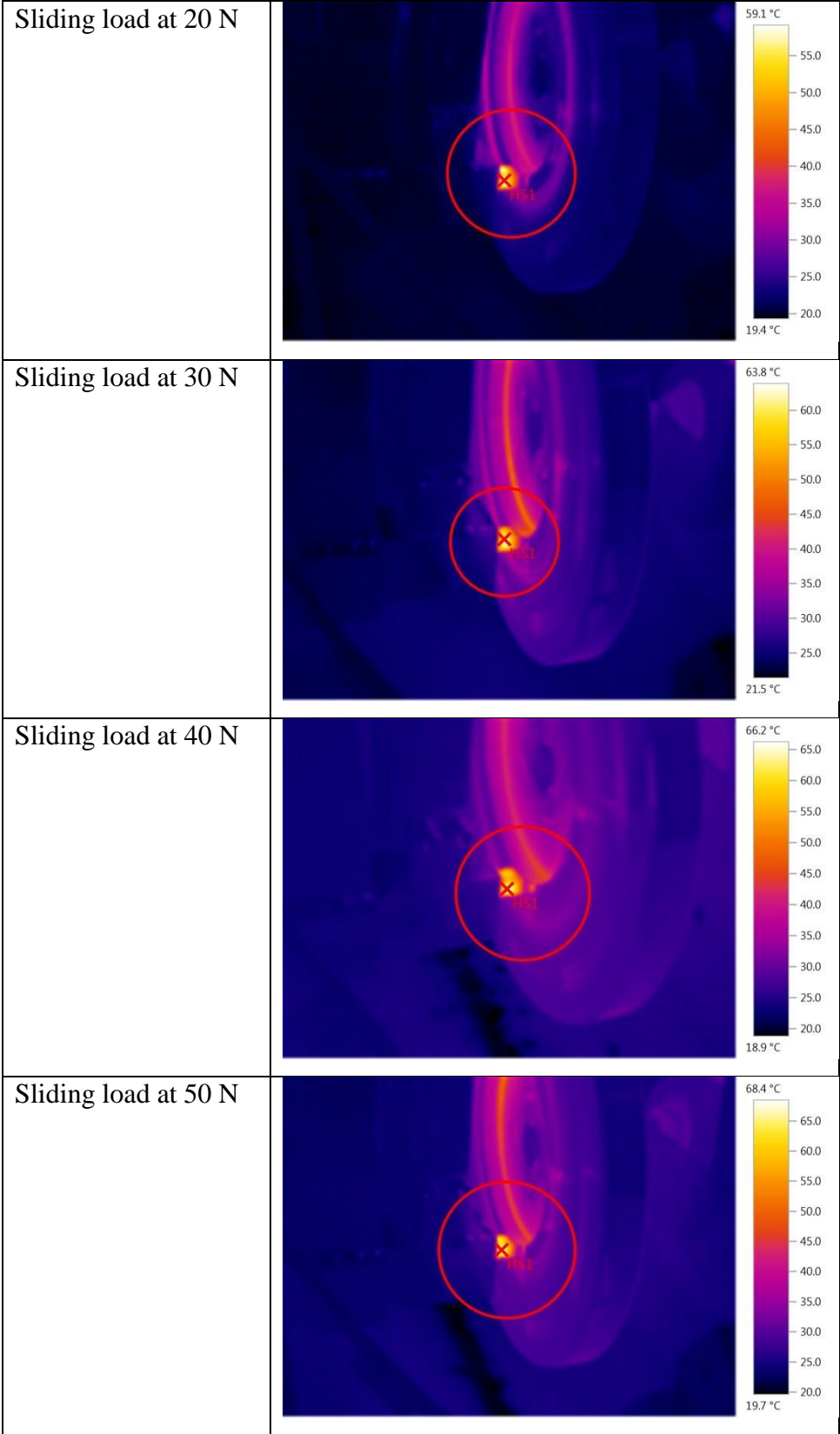
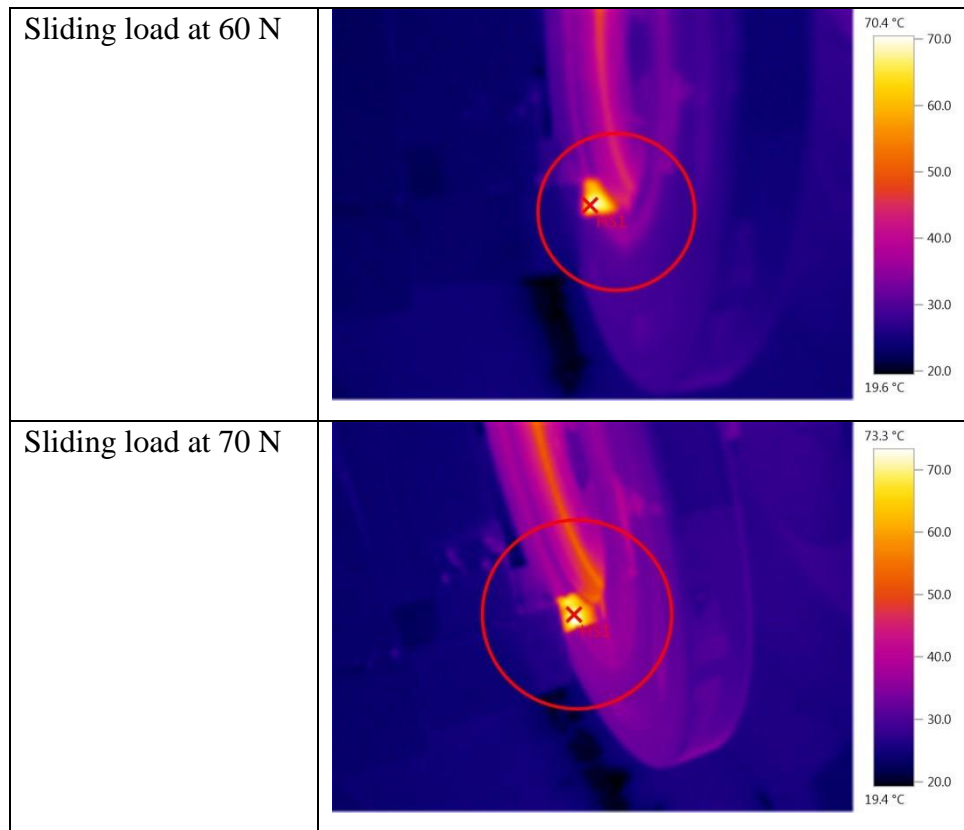
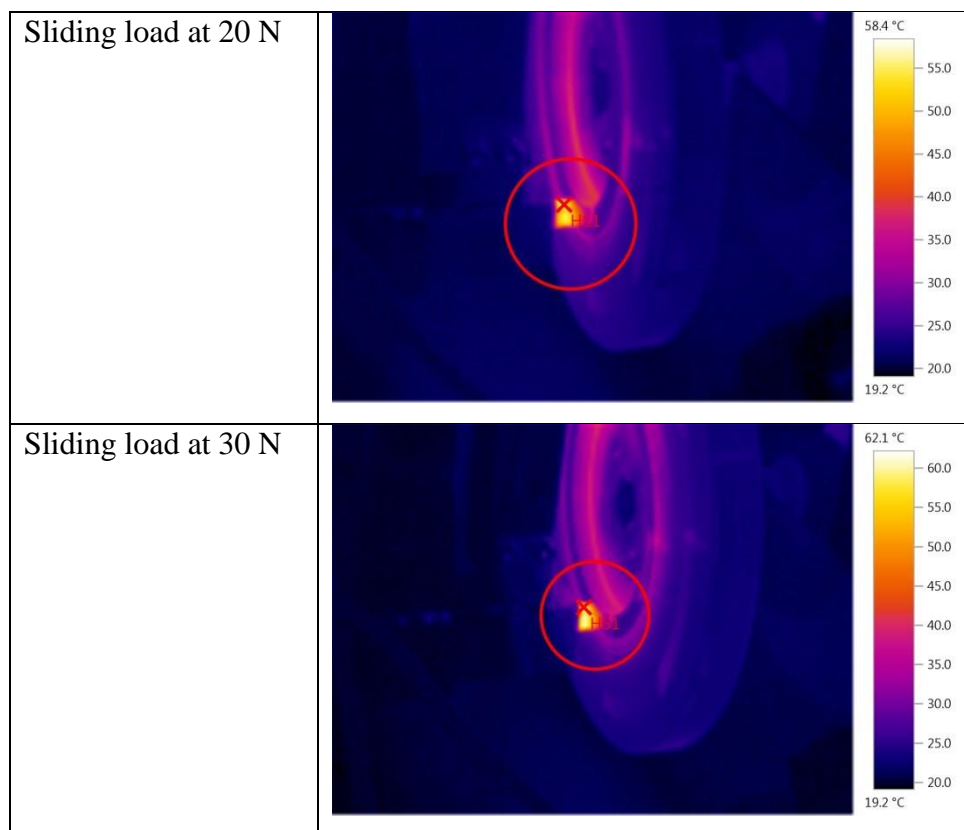


Figure B.7 continued



**Figure B.7: Heat distribution in the interface and both rubbed surfaces of the FE at 20, 30, 40, 50 N sliding loads at sliding velocity of 2.8 m/s and sliding distance 2.52 km (BOD)**



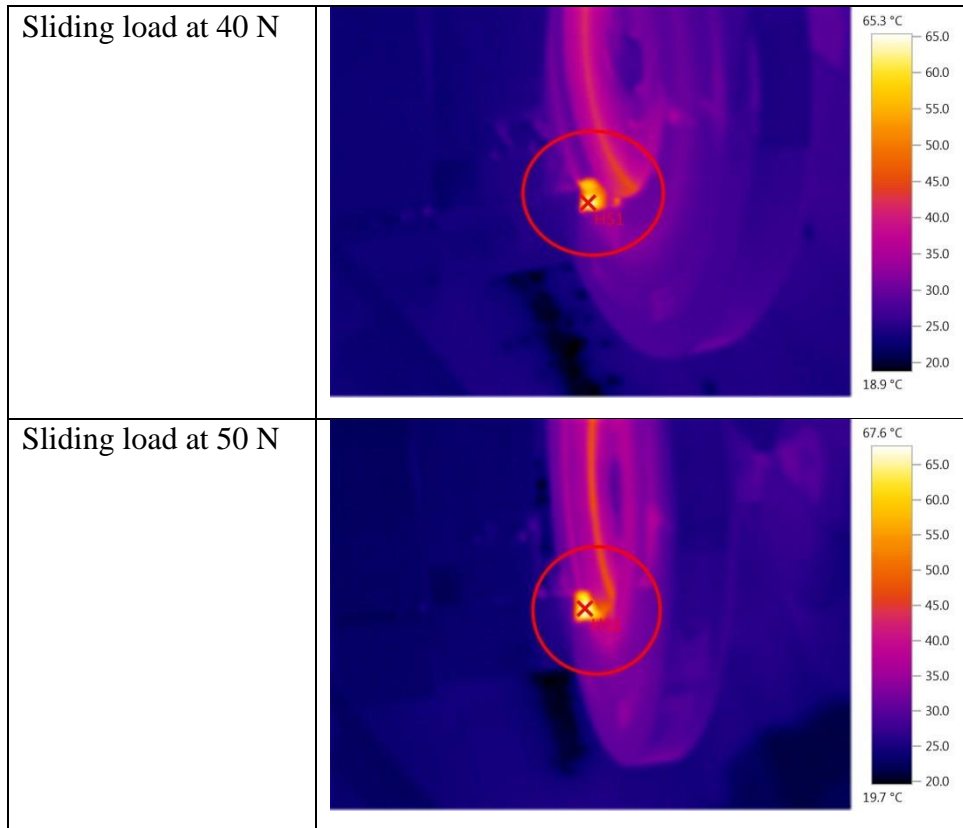


Figure B.8 continued

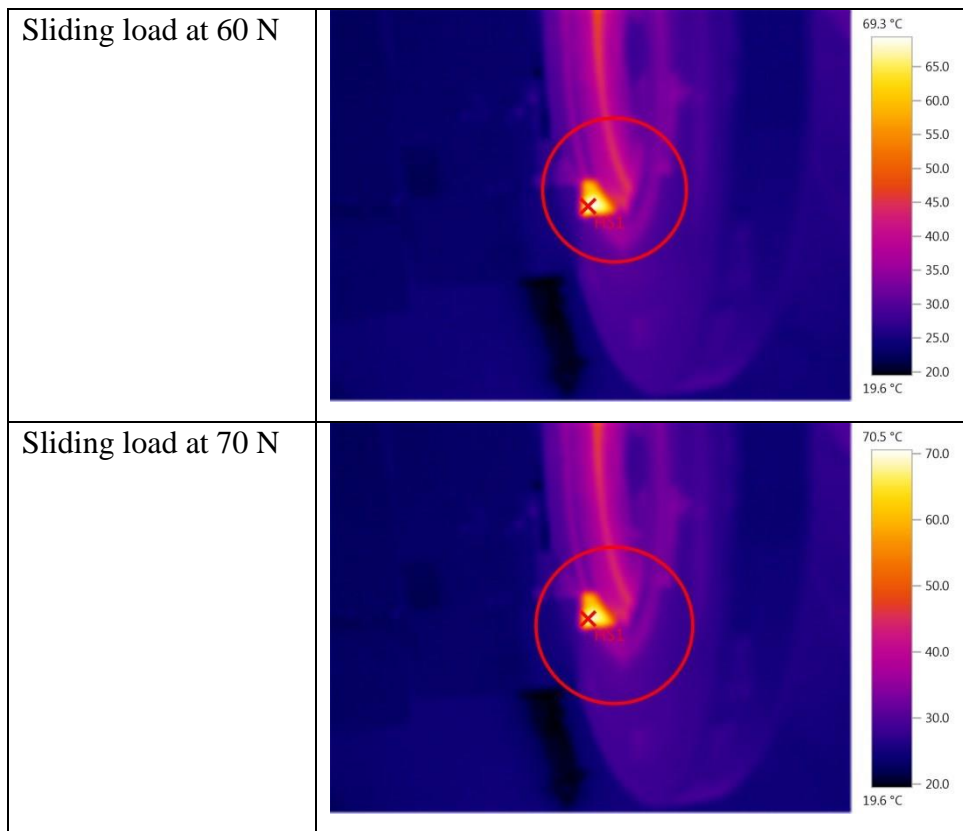
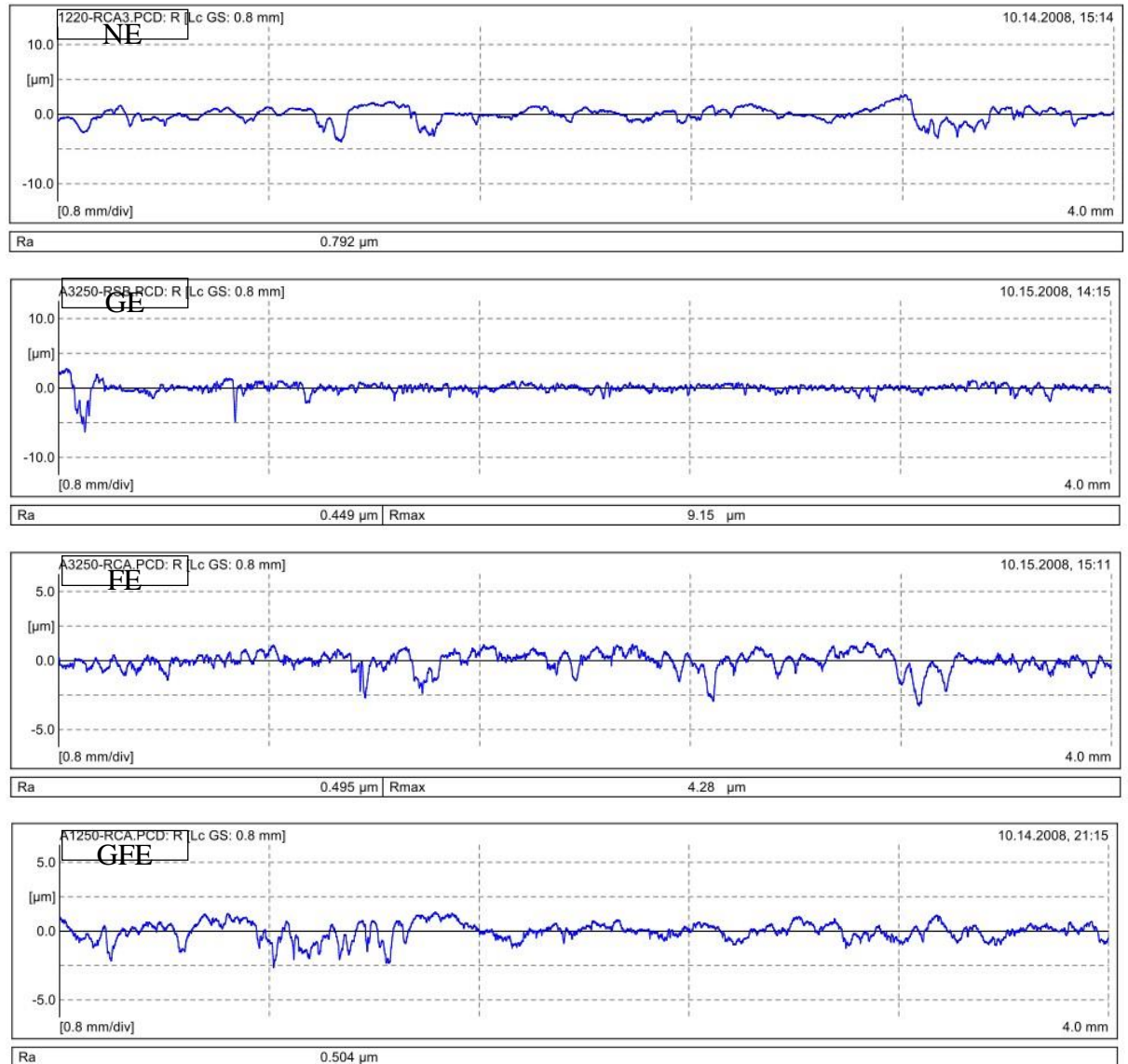


Figure B.8: Heat distribution in the interface and both rubbed surface of the GFE at 20, 30, 40, 50 N sliding loads at sliding velocity of 2.8 m/s and sliding distance 2.52 km (BOD)



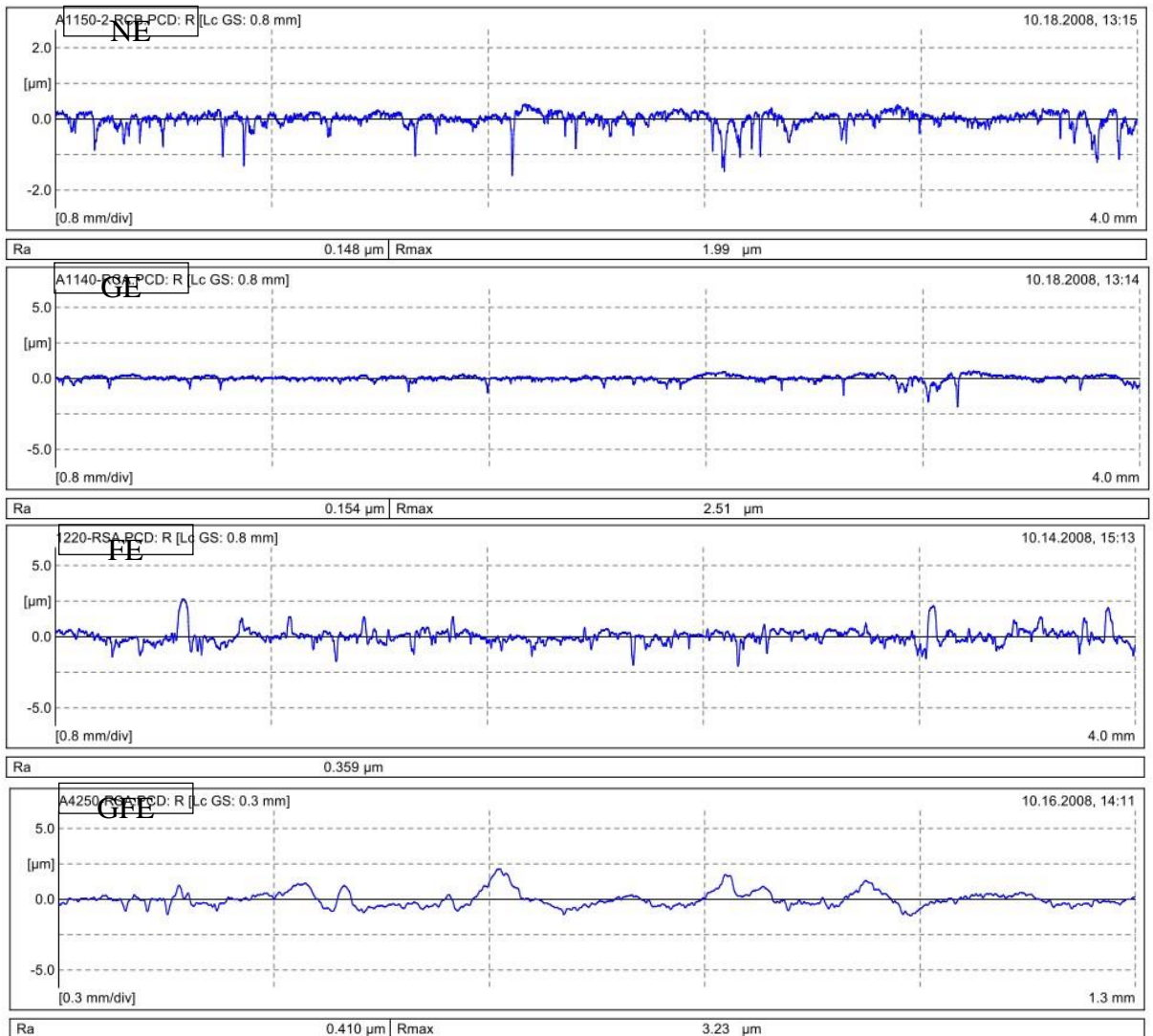
## B.2 Roughness image samples

### B.2.1 Roughness image counterface surface after the sliding of the composites (BOR)



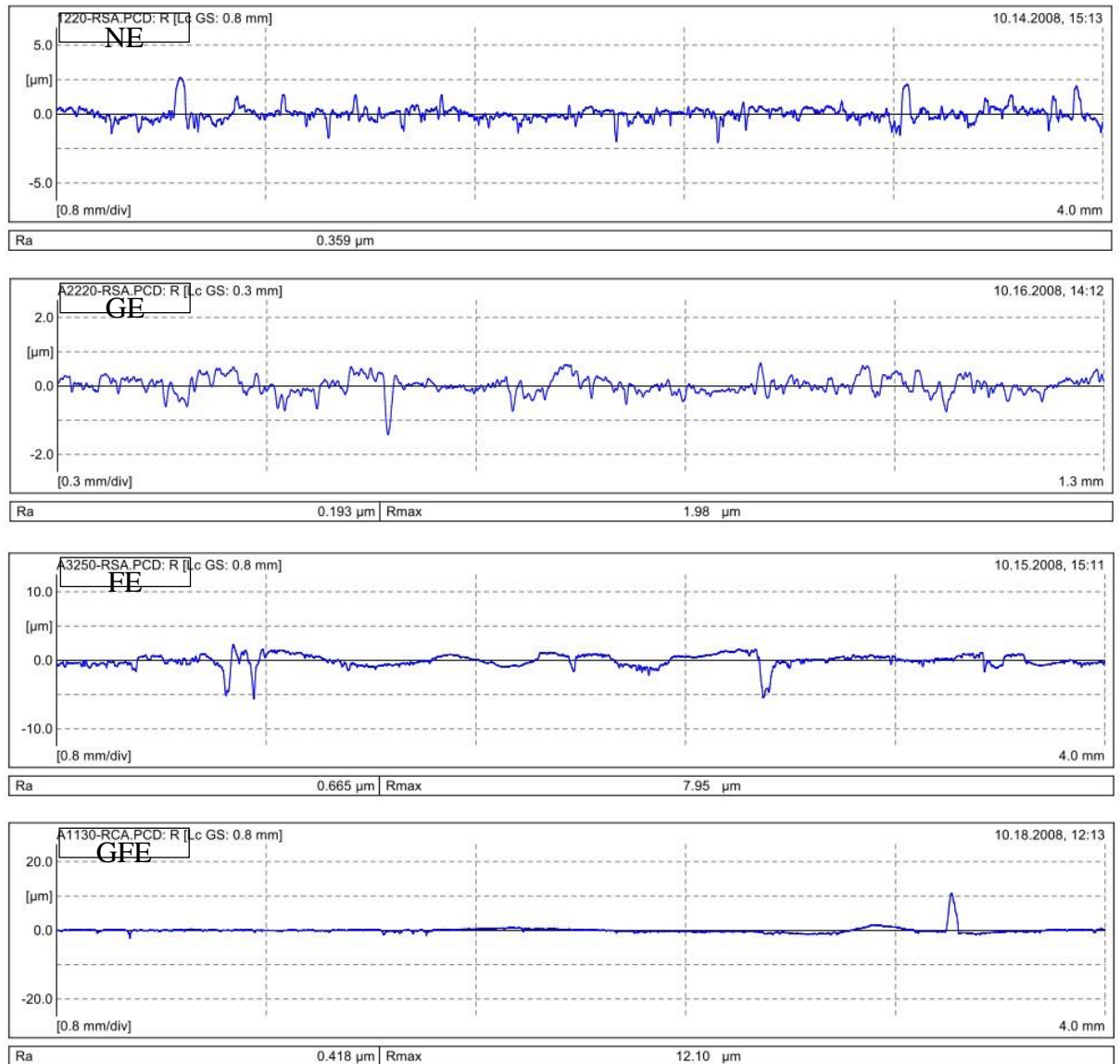
**Figure B.9: Roughness values of the counterface surface after adhesive loadings of different ECs based on graphite and/or DPF at 50 N applied load using BOR technique**

### B.2.2 Roughness image specimen surface before the sliding of the composites (BOR)



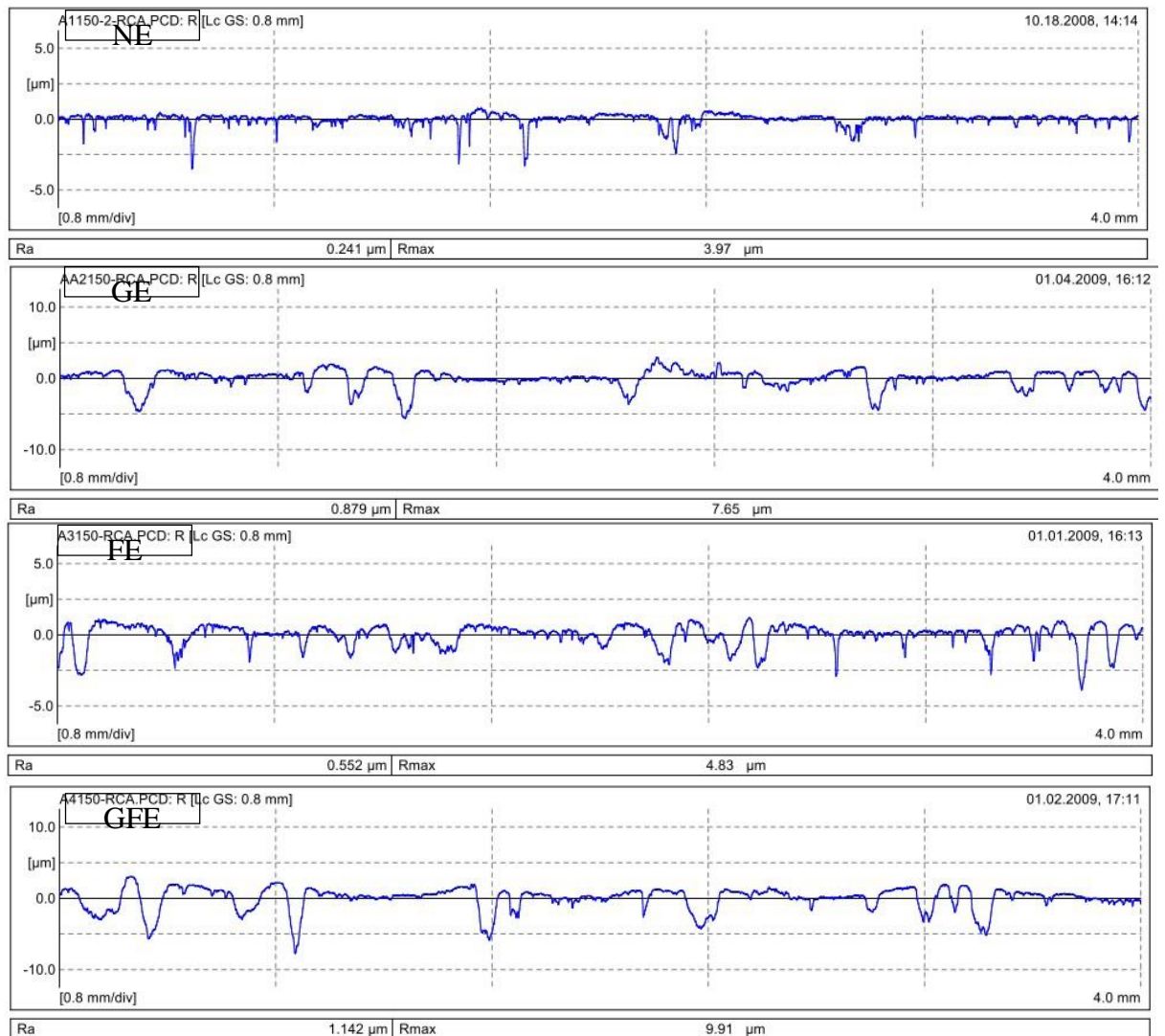
**Figure B.10: Roughness values of the specimen surface of different ECs based on graphite and/or DPF before adhesive loadings at 50 N using BOR technique**

**B.2.3 Roughness image specimen surface after the sliding of the composites (BOR)**



**Figure B.11: Roughness values of the specimen surface of different ECs based on graphite and/or DPF after adhesive loadings at 50 N using BOR technique**

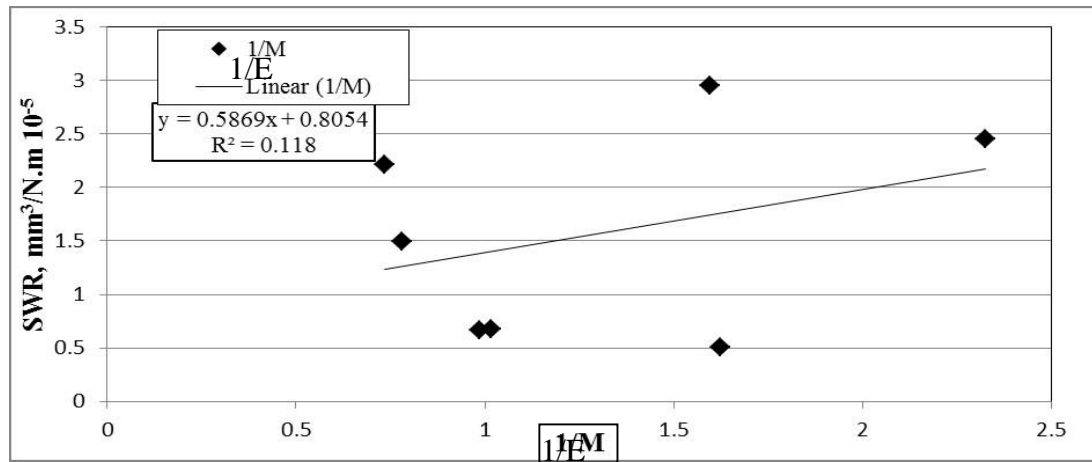
### **B.2.4 Roughness image counterface surface after the sliding of the composites (BOD)**



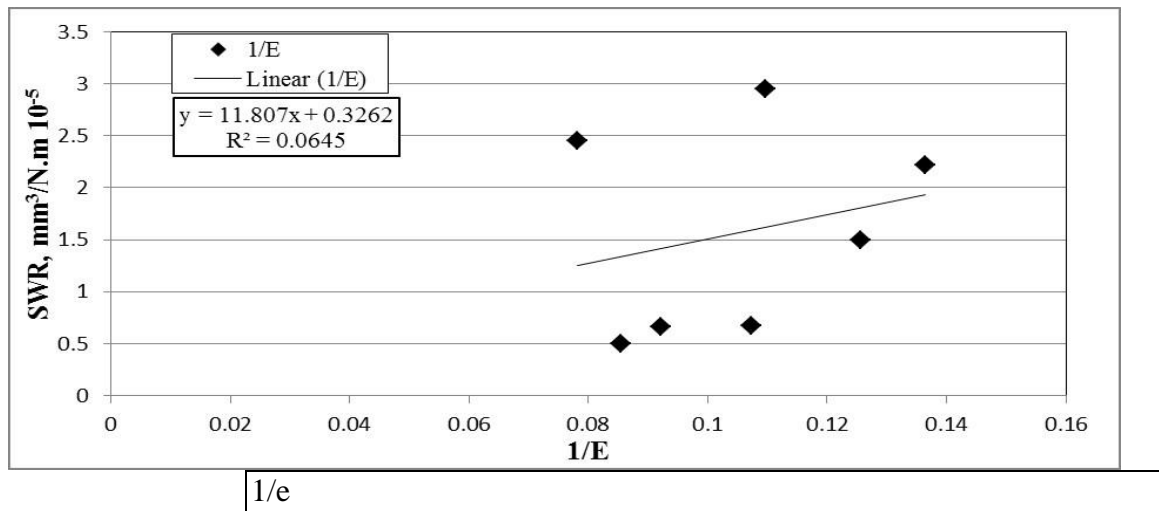
**Figure B.12: Roughness values of the counterface surface after adhesive of different ECs based on graphite and/or DPF loadings at 50 N using BOD technique**

**Appendix C: Figures of the correlation between mechanical and tribological properties**

**C.1 Completed figures of the correlation between mechanical properties and specific wear rate**

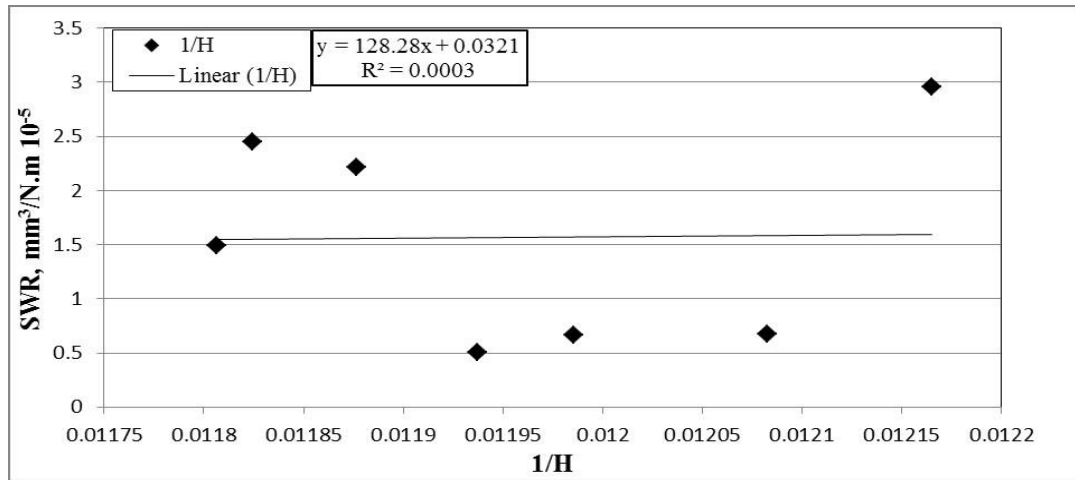


**Figure C. 1 correlation between specific wear rate and modulus of elasticity**

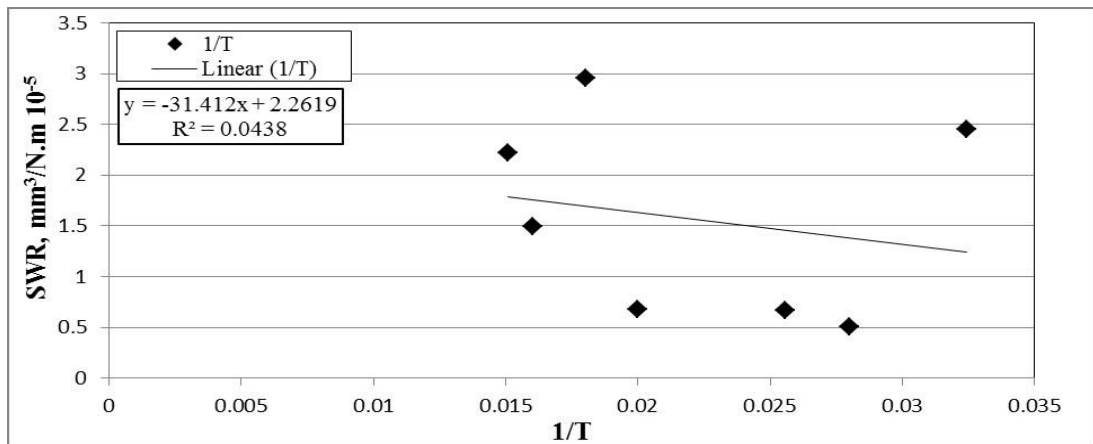


1/e

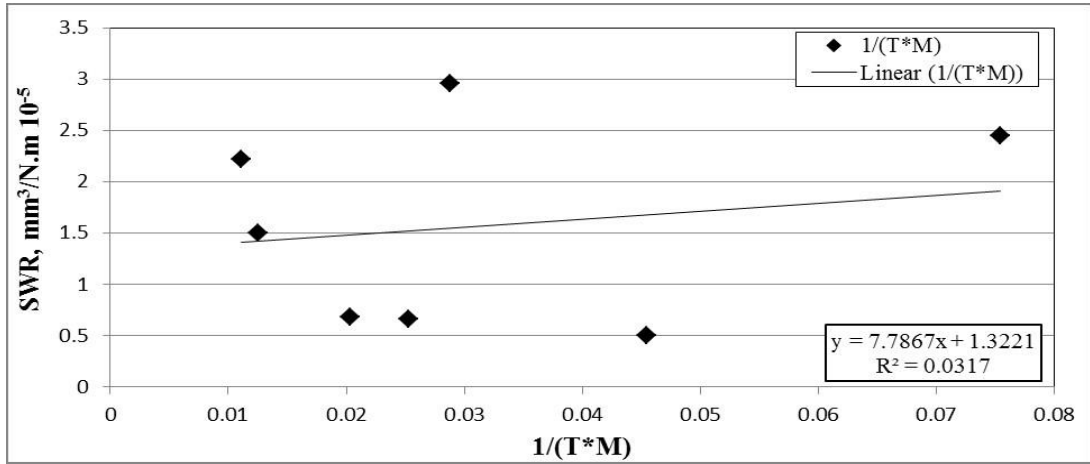
**Figure C. 2 correlation between specific wear rate and elongation at break**



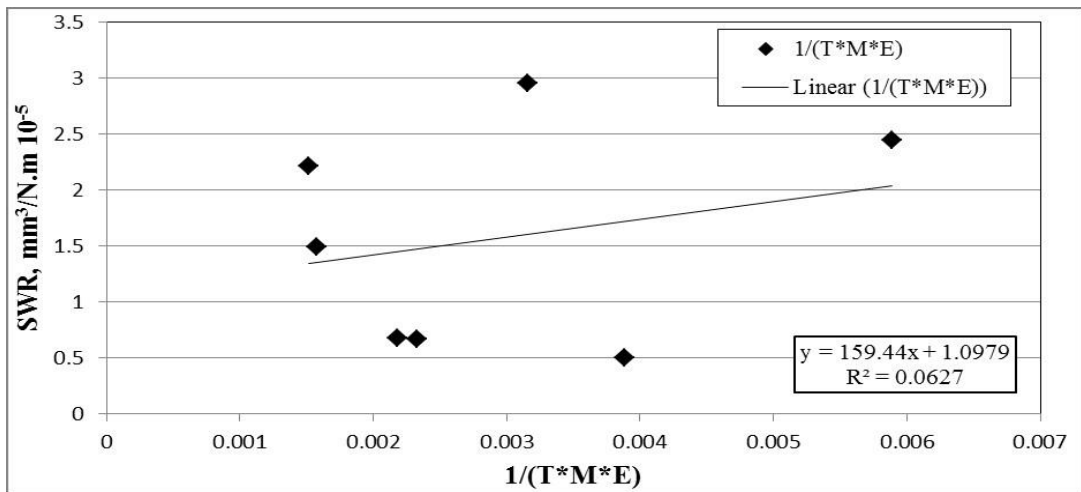
**Figure C. 3 correlation between specific wear rate and hardness**



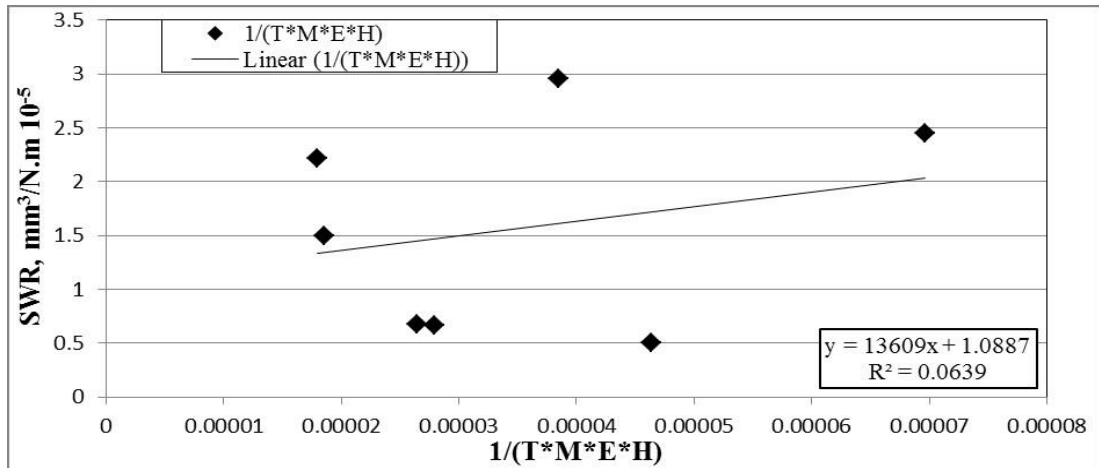
**Figure C. 4 correlation between specific wear rate and tensile strength**



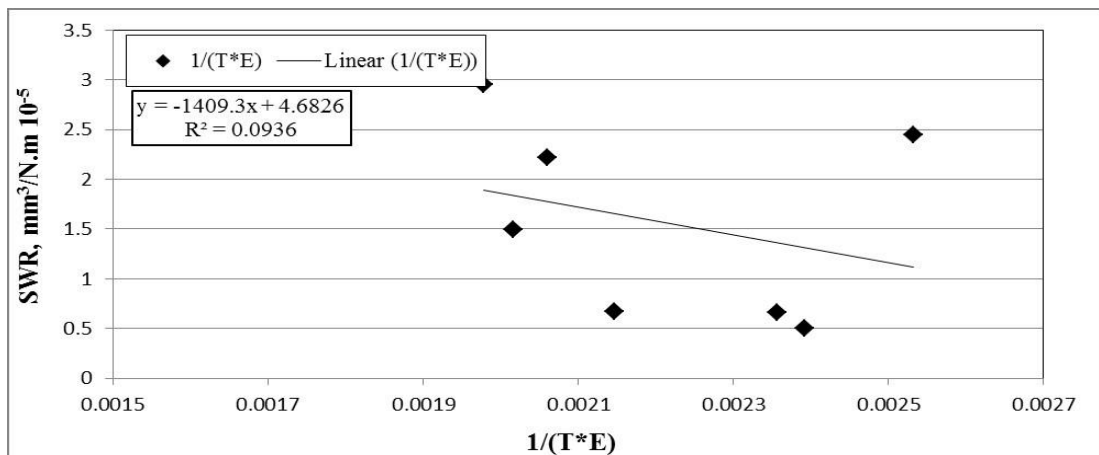
**Figure C. 5 correlation between specific wear rate and the combination of modulus of elasticity and tensile strength**



**Figure C. 6 correlation between specific wear rate and the combination of modulus of elasticity, tensile strength and elongation at break**

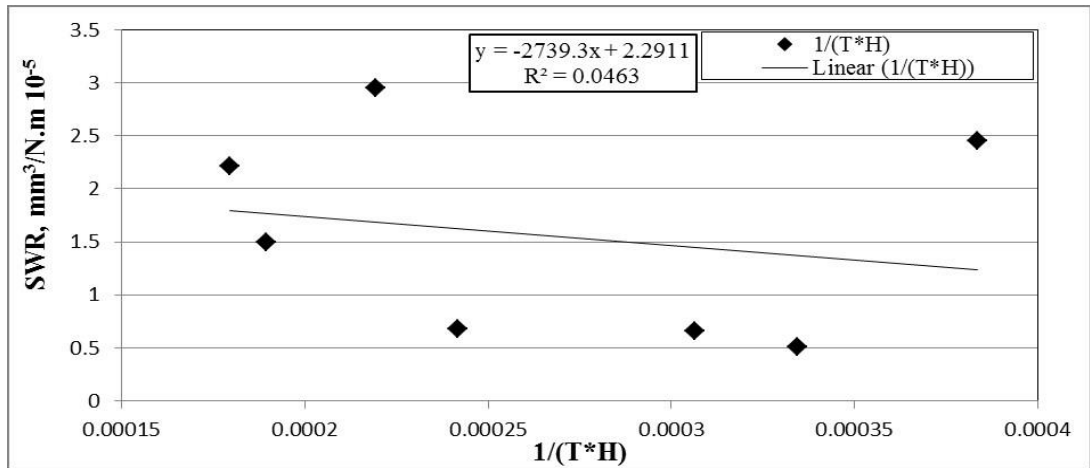


**Figure C. 7 correlation between specific wear rate and the combination of modulus of elasticity, tensile strength, hardness and elongation at break**

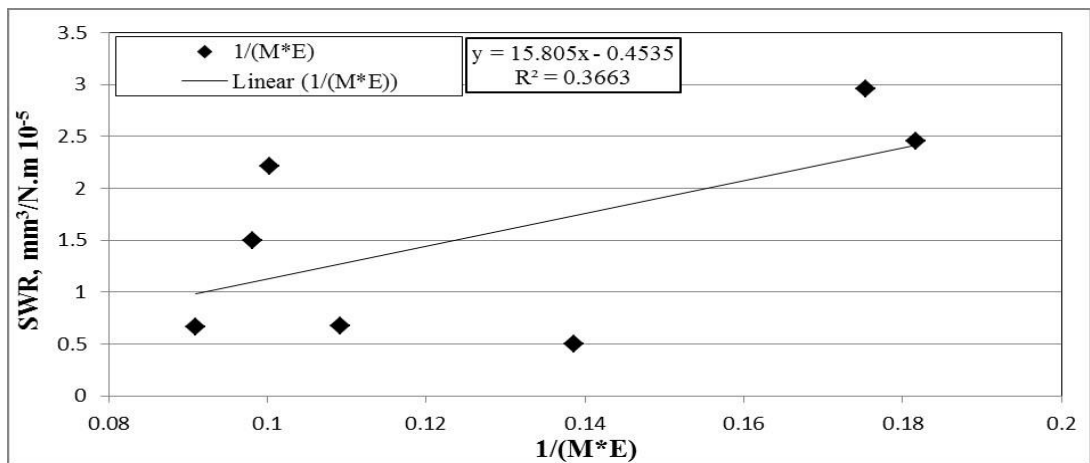


**Figure C. 8 correlation between specific wear rate and the combination of tensile strength and elongation at break**

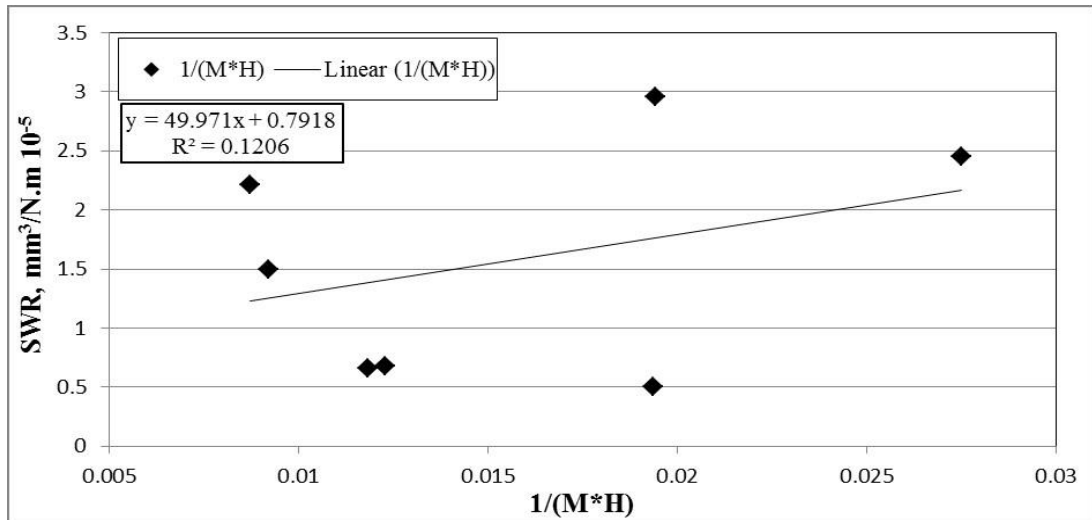




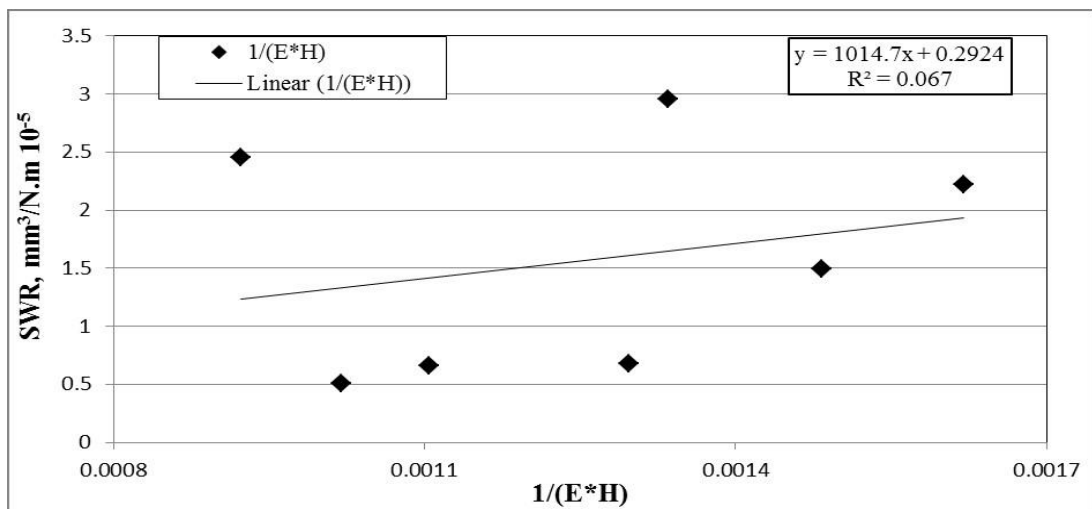
**Figure C. 9 correlation between specific wear rate and the combination tensile strength and hardness**



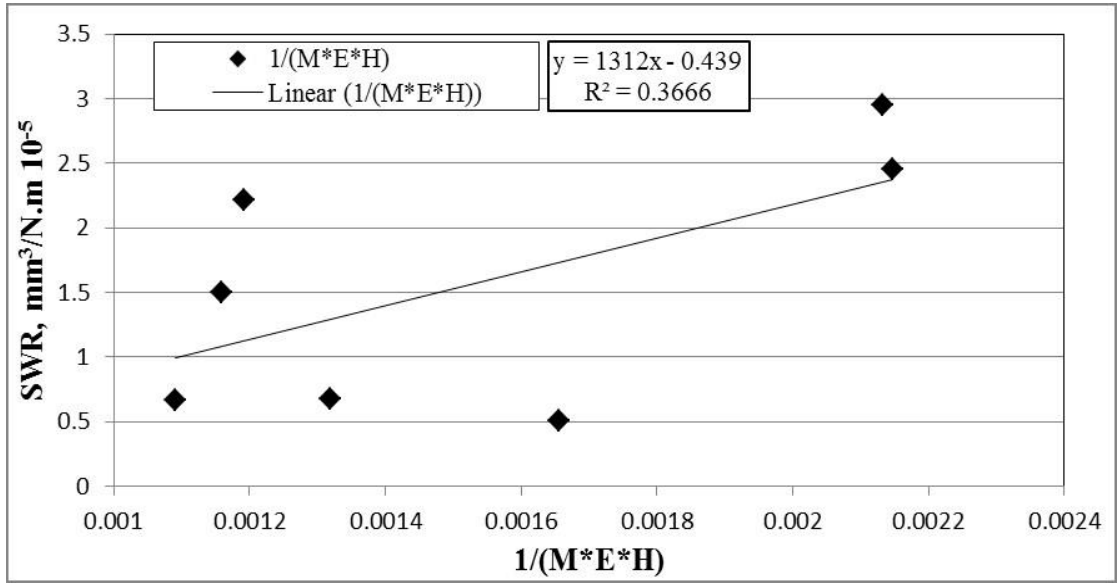
**Figure C. 10 correlation between specific wear rate and the combination of modulus of elasticity and elongation at break**



**Figure C. 11 correlation between specific wear rate and the combination of modulus of elasticity and hardness**



**Figure C. 12 correlation between specific wear rate and the combination of hardness and elongation at break**



**Figure C. 13 correlation between specific wear rate and the combination of modulus of elasticity, hardness and elongation at break**

## C.2 Completed figures of the correlation between mechanical properties and friction coefficient

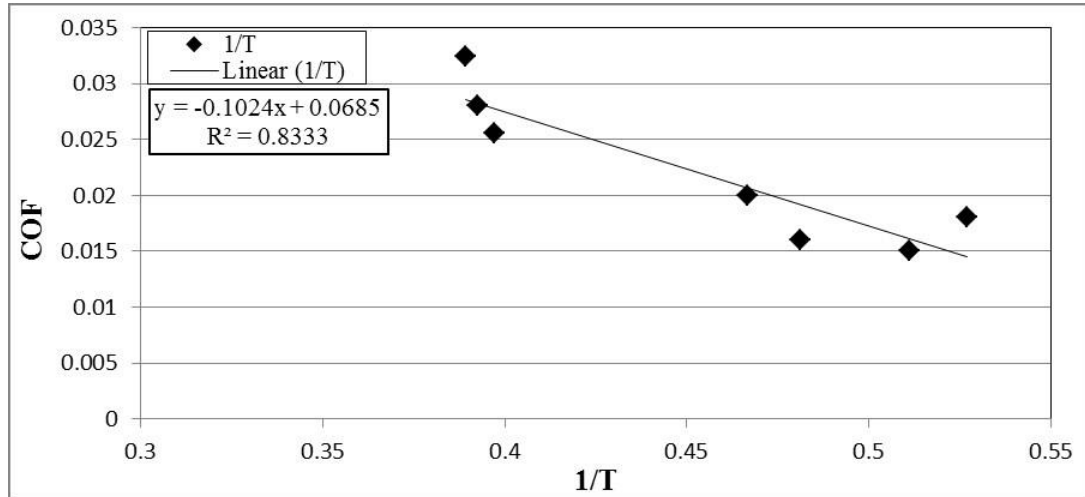


Figure C. 14 correlation between friction coefficient and tensile strength

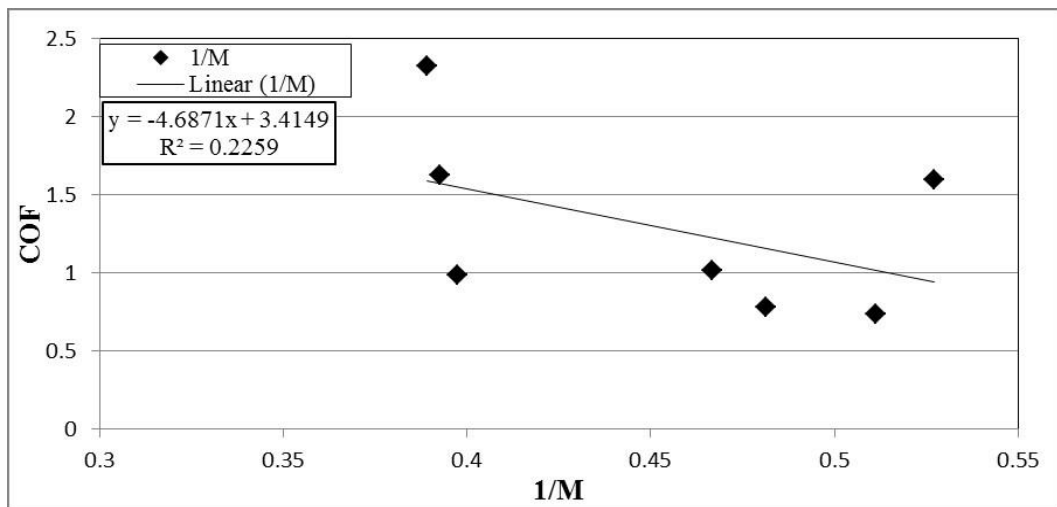
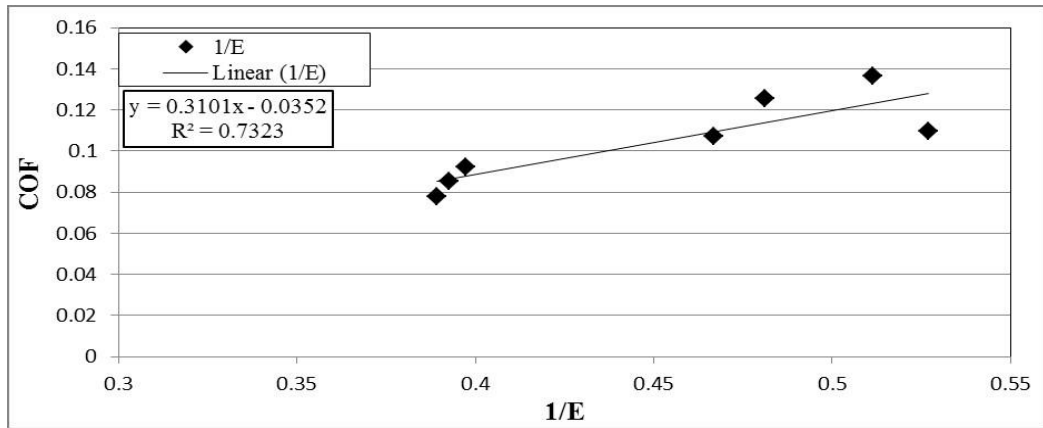
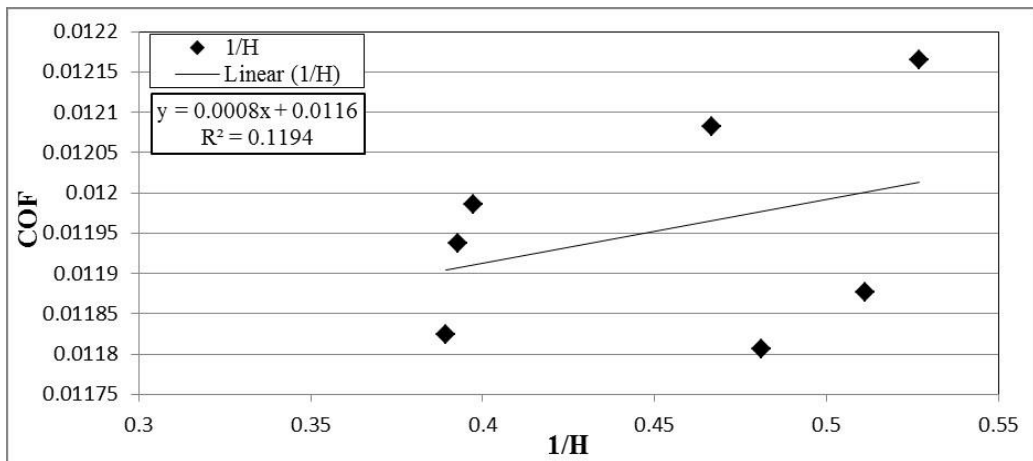


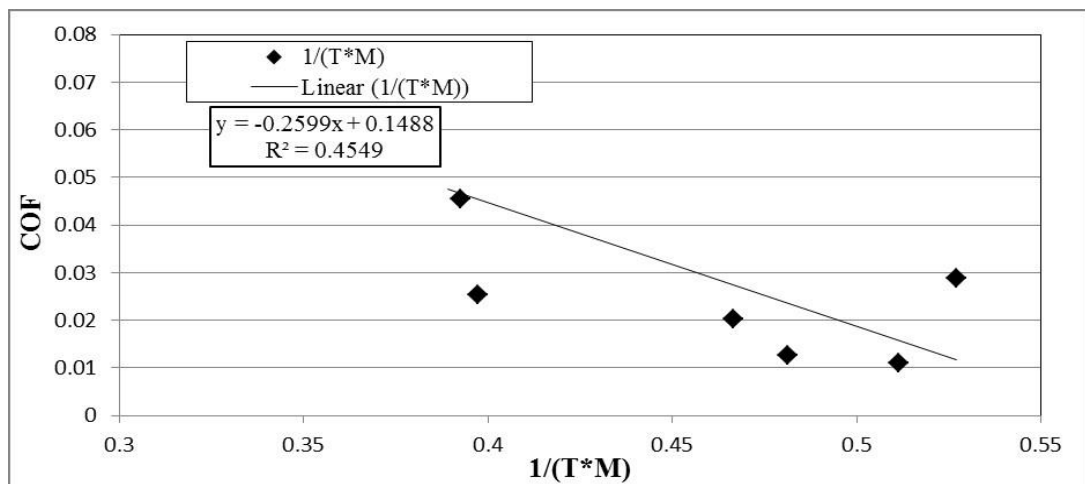
Figure C. 15 correlation between friction coefficient and modulus of elasticity



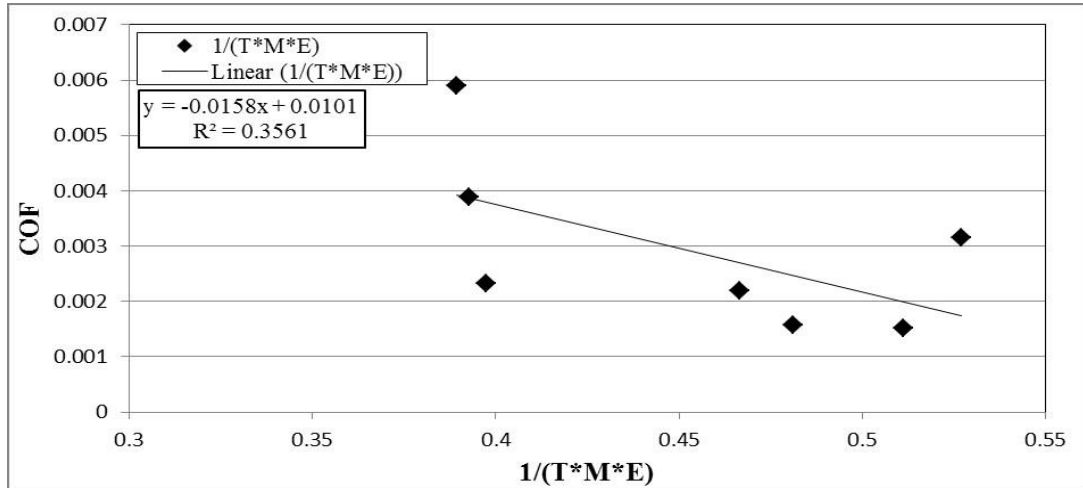
**3 Figure C. 16 correlation between friction coefficient and tensile elongation at break**



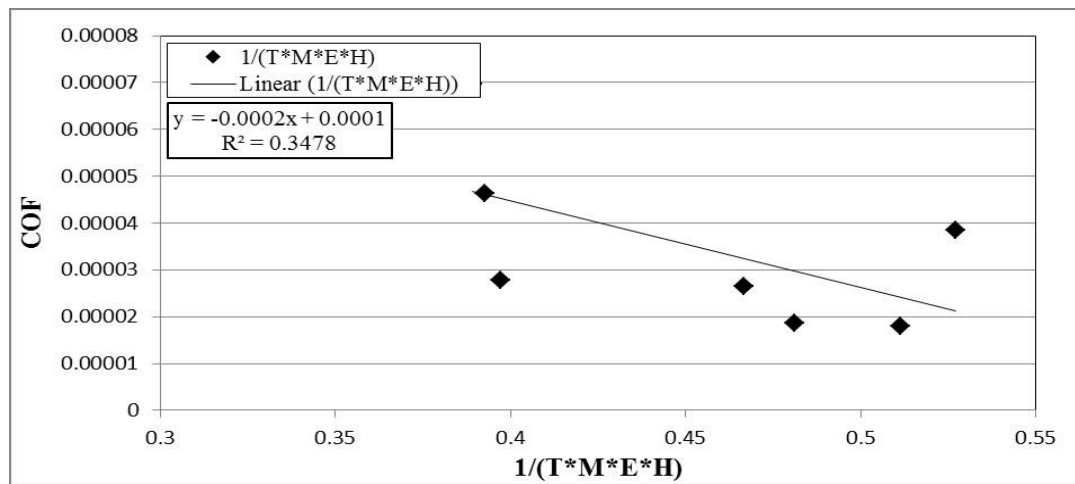
**Figure C. 17 correlation between friction coefficient and hardness**



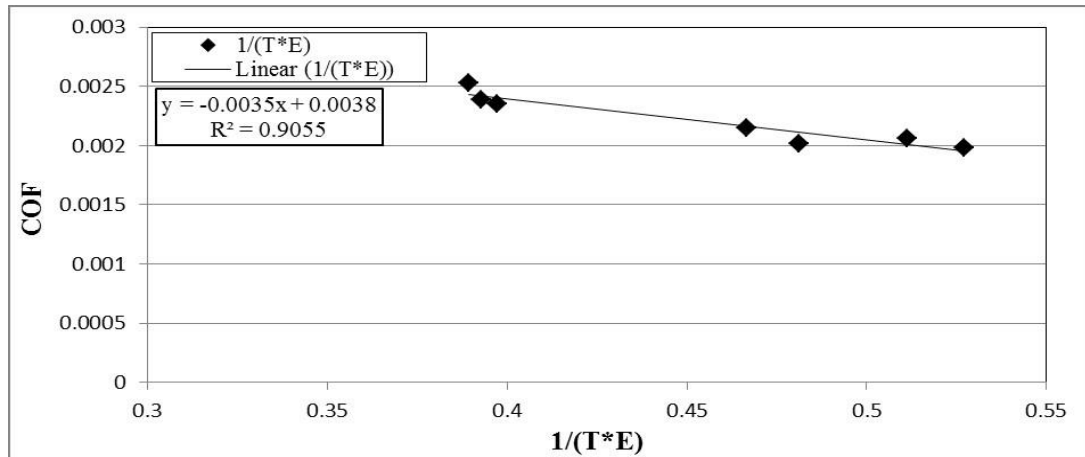
**Figure C. 18 correlation between friction coefficient and the combination of modulus of elasticity and tensile strength**



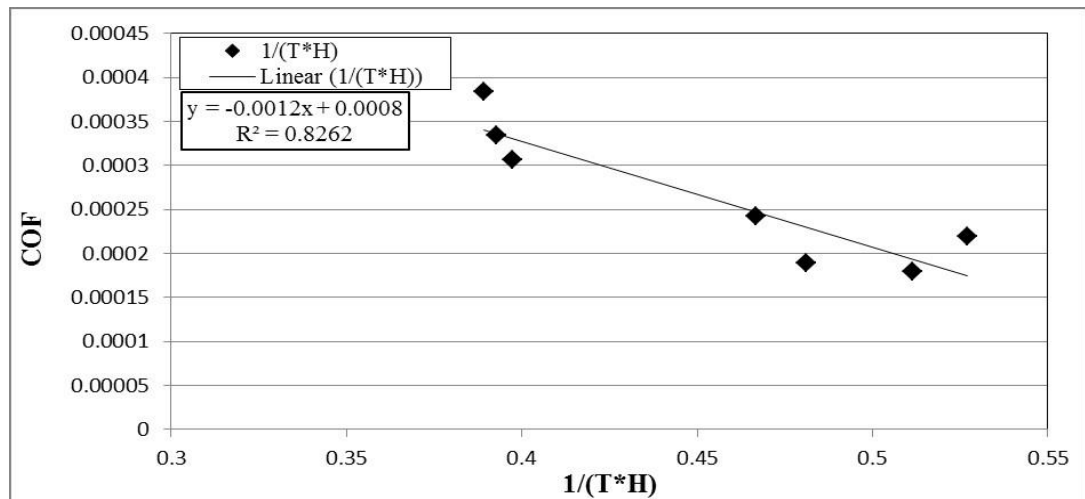
**Figure C. 19 correlation between friction coefficient and the combination of modulus of elasticity, tensile strength and elongation at break**



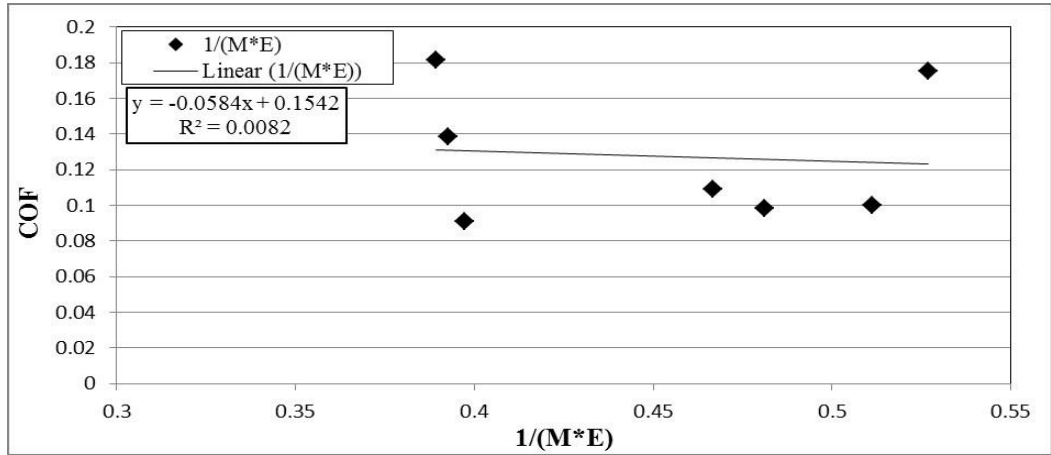
**Figure C. 20 correlation between friction coefficient and the combination of modulus of elasticity, tensile strength, hardness and elongation at break**



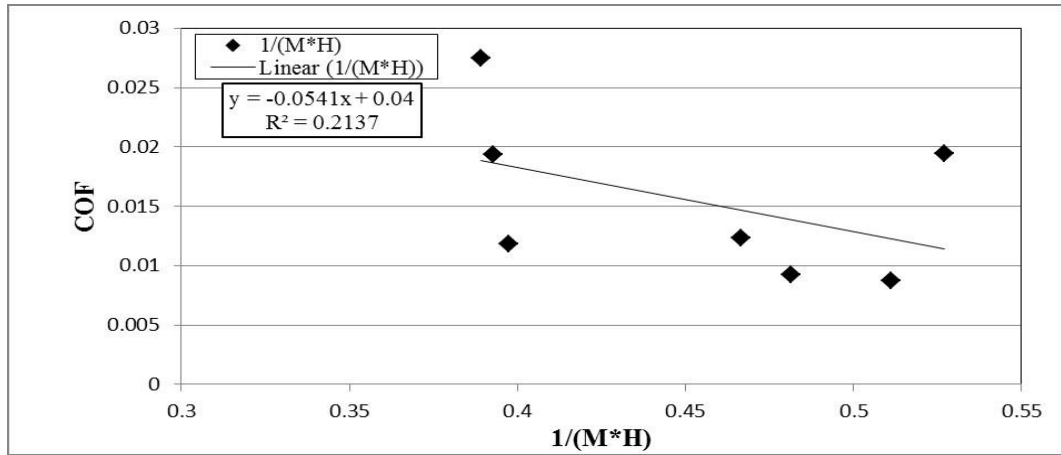
**Figure C. 21 correlation between friction coefficient and the combination of tensile strength and elongation at break**



**Figure C. 22 correlation between friction coefficient and the combination of tensile strength and hardness**

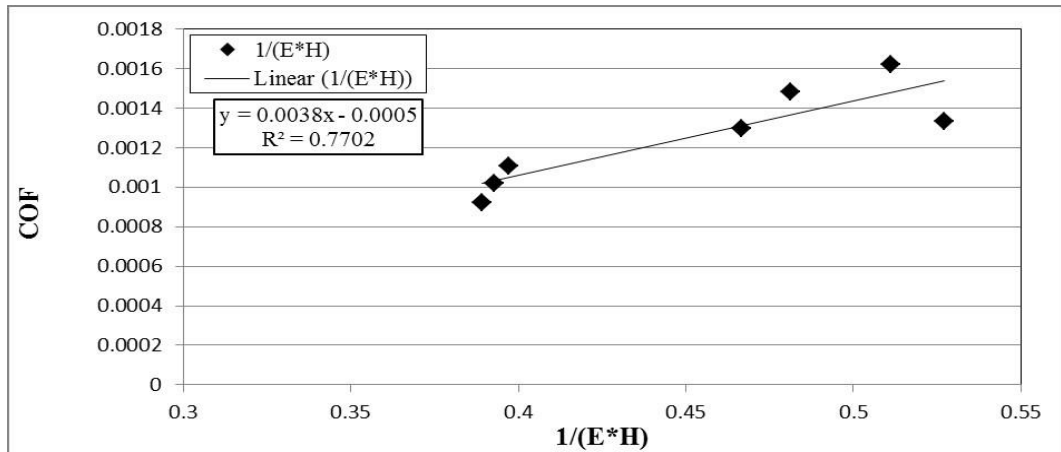


**Figure C. 23 correlation between friction coefficient and the combination of modulus of elasticity and elongation at break**

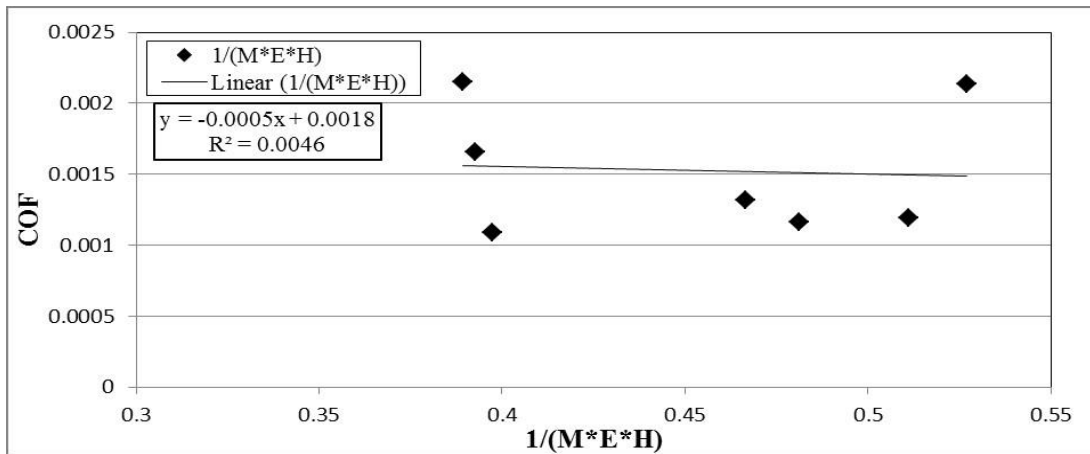


**Figure C. 24 correlation between friction coefficient and the combination of modulus of elasticity and hardness**





**Figure C. 25 correlation between friction coefficient and the combination of hardness and elongation at break**



**Figure C. 26 correlation between friction coefficient and the combination of modulus of elasticity, hardness and elongation at break**

## Glossary of Terms

<b>Terms</b>	<b>Definition</b>
<b>Biodegradability</b>	It is a process of decomposing the materials rapidly by the action of microorganisms.
<b>Block on disk</b>	It is a configuration of tribology test in which the contact between the rubbed parts is in area form
<b>Block on ring</b>	It is a configuration of tribology test in which the contact between the rubbed parts is in line form
<b>Chemical treatment</b>	It is chemical modification used to enhance the surface of the fibres to increase its interfacial adhesion with the matrix.
<b>Composites</b>	The materials made from two or more constituent materials
<b>Copolymerisation</b>	A form of addition polymerisation, in which two or more types of monomer are used.
<b>Counterface</b>	The rotational part of tribology machine which causes the material removal from the samples. It always harder than the samples
<b>Dry condition</b>	The contact between the body are in dry in which there is no liquid or gas in the interface
<b>fragmentation test</b>	It is a new technique used to determine the interfacial adhesion of the fibre with the matrix. in this technique the hole fibres are embedded in the sample
<b>Frictional heat</b>	It is the heat generated by friction and dissipated in the contacted bodies

**Plant fibre**

It is a natural fibres extracted from plants such as date palm, oil palm, and kenaf

**Running in state**

It is a term used to represent the initial stage of the adhesive rubbing process where the integration between the asperities is initiated.

**Single fibre Pull out****test**

It is an old technique used to determine the interfacial adhesion of the fibre with the matrix. In this technique the end of the fibres are free and subjected to the pull out loading through the experiments.

**Sliding direction**

It is the direction of the counterface with respect to the sample orientation during the sliding.

**Specific wear rates**

It is the unit to present the wear data of the materials. It is determined by the volume loss divided by the applied load times the sliding distance.

**Steady state**

It is a term used to represent the wear behaviour of materials after the running in stage.

**Worn surface**

The surface of the samples after the tribological tests.